Papers presented to the

ELEVENTH SYMPOSIUM

ON ANTARCTIC METEORITES

25–27, March 1986

NATIONAL INSTITUTE OF POLAR RESEARCH,
TOKYO

国立極地研究所

Papers presented to the

ELEVENTH SYMPOSIUM

ON ANTARCTIC METEORITES

25–27, March 1986

NATIONAL INSTITUTE OF POLAR RESEARCH,
TOKYO

NOTICE

Manuscripts Deadline: June 30, 1986

The publication of the full papers, which are here presented as abstracts, will be in the Proceedings of the Eleventh Symposium on Antarctic Meteorites, a special issue of the Memoirs of the National Institute of Polar Research. For inclusion in this publication the full text and illustrations of papers must be received by the organizing secretary (Dr. K. Yanai) by June 30, 1986.

Please send manuscripts to:

Dr. K. Yanai
Curator of meteorites
National Institute of Polar Research
9-10 Kaga 1-chome, Itabashi-ku
Tokyo 173
Japan

Telephone: Tokyo (03) 962-4711
Cable Address: POLARESEARCH TOKYO
Telex: 2723515 POLRSC J

Tuesday, March 25, 1986

0830-1200 Registration Auditorium (6th Floor)

0930 - 0935 Opening Address Tatsuro Matsuda:
Director-General
National Institute of
Polar Research

* Speaker

Chairmem: Yasunori Miura and Akira Shimoyama

1 0935 - 0950 Yanai K.* and Kojima H.
Antarctic search for meteorites: Past, present and future

2 0950 - 1005 Yanai K.* and Kojima H.
Curatorial work on the Japanese collections of Antarctic meteorites

3 1005 - 1020 Shimoyama A.* Harada K. Yanai K. and Kojima H.
Carbon and Nitrogen contents of carbonaceous chondrites from Antarctica, and their implication

4 1020 - 1035 Shimoyama A. Naraoka H.* Harada K. and Yamamoto H.
Carboxylic acids from the Yamato-791198 carbonaceous chondrite from Antarctica

5 1035 - 1050 Murae T.* Masuda A. and Takahashi T.
Pyrolytic studies on major carbonaceous matter in carbonaceous chondrites Y-791198, Y-791717, Y-793321 and B-7904

6 1050 - 1105 Matsunami S.
Kinetics of Fe/Mg exchange between chondrule and matrix and the implications for metamorphism of type 3 ordinary chondrites

7 1105 - 1120 Matsunami S.
Formation processes of matrix iron-rich olivine in ALH-764 (LL3.3), Y-790448 (LL3) and Krymka (L3.0) chondrites

8 1120 - 1135 Miura Y.
Determination of phyllo-silicates in carbonaceous chondrites

9 1135 - 1150 Momose K. and Nagai H.*
Thermo-remanent magnetization of Fe-Ni alloy

1150 - 1300 Lunch Time

- Special session: Lunar meteorites -

Chairmen: Yukio Ikeda and Takaaki Fukuoka

10 1300 - 1310 Yanai K.* Kojima H. and Ikadai S.
Four lunar meteorites including new specimen of Yamato-82193, prelimimary examination, curation and allocation for consortium studies

11 1310 - 1325 Bischoff A.* and Palme H.
Volatile-rich clasts from lunar meteorite Yamato-791197

12 1325 - 1400 Warren P.H.* and Kallemeyn G.W.
Geochemistry of lunar meteorite Yamato-82192: Comparison with Yamato-791197, ALHA81005 and other lunar samples

13 1400 - 1420 Bischoff A.* Palme H. Spettel B. Stöffler D. Wänke H. and Ostertag R.
Yamato-82192 and 82193: Two other meteorites of lunar origin

14 1420 - 1435 Takeda H.* Mori H. and Tagai T.
Mineralogy of lunar meteorites, Yamato-82192 and 82193 with reference to exploration of lunar highlands

15 1435 - 1450 Fukuoka T.* Laul J.C. Smith M.R. and Schmitt R.A.
Chemistry of Yamato-82192 and 82193 Antarctic meteorites

16 1450 - 1505 Takahashi K.* Shimizu H. and Masuda A.
Cosmochronological studies and REE abundances of lunar meteorites

1505 - 1530 Tea Time

17 1530 - 1545 Kaczaral P.W. Dennison J.E. Verkouteren R.M. and Lipschutz M.E.*
Consortium studies on lunar meteorite Yamato-82192

18 1545 - 1600 Nakamura N. Unruh D.M. Tatsumoto M. Fujiwara T. and Okano O.*
REE abundance and Pb-Pb isotopic characteristics of the lunar meteorite, Yamato-82192

19 1600 - 1615 Takaoka N.
Noble-gas study of lunar meteorite Y-82192

20 1615 - 1630 Weber H.W. Braun O. and Begemann F. (Bischoff A.*)
A new noble gas abundance pattern in a lunar meteorite: Yamato-82192

21 1630 - 1645 Kaneoka I.* and Takaoka N.
40Ar-39Ar analyses of Yamato-82192, an anorthositic regolith breccia from Antarctica

22 1645 - 1700 Nishiizumi K. Klein J. Middleton R. Elmore D. Kubik P.W. and Arnold J.R. (Imamura M.*)
Exposure history of four lunar meteorites

-- Special Lecture --

23 1700 - 1800 William A. Cassidy (Invited Speaker, Professor University of Pittsburgh, USA)

Title: Early history of the United States Antarctic meteorite program and the value of Antarctic meteorites

1800 - 2000 Reception (Lecture Room, 2nd Floor in Research Building)

Wednesday, March 26, 1986

Chairmen: Nobuo Morimoto and Jun-ichi Matsuda

24 0900 - 0915 Ikeda Y.* Palme H. Wlotzka F. Spettel B. and Wänke H.
A siderophile-rich clast in the polymict eucrite Y-790266

25 0915 - 0930 Toyoda H.* Takeda H. and Ishii T.
Mineralogy of some clasts in new Antarctic polymict eucrites and howardites with reference to their parental masses

26 0930 - 0945 Aoyama T.* Hiroi T. Miyamoto M. and Takeda H.
Absorption spectra and compositions of achondritic polymict breccias and its application to identification

27 0945 - 1000 Tagai T.* Takeda H. and Tachikawa O.
Diffraction characteristics and thermal histories of the meteoritic and terrestrial Ca-rich plagioclases

28 1000 - 1015 Ikeda Y.* Kimura M. and Wlotzka F.
Chemical zoning of chondrules in the Allende and ALH-77003 chondrites

29 1015 - 1030 Kitamura M.* Watanabe S. and Morimoto N.
Pyroxene crystallization in chondrules
-Autometamorphic evolution of chondrites-

30 1030 - 1045 Watanabe S.* Kitamura M. and Morimoto N.
Oscillatory zoning of pyroxenes in ALH-77214 (L3)

31 1045 - 1100 Saito J.* Tagai T. Tachikawa O. and Takeda H.
Textural and chemical studies of some Antarctic iron meteorites

32 1100 - 1115 Yabuki H.* Kimura M. and El Goresy A.
Spinel-group minerals in ordinary chondrites

33 1115 - 1130 Okada A.* and Keil K.
Perryite problem

34 1130 - 1145 Miura Y.* Yanai K. and Abe T.
Mg-Fe plagioclase compositions in Antarctic chondrites (I)

35 1145 - 1205 McKay G.* Wagstaff J. and Le L.
REE partitioning and the shergotty parent melt: evidence for complex petrogenesis and against metasomatic alteration

1205 - 1300 Lunch Time

- Special session: Yamato-691 enstatite chondrite -

Chairmen: Akimasa Masuda and Ichiro Kaneoka

36 1300 - 1310 Yanai K.* and Kojima H.
Yamato-691 E3 chondrite: recovery, curation and allocation

37 1310 - 1325 Ikeda Y.
A review of Y-691

38 1325 - 1350 Kallemeyn G.W.
Compositional characterization of Y-691 and other EH3 chondrites

39 1350 - 1410 Kimura M.
Mineralogical study on Y-691 enstatite chondrite

40 1410 - 1430 Kitamura M.* Watanabe S. and Morimoto N.
Pyroxenes in Y-691

41 cancel Akai J.
Mineralogy of Y-691 by AEM and HREM (Preliminary report)

42 1430 - 1445 Miura Y.
Formation process of Yamato-691 chondrite from Mg-Fe plagioclases and osumilite-group minerals

43 1445 - 1500 Fukuoka T.
Chemistry of enstatite chondrite, Yamato-691 (E3) Antarctic meteorite

1500 - 1530 Tea Time

44 1530 - 1550 Dennison J.E. Kaczaral P.W. Verkouteren R.M. and Lipschutz M.E.*
Consortium studies on E3 chondrite Yamato-691

45 1550 - 1605 Miyamoto M.
Spectral reflectance (0.25-25 μm) of the Yamato-691 enstatite chondrite

46 1605 - 1620 Ebihara M.
Distribution of rare earth elements in some enstatite chondrites including Yamato-691

-- Special Lecture --

47 1620 - 1720 Ahmed El Goresy* (Invited speaker; Professor, Max-Planck-Institut für Kernphysik in Heidelberg, F.R. Germany), Woolum D.S. and Ehlers K.

Title: Yamato-691: Evidence for planetary metamorphism $t<1.1$ billion years in the EH parent body

Thursday, March 27, 1986

Chairmen: Nobuo Takaoka and Mitsuru Ebihara

48 0900 - 0915 Misawa K.* and Nakamura N.
Primitive REE fractionation in Allende chodrules

49 0915 - 0930 Nakayama T.* and Nakamura N.
Fractionation of REE among individual chondrules from the Bjurböle (L4) chondrite

50 0930 - 0945 Ebihara M.
Distribution of rare earth elements in unequilibrated ordinary chondrites

51 0945 - 1000 Honda M.* Nagai H. and Shimamura T.
Trace elements in some iron meteorites

52 1000 - 1015 Okano O.* Nakamura N. Nagao K. and Honma H.
A 1.2 B.Y. impact event on LL-chondrite parent body: evidence from Rb-Sr systematics and rare gas compositions of paired LL-chondrites from Antarctica

53 1015 - 1030 Takigami Y.* and Kaneoka I.
Investigation of the shock effect on the Antarctic meteorites by the 40Ar-39Ar method

54 1030 - 1045 Okano J.* Uyeda C. Suzuki M. and Nishimura H.
Magnesium isotope abundance in Allende and Antarctic meteorites

55 1045 - 1100 Nagao K.* and Matsuda J.
Rare gas studies of Antarctic meteorites

56 1100 - 1115 Amari S.* and Ozima M.
The extra-terrestrial noble gas in deep-sea sediments

57 1115 - 1145 Grady M.M.* Barber D. Graham A. Kurat G. Ntaflos T. Palme H. and Yanai K.
Yamato-82042: an unusual carbonaceous chodrite with CM affinities

58 1145 - 1205 Wright I.P.* McGarvie D.W. Grady M.M. Gibson E.K. Jnr. and Pillinger C.T.
An ivestigation of 13C-rich material in C1 and C2 meteorites

1205 - 1300 Lunch Time

Chairmen: Hiroichi Hasegawa and Masamichi Miyamoto

59 1300 - 1320 Mukherjee A.* and Viswanath T.A.
Thermobarometry of diogenites

60 1320 - 1340 Nagata T. Funaki M. and Danon J.*
Magnetic properties of tetratanite in Ni-rich at ataxites

61 1340 - 1355 Sugiura N.* Arkani-Hamed J. and Strangway D.W.
On the possible transport of volatile trace elements in meteorite parent bodies

62 1355 - 1410 Fujii N.* Ito K. and Miyamoto M.
Shape analysis of metallic grains among Antarctic ordinary chondrites

63 1410 - 1425 Masuda A. Taguchi I.* and Tanaka K.
Non-destructive analysis of meteorites by using a high-energy X-ray CT scanner

64 1425 - 1440 Matsui T. Kani K.* and Matsushima Y.
Hugoniot of some ordinary chondrites

65 1440 - 1455 Funaki M.* and Nagata T.
Thermomagnetic "Hump" in Antarctic stony meteorites

66 1455 - 1510 Nagata T.* and Funaki M.
Tetrataenite phase in Antarctic stony meteorites

1510 - 1540 Tea Time

-- Special Lecture --

67 1540 - 1630 Michael E. Lipschutz* (Invited Speaker; Professor Purdue University, USA), Dennison J.E. Kaczaral P.W.

Title: Antarctic and non-Antarctic meteorites: Different populations

---

Abstract only, no oral presentation

68 Wang Daode
Study on the primitive materials forming terrestrial planets

69 Jerde E.A. Warren P.H. Heiken G.H. and Vaniman D.T.
A potpourri of Apollo regolith breccias: Analogs of lunar meteorites

Tuesday, March 25, 1986

0830 - 1200	*Registration, 6th Floor*
0930 - 0935	*Opening address, Auditorium*
0935 - 1150	*Symposium, Auditorium*
1300 - 1700	*Special session: Lunar meteorites*
1700 - 1800	*Special Lecture* *Professor William A. Cassidy* *(University of Pittsburgh, Pittsburgh)*
1800 - 2000	*Reception, Lecture Room, 2nd Floor*

Antarctic search for meteorites: Past, present and future

Yanai K. and Kojima H.
National Institute of Polar Research, 9-10, Kaga 1-chome, Itabashi-ku, Tokyo 173

The systematic meteorite search in Antarctic continent has been started as a result of unbelievable discovery in 1974 of a dense concentration over six handred and sixty pieces of meteorites on the bare ice field adjacent to the Yamato Mountains, East Antarctica (1) by the fifteenth Japanese Antarctic Research Expedition (JARE).

Until 1969 only six meteorites had been recovered from whole Antarctic. In 1969, JARE parties collected nine of meteorite from the Yamato Mountains area (2). The first nine pieces were found accidentally and have been believed that they were not only individual fall but they were as one or few meteorite shower. However, succeeding identifications and classifications of them showed that most of them were individual specimens and belonged to several kinds of meteorite types and classes. The nine specimens collected in the Yamato Mountains in 1969, had been classidied into four types of meteorites indicating they did not derive from common fall. The types include an enstatite chondrite (EH3), adiogenite (granoblastic), a carbonacious chondrite (C4) and six ordinary chondrite belonging to several petrologic tiypes and classes.

The 1973 field season, more 12 specimens including a howardite, were found at the Yamato Mountain area (3). Eight specimens of them were collected from the same bare ice field as those of previous find, while the others were found on a bare ice field 30-40 km apart from previous sites. This fact seemed that more meteorites could be recovered on other bare ice field.

In 1974 field season, 663 meteorite pieces were collected from the Yamato Mountains area. About 200 of these specimens were found in the same vicinities of the 1969 and 1973 finds, while over 400 specimens were found in previously unsearched area. It has been definitely shown by this find that meteorites could be found on all over the bare ice field adjacent to the Yamato Mountains. The 1974 collection included many meteorite types including a lodranite, a pallasite, numbers of achondrites, and six ungrouped meteorites, but no irons (2,4).

In 1975 the systematic search techniques initiated in 1974 resulted in a find of 308 new pieces including two irons and unique diogenite (5). The most systematic search up to that time was carried out in 1979 field season. Over 3,600 meteorite specimens were recovered in more wide area of the bare ice field. The specimens were included a most pecular specimen (lunar meteorite) and a lot of rare specimens with many iron, lodranites, various kinds of achondrite and carbonacious chondrites (6).

In the 198, 1981, 1982, 1983 and 1984 field seasons, 13, 133, 211, 42 and 59 specimens were collected respectively. In particular, the 1982 collection included a lot of unique specimens such as lunar meteorites and C1 chondrites classified preliminary.

A Japan-U.S. program titled "Antarctic Search for Meteorites" (ANSMET) was initiated as a result of the discoveries of meteorites in the Yamato Mountains. This joint program continued for three years (1976-1979) in the area of the bare ice fields of Victoria Land. The joint party collected about 900 specimens from mainly of Allan Hills in Victoria Land and other several places for three field seasons since 1976. The collections included many ordinary chondrites, several irons, a few carbonaceous chondrites and

achondrites including a shergottite (7, 8, 9, 10).

Until 1985, over 7,000 meteorite fragments were recovered from the a lot of places of the exposed bare ice field in entire Antarctic continent. Antarctic meteorites included a lot of rare and unique meteorite types, and previously unknown types of meteorites. (Figure and Table).

Recently it does not much difficult to expect the places where meteorites could be revovered form Antarctic continent, because most of Antarctic meteorites had been knowing to be found on the bare ice field except those of the costal area. It is not difficulty to estimate the possible numbers of meteorites which will be recovered from Antarctica in the future.

Several bare ice fields in Antarctic continent are expected as places of high possibility being meteorites. In particular, the Sor Rondane Mountains area is one of the most promising bare ice field, being of several thousand meteorite specimens will be expected on the southern and eastern bare ice field of the mountains. The Trans- Antarctic Mountains area has high ability of meteorites concentration, too. Western Queen Moud Land and Prince Charles Mountains my be good places for meteorites, however there are small scale bare ice fields around their mountains. The area around the Yamato Mountains was the most valuable place for meteorites. The total area of exposed bare ice around the Yamato Mountains is on the order of 4,000 square km. Eleven JARE parties have searched for meteorites there in the face of a great deal of danger, however, much of it still remains to be searched. The Yamato Mountains are the one place in Antarctica with the greatest possibility for many more meteorites findings.

REFERENCES: (1) Yanai K. (1976) Antarctic Record, Japan 56, p. 70-81. (2) Yoshida M., Ando H., Naruse R. and Ageta Y. (1971) Antarctic Record, Japan 39, p. 62-65. (3) Shiraishi K., Naruse R. and Kusunoki K. (1976) Antarctic Record, Japan 55, P. 49-60. (4) Yanai K. (1978) Memoirs of NIPR, Special Issue 8, p. 1-37. (5) Matsumoto Y. (1978) Memoirs of NIPR, Special Issue 8, p. 38-50. (6) Yanai K. (1981) Memoirs of NIPR, Special Issue 20, p. 1-8. (7) Cassidy W.A. (1977) Antarctic Journal of the United States 12, p. 96-98. (8) Yanai K., Cassidy W.A., Funaki M. and Glass B.P. (1978) Proc. Lunar Sci. Conf. 9th, p. 977-987. (9) Cassidy W.A. (1979) Antarctic Journal of the United States 15, p. 41-42. (10) Shiraishi K. (1979) Memoirs of NIPR 15, p. 1-12.

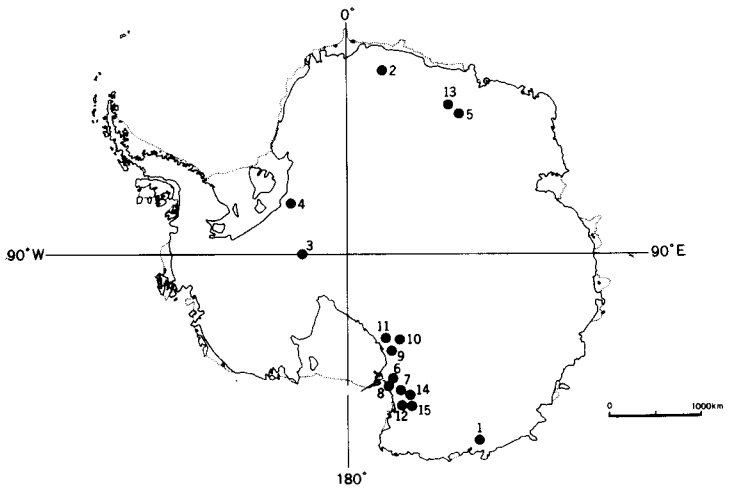

Figure. The locations of Antarctic meteorites collected since 1912.

The Collections of Antarctic Meteorites (1912-1985)

Location	Meteorite Name	Date of find	Iron	Stony-Iron	Chondrite	Achondrite	C.C.	*	Total	Search Party
1	Adelie Land	1912.12	-	-	1	-	-	-	1	Australia
2	Lazarev	1961.1	2	-	-	-	-	-	2	CCCP
3	Thiel Mts.	1961.12	-	2	-	-	-	-	2	USA
4	Neptune Mts.	1964.12	1	-	-	-	-	-	1	〃
5	Yamato-69	1969.12	-	-	7	1	1	-	9	JARE-10
5	Yamato-73	1973.12	-	-	11	1	-	-	12	JARE-14
5	Yamato-74	1974.11-12	-	2	630	28	3	-	663	JARE-15
5	Yamato-75	1975-76	2	1	290	12	3	-	308	JARE-16
6	Mt.Baldr	1976.12	-	-	2	-	-	-	2	Japan-USA
7	Allan Hills-76	1977.1	1	-	7	1	-	-	9	〃
7	Allan Hills-77	1977-78	6	1	292	4	3	4	310	〃
8	Purgatory Peak	1978.1	1	-	-	-	-	-	1	〃
9	Derrick Peak	1978.12	6	-	-	-	-	-	6	New Zealand
9	Derrick Peak	1978-79	10	-	-	-	-	-	10	Japan-USA
10	Meteorite Hills-78	〃	-	-	28	-	-	-	28	〃
11	Bates Nunatak-78	〃	-	-	5	-	-	-	5	〃
7	Allan Hills -78	〃	2	-	249	8	1	2	262	〃
12	Reckling Peak-78	〃	-	-	5	-	-	-	5	〃
7	Allan Hills-79	1979-80	-	-	52	1	-	2	55	USA
12	Reckling Peak-79	〃	1	-	14	-	-	-	15	〃
14	Elephant Moraine	〃	-	-	7	5	-	-	12	〃
5	Yamato-79	〃	7	1	3,558	79	31	-	3,676	JARE-20
13	Belgica-79	1979.12	-	-	4	-	1	-	5	〃
7	Allan Hills-80	1980-81	1	-	29	1	1	-	32	USA(WG)
12	Reckling Peak-80	〃	1	4	61	3	1	-	70	〃
15	Outpost Nunatak-80	〃	-	-	1	-	-	-	1	〃
5	Yamato-80	〃	-	1	11	1	-	-	13	JARE-21
7	Allan Hills-81	1981-82	2	-	359	8	4	-	373	USA(WG)
5	Yamato-81	〃	-	-	123	2	7	1	133	JARE-22
	TAMS	1982-83	-	-	-	-	-	113	113	USA(Denmark)
5	Yamato-82	〃	-	-	179	21	10	1	211	JARE-23
	TAMS	1983-84	-	-	-	-	-	360	360	USA(France)
5	Yamato-83	1983.12	-	-	42	-	-	-	42	JARE-24
	TAMS	1984-85	-	-	-	-	-	292	292	USA
5	Yamato-84	1984.12	-	-	-	-	-	59	59	JARE-25
	Frontier Mts	1984-85	-	-	42	-	-	-	42	W. Germany
	Total		43	12	6,009	176	66	834	7,140	

(March 1986)

C.C. : Carbonaceous Chondrite
* : Unidentified
JARE : Japanese Antarctic Research Expedition
TAMS : Trans-Antarctic Mountains

2—1

Curatorial work on the Japanese collections of Antarctic meteorites

Yanai K. and Kojima H.
National Institute of Polar Research, 9-10, Kaga 1-chome, Itabashi-ku, Tokyo 173

The present Japanese collection of Antarctic meteorites with the including of Victoria Land specimens is estimated to total 5,618 specimens (Table 1). The Department of Antarctic Meteorites, NIPR, Tokyo has been processing the Japanese collection since 1975. All collected specimens have been numbered, weighed, photographed, identified, and classified as preliminary. The specimens are stored in an air conditioned clean room.

Table 1. Japanese Collections of Antarctic Meteorites

National Institute of Polar Research (NIPR), Tokyo, 173 Japan

Meteorite Name	Date of find	Iron	Stony-Iron	Chond-rite	Achond-rite	*	**	Total	Search Party
Yamato-69	1969.12			7	1	1		9	JARE-10
Yamato-73	1973.12			11	1			12	JARE-14
Yamato-74	1974.11-12		2	630	28	3		663	JARE-15
Yamato-75	1975-76	2	1	290	12	3		308	JARE-16
Mt.Baldr	1976.12			2				2	Joint Japan-U.S.A.
Allan Hills-76	1977.1	1		7	1			9	
Allan Hills-77	1977-78	6	1	234	4	3		248	
Purgatory Peak	1978.1	1						1	
Derrick Peak-78	1978-79	5						5	
Meteorite Hills-78	1978-79			28				28	
Bates Nunatak-78	1978-79			5				5	
Allan Hills -78	1978-79	2		173	8	1		184	
Reckling Peak-78	1978-79			5				5	
Yamato-79	1979-80	7	1	3,558	79	31		3,676	JARE-20
Belgica-79	1979.12			4		1		5	JARE-20
Yamato-80	1980-81		1	11	1			13	JARE-21
Yamato-81	1981-82			123	2	7	1	133	JARE-22
Yamato-82	1982-83			179	21	10	1	211	JARE-23
Yamato-83	1983.12			42				42	JARE-24
Yamato-84	1984.12						59	59	JARE-25
Total		24	6	5,309	158	60	61	5,618	

* : Carbonaceous Chondrite
** : Unidentified
JARE : Japanese Antarctic Research Expedition

(March 1986)

The Yamato collection icludes 9 irons, 5 stohy-irons (three lodranites), over 60 carbonaceous chondrites including the largest mass over 25 kg, many achondrites including aubrite, ureilites, diogenites, howardites, eucrites and anorthositic breccias (lunar meteorites), 4 enstatite chondrites and many ordinary chondrites including several unique (ungrouped) specimens. The collection may also contain more new and as of yet unidentified specimens (Table 2).

Table 2. Types of Meteorite in the Japanese Collections of the Yamato Meteorites

	Y-69	Y-73	Y-74	Y-75	Y-79	Y-80	Y-81	Y-82	Y-83	Y-84	Total
E chondrite	1		2		205						208
H3			9	5	15			1			30
L3			5		1			1			7
LL3			2	1	1						4
L-LL3				2							2
H4	1	3	52	11	213						280
L4			9	11	4						24
LL4			3	1							4
H5	3	2	236	11	68			1			321
L5			7	5	6						18
LL5			1	3							4
H6	2	2	218	14	33						269
L6		3	71	216	71			2			363
LL6		1	5	5	2						13
C.chondrite	1		4	3	31		7	15			61
Shocked ch.			2		179						181
Ungrouped ch.			6	5							11
Iron				2	7						9
Pallasite			1								1
Mesosiderite											0
Lodranite			1	1	1	1					4
Aubrite					1						1
Ureilite			4		3			1			8
Diogenite	1		22	7	30	1	2	5			68
Howardite		1			15			3			19
Eucrite			3	5	39			10			57
Anorth.Br.					1			2			3
Unclassified	0	0	0	0	2750	11	124	170	42	59	3156
Total	9	12	663	308	3676	13	133	211	42	59	5126

The Japanese portion of the Victoria Land Meteorites include 15 irons, one mesosiderite, 11 achondrites including aubrite, ureilites, diogenite, howardite, eucrites and shergottite, 2 enstatite chondrites, and many ordinary chondrites including two unique (ungrouped) specimens and the largest mass over 400 kg. The Victoria Land collection includes no pallasite and no lodranite (Table 3).

Since 1975, the meteorite curator of the NIPR has received 454 research proposals from scientists representing fifteen countries. Those proposals also include several consortium studies such as the lunar meteorite(s) and the Yamato-691 enstatite chondrite. All research proposals are judged for scientific merit by the Committee on Antarctic Meteorite Research of Japan. To date, over 2,400 samples have been allocated to scientists throughout the world.

Table 3. Types of Meteorite in the Collections of the Victoria Land Meteorites

	MBR	ALH-76	ALH-77	ALH-78	BTN-78	MET-78	RKP-78	DRP-78	PGP-78	Total
E chondrite			2							2
H3			1	1						2
L3			40	4						44
LL3		1	2	2						5
L-LL3			2	1						3
H4			34	15		1	2			52
L4			2	3						5
LL4				2						2
H5	1		131	57		1				190
L5			5							5
LL5			1	2						3
H6	1	2	26	23		2				54
L6		4	33	27	2	4	2			72
LL6			1	1	1					3
Shocked			1							1
Ungrouped			1	1						2
C.C			4	1						5
Iron		1	6	2				9	1	19
Pallasite										0
Mesosiderite			1							1
Lodranite										0
Aubrite				1						1
Ureilite			1	2						3
Diogenite			1							1
Howardite				1						1
Eucrite		1	1	3						5
Shergottite			1							1
Anorth.Br.										0
Unclassified	0	0	0	112	1	20	1	0	0	134
Total	2	9	297	261	4	28	5	9	1	616

CARBON AND NITROGEN CONTENTS OF CARBONACEOUS CHONDRITES FROM ANTARCTICA, AND THEIR IMPLICATION

SHIMOYAMA, A.,[1] HARADA, K.,[1] YANAI, K.,[2] and KOJIMA, H.[2]

1 Department of Chemistry, University of Tsukuba
Sakura-mura, Ibaraki 305

2 National Institute of Polar Research, Kaga-cho
Itabashi-ku, Tokyo 173

Carbonaceous chondrites contain organic compounds of extraterrestrial origin. Contents of these compounds vary from C1 to C3 chondrites and are reflected by carbon and nitrogen contents. We have analyzed C and N contents of carbonaceous chondrites from Antarctica. These analyses were duplicated and the two contents are listed in Table 1. We plotted these contents in a log-log diagram as seen in Fig. 1. In addition, the two contents of non-Antarctic carbonaceous chondrites reported[1] are plotted in Fig. 1. Four Antarctic chondrites appear in the pre-existed empty space between the point 7 and 8 of non-Antarctic carbonaceous chondrites. It is likely that the C and N contents change almost continuously from C1 to C3. We propose a logarithmic linear relation in between the two contents. The least-squares fit of the 11 points of Antarctic chondrites gives an equation,

$$\log N = 1.84 \log C - 1.46 \qquad (1)$$

where C and N are contents(%) of carbon and nitrogen, respectively, and the correlation coefficient(r) is 0.97. The 18 points of the non-Antarctic carbonaceous chondrites give,

$$\log N = 1.43 \log C - 1.43 \qquad (2)$$

and r is 0.90. Apparently a better logarithmic linear relation exists for Antarctic carbonaceous chondrites. It has been known that Antarctic carbonaceous chondrites were less contaminated by terrestrial organic matter as observed by the amino acid examination.[2,3] Therefore, a straight line by equation (1) is drawn in Fig. 1 in order to present a possible relation between C and N contents of carbonaceous chondrites. This relation

indicates that, as the contents of organic compounds become smaller, these compounds change toward C-rich and N-poor compounds. If this line is accurate, extrapolation of the line toward more primitive than C1 chondrites gives C and N contents of lower temperature condensates. We will discuss our postulate for such a primitive condensate.

References

1. E.K. Gibson, et al.(1971) Geochim. Cosmochim. Acta, 35, 599.
2. A. Shimoyama, et al.(1979) Nature, 282, 394.
3. A. Shimoyama, et al.(1985) Chem. Lett., 1183.
4. A. Shimoyama and K. Harada(1984) Geochem. J., 18, 286.

Table 1. Carbon and Nitrogen Contents of Antarctic Carbonaceous Chondrites

Chondrite	C (%)	N (%)	Chondrite	C (%)	N (%)
Y-791198[3]	2.33, 2.31	0.12, 0.13	B-7904.2[4]	1.13, 1.12	0.062, 0.066
Y-74662	1.94, 1.94	0.13, 0.13	B-7904.3[4]	0.87, 0.89	0.041, 0.048
Y-74642	1.91, 1.91	0.11, 0.10	Y-74135	1.08, 1.08	0.033, 0.033
Y-793321[4]	1.63, 1.68	0.12, 0.11	ALH-77307	0.79, 0.79	0.023, 0.027
Y-82042	1.71, 1.67	0.065, 0.069	Y-81021	0.89, 0.88	0.018, 0.016
			Y-791717	0.21, 0.20	0.0018, 0.0017

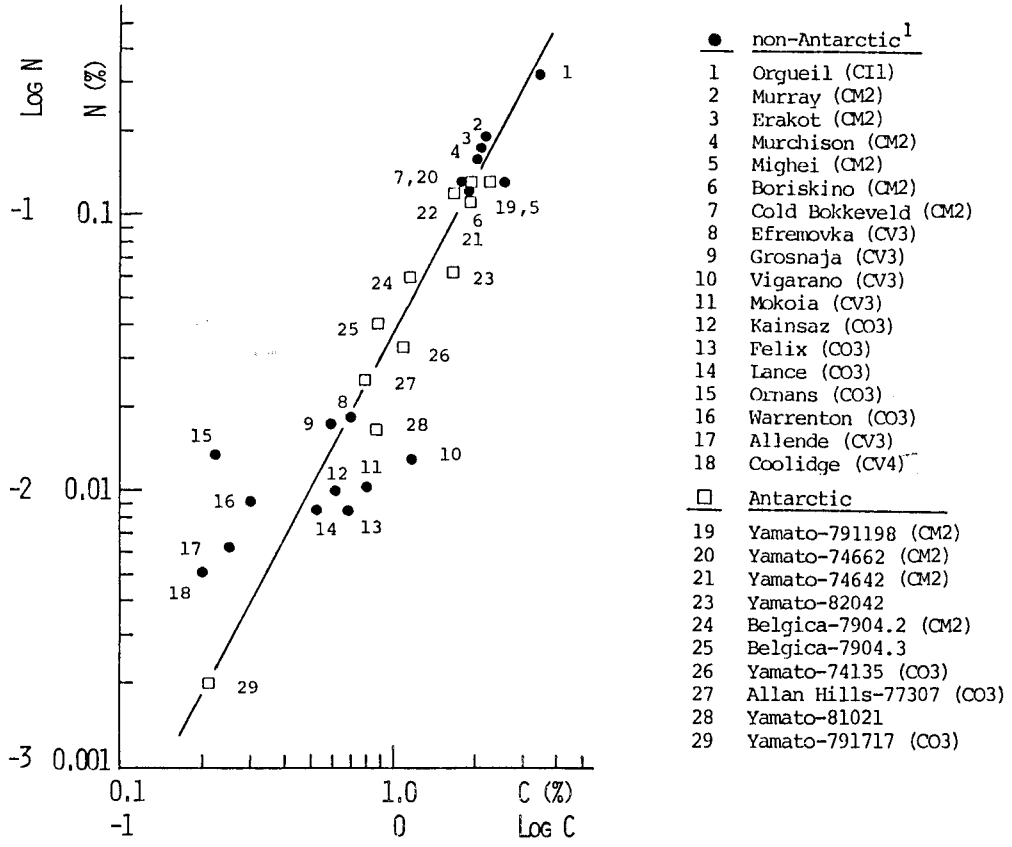

Fig. 1. Carbon and nitrogen contents of carbonaceous chondrites.

CARBOXYLIC ACIDS FROM THE YAMATO-791198 CARBONACEOUS CHONDRITE FROM ANTARCTICA

SHIMOYAMA, A., NARAOKA, H., HARADA, K., and YAMAMOTO, H.*

Department of Chemistry, University of Tsukuba, Sakura-mura, Ibaraki 305
*Faculity of Education, Ibaraki University, Mito, Ibaraki 310

Recently, it was found that the YAMATO-791198 carbonaceous chondrite yielded many kinds of extraterrestrial amino acids[1]. Because of this finding, this chondrite is considered to be very suitable for the study of organic compounds. We analyzed this specimen for carboxylic acids.

The sample of Y-791198,22 was processed on a clean bench set inside of a clean room with care. A powdered sample was extracted with methanolic potassium hydroxide by refluxing in sealed tube. The supernatant, after centrifugation, was added to distilled water. After the water solution was extracted with dichloromethane, the solution was evaporated to dryness under reduced pressure. The acidified solution (pH 1) by 6M HCl was extracted with dichloromethane.

Monocarboxylic acids were identified by gas chromatography combined with mass spectrometry(Fig.1). It was found that monocarboxylic acids in this specimen contained straight and branched-chain structures having two to twelve carbon atoms(C_2-C_{12}). The quantities of n-alkyl carboxylic acids are shown in Table 1, being butanoic acid the largest. Most of structural isomers were found with C_4, C_5 and C_6. Further, we found a few of C_7 isomers. As to C_6, various isomers was observed as seen in the enlarged portion in Fig.1. Straight chain isomer was predominant with increasing carbon atoms. Beside these aliphatic carboxylic acids, we also found aromatic carboxylic acids.

From these results, carboxylic acids analyzed were apparently extraterrestrial in origin and not from comtaminants. Results of

4—2

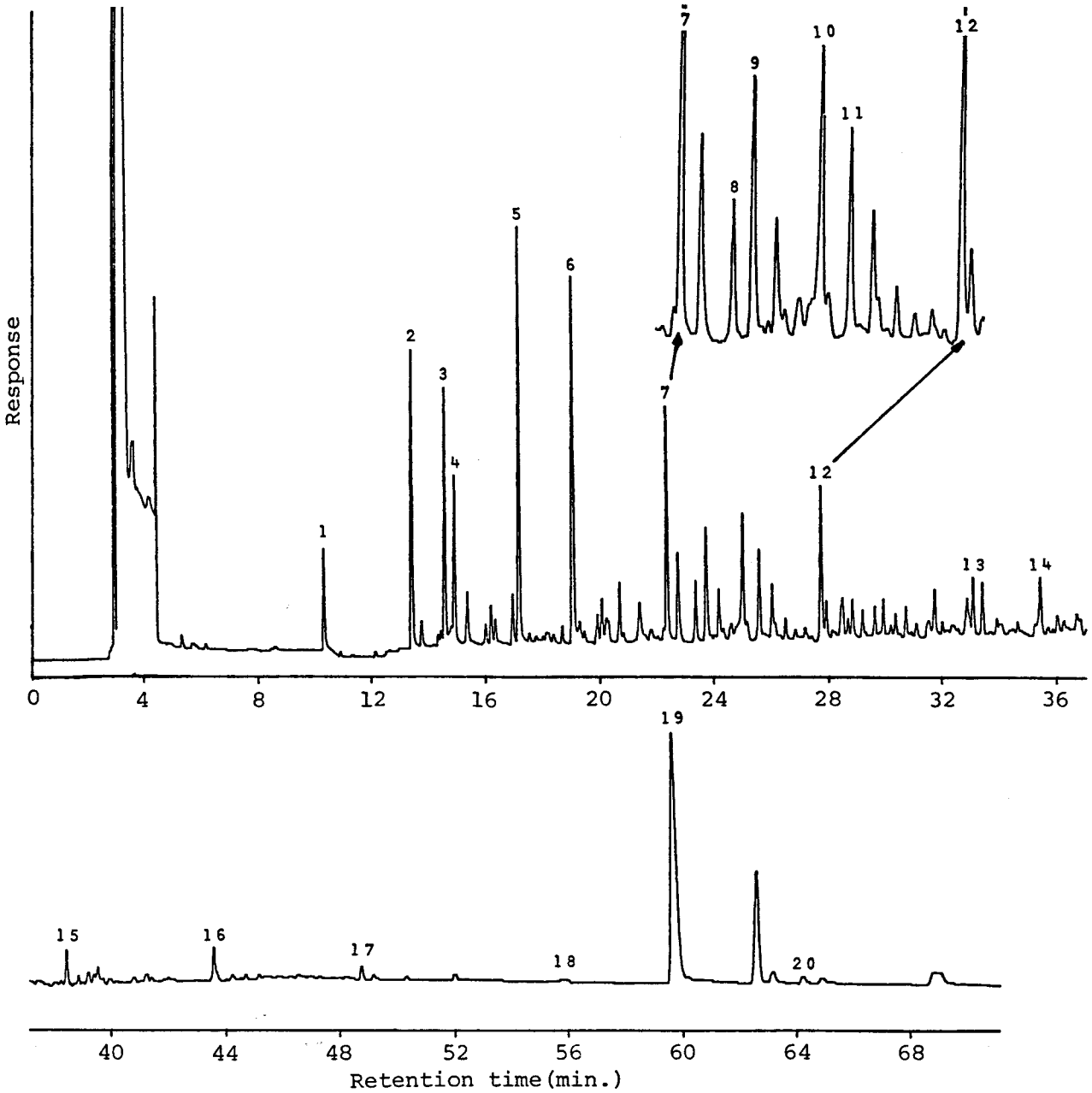

Fig.1 Gaschromatogram of monocarboxylic acids

Peak No., 1. acetic acid, 2. propionic acid, 3. 2-methyl propionic acid, 4. 2,2-dimethyl propionic acid, 5. butanoic acid, 6. 3-methyl butanoic acid, 7. pentanoic acid, 8. 2-ethyl butanoic acid, 9. 2-methyl pentanoic acid, 10. 3-methyl pentanoic acid, 11. 4-methyl pentanoic acid, 12. hexanoic acid, 13. heptanoic acid, 14. phenol, 15. octanoic acid, 16. nonanoic acid, 17. decanoic acid, 18. undecanoic acid, 19. benzoic acid, 20. dodecanoic acid.

Chromatographic conditions: Shimazu GC-8A(FID) with FS-WCOT capillary column (0.25mm i.d.x50m) with FFAP chemical bonded. Temperature programmed at 2°C/min. from 90-180°C

the present study will be further discssed in comparison with other organic compounds found from this YAMATO carbonaceous chondrite, and other studies on carboxylic acids[2,3].

Table Quantities of n-alkyl monocarboxylic acids(/g)

carbon number	abundance(ng)	carbon number	abundance(ng)
2	650	8	90
3	1100	9	130
4	1200	10	50
5	720	11	10
6	430	12	70
7	150		

Referrence

1) A.Shimoyama, K.Harada and K.Yanai, Chemistry Letters, 1183, (1985)
2) G.U.Yuen and K.A.Kvenvolden, Nature, 301, 246(1973)
3) J.G.Lawless and G.U.Yuen, Nature, 396, 282(1979)

5—1

PYROLYTIC STUDIES ON MAJOR CARBONACEOUS MATTER IN CARBONACEOUS CHONDRITES Y-791198, Y-791717, Y-793321, AND B-7904

Murae, T., Masuda, A., and Takahashi, T.
Department of Chemistry, Faculty of Science, University of Tokyo, Bunkyo-ku, Tokyo 113

Major carbonaceous matter in four Antarctic carbonaceous chondrites Y-791198 (C2), Y-791717 (C3), Y-793321 (C2), and B-7904 (C2) was examined by means of pyrolysis-gas chromatography. Partial mineral dissolution by treatment with HCl and/or HF was carried out on two Antarctic carbonaceous chondrites Y-791717 (C3), ALH-77307 (C3) and a carbonaceous chondrite Allende (C3) for further clarification of major carbonaceous matter in the carbonaceous chondrites.

No change was observed in the pyrograms at 740 ^{o}C for Y-74662 (C2) before and after extraction with benzene-methanol (2:1) (Fig. 1). This fact suggests that the components in the pyrograms were obtained by the thermal degradation of major carbonaceous polymer in the meteorite.

The pyrogram at 740 ^{o}C for Y-791198 (C2) was almost identical in the chromatographic pattern with that for Y-74662 (C2). The pyrograms at 740 ^{o}C for Y-793321 (C2), Y-791717 (C3), and B-7904 (C2) were closely similar to that of ALH-77307(C3) in the pattern (Figs. 2 and 3 B). A large aromatic structure (small size monolayer of graphite) bearing edge defects has been proposed for major carbonaceous matter in carbonaceous chondrite by the authors. On the basis of the proposed structure and of the amount of carbon contained and the amount of naphthalene yielded on pyrolysis, it was suggested that the structures and amount of the edge defects were almost the same for the carbonaceous matter in Murchison (C2), Allende (C3), Y-74662 (C2), and Y-791198 (C2). The similarity of the edge defects of the carbonaceous matter in B-7904, ALH-77307, and Y-791717 was also suggested.

Pyrograms for the residue which was obatained on partial mineral dissolution with conc. HCl and then HF (ca. 8%) are shown in Figures 3, 4, and 5. Most of carbon originally contained in the chondrites was found in the partially mineral dissolved residues (Table 1). The pyrograms for the residues show that 1) the structure of major carbonaceous matter in the chondrites was not affected seriously by HCl treatment: 2) differences of relative intensity of the peaks in the pyrograms before and after the HCl treatment were caused by the change of coexisting minerals which were related with the formation of secondary products on pyrolysis: 3) although HF treatment made a considerable change in the pyrogram for Allende (Fig. 5 A), no remarkable change was observed in that for ALH-77307 on the same treatment (Fig. 4 A). This fact is considered to reflect the amount and nature of edge defects of the major carbonaceous matter in the carbonaceous chondrites.

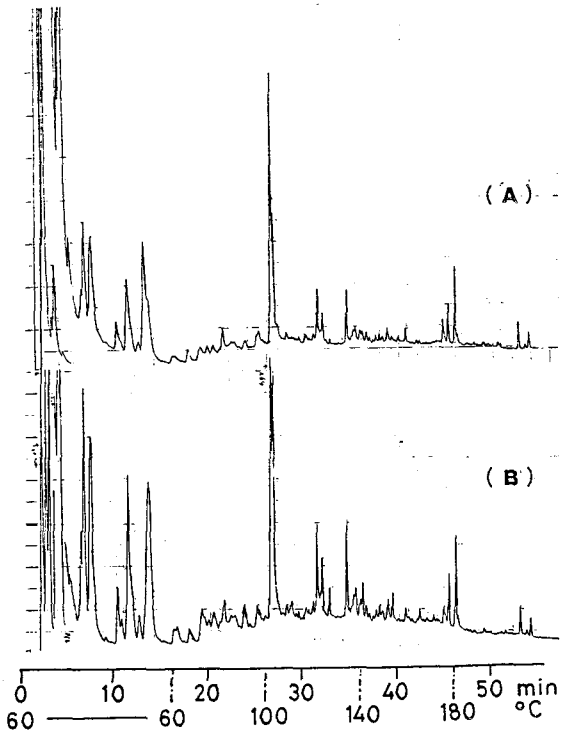

Fig. 1 Pyrograms for Y-74662
A: 3 mg, after extraction
B: 6 mg, before extraction

Colum: OV-101, 25m x 0.25mm i.d.
Detector: FID, attenuation 1, range 16
Pyrolized for 3 sec at 740 °C

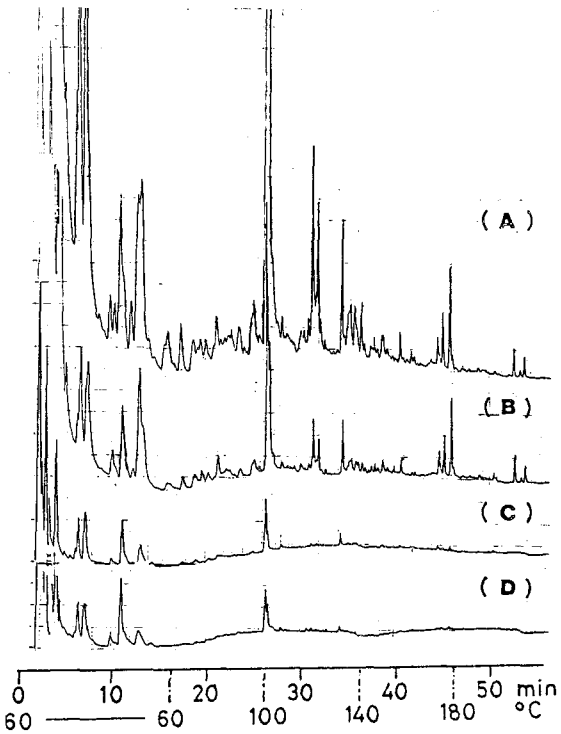

Fig. 2 Pyrograms for
A:5 mg of Y-791198
B:3 mg of Y-74662
C:6 mg of B-7904
D:15 mg of Y-793321
Conditions are the same as those for Fig. 1

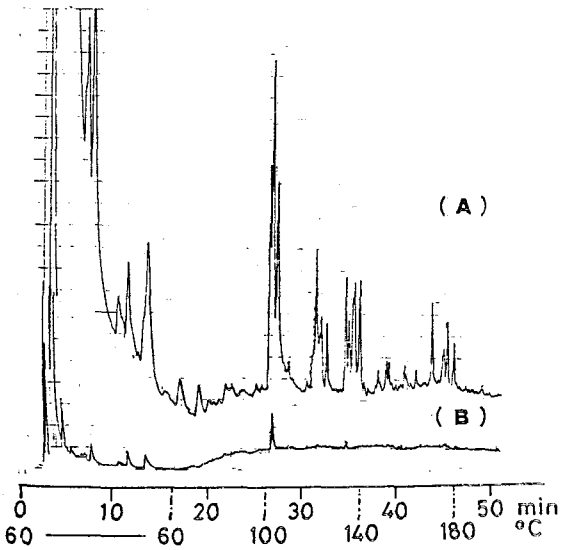

⇐

Fig. 3 Pyrograms for Y-791717
A: 9.2 mg, treated with HCl
B: 15.8 mg, before treatment
Conditions are the same as those for Fig. 1 excepting range (8) for A.

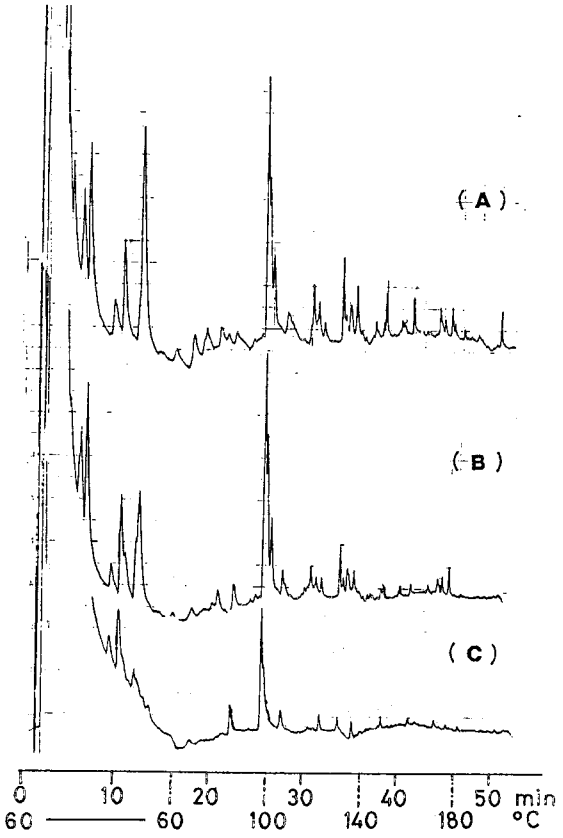

Fig. 4 Pyrograms for ALH-77307
A: 1.79 mg, HCl & HF treated
B: 6.57 mg, HCl treated
C: 15.1 mg, before treatment
Conditions are the same as those for Fig. 3 A.

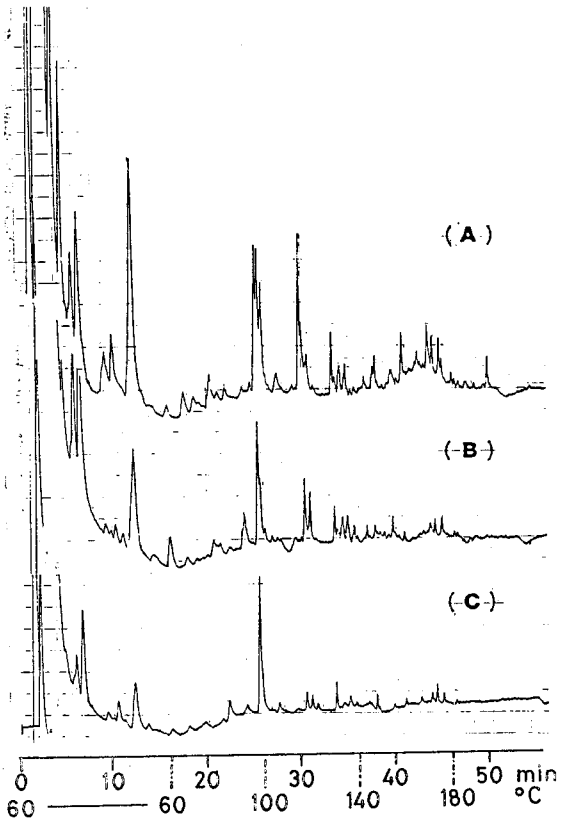

Fig. 5 Pyrograms for Allende
A: 2.28 mg, HCl & HF treated
B: 3.26 mg, HCl treated
C: 9.18 mg, before treatment
Conditions are the same as those for Fig. 4.

Table 1. Amount of the meteorite used for mineral dissolution and of recovered residue after treatment with conc. HCl and then HF (ca. 8%). Carbon content of each sample is shown in parentheses.

	Used for HCl treatment	Treated with HCl recovered	Treated with HCl used for HF	Treated with HF recovered
Allende	570 mg (0.23 %)	285 mg (0.51 %)	250 mg	56.0 mg (1.46 %)
ALH-77307	144 mg (0.74 %)	69.3 mg (1.17 %)	41.1 mg	13.0 mg
Y-791717	152 mg (0.12 %)	64.2 mg (0.22 %)		

KINETICS OF FE/MG EXCHANGE BETWEEN CHONDRULE AND MATRIX AND THE IMPLICATIONS FOR METAMORPHISM OF TYPE 3 ORDINARY CHONDRITES.

Satoshi MATSUNAMI: Geological Institute, University of Tokyo.

Several authors have suggested that composition of matrix olivine and texture of matrix in type 3 ordinary chondrites would have been affected remarkably by thermal metamorphism (Huss et al. 1981; Sears et al. 1980). It is shown that matrix olivine composition has sufficient sensitivity to thermal history of type 3 ordinary chondrites, compared to rare gas, carbon, water, and volatile trace elements contents, $\delta^{18}O$, and TLS. Although many heating experiments of primitive chondrites have been conducted to clarify compositional and mineralogical changes due to thermal metamorphism quantitatively (e.g., Lipschutz and coworkers 1975-), kinetics of Fe/Mg exchange process between chondrules and matrix has never been studied. Recently, Matsumami, Nagahara and Kushiro (1985) have conducted an experimental study on textural and compositional variation of matrix materials in primitive type 3 ordinary chondrites and have shown experimentally that matrix olivine composition may reflect small differences in their metamorphic history. In the present paper, the author reports the rate law of compositional change of matrix olivine associated with Fe/Mg exchange between magnesian chondrules and FeO-rich opaque matrix. From the kinetic data, he discusses the nature of metamorphism and the origin of type 3 ordinary chondrites.

-- Experiments and Results -- Details of experimental method have already been mentioned in Matsunami et al. (1985). In addition to their results, three additional experiments at 950°C were carried out and added to this analysis of experimental results. It is shown that rate of compositional change of matrix olivine is expressed by the following Arrhenius relation for matrix olivine grains less than 6 micron in diameter (Fig. 1):

$$|\Delta Fa/\Delta t| = k0*\exp(-Ea/RT),$$

where Fa is average Fayalite content of matrix olivine, t is time (hour), $k0=2.52*10^6$ (Fa mole %/hr), activation energy Ea=39.4 kcal/mol, R is gas constant and T is temperature (°K). Activation energy of exchange process is about 2/3*(Ea of interdiffusion coefficient of Fe and Mg in olivine lattice: Misener, 1974), suggesting that grain boundary diffusion process through micron-sized materials in opaque matrix would be important in Fe/Mg exchange between magnesian chondrule and ferrous matrix olivine.

-- Implications -- Fe/Mg exchange reaction between chondrules and matrix in type 3 ordinary chondrites is experimentally shown to be rapid sufficiently. It is suggested that Fe/Mg exchange between chondrule and matrix is one of good indicators of metamorphism of type 3 chondrites. Kinetics of

Fe/Mg exchange shows remarkable dependences on grain size (or grain size distribution) of matrix olivine (Fig. 2). This effect must be taken into account to interpret matrix olivine composition of type 3 ordinary chondrites.

The exchange reaction is so rapid that matrix olivine composition might have been easily affected in unmetamorphosed type 3 ordinary chondrites during various formation processes in the nebular and planetary settings. For example, fine-grained chondrule rim material surrounding a chondrule might have easily exchanged Fe and Mg with the chondrule interior during the sedimentation stage to the mid-plane of the PSN in the cooling nebular gas after chondrule formation. After accretion of chondritic materials to planetesimals (probably due to gravitational instabilities of dust-gas layer), composition of matrix materials would have been altered due to metamorphic heating and/or impact heating. To evaluate this possibility quantitatively, a computer simulation on metamorphic equilibration of matrix olivine with chondrule olivine associated with the cooling of chondritic impact ejecta on the meteorite parent body has been developed to understand relationships among ejecta thickness, accretion temperature, and fraction of ejecta which preserve relatively primitive composition of matrix olivine (Fa40<). Effects of porosity reduction due to sintering of hot impact ejecta to thermal conduction and rate of Fe/Mg exchange between chondrule and matrix olivine have been taken into account to calculations. From results of calculation, in the case where velocity and size of projectile are sufficiently large, it is suggested that metamorphic equilibration during cooling of chondritic impact ejecta would have sufficiently caused chemical and petrological changes such as those observed in the transition from petrologic subtype 3.0 to 4 in the central part of hot ejecta thicker than several hundred meters at the crater rim.

References:

Huss,G.R., Keil,K. and Taylor,G.J. (1981): G.C.A.,45,33-51; Matsunami,S., Nagahara, H. and Kushiro,I. (1985): In 'Papers presented to the Tenth Symposium on Antarctic Meteorites',pp.61-63; Misener,D.J. (1974): In 'Geochemical Transport and Kinetics',(ed. A.W.Hofmann),Carnegie Inst. Wash. Publ.634, pp.117-129; Sears,D.W., Grossman,J.N., Melcher,C.L. and Mills,A.A. (1980): Nature,287,791-795.

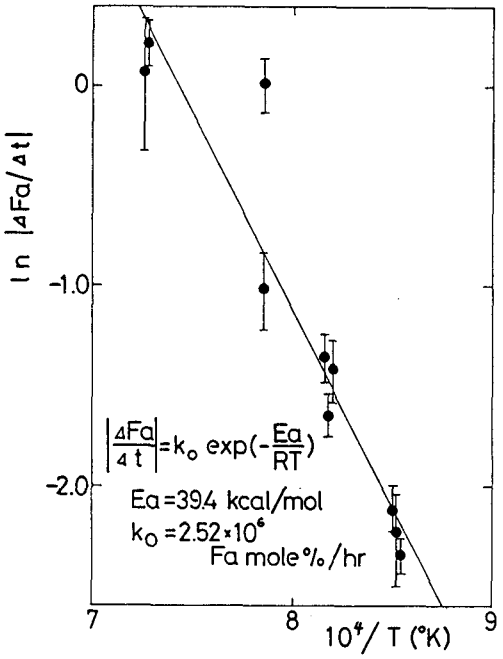

Figure 1. Arrhenius plot for the rate of compositional change of matrix olivine due to Fe/Mg exchange between magnesian chondrule and ferrous matrix olivine in experimentally heated ALH-77214 chondrite (L 3.4).

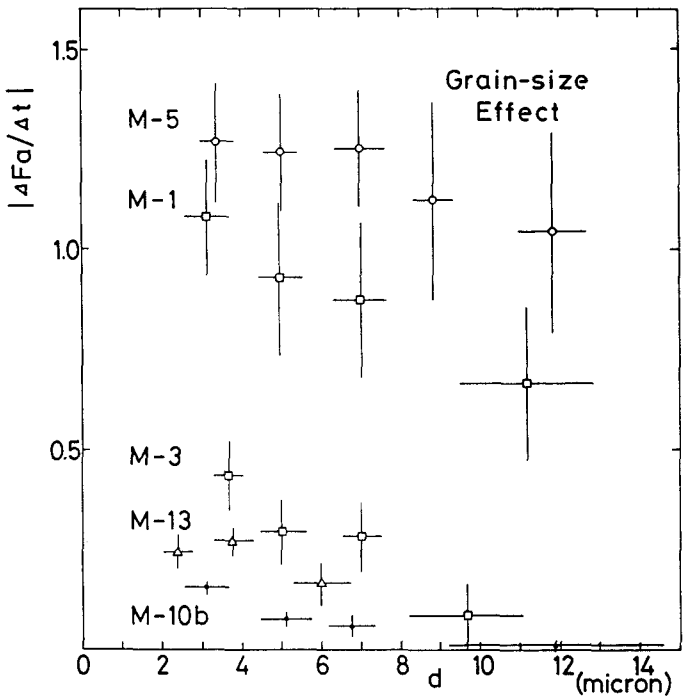

Figure 2. Grain size effect to the rate of compositional change of matrix olivine due to Fe/Mg exchange between chondrule and matrix olivine in experimentally heated ALH-77214 chondrite (L 3.4).

7—1

FORMATION PROCESSES OF MATRIX IRON-RICH OLIVINE IN ALH-764 (LL 3.3), Y-790448 (LL 3) AND KRYMKA (L 3.0) CHONDRITES.

Satoshi MATSUNAMI: Geological Institute, University of Tokyo.

The fine-grained opaque matrix in highly unequilibrated ordinary chondrites is characterized by wide variability of chemical composition of Fe-rich matrix olivine, ranging Fa1 to Fa95 (1,2,3). This paper focusses on formation processes of Fe-rich olivine in opaque matrix, and reports the occurrences and chemical composition of micron-sized Fe-rich olivine and olivine--like materials to discuss their formation processes.

Representative occurrences suggesting their formation processes observed in opaque matrix materials of chondrite samples studied here (ALH-764, Y-790448 and Krymka) are classified into the following four types: (i) Fe-rich olivine or Al-bearing olivine-like material on enstatite, (ii) Al-bearing olivine-like material on sodic plagioclase-like Si,Al-rich material, (iii) Fe-rich olivine on fine-grained aggregate of Fe-Ni metals, and (iv) Fe-rich olivine on magnesian olivine. As already suggested by several authors (2,3,4,5,6,7,8,9), these observations strongly suggest that the reaction of mixtures composed of varing proprotions of micron-sized condensates such as enstatite, silica, albite and/or magnesian olivine with metallic iron or iron-rich gas to form iron-rich olivine would have taken place in the cooling gas of the primordial solar nebula. Since Fe-rich olivine and metallic Fe-Ni is a common assemblage in opaque matrix materials of highly primitive type 3 chondrites, PO2 condition would have been between iron-wustite buffer and iron-quartz-fayalite buffer, indicating that Fe-rich olivine would have formed under relatively high oxygen fugacity condition.

To determine whether the formation reactions are subsolidus ones or not, contents of minor element in Fe-rich olivine, Al-bearing olivine-like material, matrix pyroxene, and Si,Al-rich sodic plagioclase-like material in the matrices are studied in detail. Particularly, MnO contents of matrix Fe-rich olivine and Al-bearing olivine-like material show a strong positive correlation with their FeO contents and that their Mn/Fe ratios are nearly that of solar composition gas (10) (Figs. A, B and C). Since MnO contents of enstatite, or Si,Al-rich sodic plagioclase-like material is commonly less than 0.8 wt % and Mn content is very low in metallic Fe-Ni grains (<0.1 wt %), this characteristic feature can not be explained solely by the subsolidus reactions of mixtures (including selective oxidation of iron from Fe-Ni metal to form FeO component of Fe-rich olivine) with Fe-Ni metal (kamacite or taenite). A possible mechanism which would explain MnO-FeO positive correlation of Fe-rich olivine component is probably the reaction of precursor mixtures with gaseous Fe and Mn at relatively high oxygen

fugacity. Since occurrence (iii) is not so common and FeO contents of matrix pyroxene and Si,Al-rich material are low, it is suggested that Fe in matrix Fe-rich olivine component would have been mainly derived from gaseous iron in the nebular gas.

References: (1) Huss,G.R., Keil,K. and Taylor,G.J. (1981): G.C.A.,45,33-51; (2) Nagahara,H. (1984): G.C.A.,48,2581-2595; (3) Matsunami,S. (1984): Unpubl. Master Thesis; (4) Grossman,L. and Larimer,J.W. (1974), Rev.Geophys Space Phys.,12,71-101.; (5) Ikeda,Y., Kimura,M., Mori,H. and Takeda,H. (1981): Mem.Natl. Inst.Polar Res.Spec.Issue,20,124-144; (6) Housley,R.M. and Cirlin,E.H. (1982): Meteoritics,17,229; (7) Housley,R.M. and Cirlin,E.H. (1983): In'Chondrules and Their Origins' (ed. E.A. King),pp.145-161,Lunar Planetary Institute; (8) Nagahara,H. and Kushiro,I. (1984): Lunar Planet. Sci.,XV,583-584; (9) Kornacki,A.S. and Wood,J.A. (1984): G.C.A.,48,1663-1676; (10) Anders,E. and Ebihara,M. (1982): G.C.A.,46,2362-2380.

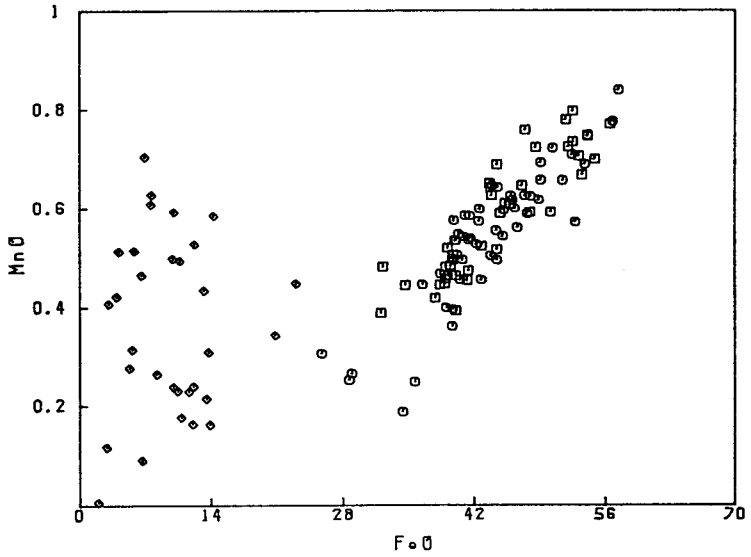

Figure A.

ALH-764 (LL 3.3)

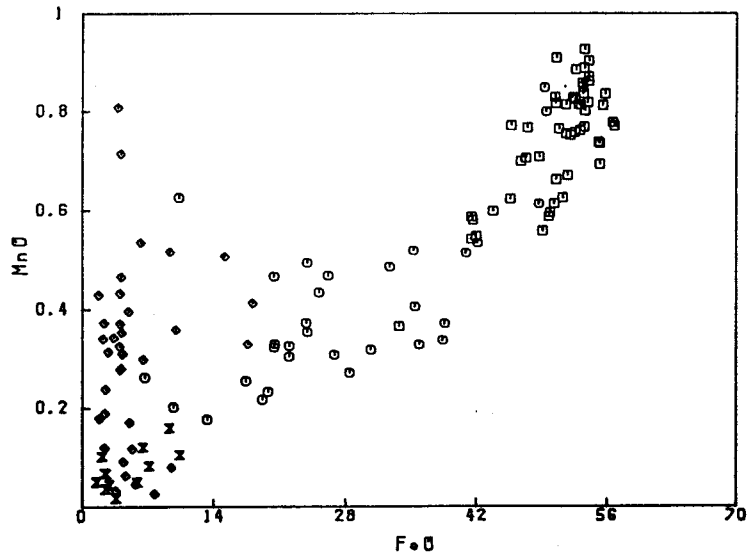

Figure B.

Y-790448 (LL 3)

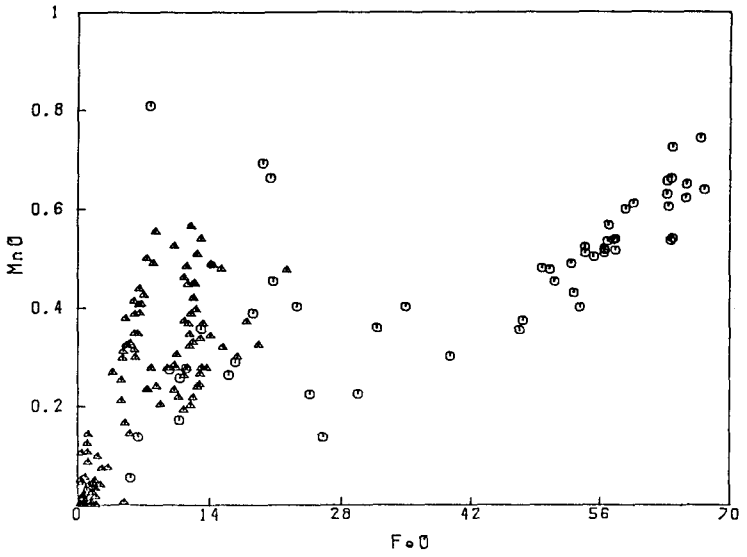

Figure C.

Krymka (L 3.0)

Figure A. FeO vs MnO variations in matrix olivine (⊙), matrix Al-bearing olivine-like material (⊡), and matrix pyroxene (◈) of ALH-764(LL 3.3)chondrite.

Figure B. FeO vs MnO variations in matrix olivine (⊙), matrix Al-bearing olivine-like material (⊡), matrix pyroxene (◈), and matrix Si,Al-rich material (⧖) of Y - 790448(LL 3) chondrite.

Figure C. FeO vs MnO variations in matrix olivine (⊙), and chondrule olivine (△) of the Krymka L 3.0 chondrite.

DETERMINATION OF PHYLLO-SILICATES IN CARBONACEOUS CHONDRITES

Miúra, Y. Department of Mineralogical Sciences and Geology, Faculty of Science, Yamaguchi University, Yoshida, Yamaguchi, 753.

The phyllo-silicate minerals in the carbonaceous chondrite are determined mineralogically in this study, by applying the definition of the terrestrial phyllo-silicates which is recently applied into the chlorine-bearing serpentines from Precambrian ultramafic body of dunite [1, 2].

The terrestrial serpentine-group minerals with minor Fe content are classified as lizardite (OC/TC=1.70~1.95), chrysotile (OC/TC=1.52~1.70) and antigorite (~1.52) by EPMA and TEM data, where OC and TC means octahedral and tetrahedral cations, respectively. Thus, the lizardite with and without chlorine is the first product from olivine (OC/TC=1.95~2.00) under hydrous condition [2]. The serpentine minerals in the Allende and ALH-77307,85-1 chondrites are classified by the above definition as follows (cf. Fig. 1):

1. Chlorine-bearing antigorite (OC/TC=1.31) are observed in the Allende chondrite, where the chlorine is assumed to be existed into crystal structure and/or grain boundary if the TEM data of the terrestrial chlorine-bearing serpentines are applied [2].
2. Ordinary aqueous serpentine (but with higher Fe or Si content in the meteorites) are determined as lizardite (1.88), chrysotile (1.53) and antigorite (1.40) in the ALH-77307,85-1 chondrite.
3. The other phyllo-silicates of smectite (OC/TC=0.53~0.64) are found in the Allende chondrite.

The detail study of the formation process will be discussed in the next paper.

The author thanks Mr. M. Hironaka, undergraduate student of Yamaguchi University, for his help of the calculation of EPMA data.

REFERENCES:

[1] Miúra, Y., Rucklidge, J. and Nord,G.(1981): Contrib. Mineral. Petrol, 76, 17-23.
[2] Miúra, Y. et al.(1986): Technical report of the Fundamental Scientific Research of 1985. pp. 4.

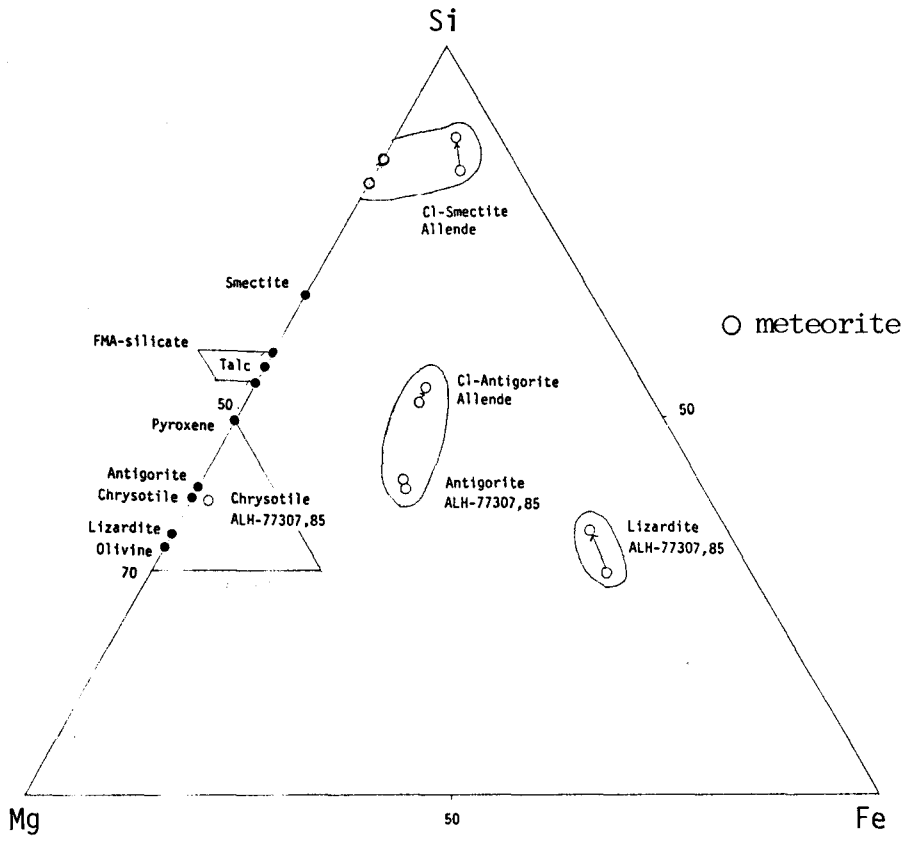

Fig. 1. Phyllo-silicates in carbonaceous chondrites, together with IDPs and terrestrial data.

Thermo-Remanent Magnetization of Fe-Ni Alloy

Kan-ichi Momose* and Hiroyuki Nagai**
Department of Geology* and Department of Physics**, Faculty of Science,
Shinshu University, Matsumoto, 390 Japan

The Fe-Ni alloy is the original substance of the remanent magnetization (RM) of meteorites. Some of rock-forming minerals contain Fe-Ni alloys which transform martensitically from fcc phase to bcc phase. In order to deduce the cosmic paleomagnetic field from RM of meteorites, it is very important to know whether or not the RM obtained in the temperature range from Curie temperature (T_c) to room temperature (T_0) preserve in bcc phase after martensitic transformation. The martensitic transformation occurs by cooling below the martensitic transform point (T_{Ms}), rolling or grinding.

From the previous experiments of 20at%~29at%Ni-Fe alloys, the RM obtained by cooling from T_c to T_0 are phenomenologically resemble in each other in magnetic behaviour as follows:

(i) TRM obtained by cooling at 77K in geomagnetic field is stable, while TRM obtained by cooling in zero magnetic field is broken.

(ii) The direction and the intensity of TRM obtained by cooling at 77K in geomagnetic field are unchanged by 2nd cooling in geomagnetic and zero magnetic fields.

The present work is to investigate the magnetic properties of 5at%~15at% Ni-Fe alloys by the same method for the previous alloys, where the martensitic transformation occurs above T_0. The experimental results are shown in Figs.1-3 and in Table I. The Mössbauer spectra of ^{57}Fe show the existence of small amount of fcc phase at T_0 in all samples.

As shown in figures the directions of RM of 5at% and 15at%Ni-Fe alloys are nearly same. The direction of RM of 10at%Ni-Fe alloy changes after cooling at 77K in zero magnetic field ($B_0 \rightarrow B_1$ in Fig.2). The intensity of RM after cooling in magnetic field is stable, while it decreases after 1st cooling at 77K in zero magnetic field.

Finally, the intensities of TRM (bcc phase) of 5at%~15at%Ni-Fe alloys decrease by cooling in zero magnetic field. This decrease may be due to the martensitic transformation from fcc phase to bcc phase.

Table I. TRM of Fe-Ni alloys (powder) after cooling at 77K in zero and geomagnetic fields.

Samples	Heat treatment	D	I	J ($\times 10^{-3}$ emu/g)	J/J_0
5 at%Ni-Fe	(A_0)TRM (800°C,10^{-3}Pa) bcc	-6.02°	47.79°	18.422	J_0
	(A_1)cooled (A_0) at 77K in parallel to geomag. field	-6.31°	49.00°	19.045	1.03
	(A_2)2nd TRM (920°C,10^{-3}Pa)bcc	-8.56°	58.59°	23.161	2nd J_0
	(A_3)cooled (A_2) at 77K in zero magnetic field	-4.98°	58.91°	20.034	0.865
10 at%Ni-Fe	(B_0)TRM (700°C,10^{-3}Pa) bcc	15.94°	57.48°	5.725	J_0
	(B_1)cooled (B_0) at 77K in zero magnetic field	37.47°	65.77°	3.263	0.570
	(B_2)2nd TRM (700°C,10^{-3}Pa) bcc	14.87°	65.75°	5.711	2nd J_0
	(B_3)cooled (B_2) at 77K in parallel to geomag. field	25.60°	68.91°	5.237	0.917
15 at%Ni-Fe	(C_0)TRM (700°C,10^{-3}Pa) bcc	3.10°	56.37°	9.670	J_0
	(C_1)cooled (C_0) at 77K in parallel to geomag. field	3.98°	57.00°	9.369	0.969
	(C_2)cooled (C_1) at 77K in zero magnetic field	4.30°	57.75°	8.117	0.840
	(C_3)2nd TRM (700°C,10^{-3}Pa) bcc	4.05°	55.41°	7.652	2nd J_0
	(C_4)cooled (C_3) at 77K in zero magnetic field	8.97°	53.68°	5.356	0.699

* D = declination, I = inclination, J = intensity of magnetization, J_0 = original intensity

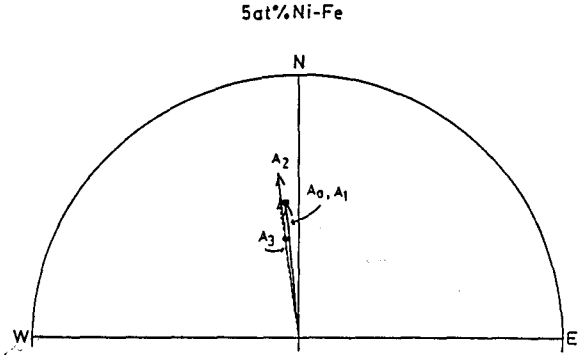

Fig.1

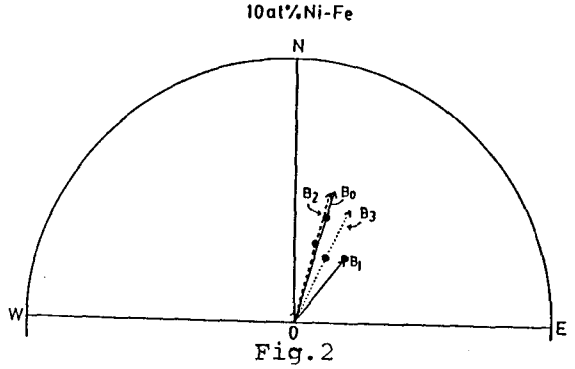

Fig.2

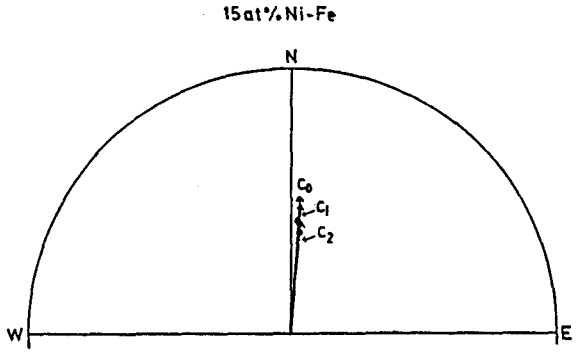

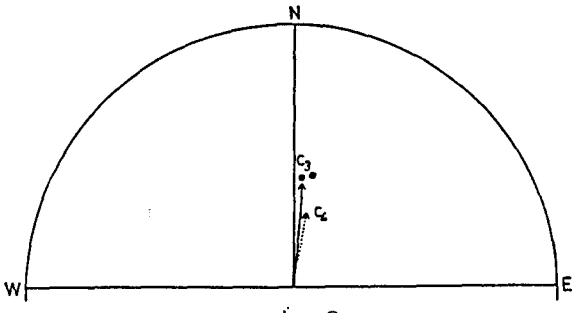

Fig.3

Special Session: Lunar Meteorites

Tuesday, March 25, 1986

1300 - 1700

Four lunar meteorites including new specimen of Yamato-82193, preliminary examination, curation and allocation for consortium studies

Yanai K. Kojima H. and Ikadai S.
National Institute of Polar Research, 9-10, Kaga 1-chome Itabashi-ku, Tokyo 173

ALHA-81005, Yamato-791197 and Yamato-82192 meteorites had been reported as lunar meteorites, an anorthositic regolith breccia(1, 2, 3, 4, 5). Yamato-82193 and was identified as a new specimen of lunar meteorite. This specimen can be classified as an anorthositic regolith breccia. This new specimen was collected from the closed area to that of the Yamato-82192 on January 13, 1983. This specimen likely represents an individual meteorite, 37.04 grams and measured 3.4 x 3.0 x 2.2 centimeters. The original volume of the specimen was 9.47 cubic centimeters and specific gravity is 2.85 g/cm3. The meteorite corted with pale yellowish-tan color. Very thin fusion crust is partly recognized on the original surfaces and most of fusion crust had been already abrated. Fresh surface and interior show light-grey pale violet color. The interior consists many of angular clasts which range from one millimeter to several millimeters across. These clasts are dark grey to white in color, set in a pale grey-light greyish brown matrix.

Petrographically Yamato-82193 is a polymict microbreccia containing kinds of clasts. Few types of clast were observed in thin section, polyminerallic, monominerallic and melted clasts. Most larger clasts are polyminerallic and composed of calcic plagioclase(anorthite), olivine and pyroxene. The small clasts are mineral fragments dominantly of calcic plagioclase with minor pyroxene and olivine. A lot of melt clasts are observed in the section. The clasts show a variety of texture including troctolitic, gabrroic, basaltic and shock-melted glassy clasts. The texture of the specimen is similar to those of eucrites and howardites, but the specimen are much more feldspathic.

Yamato-82193 meteorite appears to be a regolith breccia with an abundance feldspathic clasts set in light-greyish brown matrix. From its texture and kinds of clasts, Yamato-82193 meteorite resembles the lunar regolith breccia of 60019, however this meteorite does not contains any swirly brown glass. Feldspar compositions range An88.3 to 97.8 with most composition ranging from 93.3 to 97.8. Pyroxenes and olivines show also variable compositions. The composition range in pyroxenes is En30.1-75.2, Fs16.2-47.0, Wo3.1-38.0. Olivines are Fo48.7-81.1. Yamato-82193 is similar to Yamato-82192 in most respect, petrography, chemistry, textures and kinds of clast, but Yamato-82193 is slight different from Yamato-971197 in some respects matrix and others.

Table 1 shows some basic informations of all lunar meteorites, in which contain type, original weights, demensions, volumes, densities, chemical compositions of the few minerals, metal and troilite, and magnetic property, especially NRM. These four meteorites belong to anorthositic regolith breccia for their mineral assemblages compositions, textures and some physical properties. However, there are some differences among those meteorites, especially Yamato-82192 and 82193 free from metal or very rare and their NRM are extremely weak. Yamato-82192 and 82193 have much more troilite than Yamato-791197. ALHA81005 free from troilite (6). It seems that two Yamato-82 lunar meteorites are pair and were brought to earth by another impact onto the Moon's surface from those of Yamato-79 and ALHA81 lunar meteorites.

References: (1) Bogard, D. et al. 1983 Geophys. Res. Lett. 10, No.9 (Special ALHA81005 issue). (2) Yanai, K. and Kojima, H. (1984a) Abstr. 9th Sympo. 42-43, Tokyo. (3) Yanai, K. and Kojima, K. (1984b) Mem. Natl Inst. Polar Res., Spec. Issue 35. 18-34. (4) Yanai, K. and Kojima, K. (1985) Abstr. 10th Sympo. Antarctic Meteorites. NIPR, p. 87-89, Tokyo. (5) Yanai, K., Kojima, H. and Katsushima, H. (1984) 47th Annual Meeting. Meteoritical Soc., Albuquerque. p. 342. (6) Antarctic Meteorite newsletter vol.6, No.1.

Table 1. Some basic informations of the lunar meteorites

Name	Yamato-791197	Yamato-82192	Yamato-82193	ALHA81005
Find	Nov. 20, 1979	Jan. 13, 1983	Jan. 13, 1983	Jan. 18, 1982
Type	An. regolith br.	An. regolith br.	An. regolith br.	An. regolith br.
Weight(orig)	52.40g	36.67g	27.04g	31.4g
Dimension(cm)	4.5x4.2x2.8	4.3x3.3x2.3	3.4x3.0x2.2	3x2.5x3
Volume(cm3)	18.45	12.87	9.47	
Density(g/cm3)	2.840	2.849	2.855	
Olivine, %Fa	13.6-92.1	6.8-89.1	48.7-81.1	11-40
En	18.0-83.1	13.8-79.4	30.1-75.2	44-79
Pyroxene Fs	9.0-58.9	8.1-57.6	16.2-47.0	7-47
Wo	1.7-44.1	1.8-43.2	3.1-38.0	1-41
Plagioclase An	92.0-98.2	83.0-98.2	88.3-97.8	95-98
Fe-Ni Metal	common(5.8%Ni)	very rare(7.2%Ni)	absent(?)	1mm grain
Troilite	less	common	common	absent
magnetic property(NRM)	weak	extremely weak	extremely weak	

Table 2. Sample allocation of the Yamato-82192 (anorthositic regolith breccia)

No	P.I.Name	Bulk	clast	matrix	Remarks
374	L. Haskin	,141A 0.035g			thermoluminescence & tracks
397	M. Lipschutz	,52C 0.088g	,83C 0.011g		trace & ultratrace elements
398	L. McFadden	PTS ,53 0.164g			spectral reflectance
399	T. Fukuoka		,52B 0.029g ,83B 0.036g		major & trace elements
401	J. Laul	,141B 0.025g			major & trace elements
403	R. Ostertag	,50-1 PTS ,75 0.097g			petrology, especially shock feature INAA

408	K. Keil	,50-3 PTS			mineralogy-petrology
411	C. Koeberl	,72 0.191g			halogenes & trace elements
421	P. Warren	,71 0.169g	,52A 0.007g ,83B 0.004g		petrographic & INAA, PTS
430	H. Takeda	,50-6 PTS		,55D 0.053g	mineralogy, comparison
438	O. Eugster	,82 0.297g			terrestrial age
439	K. Nishiizumi	,73 0.295g			terrestrial age
448	N. Takaoka			,63C 0.097g	noble gas
449	N. Nakamura	,63A 0.092g ,74 0.111g			Rb-Sr, U-Th-Pb
A	I. Kushiro	finish			bulk composition
B	R. Clayton	finish			oxygen isotope
C	I. Kaneoka			,63D 0.090g	Ar-Ar age
D	K. Yanai				processing, whole
E	A. Masuda	,63B 0.092g ,141C 0.102g			Rb-Sr, Sm-Nd
F	T. Nagata	,55A 0.258g			magnetic properties

Table 3. Sample allocation of the Yamato-82193 (anorthositic regolith breccia)

No	P.I.Name	Bulk	clast	matrix	Remarks
399	T. Fukuoka		,112 0.008g	,110 0.026g ,111 0.026g	major & trace elements
403	R. Ostertag	,91-2 PTS			petrology
408	K. Keil	,91-3 PTS			mineralogy-petrology
430	H. Takeda	,91-4 PTS			mineralogy, comparison
438	O. Eugster	,100 0.326g			terrestrial age
439	K. Nishiizumi	,101 0.306g			terrestrial age
A	R. Clayton	0.02g			oxygen isotope
C	K. Yanai				processing

11—1

VOLATILE-RICH CLASTS FROM LUNAR METEORITE YAMATO-791197

A. Bischoff[1] and H. Palme[2].
[1]Institut für Mineralogie, Correnssstr. 24, 44 Münster, F. R. of Germany;
[2]Max-Planck-Institut für Chemie, Saarstr.23, 65 Mainz, F. R. of Germany.

The Antarctic meteorite, Allan Hills 81005, was recognized as the first meteorite of lunar origin and described as a lunar highland regolith sample ejected by an impact from the moon (Ostertag et al., 1985; Warren and Kallemeyn, 1985).
Meanwhile three additional Antarctic meteorites (Y-791197, Y-82192, Y-82193) were found to be of lunar origin. Y-791197 is a polymict regolith breccia (Bischoff and Stöffler, 1985) similar to ALHA81005; however, distinct chemical differences are obvious concerning the abundances of volatile elements (Ostertag et al., 1985; Kaczaral et al, 1985).
Ostertag et al. (1985) reported high concentrations of the volatile elements Ga and Zn compared to ALHA81005 and other lunar anorthothitic breccias. Kaczaral et al. (1985) found similar enrichments in these and other more volatile elements and suggested that the trace element contents in Y-791197 resemble those in Apollo 66095 ("Rusty Rock"), a unique sample rich in condensed lunar volcanic exhalation.
By following the Ga and Zn activity of neutron-irradiated samples of Y-791179 we have separated two Ga- and Zn-rich clasts from the bulk sample (59.3 mg). The concentrations of some major and trace elements for these clasts (together 4.1 mg) are listed in Tab. 1. The Ga and Zn concentrations are higher than in any other lunar sample. Compared to ALHA81005 Ga is enriched by a factor of 20.1 and Zn by 16.3. In addition these clasts show remarkable enrichments in Br and Sb, compared to other lunar highland rocks. The bulk chemistry of the clasts is not too different from the composition of the mayor fraction of the meteorite, except for two times higher contents of REE and other incompatible elements (U, K).
The high values of Zn and Ga agree well with those obtained by Kaczaral et al. (1985). However, we did not find the extremely high concentration of Au observed by these authors. The Ni/Au ratio of our separate is within the range of lunar highland rocks of this type.
After determination of the bulk chemistry from one fragment a thin section was made for petrographic studies.
The fragment itself is a polymict breccia with abundant interstitial melts and was lithified by shock in the regolith (Bischoff et al., 1983). The sample is extremely fine-grained with rounded (partly digested) clasts. Mainly mineral clasts were found; only some clasts are granulites. Additionally, some devitrified glass spheres and a chondrule-like object were observed. Interestingly, at least one half of all fragments >30 µm are mafic mineral clasts. A SEM study revealed that this sample contains abundant fayalite next to hedenbergite and an SiO_2-phase. This paragenesis was observed in several samples from the Luna 24 mission (Ma et al., 1977; Papike and Vaniman, 1977). By systematically searching for Zn and Ga we detected a Zn-sulfide ((Fe,Zn)S) and an unidentified Ga-rich phase (Tab. 2). In addition, elemental Ge (up to 1.85 wt%) was analyzed within metals (Tab. 3).
We believe that the high content of volatile elements is a result of processes occurring on the lunar surface and is not caused by terrestrial contamination. Ge-rich metal separates were found in Apollo 14 rocks (14306, 14258; Ganapathy et al. (1974)) and high amounts of Zn and other

volatile elements in the "Rusty Rock" Apollo 66095. Additionally, the fayalite-hedenbergite-SiO_2-paragenesis is a distinct component in Lunar 24-rocks (Ma et al., 1977; Papike and Vaniman, 1977). However, the observed paragenesis as well as the volatile element characteristic of these clasts from Y-791197 have never been described in other lunar samples. Unpublished analytical data from Luna 24 samples indicated the presence of relatively Zn- and Ga-rich phases. A bulk sample (Luna 24114.1-4.1) contained 91 ppm Zn, and an anorthite with 14.5 ppm Ga was measured. These results could provide clues on the formation location of these Ga- and Zn-rich materials.
Wether these enrichments of volatiles are due to volcanic exhalations or wether they merely represent local concentrations of relatively volatile elements present in the lunar highlands is presently not clear. One way to test this would be the analysis of lead isotopes. The possibility remains that the volatile-rich clasts may indicate a more volatile-rich lunar interior than presently thought.
These data demonstrate that the study of lunar meteorites may ultimately provide new evidence on the composition and evolution of the Moon, besides evidence that is available from the lunar samples returned by spacecraft.

References:

Bischoff A. and Stöffler D. (1985) Lunar Planet. Sci. XVI, 63-64.
Bischoff A. et al. (1983) Earth Planet. Sci. Lett. 66, 1-10.
Ganapathy R. et al. (1974) Proc. 5th. Lunar Conf., Geochim. Cosmochim. Acta, Vol. 2, 1659-1683.
Kaczaral P. W. et al. (1985) Submitted to "Proc. 10th. Symposium on Antarctic Meteorites".
Ma M.-S. et al. (1977) Mare Crisium: The View from Luna 24, Geochim. Cosmochim. Acta, Suppl. 9, 569-592.
Ostertag R. et al. (1985) Submitted to "Proc. 10th. Symposium on Antarctic Meteorites"
Palme H. et al. (1983) Geophys. Res. Lett. 10, 817-820.
Papike J. J. and Vaniman D. T. (1977) Mare Crisium: The View from Luna 24, Geochim. Cosmochim. Acta, Suppl. 9, 371-401.
Warren P. H. and Kallemeyn G. W. (1985) "10th Symposium on Antarctic Meteorites" (abstract), 90-92, National Institute of Polar Research.

Tab. 2: Zn-rich phases within the Ga- and Zn-rich aliquot. Data in wt%; n.d. = not detected; n.a. = not analyzed; normalized totals due to the small grain sizes; *) close to metals

S	34.4	31.5	27.3	22.6
Fe	30.4	51.8*	42.7*	47.7*
Ni	n.d.	n.a.	0.91	1.17
Zn	35.2	16.8	29.1	28.5
Total	100.0	100.1	100.01	99.97

Tab. 1: Concentrations of major, and trace elements in aliquots from Y-791197 and ALHA81005.

	Y-791197 59.3 mg Ostertag et al. (1985)		Y-791197 4.1 mg This work		ALHA81005 128 mg Palme et al. (1983)		Fragments ALHA81005
%		Error		Error		Error	
Ca	11.4	5	10.9	10	10.8	3	1.01
Fe	5.05	3	5.44	3	4.20	3	1.30
ppm							
Na	2410	3	2574	3	2250	3	1.14
K	290	5	595	10	230	5	2.59
Sc	16.5	3	19.3	3	9.24	3	2.01
Cr	1034	3	953	3	862	3	1.11
Co	16.9	3	37.2	3	20.2	3	1.84
Ni	100	15	239	20	186	5	1.28
Zn	50	20	361	5	18	20	20.1
Ga	9.87	5	45.7	5	2.8	5	16.3
Br			1.39	15			
Sb			0.11	40			
La	3.24	4	7.20	3	2.44	3	2.95
Ce	8.76	8	19.3	20	6.9	5	2.80
Sm	1.56	4	3.05	3	1.18	3	2.58
Eu	0.723	3	1.17	5	0.704	3	1.66
Ho	0.48	10	0.733	10	0.37	15	2.0
Yb	1.34	4	2.50	5	1.06	5	2.36
Lu	0.19	4	0.337	20	0.15	3	2.25
Hf	1.11	5	2.66	10	0.93	3	2.85
Au	0.0013	15	0.0022	45	0.0021	7	1.05
Th	0.43	15	1.75	20	0.35	8	5.0
U	0.14	15	0.219	35	0.103	15	2.06

Tab. 3: Metal analyses within the Ga- and Zn-rich fragment. Data in wt%; n.d. = not detected; most analyses normalized to 100%; 1-5: Ge-rich metals; 6: meteoritic component

	1	2	3	4	5	6
Fe	94.1	93.3	92.5	92.6	92.7	75.7
Co	1.40	1.01	0.95	0.93	0.84	1.31
Ni	4.2	3.9	5.1	5.0	4.7	23.0
Ge	1.73	1.85	1.44	1.39	1.74	n.d.
Total	101.43	100.06	99.99	99.92	99.98	100.01

GEOCHEMISTRY OF LUNAR METEORITE YAMATO-82192: COMPARISON WITH YAMATO-791197, ALHA81005, AND OTHER LUNAR SAMPLES

Paul H. Warren and Gregory W. Kallemeyn

Institute of Geophysics and Planetary Physics
University of California, Los Angeles, CA 90024, USA

Yanai and Kojima [1], who described Yamato-82192 petrographically, concluded from the overall mineralogy and texture, particularly the low MnO/FeO ratios of the mafic silicates, that this meteorite originated as a regolith breccia on the Earth's Moon. Our instrumental neutron activation analysis supports this conclusion. This meteorite appears nearly identical to Y-791197, which was recovered only about 80 km from Y-82192. Hence, these two samples may be a pair from a single meteorite shower. In fact, Y-82192 and Y-791197 are both so similar to ALHA81005, which is also a lunar regolith breccia [2], it seems possible that all three meteorites were brought to Earth by a single impact onto the Moon's surface.

Our data for 36 elements in bulk-rock sample Y82192,71, and for two small white clasts separated from the matrix, are shown in the Table. Some of these data are preliminary, as we have not quite completed gamma-ray counting of our samples. Parentheses around a datum indicate a relatively high uncertainty (up to 30%). For comparison, the Table also shows average literature data for Y791197 [3] and ALHA81005 [4], and new data for 14315, another unusual lunar regolith breccia [companion abstract by Jerde et al.]. For ALHA81005, a mass-weighted mean is shown, because all six analyses were based on the same technique (neutron activation). However, because different laboratories applied several different techniques for major elements (Na, Mg, Al, Ca, Ti, Cr and Fe) in Y791197, in these cases a simple average is used.

Regolith breccias such as Y82192, Y791197, and ALHA81005 form by mechanical consolidation of former lunar soil. Compositional data for these samples may be appropriately compared with corresponding data for actual lunar soils artificially brought to Earth [4]. Other than the recently-discovered lunar meteorites, the Luna 20 and Apollo 16 sites are generally considered to be our only sources of representative samples of lunar highlands soil. Apollo 11 and 12 soils are dominated by mare components. Apollo 14 soils not only contain a considerable mare component, they are also extraordinarily rich in incompatible elements such as Th and K [5]. Most Apollo 15 and 17 soils contain considerable mare components. However, 14315, a uniquely Al-rich and Ti-poor regolith breccia from Apollo 14, is comparatively low in KREEP and mare components; and 73141, the most Al-rich soil from Apollo 17 [4], appears to be nearly free of mare material. These samples are probably representative of appreciable fractions of the central near side highlands.

The Y82192 whole-rock Fe/Mn ratio (74.5, Table) is typical for a lunar regolith sample. As noted by Laul and Schmitt [6], Fe/Mn is nearly constant at 80 (± about 5) among all Apollo and Luna soils. The Y82192 Fe/Mn ratio is essentially identical with the Fe/Mn ratios of Y791197 and ALHA81005 (71.2 and 73.6, respectively), and distinctly higher than the Fe/Mn ratios for plagioclase-rich meteorites from parent bodies other than the Moon: eucrites, howardites, and "SNC" achondrites, all have Fe/Mn ratios close to 40 [4].

Despite pervasive mixing by great impacts, the ancient, nonmare lunar crust manifests considerable lateral heterogeneity [5]. The Apollo and Luna missions only sampled a tiny region near the center of the Moon's near side, encompassing just 4.7% of the lunar surface. Although exact sources of lunar meteorites may never be unambiguously determined, the majority are presumably not from the limited region sampled by the Apollo and Luna programs. Lunar

meteorites are therefore extremely valuable sources of information about lateral variations in the composition and petrology of the Moon's crust.

Incompatible element concentrations (Fig. 1; shown normalized to high-K KREEP [7]) are remarkably similar to those of ALHA81005 and Y791197, and far lower than those of most other lunar regolith samples. The crust in the region(s) that spawned these meteorites was apparently close to, if not entirely, devoid of KREEP. However, the striking similarity among the three meteorites on Fig. 1 is potentially misleading. Orbital spectrometry data [5] that indicate that abundant KREEP is found almost exclusively in the central near side, i.e., the very region sampled by the Apollo and Luna missions.

Enrichments of volatile elements such as Zn and Ga in several analyses of Y791197 led to a suggestion [8] that Y791197 could not have come from the same

	Y-82192 whole-rock 171.1 mg	Y-791197 average, liter. [3]	ALHA81005 wtd. mean, liter. [4]	Ap-14 Al-rich reg. brec. 14315	Y-82192 Clasts ,52A 6.4 mg	Y-82192 Clasts ,83B 3.5 mg
Na mg/g	2.73	2.42	2.24	4.20	2.71	4.39
Mg mg/g	36	36	49.4	47.6	–	–
Al mg/g	123	139	136	117	–	–
K mg/g	0.173	0.237	0.194	2.60	0.14	0.26
Ca mg/g	101	109	107	92.8	(150)	130
Ti mg/g	(2.0)	2.0	1.57	5.1	–	–
Fe mg/g	44.7	49.7	42.7	57.8	26.2	13.1
Sc µg/g	13.5	13.4	9.1	15.6	6.6	6.2
V µg/g	(33)	33	24.6	–	–	–
Cr µg/g	1010	910	890	1240	700	500
Mn µg/g	600	670	580	780	380	225
Co µg/g	16.7	25	21.0	33.0	12.8	(4)
Ni µg/g	122	250	198	430	(115)	<200
Zn µg/g	7	34.5	8.7	–	(23)	45
Ga µg/g	2.8	5.9	2.7	6.6	4.0	5.5
Br ng/g	<200	176	190	–	–	–
Sr µg/g	140	137	135	140	(150)	(250)
Zr µg/g	24	32	26.8	520	<360	(235)
Cs ng/g	<160	64	24	420	<770	<800
Ba µg/g	(22)	33	28.4	380	<140	<180
La µg/g	1.54	2.38	1.98	36	1.34	1.91
Ce µg/g	3.8	6.0	5.2	91	(3.3)	(2.4)
Nd µg/g	2.3	3.7	3.2	53	–	–
Sm µg/g	0.68	1.13	0.95	14.3	0.46	0.33
Eu µg/g	0.87	0.79	0.69	1.56	0.83	1.30
Tb µg/g	0.17	0.256	0.214	3.1	–	–
Dy µg/g	1.28	1.60	1.33	19.9	(0.75)	–
Ho µg/g	0.24	0.34	0.31	4.3	(0.15)	(0.17)
Yb µg/g	0.79	1.07	0.84	10.4	(0.47)	(0.70)
Lu µg/g	0.121	0.157	0.124	1.55	(0.063)	–
Hf ug/g	0.73	0.86	0.73	11.3	(0.31)	(0.3)
Ta µg/g	(0.038)	0.103	0.093	1.32	<0.5	<0.7
Ir ng/g	6.4	6.6	6.8	18.8	<8	<4
Au ng/g	(1.4)	6.6	2.2	12.7	–	–
Th µg/g	0.19	0.33	0.29	5.6	<0.32	<0.43
U µg/g	0.058	0.119	0.098	1.38	–	–
mg	0.649	0.624	0.737	0.654	–	–

lunar region as ALHA81005. Our own analysis [4] found only modest Zn and Ga enrichments in Y791197 vs. ALHA81005, and we find that Y82192 has considerably lower Zn and Ga concentrations than Y791197 (Table). Further, the upper limit we find for Br indicates modest overall contents of volatile elements (as we also inferred from our Br datum for Y791197 [4]). Note, however, that the two clasts have far higher Zn and Ga than the bulk rock.

One probably significant difference between Y791197 and ALHA81005 is that Y791197 has a far lower mg ratio [4]. Our Y82192 Mg datum has a relatively high uncertainty (nominally 14%); we expect to acquire a more precise Mg datum through further analysis. However, Nakamura et al. [9] report a similar mg ratio. Whereas ALHA81005 analyses [2] consistently indicate an mg ratio higher than that of any other lunar regolith sample, Y82192 and Y791197 both have unusually low mg ratios (Fig. 2). The mg range between Y82192 and ALHA81005 exceeds the range among regolith breccias from Apollo 16, which come from as far as 8 km apart in an area specifically chosen to straddle two separate formations (Cayley and Descartes); the mg range between Y791197 and ALHA81005 is even greater. These huge disparities in mg impose key constraints on the origins of these meteorites. If all three were blasted off the Moon by a single impact, evidently they were not close together before the impact, or else the impact happened to strike an exceptionally heterogeneous area.

The aluminum (plagioclase) content of Y82192 is similar to those of previously analyzed lunar highlands regolith samples (Fig. 2). The average plagioclase content of the ancient crust is a key line of evidence in support of the lunar magmasphere hypothesis. A magmasphere is probably the only plausible means of producing a crust with an average plagioclase content much greater than that of a basaltic partial melt (i.e., much greater than about 55 wt%). The Al content of Y82192 is high enough to strengthen the case for a primordial lunar magmasphere; especially to the degree that Y82192, Y791197, and ALHA81005 come from widely-separated lunar locations.

REFERENCES [1] Yanai K. and Kojima H. (1984) Proc. 9th Symp. Antarc. Meteor. [2] Bogard, D. et al. (1983) Geophys. Res. Lett. 10, No. 9 (special ALHA81005 issue). [3] Various authors (1985) Abstracts, 10th Symp. Antarc. Meteor. [4] Warren P. H. and Kallemeyn G. W. (1985) Proc. 10th Symp. Antarc. Meteor. [5] Adler I. and Trombka J. I. (1977) Phys. Chem. Earth 10, 17-43. [6] Laul J. C. and Schmitt R. A. (1973) Proc. Lunar Sci. Conf. 4, 1349-1367. [7] Warren P. H. and Wasson J. T. (1979) Rev. Geophys. Space Phys. 17, 73-88. [8] Kaczarel P. W. et al. (1985) Abstracts, 10th Symp. Antarc. Meteor. [9] Nakamura N. et al. (1986) Lunar and Planetary Science XVII, 601-602.

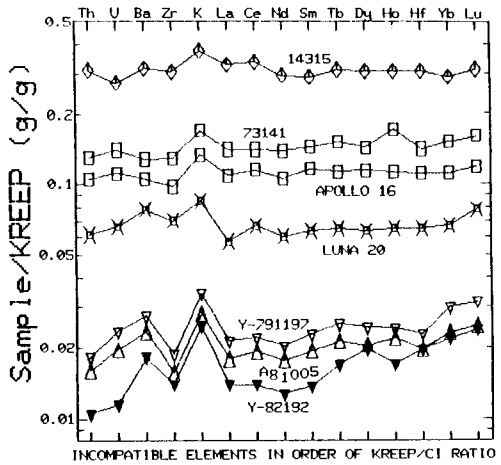

Fig. 1

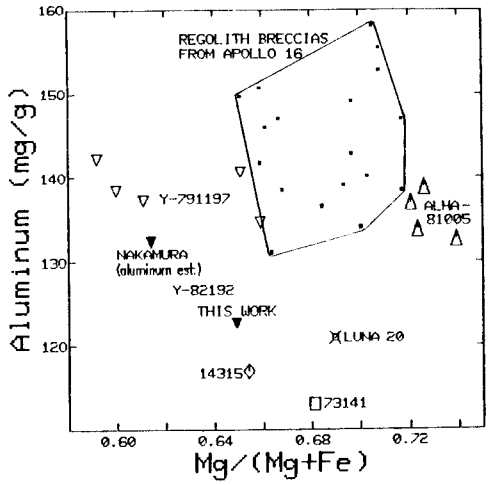

Fig. 2

YAMATO 82192 AND 82193: TWO OTHER METEORITES OF LUNAR ORIGIN.

A. Bischoff,[1] H. Palme,[2] B. Spettel,[2] D. Stöffler,[1] H. Wänke,[2] and R. Ostertag[1];
[1]Institut für Mineralogie, Correnssstr. 24, 4400 Münster, F.R. of Germany;
[2]Max-Planck-Institut für Chemie, Saarstr. 23, 6500 Mainz, F.R. of Germany

Allan Hills 81005 and Yamato 791197 were described as the first meteorites of lunar origin that were ejected from the moon by impact. Both are polymict lunar highland regolith breccias.
Here, we present mineralogical and chemical data of two other lunar meteorites: Yamato 82192 and 82193. These two lunar samples are regolith breccias that are composed of a great variety of lithic and mineral fragments embedded in a fine-grained matrix of clasts. Both samples are densely compacted by shock.
A 85.3 mg piece of the meteorite was analyzed by INAA, in the same way as the other lunar meteorites (1,2). The results are presented in Table 1. The chemical composition of Y-82192 is very similar to that of the other lunar meteorites. Major differences are the low abundances of REE and their flat pattern. This difference can be extended to all incompatible elements (Hf, Th, U, Ba, and K). Their abundances are approximately a factor of two lower than in ALHA81005 and Y-791197. Their relative abundances are, except for Ba and K, chondritic within the limits of error. The siderophile elements Ni, Co, Ir, and Au have similar abundances to other lunar highland samples. There appears to be a uniform signature of siderophile elements in the old lunar highlands, away from the large basins of the front side of the moon.
The frequency distribution of mineral and lithic clasts within Y-82192 and 82193 gives important information about the nature of the regolith and subregolith basement at the impact site of these samples. As done for ALHA81005 (3) and Y-791197 (2,4), we have determined the clast population statistics of the thin sections Y-82192,50-1, and Y-82193,91-2. The volumes and the proportions of clasts ($\gtrsim$0.1 mm) were measured with a Zeiss Mop Videoplan, and the data were compared with those obtained for Y-791197 and ALHA81005 (Tab. 2,3). Both samples contain about 26 vol% clasts larger than $\sim$0.1 mm in size. Recrystallized feldspathic rocks and breccias, and granulitic lithologies are by far the dominant rock types (Tab. 2). Similar values were obtained by the study of the two previous lunar meteorites ALHA81005 and Y-791197. Crystalline melt breccias (CMBs) are common, and the amount of devitrified glasses is negligible. The CMBs are similar to those within Y-791197. The feldspathic microporphyritic melt breccias are different from those within Apollo 16 fragmental breccias because of their very fine-grained texture. A second variety of fine-grained melt breccias is extremely fragment-laden and mafic-rich. This was already pointed out by the study of CMBs from Y-791197. In all Yamato samples the feldspathic CMBs are more abundant than the mafic ones. This is different from the abundances of CMBs in ALHA81005. In contrast to ALHA81005 and Y-791197, Y-82192 and Y-82193 contain basaltic clasts (Tab.3). Glasses are a common and characteristic lithology in A81005. Especially the irregularly-shaped brown layers of impact glasses in A81005 are missing in Y-82192 and Y-82193 as well as in Y-791197 (2,4). As a whole Y-82192 and 82193 have less regolith components (vesiculated brown glass, glass spherules) than the other lunar meteorites. From the optical study it appears to be certain that Y-82192 and 82193 are derived from the same rock. The basaltic clasts (not observed in A81005 and Y-791197) and the fine-grained textures of the CMBs are identical. Furthermore, both lunar samples have approximately the same abundances of the various types of clasts.

In comparison to the first lunar meteorites ALHA81005 and Y-791197, the samples described here are optically more related to Y-791197 than to A81005 despite the lack of the basaltic clasts in Y-791197. Y-82192 and Y-82193 must be lunar highland samples, essentially by the same arguments as those given for the other lunar meteorites, except for the rare gases of Y-82192 (5). However, because of the differences in incompatible elements this meteorite (Y-82192) cannot be a piece of one of the other lunar meteorites.

TABLE 1	Y-82192 85.29 mg	Error	Y-791197 59.3 mg	Error	ALHA81005 128 mg	Error
%						
Mg			4.25	5	4.78	5
Al			13.30	3	13.4	3
Ca	10.6	6	11.4	5	10.80	3
Ti	0.22	15	0.22	10	0.14	10
Fe	4.74	3	5.05	3	4.20	3
ppm						
Na	2650	3	2410	3	2250	3
P			100	30	90	25
K	150	17	290	5	230	5
Sc	14.5	3	16.5	3	9.24	3
V	40	5	39	10	26	8
Cr	1020	3	1034	3	862	3
Mn	657	3	734	3	587	3
Co	19.9	4	16.9	3	20.2	3
Ni	120	10	100	15	186	5
Zn	30	15	50	20	18	20
Ga	3.78	11	9.87	5	2.8	5
As	<0.2					
Se	<0.2				0.6	
Br	<0.2					
Rb	<3				1.5	
Sr	136	15	118	20	128	10
Zr	14				30	
Sb	<0.1					
Cs	<0.1					
Ba	21	21	34	25	34	20
La	1.13	4	3.24	4	2.44	3
Ce	2.98	6	8.76	8	6.9	5
Nd	1.97	11	5.24	10	3.9	10
Sm	0.631	4	1.56	4	1.18	3
Eu	0.754	3	0.723	3	0.704	3
Gd	1.2	35			1.4	20
Tb	0.17	12	0.33	10	0.27	5
Dy	1.13	5	2.22	5	1.7	10
Ho	0.26	10	0.48	10	0.37	15
Tm	0.15	30	0.23	20	0.18	20
Yb	0.76	6	1.34	4	1.06	5
Lu	0.115	4	0.19	4	0.15	3
Hf	0.44	6	1.11	5	0.92	3
Ta			0.16	8	0.12	8
Ir	0.0056	13	0.0059	15	0.0073	10
Au	0.0011	15	0.0013	15	0.0021	7
Th	0.2	20	0.43	15	0.35	8
U	0.05	20	0.14	15	0.103	15

TABLE 2

Type of rock		Y-82192 No.	Y-82192 area [mm²]	Y-82192 vol. %	Y-82193 No.	Y-82193 area [mm²]	Y-82193 vol. %
Granulitic anorthosite		7	1.72	7.9	10	0.52	6.0
Granulitic (gabbroic, noritic) anorthosite		2	0.14	0.7	2	0.91	10.5
Intragranularly recrys. cataci. anorthosite		13	1.89	8.9	23	1.36	15.6
Intragranularly recrystallized plagioclase		87	4.04	19.1	45	1.02	11.7
Recrystallized feldspathic melt breccia		2	2.62	12.4	1	0.05	0.6
Recrystallized feldspathic rocks and breccias, and granulitic lithologies		111	10.41	49.0	81	3.86	44.4
Feldspathic fine-grained to microporphyritic CMB	feldspathic	33	2.47	11.7	27	1.13	13.0
Feldspathic, subophitic CMB	feldspathic	1	0.54	2.6			
Micropoikilitic CMB	mafic	1	0.20	0.9			
Fine-grained, mafic-rich CMB	mafic	12	1.44	6.8	5	0.07	0.8
Fine-grained, subophitic CMB	mafic	11	1.17	5.5	5	0.30	3.5
Crystalline melt breccias		58	5.82	27.5	37	1.40	17.3
Devitrified glass spherules		1	0.01	0.1	1	0.02	0.2
(Partly) devitrified impact glass		4	0.31	1.5	4	0.36	4.1
Impact melt with variolitic texture					1	0.02	0.2
Devitrified (impact) glasses		5	0.32	1.6	6	0.40	4.5
Plagioclase mineral fragments		45	1.82	8.6	27	0.82	9.4
Mafic mineral fragments		11	0.31	1.5	7	0.10	1.1
Mineral fragments		56	2.13	10.1	34	0.92	10.5
Feldspathic and mafic basalts		4	1.66	7.8	1	1.67	19.2
Cataclastic gabbro		1	0.22	1.0			
Quenched spinel-troctolite		1	0.03	0.2			
Polymict fragmental breccia		1	0.45	2.1	1	0.35	4.0
others		2	0.13	0.6			
All others		13	2.49	11.7	2	2.02	23.2
	TOTAL	239	21.17	99.9	158	8.70	99.9

TABLE 3

	Y-82192	Y-82193	Y-791197	A81005
Recystallized and granulitic lithologies	49.0	44.4	53.9	56.5
Feldspathic crystalline melt breccias	14.3	13.0	12.7	6.5
Mafic crystalline melt breccias	13.2	4.3	10.9	15.7
Vitric to devitrified (impact) glasses	1.6	4.5	6.5	11.0
(Vitric impact glasses)	-	-	(0.4)	(1.5)
Mineral fragments	10.1	10.5	4.1	2.1
Feldspathic and mafic basalts	7.8	19.2	-	-
Polymict fragmental breccias	2.1	4.0	11.5	7.4
Others	1.8	-	0.4	1.0
TOTAL	99.9	99.9	100.0	100.2

References: (1) Palme et al. (1983), Geophys. Res. Lett. 10, 817-820; (2) Ostertag et al. (1985), Submitted to Proc. of the 10th Symposium on Antarctic Meteorites. (3) Bischoff and Stöffler (1984), Lunar and Planet. Sci. XV, 62-63. (4) Bischoff and Stöffler (1985), Lunar and Planet. Sci. XVI, 63-64. (5) Weber et al., this volume.

MINERALOGY OF LUNAR METEORITES, YAMATO-82192 AND 82193 WITH REFERENCE TO EXPLORATION OF LUNAR HIGHLANDS

Takeda, H., Mori, H. and Tagai, T.
Mineralogical Institute, Faculty of Science, University of Tokyo, Hongo, Tokyo 113, Japan

Since all lunar meteorites, ALH81005 (e.g. 1), Y-791197 (2), Y-82192 (3), and Y-82193 (4), are lunar highland, regolith breccias, studies of lunar meteorites provide us with information of various samples of the lunar highland rock types of a wider area of the moon, from where the meteorite was derived. Warren and Wasson (5) have been searching for pristine nonmare rocks for many years. Pristine rocks are important because only they preserve faithfully the compositional variety of the original lunar crust. Comparisons of four lunar meteorites are also important, because they inform us about portions of the Moon's crust never sampled by either the U.S. Apollo or the Soviet Lunar mission. If some interesting pristine clasts will be found, the impact sites of the lunar meteorites will be a good candidate for a furture exploration of the lunar highland, and the nature of the lunar crust in different locations will give us important clue to solve the orogin of the moon.

We studied two thin sections Y-82192,50-6 and Y-82193,91-4 supplied from NIPR by the electron microprobe and photomicroscope method and a small rock fragment of Y-82192 by the analytical transmission electron microscope (TEM) technique. Sample Y-82192 is a regolith breccia (4) partly coated with a thick devitrified impact glass. Our thin section does not include this glass.

Y-82192,50 is a regolith breccia, but the matrix is not crystalline as was reported previously (3). The matrix is fine-grained comminuted fragments of regolith components and has smaller amounts of glass than Y-791197, and is similar to that of mega regolith breccia 60016. 60016 and 60019 are lunar analogs of the lunar meteorites, and 60016 contains less matrix glass than 60019. Since 60016 contains smaller amount of solar wind gas components than normal regolith breccias, Y-82192 may also contains a fewer amount of such gases. The amount of glass differs from one place to another and glass-rich areas are similar to Y-791197. The clasts vary in size and the largest clast reaches up to 3.6 x 1.7 mm in size. This clast is another regolith breccia (BB). This type of "breccia in a breccia" is common in lunar samples, but such a good example is not reported in the lunar meteorites. The amount of matrix glass of BB is smaller than the host matrix and the bulk chemical composition of the matrix glass obtained by a broad beam analysis by the microprobe is more feldsparthic than the matrix of Y-82192 (Fig. 1).

The second largest clast is a glassy melt breccia with plagioclase fragments. The matrix glass is slightly devitrified. The outline of another such clast is not clear and the glass matrix is merged into the glassy matrix surrounding the clast, and in some cases it looks like a glass-rich matrix. Other common clasts are cataclastic anorthosites, and most of the plagioclase fragments are shocked. Only one crystalline clast found within the thin section is a troctolitic anorthosite 0.85 mm in diameter with small amount of pyroxene with $Ca_{4.4}Mg_{59.0}Fe_{36.6}$. The plot of mole % An (96.0) in plagioclase versus mole % Mg/(Mg+Fe) in coexisting mafic minerals (mg of olivine = 56.6 for $Fa_{43.4}$ and mg of pyroxene = 61.7) for this clast are within the ferroan anorthosite field.

The Y-82192 pyroxene compositions of small fragments in the matrix plotted in the pyroxene quadrilateral (Fig. 2) distribute within the Mg-rich field. This pattern is rather similar to 60019 than Y-791197. The pyroxene compositions of the BB clast is within this field. The largest pyroxene fragment is an inverted pigeonite crystal 0.55 x 0.35 mm in size and has coarse exsolution lamellae of augite 0.01 mm thick with about 0.05 mm intervals with common (001). The pyroxene composition is within the ferroan anorthosite field (Data with the tie line in Fig. 2), but such pyroxene is found in noritic rocks also. The compositions of plagioclase fragments is similar to those of the other lunar meteorites.

TEM observation showed the fine-grained matrix material consists of micron-sized angular clastic fragments of silicate minerals and some very fine-grained (submicron-sized) interstitial silicate minerals. Both of the silicate minerals are primarily composed of plagioclase with small amounts of pyroxene and olivine. Very minor amounts of troilite and Ca-phosphate were also observed. The very fine-grained interstitial silicate minerals can be interpreted as a result of solid-state recrystallization and to play a role of glue in the matrix material.

Y-82193,90 is a thin section of the matrix portion of the regolith breccia and has a coherent texture. The size of the clast fragments is smaller than the other lunar meteorites and range from 0.1 to 0.9 mm in diameter. Large lithic clasts are not present. Cataclastic anorthosite clasts and very fine-grained recrystallized matrix breccias are among the small clasts. The matrix glass is smaller than Y-791197 and distribute evenly. The glassy matrix compositions are rich in mafic components than those of Y-82192 (Fig. 1). This is consistent with the presence of abundant mafic silicate grained in the matrix.

Only lithic clast found in our thin section of Y-82193 is a basaltic clast 0.94 x 0.47 mm in size, which appears to be recrystallized noritic anorthosite. The pyroxene is zoned with compositional range from $Ca_6Mg_{59}Fe_{35}$ to $Ca_{42}Mg_{34}Fe_{24}$ with a gap in the middle. The plagioclase composition is from An 90 to 96. The compositions of pyroxene fragments in the matrix distribute as in Fig. 3, which is similar to that of Y-82192. The compositions of plagioclase fragments in the matrix distribute also in a similar manner with the mean composition of An 96.0.

Comparisons of the two lunar meteorites revealed that clast population, the textures and composition of the matrix glasses are different. The absence of iron-rich variety of Y-82192 and Y-82193 pyroxenes may partly due to small number of sampling points, but suggests that they came from a region far from all mare flows. Another interpretation may be that Fe-rich metastable pyroxenes may have been melted by a shock event to produce iron-rich glassy matrix. Considering the differences between 60016 and 60019, we can not definitely state that Y-82192 is different from Y-82193 or Yamato-82 lunar meteorites are different from other lunar meteorites. To answer this question, we have to study local variations of more regolith breccias recovered by the Apollo mission. There was found no unique clast which might locate the impact sites on the moon or to show new differentiation trends of the highlands. All clasts and pyroxene types are common ones among the lunar meteorites and lunar highland breccias. The presence of "breccia in a breccia" in Y-82192 suggests complex impact and excavation histories known in lunar regolith breccias.

We thank Dr. K. Yanai and Mr. H. Kojima for the sample preparation and thin-sectioning of this interesting HPF clast. A part of this study was supported by a Fund for Scientific Research from the Ministry of Education.

References: (1) Warren P. H., Taylor G. J. and Keil K. (1983) Geophys. Res. Lett. 10, 779-782. (2) Yanai K. and Kojima H. (1984) Abstr. 9th Symp. Antarctic Meteorites. NIPR, p. 42-43, Tokyo. (3) Yanai K., Kojima H., and Katsushima T. (1984) Meteoritics 19, 342-343. (4) Yanai K. and Kojima H. (1985) Abstr. 10th Symp. Antarctic Meteorites, p. 87-89, NIPR, Tokyo. (5) Warren P. H. and Wasson J. T. (1979) Proc. Lunar Planet. Sci. Conf. 10th, p. 583-610.

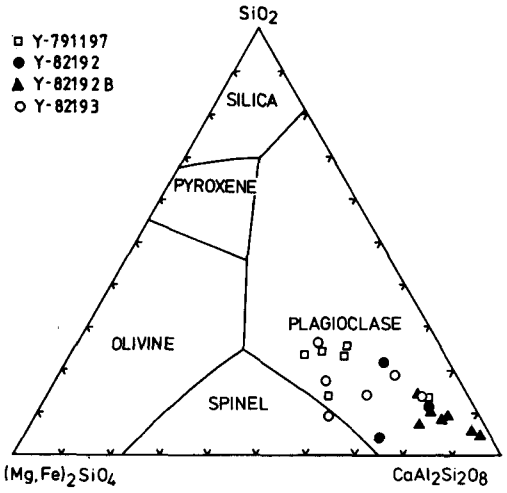

Fig. 1 Compositions of matrix glasses in Y-791197, Y-82192 and Y-82193. Each symbol represents average values of five to ten individual analyses. Triangles: glasses in the BB clast.

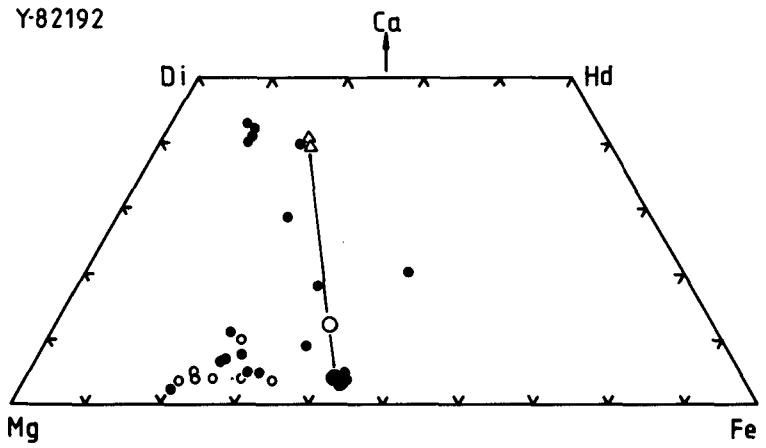

Fig. 2 Pyroxene quadrilateral of Y-82192. Small open circles are from the BB clast. The tie line indicates exsolved pair. Large open circle: bulk composition.

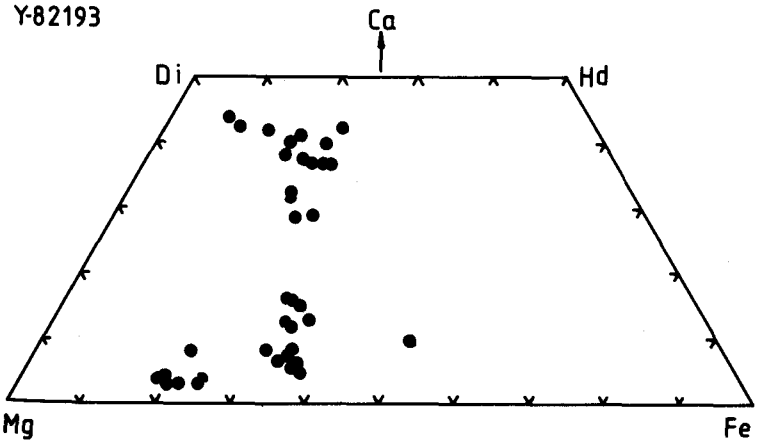

Fig. 3 Pyroxene quadrilateral of Y-82193.

CHEMISTRY OF YAMATO-82192 AND-82193 ANTARCTIC METEORITES

Fukuoka, T.[1], Laul, J. C.[2], Smith, M. R.[2] and Schmitt, R. A.[3]

1 Dept. of Chemistry, Gakushuin University, Toshima, Tokyo 171
2 Chemical Technology Dept., Battelle, Pacific Northwest Laboratories, Richland, WA 99352
3 Dept. of Chemistry and Geology, Radiation Center, Oregon State University, Corvallis, OR 97331

We analized more than 30 major, minor and trace elements in two white clasts and two matrices from Yamato 82192 meteorite and one white clast and three matrices from Yamato 82193 meteorite by instrumental neutron activation analysis (INAA). Two matrix samples with white clasts (Sub. Nos. 52B and 83B)and two matrix samples(Sub.Nos.110 and 111) and one matrix sample with white clast (Sub. No. 112) were provided from National Institute of Polar Research of Japan. We separated the clasts and the matrices from those samples and purified them prior to INAA.

Preliminary analytical results are shown in Table 1 together with the results for standard rocks, BCR-1 and JB-1. The chemical abundances of the clast and matrix of Yamato 791197 (1) are compiled in Table 1 for comparison. The most of chemical compositions of both meteorites are low compared with those in the lunar meteorites Y-791197 (1) and ALHA 81005 (2). Thus errors are relatively large for the analytical results. The Cl chondrites (non-volatile) normalized LIL patterns (Figs. 1 and 2) of Y-82192 and -82193 are typical of lunar anorthositic gabbros with positive Eu anomaly at 10 X (Cl chondrites).

Based on the well-established characteristic lunar and meteoritic ratios of FeO/MnO and Cr_2O_3/V, and LIL patterns, Y-82192 and -82193 meteorites are undoubtedly of lunar highland origin like Y-791197 and ALHA 81005 meteorites. Our conclusion is consistent with petrographic studies (3, 4). The high content of siderophiles, Ni, Ir and Au in the most of samples of Y-82192 and -82193 suggests strongly that these rocks were subjected to a meteoritic impact on the moon like Y-791197 and ALHA 81005.

Sample heterogeneity of both breccias may explain the chemical discrepancies in the matrix samples which are attributed to their polymict character (3, 4) and to the small sample size. Both meteorites were collected from the close points (4). The similarity of the chemical compositions of matrices (weighted mean) of both meteorites suggests that the two meteorites are possibly paired origin, although the chemical similarity of both meteorites is small compared with it between Y-791197 and ALHA 81005. The chemical compositions of matrices of both meteorites are largely different from those of Y-791197 and ALHA 81005.

The lack of an appreciable KREEP component in Y-82192 and -82193 lunar breccias implies a far side origin of both meteorites as discussed before for the origin of Y-791197 and ALHA 81005 (1).

REFERENCES: (1) Fukuoka, T. et al.(1985) Mem. Natl Inst. Polar Res. Spec. Issue 41. (2) Laul, J. C. et al.(1983) Geophys, Res. Lett. 10, 825-828. (3) Yanai, K. et al.(1984) Meteoritics 19, 342. (4) Yanai, K. et al.(1985) Meteoritics 20.

Table 1. Preliminary results of chemical abundances by INAA

		YAMATO 82192					YAMATO 82193					YAMATO 791197		CONTROLS		
		Clast 52B-1	Clast 83B-1	Matrix 52B-2	Matrix 83B-2	Matrix Wtd.mean	Clast 112-1	Matrix 110	Matrix 111-1	Matrix 112-2	Matrix Wtd.mean	Clast 99-1	Matrix Wtd.mean	BCR-1	JB-1	Error* %
Wt	mg	6.80	2.25	16.6	26.7		2.47	25.2	22.3	3.01		5.39		12.6, 19.4	11.9, 19.8	
TiO_2	%	0.14	0.15	0.16	0.26	0.22	0.49	0.31	0.21	0.36	0.27	0.15	0.30	2.25	1.22	16-40
Al_2O_3	%	28.4	30.9	27.2	26.9	27.0	26.7	24.8	26.2	30.9	25.8	24.7	27.1	13.3	14.1	1
FeO	%	4.34	2.93	4.33	4.77	4.60	6.59	5.90	5.51	4.47	5.64	6.9	6.7	12.2	7.64	0.5-1
MgO	%	4.4	1.4	4.4	4.5	4.5	8.3	4.9	5.4	4.7	5.1	12.3	6.4	4.7	9.0	10-25
CaO	%	16.3	21.6	15.4	14.9	15.1	16.2	16.1	17.2	17.2	16.7	16.1	15.3	7.2	9.0	4-9
Na_2O	%	0.32	0.49	0.54	0.45	0.49	0.36	0.38	0.44	0.42	0.41	0.30	0.34	3.20	2.58	0.5-1
K_2O	%	0.014	0.034	0.018	0.022	0.020	0.042	0.035	0.039	0.031	0.037	0.038	0.029	1.70	1.42	17-50
MnO	%	0.062	0.048	0.058	0.072	0.067	0.106	0.086	0.077	0.066	0.081	0.111	0.085	0.197	0.159	0.5-1
Cr_2O_3	%	0.107	0.071	0.095	0.119	0.110	0.236	0.158	0.154	0.115	0.154	0.188	0.120	0.0021	0.067	0.5
Sr	ppm	170	220	220	170	190	150	170	180	220	180	150	137	330	430	6-11
Ba	ppm	20	28	21	29	26	77	33	21	36	28	78	39	670	440	12-20
Sc	ppm	7.69	6.21	7.26	9.57	8.68	16.3	13.2	11.8	7.46	12.2	14.5	12.9	32.0	25.6	0.5
V	ppm	10	15	11	37	27	18	33	33	6	31	27	28	447	225	15-70
La	ppm	0.91	0.78	0.87	1.26	1.11	2.49	1.26	1.21	1.74	1.27	5.07	2.17	25.5	36.5	1-3
Ce	ppm	2.2	1.7	2.0	3.2	2.7	6.1	2.9	3.0	3.7	3.0	13.0	5.4	54.0	64.2	3-10
Nd	ppm	1.3	0.8	1.1	1.8	1.5	3.3	2.1	1.9	2.3	2.0	7.3	3.4	30.0	26.8	5-10
Sm	ppm	0.44	0.34	0.43	0.60	0.54	1.03	0.65	0.62	0.80	0.65	2.25	1.04	6.70	4.95	0.5-1
Eu	ppm	0.75	1.10	1.06	0.87	0.94	0.82	0.77	0.88	0.87	0.82	0.81	0.78	1.90	1.39	1
Gd	ppm	0.48	0.70	0.67	0.59	0.62	0.78	0.50	0.60	0.84	0.57	2.7	1.3	6.6	3.9	20-35
Tb	ppm	0.09	0.06	0.08	0.14	0.12	0.22	0.14	0.13	0.14	0.14	0.52	0.24	1.10	0.72	10-30
Dy	ppm	0.4	0.7	0.7	1.1	0.9	1.4	1.0	1.0	1.1	1.0	3.3	1.5	6.3	4.1	15-40
Yb	ppm	0.43	0.36	0.43	0.63	0.55	1.12	0.77	0.70	0.68	0.73	2.02	1.03	3.40	2.24	2-6
Lu	ppm	0.061	0.061	0.063	0.094	0.082	0.174	0.126	0.109	0.096	0.117	0.30	0.15	0.52	0.31	2-5
Hf	ppm	0.34	0.20	0.27	0.42	0.36	0.89	0.45	0.43	0.57	0.45	1.66	0.81	4.76	3.24	5-10
Th	ppm	0.10	0.06	0.12	0.16	0.14	0.47	0.18	0.22	0.26	0.20	1.08	0.35	5.95	8.63	6-20
U	ppm	0.029	0.011	0.027	0.034	0.031	0.066	0.043	0.034	0.055	0.040	0.26	0.09	1.74	1.52	10-40
Ta	ppm	0.020	0.024	0.023	0.055	0.043	0.048	0.025	0.039	0.074	0.034	0.25	0.11	0.76	2.64	20-45
Co	ppm	15.6	5.48	13.9	14.7	14.4	13.4	22.6	15.4	19.4	19.2	28.2	19.8	36.0	34.0	0.5-2
Ni	ppm	167	46	104	132	121	71	158	120	268	148	430	180	15	162	3-10
Ir	ppb	2.9	1.0	2.2	3.3	2.9	2.8	5.1	6.2	7.2	5.7	18.3	6.5	n.d.	n.d.	7-25
Au	ppb	1.0	n.d.	0.4	0.9	0.7	0.4	0.9	1.6	1.9	1.3	6.4	2.5	n.d.	n.d.	20-50

* Errors for INAA are due to counting statistics.

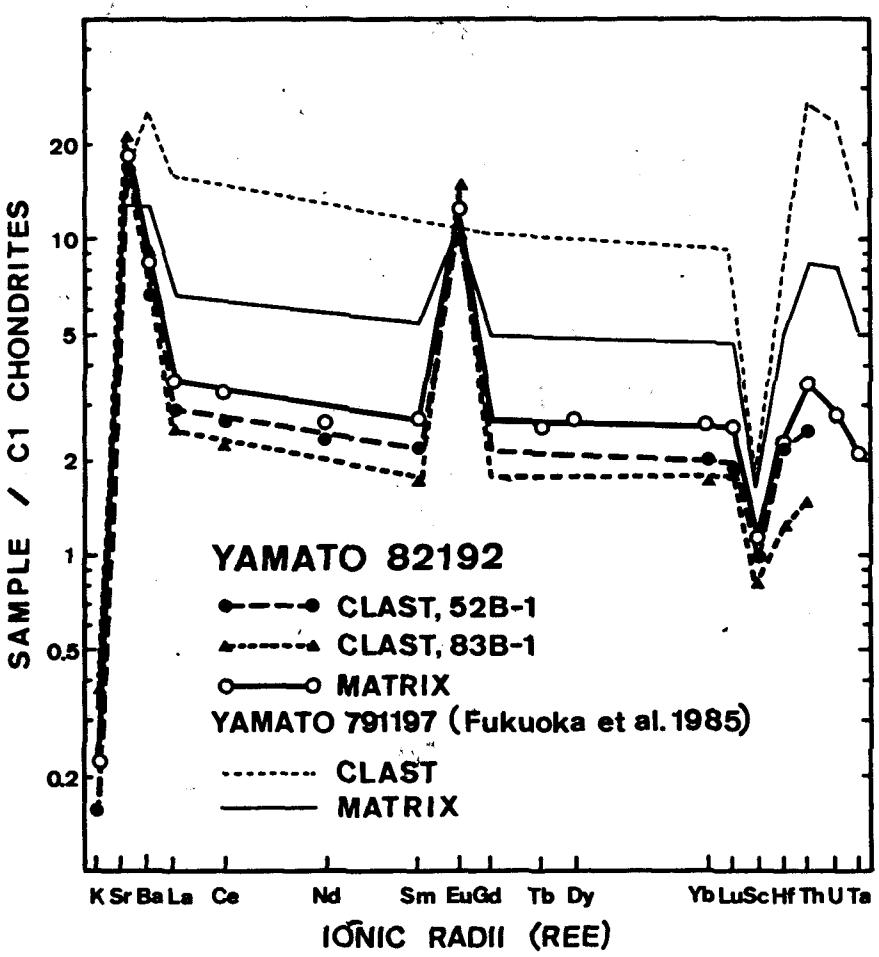

Fig.1. C1 chondrites (non-volatile) normalized abundance patterns of the large-ion lithophile (LIL) elements in clasts and matrix of Y-82192 and -791197 meteorites.

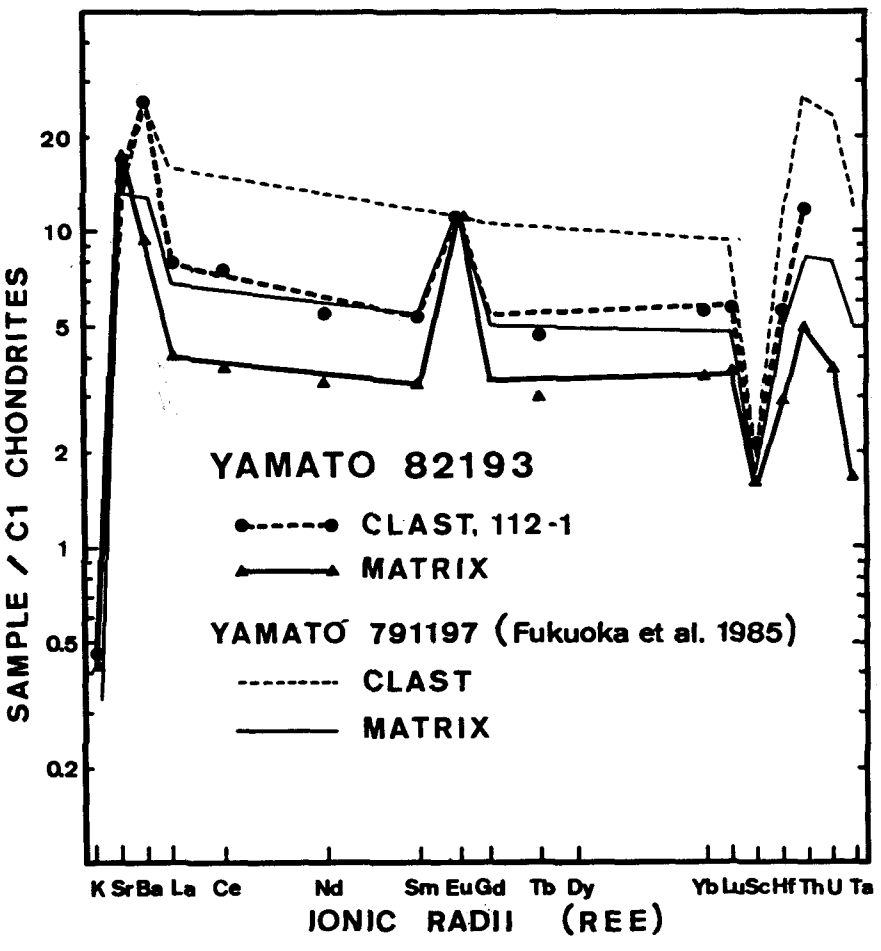

Fig.2. C1 chondrites (non-volatile) normalized abundance patterns of the LIL elements in clast and matrix of Y-82193 and -791197 meteorites.

Cosmochronological studies and REE abundances of Lunar meteorites

Kazuya Takahashi, Hiroshi Shimizu and Akimasa Masuda
Department of Chemistry, The University of Tokyo

Recently, a few meteorites from the Antarctic have been classified as an anorthositic breccia and they have been considered to be of the lunar origin. We precisely determined REE, Sr and Ba abundances for several samples from two lunar meteorites, Y-791197 and Y-82192. Furthermore, by using ^{87}Rb-^{87}Sr system, we will discuss the genesis of these lunar meteorites.

Fig. 1 shows the REE patterns of two clasts in Y-791197 and matrix samples in Y-791197 and Y-82192 with the patterns of one lunar sample (Haskin et al.,1973) and ALH-81005. The clast in the chip, SubNo.115 in Y-791197, is composed of Ca-rich plagioclase (An=97.7%, Ab=1.9%) and the clast in the chip, SubNo.109, is composed of Ca-rich plagioclase with Mg, Fe-rich parts. As shown in Fig. 1, all REE patterns except the clast in SubNo.109 resemble well the pattern of the anorthosite. The pattern of the clast in SubNo.109 shows a negative Eu-anomaly and the REE abundances are higher than those of the others. This clast appears to be the mixture of anorthositic component and the material with the REE pattern like to the Fra mauro basalts. Both of the patterns of Y-82192,63B and the clast in Y-791197,115 have features similar to ALHA-81005, namely larger Eu anomalies and relatively lower REE abundances, except Eu, than those of others. Therefore, these samples can be considered to have derived from the parts which consist of similar materials on the moon. The sample, Y-82192,63B, is regarded as a melted fragment. We are going to separate this specimen into some fractions with heavy liquids. At present we have obtained the ultra-fine sample suspended in acetone (we call this sample "suspension") from Y-82192,63B. Fig. 2 shows the REE pattern of the "suspension" and the abundance ratios between "suspension" and bulk sample of Y-82192,63B, with those of Juvinas (eucrite) and Kapoeta (howardite). The patterns of these ratios of Juvinas and Kapoeta can be considered to reflect the pattern of the residue component for a crystalization process. On the other hand, the pattern of the suspension for Y-82192,63B resembles that of bulk sample, but the REE abundances of suspension, except Eu, are slightly lower than bulk sample. The suspension for Y-82192,63B may be different in genetic characters from that for Juvinas and/or Kapoeta.

Figs. 3 and 4 show the plots of the $^{87}Sr/^{86}Sr$ ratios against the $^{87}Rb/^{86}Sr$ atomic ratios for Y-791197. The ages calculated from these plots are within the range of those of the lunar anorthosites. On these plots the clast in SubNo109 with the clast in SubNo.115 forms an isochron slightly but distinctly different from the isochron for SubNo.108. As mentioned above, the REE patterns of these clasts are also different from the pattern of SubNo.108. So it is possible that these clasts in SubNo.109 and SubNo.115 belong to a series of differenciations different from SubNo.108 on Rb-Sr system. On the other hand, the initial $^{87}Sr/^{86}Sr$ ratios are extremely low. This observation suggests

that the source material of this meteorite might have the very primitive Sr-isotope composition and the low Rb/Sr abundance ratio.

We will add some isotope and REE abundance data on these lunar meteorites.

References

Boynton W. V. and Hill D. H. (1983) Geophys. Res. Lett. 10, 837-840

Haskin L. A., Helmke P. A., Blanchard D. P., Jacobs J. W., and Telander K (1973) Proc. Lunar Sci. Conf., 4, 1275-1296

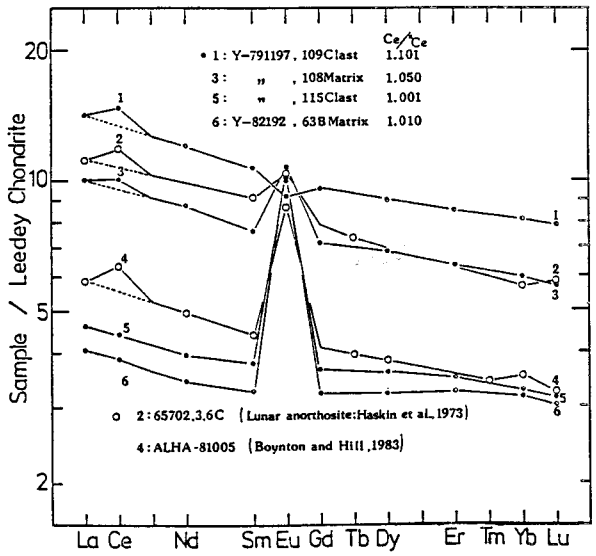

Fig. 1.

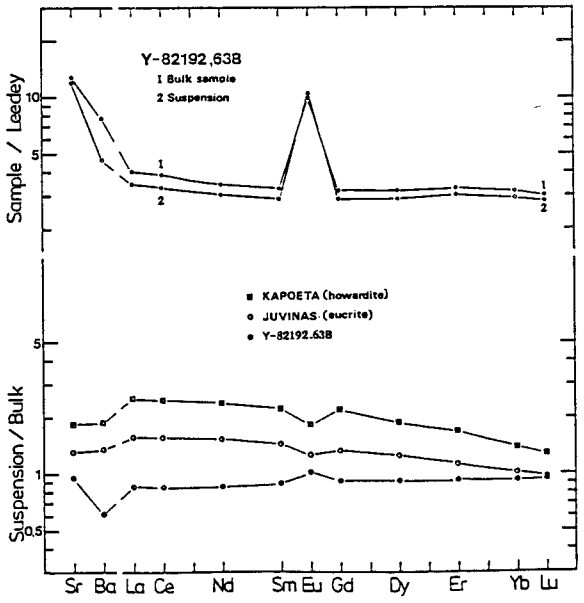

Fig. 2.

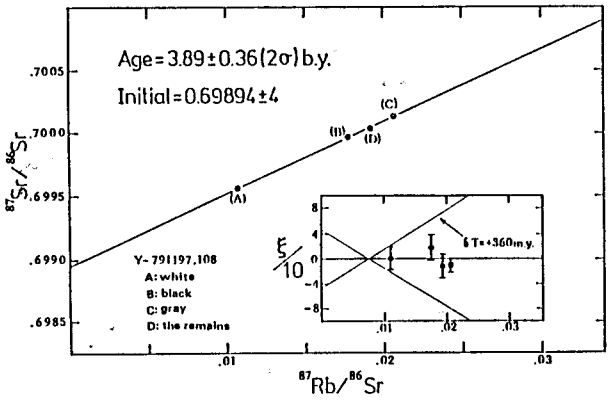

Fig. 3.

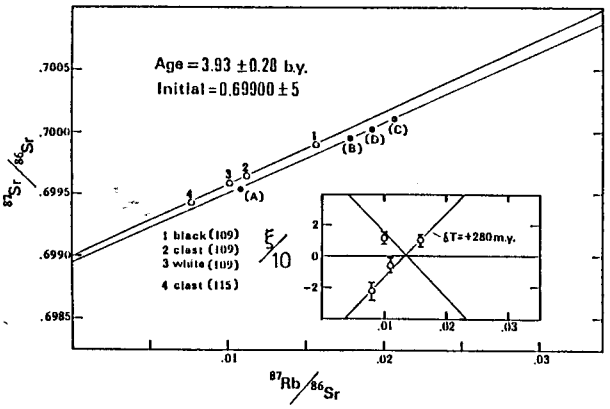

Fig. 4.

CONSORTIUM STUDIES ON LUNAR METEORITE YAMATO 82192 AND 691(E3)

Kaczaral, P. W., Dennison, J. E., Verkouteren, R. M. and Lipschutz M. E.

Department of Chemistry, Purdue University, W. Lafayette, IN 47907 USA

From the first Antarctic meteorite discoveries by JARE 10, the recovery of samples of rare or unique types has become very nearly an annual event. Such samples are usually quite complex so that a complete understanding of their history requires consortium study. Two samples studied in this mode are Yamato (Y) 82192 and 691. Here, as Consortia members, we report results of our RNAA measurements of 15 volatile/mobile trace and ultratrace elements (Ag, Au, Bi, Cd, Co, Cs, Ga, In, Rb, Sb, Se, Te, Tl, U, Zn) in them.

We analyzed 3 samples of Y 82192: black matrix (28.23 mg); coexisting matrix melt (42.21 mg); unmelted white clast (10.16 mg). Trace element contents decrease by approximately constant factors, 1.0:0.67:0.50, in the 3 samples. Lithophiles (Ga, Rs, Cs, U) are present in Y 82192 at levels 0.5-1x those in Allan Hills (ALH) 81005 while other elements are present essentially at levels twice those of ALH A81005 (Verkouteren et al., 1983). Hence, the lunar highlands regolith from which Y 82192 breccia formed was twice as mature as that forming ALH A81005. On average, Y 82192 contains 2-3% admixed meteoritic material (Cl equivalent). Au is enriched by another 3x, hinting at another component. More refractory siderophiles could give clues to this. Neither ALH A81005 nor Y 82192 shows the pattern of condensed volcanic exhalation exhibited by Y 791197 (Kaczaral et al., 1986). The three samples could well derive from the same general lunar region but, from the volatile/mobile trace elment standpoint, each has its own peculiar history.

The 15 trace elements above are normally considered chalcophile, lithophile or siderophile. Most elements are about equally abundant in the two E3 chondrites, Y 691 and Qingzhen. Three of the most volatile/mobile elements - Cd, Bi, Tl - are clearly discrepant, with Y 691 lying virtually at Cl levels (Fig. 1). Data for most elements lie within E4 chondrite ranges (Biswas et al., 1980): however, trends for Ag, Au and Co hint at somewhat lowered siderophile contents. Both E3 chondrites lie with Abee and Indarch at the head of the E chondrite Se/Te fractionation trend arguing for the absence of significant metamorphic alteration. Volatile/mobile elements in E4 chondrites are systematically higher than those of E5,6 chondrites and aubrites (Biswas et al., 1980). High volatile element contents in Y-691 argue that, among enstatite meteorites, it formed at the lowest nebular temperature. Qingzhen's formation temperature was somewhat higher.

REFERENCES: Biswas S., Walsh T., Bart G. and Lipschutz M. E., Geochim. Cosmochim. Acta **44**, 2097-2110 (1980); Verkouteren R. M., Dennison D. E. and Lipschutz M. E., Geophys. Res. Lett. **10**, 821-824 (1983); Kaczaral P. W., D. E., and Lipschutz M. E., Proc. Tenth Symp. Antarctic . in press (1986).

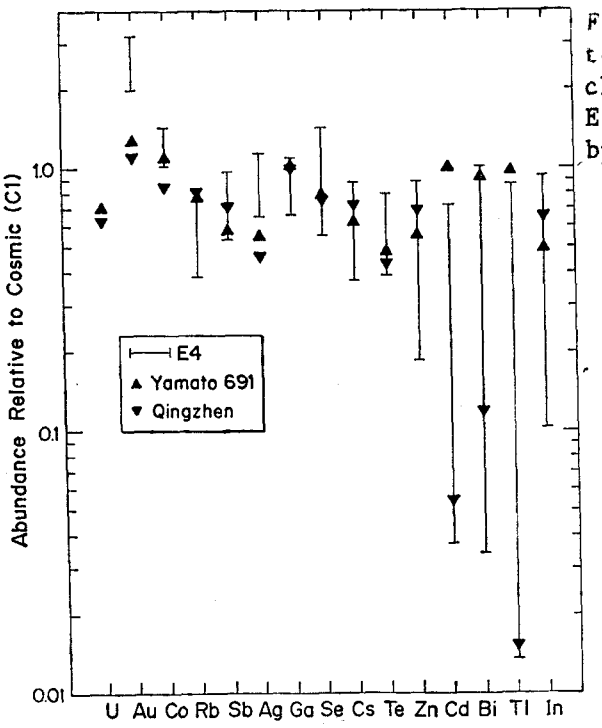

Fig. 1. Atomic abundance (normalized to cosmic or C1 levels) in E3 chondrites compared with ranges in E4. Elements are ordered from left by increasing putative volatility.

REE ABUNDANCE AND Pb-Pb ISOTOPIC CHARACTERISTICS OF THE LUNAR METEORITE, YAMATO-82192

N. Nakamura, D.M.Unruh[2], M. Tatsumoto[2],T. Fujiwara and O. Okano
Department of Earth Sciences, Faculty of Science, Kobe University Nada, Kobe 657, Japan; [2]U.S. Geological Survey, MS 963, DFC, Lake wood, CO 80225, USA.

Yamato-82192 is the third lunar meteorite identified as an anorthositic regolith breccia (Yanai & Kojima 1985). Two matrix samples (subsript Nos. 74 and 63A) investigated in this work contained many tiny (≲1mm in diameter) clasts but clasts in the samples were scarce compared to Y-791197 analyzed by us (Nakamura et al. 1975). We have undertaken REE, Rb-Sr and Pb-Pb analyses together with major element determinations of the Y-82192 samples.

Chemical compositions of two matrix samples are quite similar to each other ;CaO=15.54-15.57%, MgO=5.71-5.74%, FeO=6.13-6.54%, K=125-138ppm, Rb=0.282-0.284ppm. Chondrite-normalized trace element abundance patterns (Fig. 1) show large positive Eu and Sr anomalies and are similar to those of matrix and a clast from the Y-791197 meteorite and to those of lunar anorthositic regolith breccias, e.g. Apollo 64435. It is worth noting that, including the Y-82192 matrix, all the matrix samples of the Yamato "lunar" meteorites appear to have minor but significantly-positive Ce anomalies (+4 - +7% relative to mean O-chondrites) as typically found for lunar highland materials (Masuda et al. 1972; Nakamura 1974). Thus, all the major and trace element data obtained in this work are consistent with a lunar highland origin of the meteorite.

Lead isotopic data for a 20 mg split of Y-81292,63A are shown in Fig.2 together with data from other lunar meteorites Y-791197 (Nakamura et al. 1985) and ALHA 81005 (Chen & Wasserburg 1985). Also shown are data from selected lunar samples taken from the literature.

Lunar anorthositic samples have Pb isotopic signitures that are unique among all solar system materials. Their high $^{207}Pb/^{206}Pb$ and $^{206}Pb/^{204}Pb$ values result from two stages of U-Pb evolution involving high U/Pb from ~4.5 - 3.9 b.y. ago followed by a drastic decrease in this ratio at 3.9 b.y.

Y-791197 and ALHA 81005 data clearly show this high $^{207}Pb/^{206}Pb$ signiture and thus provide strong independent evidence of a lunar origin for these samples (Nakamura et al. 1985; Chen & Wasserburg 1985). However, data for Y-82192,63A(R) plot precisely on the geochron ($^{207}Pb/^{206}Pb$ model age = 4549 ± 6 m.y.). Furthermore, the U-Pb data are ~7% discordant and thus do not plot the "cataclysm" line. A 0.2N-HBr wash of the sample yielded a small amount of Pb (~.05pmoles ^{206}Pb= 1% of the total ^{206}Pb) with near terrestrial isotopic ratios ($^{206}Pb/^{204}Pb$= 21). The data taken at face value suggest that the Pb in Y-82192,63A is entirely meteoritic, with perhaps a small terrestrial component However, it is possibly that Y-82192,63A contains Pb with a similar isotpic composition to that in Y-791197,CL80 but is contaminated with meteorite or terrestrial Pb.

References:

Yanai K. & Kojima H. (1985) paper presented to 9th sympos. Antarc. Meteor. 87-89, NIPR, Tokyo
Nakamura et al. (1985) Mem. Natl. Inst. Polar Res. Spec. Issue (in press)
Chen J. H. & Wasserburg G.J. (1985) Lunar and Planetary Science XVI, 119-120.
Masuda A. et al. (1972) PLC3 (2) 1307-1313.
Nakamura N. (1974) Geochem. J. 8, 67-74

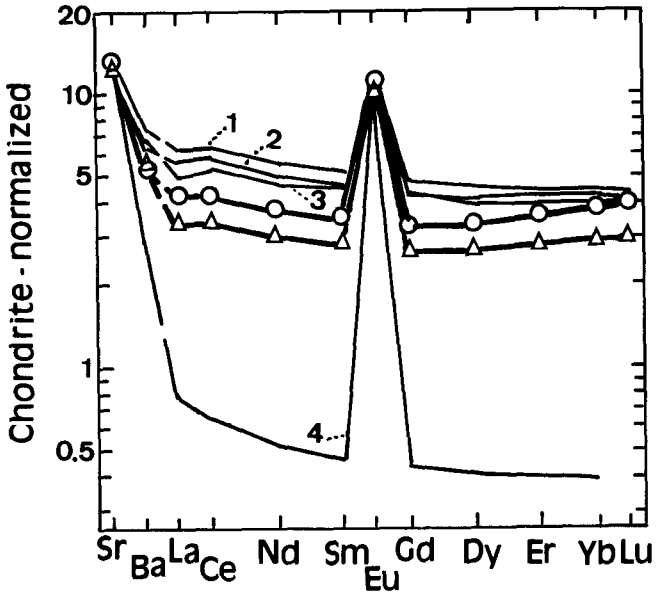

Fig. 1. REE, Ba and Sr abundance patterns for lunar meteorites;
Y-82192 Y-791197
○ Matrix-74 1: Matrix-1 3: Clast-80
△ Matrix-63A 2: Matrix-4 4: Clast-84

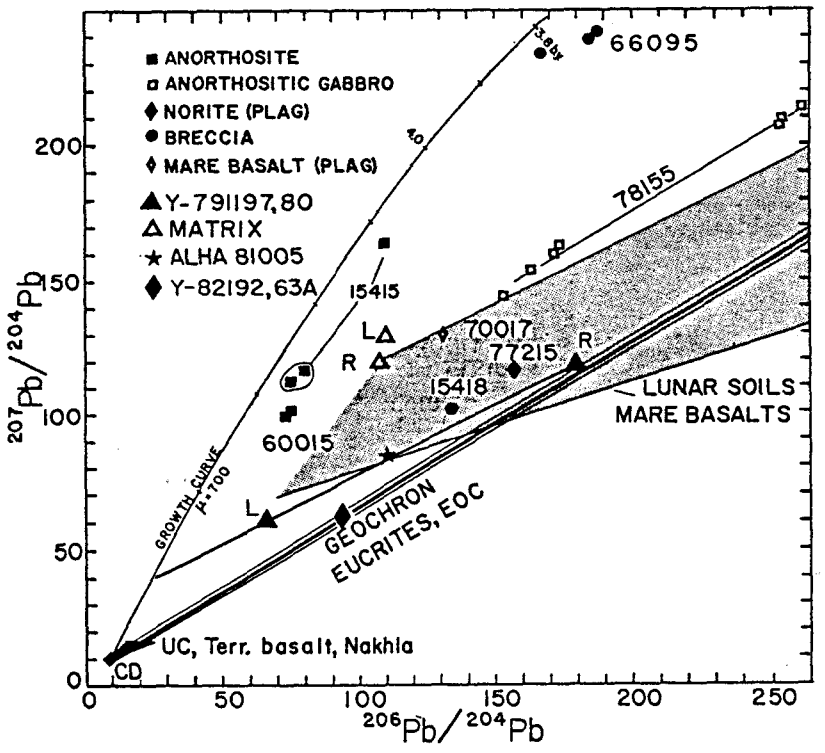

Fig. 2. $^{207}Pb/^{204}Pb$ vs. $^{206}Pb/^{204}Pb$ diagram for lunar meteorites and selected lunar samples. Shown for reference are the 4550m.y. geochron defined by chondrites and achondrites, and a Pb growth curve for $\mu(= {}^{238}U/{}^{204}Pb)=700$. Data for Y-791197 and ALHA 81005 plot significantly above the geochron and are similar to lunar highland data. Y-82192 data plot precisely on the geochron and provide no evidence for a lunar origin "L" and "R" for Y-791197 samples are 1.2N-HBr washes and residues, respectively.

Noble-gas study of lunar meteorite Y82192

Nobuo Takaoka
Department of Earth Sciences
Yamagata University

Y82192 meteorite has been classified as anorthositic breccia (Yanai et al. 1984). It includes glassy clasts resulted from impact shock. Our sample Y82192, 63C is a specimen chipped from such part (Yanai, private communication). We have analysed two samples of small chips (3.66 mg and 26.43 mg) for noble gas isotopes. Concentrations and isotopic compositions of noble gases are summerized in Table 1, together with those for the lunar meteorite Y791197 (Takaoka, 1985). The noble gas concentration is very low compared with that in the other lunar meteorites Y791197 and ALH81005 (Bogard and Johnson,1983). Thus errors are large for the Kr and Xe isotopic ratios.

Helium is mostly of cosmic-ray origin. Ne is a mixture of trapped and cosmogenic components. Figure 1 is a three-isotope plot for Ne. Y82192 falls on a line connecting between solar Ne(Ne-B)and cosmogenic Ne. This shows that the trapped gas is of solar-type. The cosmogenic $^{22}Ne/^{21}Ne$ ratio is estimated to be 1.29, a large value suggesting that the sample was irradiated by hard cosmic-rays in a small meteoroid or near the surface of a parent body. ^{36}Ar and ^{38}Ar are mixtures of trapped and cosmogenic components, whereas ^{40}Ar is a mixture of trapped and radiogenic ones.

Figure 2 is a plot of elemental abundance for the trapped gas. The abundance is lower by factors of >3700 for ^{4}He,1100 for ^{20}Ne, 1500 for ^{36}Ar, 600 for ^{84}Kr and 350 for ^{132}Xe relative to that in the Y791197 whole rock. The extremely low concentration of soler-type gas means that the sample lost most part of the trapped gas probably by impact shock, or that it resided at depth on the lunar surface and was shielded from solar-wind irradiation. The concentration of ^{40}Ar amounts to 1.12×10^{-5}cc/g, however. Because the $^{40}Ar/^{36}Ar$ ratio is 54 after correction for cosmogenic Ar, trapped ^{40}Ar is negligibly small. With assumptions that this ^{40}Ar is all radiogenic and that the K content is the same as that for Y82192 bulk (K_2O = 0.02 %, Yanai, private communication), we have 4.0 $\pm$0.4 Ga for the K-Ar age, which is in good agreement with the age for lunar high-land rocks and the lunar meteorite Y791197 (Kaneoka and Takaoka,1985). This means that the gas loss did not occur at recent time, if any, or that it was so incomplete and light to the degree that radiogenic ^{40}Ar was not lost. Partial gas-loss might be possible because the solar-type gas is a surface-

correlated component enriched near grain surfaces ($\lesssim 1\mu m$) by solar-wind implantation.

Table 2 shows the concentrations of cosmogenic gases and the cosmic-ray irradiation ages estimated under different conditions: irradiations in lunar regolith (2 pai geometry; Hohenberg et al.,1978) and in a meteoroid (4 pai geometry; Cressy and Bogard,1976; Schultz,1985). The cosmic-ray irradiation age is short, although there are uncertainties resulting from production rates which depend on target chemistry of the sample. In the calculation of the production rate, a mean value of chemical compositions for Y791197 (Fukuoka et al. 1985; Lindstrom et al.,1985; Ostertag et al.,1985; Warren and Kellemeyn,1985) was employed. It is contrast to long irradiation ages for Y791197 (Takaoka, 1985) and ALH81005(Bogard and Johnson,1983). The short irradiation age means that the meteorite was at great shielding depth on the average.

There is no significant excess in ^{131}Xe as shown in Table 1. On the Moon, ^{131}Xe is produced mainly by resonance capture of epithermal neutrons by ^{130}Ba (Eberhardt et al.,1971). No excess in ^{131}Xe indicates the heavy shielding on the Moon, or depletion of Ba in the present sample. Y82192,63C contains an appreciable amount of cosmogenic ^{126}Xe, however. From absence of the cosmogenic ^{131}Xe excess, concordance of cosmic-ray ages estimated from cosmogenic ^{21}Ne, ^{38}Ar and ^{126}Xe and others, we suppose that the present specimen was buried at great depth on the Moon and most of the cosmogenic gases were produced in a small meteoroid in inter-

Table 1. Concentrations and isotopic ratios of noble gases in Y82192 meteorite

Isotope	Y82192,63C (3.66 mg)	Y82192,63C (26.43 mg)	Y791197,105#
$^{4}He(10^{-8})$	99.1	211	4.46×10^{5}
$^{3}He/^{4}He$	0.166±0.006	0.0861±0.0023	0.000449
$^{22}Ne(10^{-8})$	9.38	10.5	7.55×10^{3}
$^{20}Ne/^{22}Ne$	7.95±0.05	7.99±0.07	12.30
$^{21}Ne/^{22}Ne$	0.320±0.008	0.319±0.004	0.0403
$^{36}Ar(10^{-8})$	19.8	23.9	3.39×10^{4}
$^{38}Ar/^{36}Ar$	0.274±0.003	0.272±0.002	0.189
$^{40}Ar/^{36}Ar$	49.1±1.7	52.8±0.3	2.536
$^{84}Kr(10^{-10})$	7.8	2.9	1700
$^{78}Kr/^{84}Kr$	0.0090±0.0040	0.0084±0.0007	0.00677
$^{80}Kr/^{84}Kr$	0.0442±0.0035	0.0475±0.0013	0.0416
$^{82}Kr/^{84}Kr$	0.201±0.011	0.212±0.008	0.203
$^{83}Kr/^{84}Kr$	0.206±0.009	0.212±0.004	0.205
$^{86}Kr/^{84}Kr$	0.299±0.014	0.305±0.008	0.306
$^{132}Xe(10^{-10})$	1.0	0.68	245
$^{124}Xe/^{132}Xe$	- - -	0.014±0.003	0.00543
$^{126}Xe/^{132}Xe$	- - -	0.019±0.006	0.00552
$^{128}Xe/^{132}Xe$	0.098±0.026	0.102±0.008	0.00857
$^{129}Xe/^{132}Xe$	1.02±0.13	0.992±0.049	1.029
$^{130}Xe/^{132}Xe$	0.152±0.018	0.171±0.015	0.1673
$^{131}Xe/^{132}Xe$	0.765±0.043	0.804±0.048	0.824
$^{134}Xe/^{132}Xe$	0.40±0.13	0.380±0.021	0.372
$^{136}Xe/^{132}Xe$	0.347±0.045	0.335±0.009	0.302

Concentration in cc/g. Errors in 1 σ. #Takaoka(1985)

planetary space. A history of the lunar meteorite we can infer is that lunar high-land regolith which had formed 4.0 Ga ago and had been buried at great, average depth, say 500 g/cm^2 or more, got hit by a meteorite impact about 12 Ma ago and was ejected into an orbit toward the Earth. Various kinds of clasts were agglomerated in a matrix of regolith by the impact shock, and part of them was partially molten to form breccia. The trapped gas which might have been enriched near grain surface was lost mostly, but radiogenic ^{40}Ar was not lost. That trapped ^{36}Ar, radiogenic ^{39}Ar and ^{40}Ar were released from matrix of Y791197 at >1200 °C shows that the matrix consists mainly of high-temperature hosts for Ar and K (Kaneoka and Takaoka,1985).

References: Bogard,D.D. and Johnson,P.(1983) Geophys.Res.Lett.10,801; Cressy,P.J. and Bogard,D.D.(1976) Geochim.Cosmochim.Acta 40,749; Eberhardt et al.(1971) Earth Planet.Sci.Lett.12,260; Fukuoka,T. et al.(1985) Abstr. 10th Symp. Antarct. Met.,93; Hohenberg,C.M. et al.(1978) Proc.Lunar Planet.Sci.Conf. 9th, 2,2311; Kaneoka,I. and Takaoka,N.(1985) Mem.Nat.Inst.Polar Res. in press; Lindstrom et al.(1985) Abstr. 10th Symp. Antarct.Met. 119; Ostertag et al. (1985) Abstr. 10th Symp.Antarct.Met. 95; Schultz,L.(1985) preprint; Takaoka,N. (1985) Mem.Nat.Inst.Polar Res. in press; Warren,P.H. and Kellemeyn,G.W.(1985) Abstr. 10th Symp.Antarct.Met. 90; Yanai,K. et al.(1984) Meteoritics 19,342; Nishiizumi,K. et al.(1980) Earth Planet.Sci.Lett. 50,156.

Table 2. Cosmogenic noble gases and cosmi-ray irradiation ages

Isotope	Y82192,63C (cc/g)	2 pai irradiation(0-225g/cm^2) Production rate[a]	Age(Ma)	4 pai irradiation Production rate[b]	Age(Ma)
^{21}Ne	3.0 x 10^{-8}	0.30 - 0.049	9.9 - 62	0.22	14
^{38}Ar	2.1 x 10^{-8}	0.61 - 0.072	3.4 - 29	0.18	12
^{126}Xe	1.0 x 10^{-12}	3.6 - 0.67	28 - 150	---	14 - 23[c]

a) Production rate(Hohenberg et al.,1978) was calculated with a mean chemical composition for Y791197(see text) and given in units of 10^{-8}cc/g.Ma for ^{21}Ne and ^{38}Ar and 10^{-14}cc/g.Ma for ^{126}Xe.

b) ^{21}Ne production rate was estimated with Cressy and Bogard(1976) modified to add ^{21}Ne produced from aluminium and multiplied by a ratio(0.65) between ^{21}Ne production rates given by Nishiizumi et al.(1980) and Cressy and Bogard(1976).

c) Calculated with the production rates for 0 - 65 g/cm^2 given by Hohenberg et al. (1978) which were doubled for 4 pai irradiation

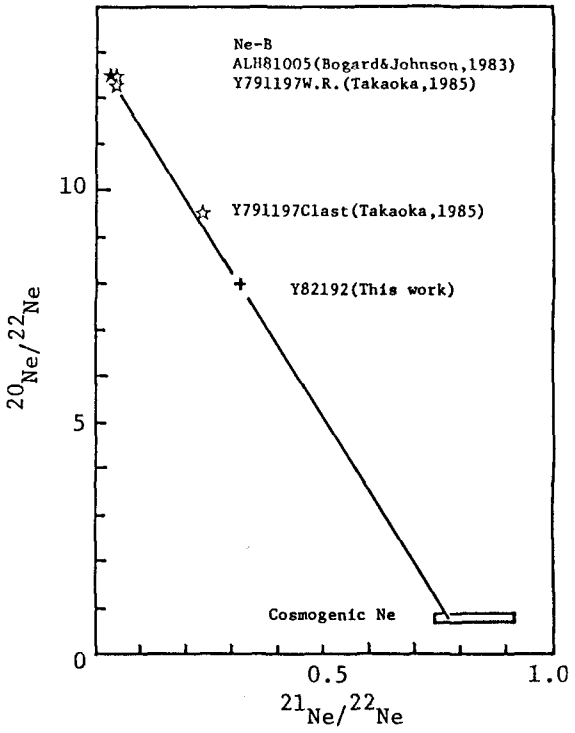

Fig. 1. Three-isotope plot for Ne

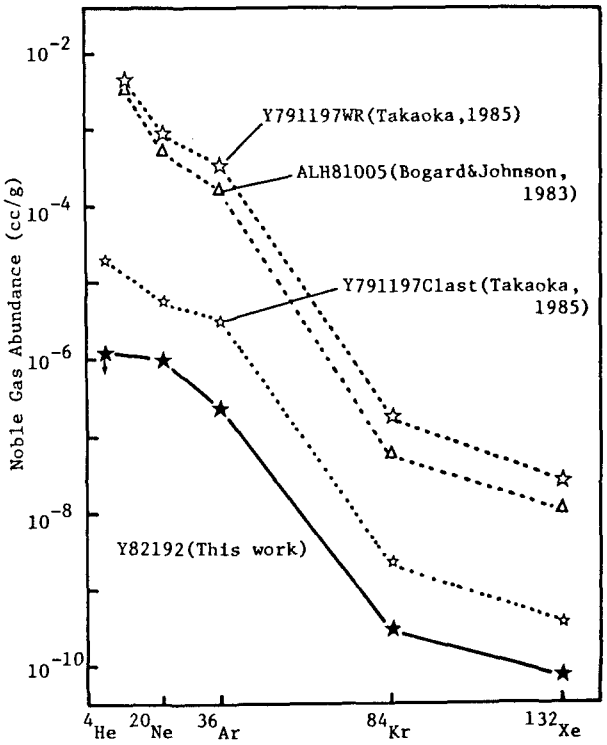

Fig. 2. Elemental abundance of trapped gas.

A new noble gas abundance pattern in a lunar meteorite: Yamato 82192

H.W.Weber, O.Braun, and F.Begemann
Max-Planck-Institut für Chemie
Saarstrasse 23, 6500 Mainz, F.R.G.

Among the many thousand meteorites recovered from Antarctica are four which are recognized to be undoubtedly pieces of the Moon. All four are compacted regolith brecciae (1-4), and it was therefore no surprise that the noble gases contained in two of them (Y 791197 and AH 81005) showed all the features of the noble gases in the lunar regolith (5,6). Y 82192 is entirely different in this respect. Its light noble gases He, Ne and Ar are dominated by spallogenic and radiogenic components, and the trapped gases are similar to those in the Apollo 17 boulder and to those in "normal" meteorites.

Two pieces were analyzed by our standard techniques. In order to exclude with certainty the possibility of a sample mix-up we have measured in addition a fragment of ca. 3 mg which had been used for the neutron activation analysis (4). This piece has yielded the chemical data which are interpreted as unambiguous evidence for a lunar origin of Y 82192 (4); its noble gases are in all their essential features identical with those of the two unirradiated samples listed here.

weight mg	^{3}He	$\frac{^{4}He}{^{3}He}$	^{21}Ne	$\frac{^{22}Ne}{^{21}Ne}$	$\frac{^{20}Ne}{^{21}Ne}$	^{38}Ar	$\frac{^{36}Ar}{^{38}Ar}$	$\frac{^{40}Ar}{^{36}Ar}$	$^{38}Ar_{sp}$	^{84}Kr	^{132}Xe
2.95	7.03	6.36	2.44	1.35	2.21	3.28	2.30	112	2.12	0.020	0.0027
7.44	5.69	5.75	2.28	1.33	1.70	2.69	2.07	153	2.07	0.017	0.0018
mean	6.36	6.06	2.36	-	-	-	-	-	2.10	0.018	0.0022

All concentrations are given in units of 10^{-8} cm^{3} STP/g. Uncertainties in isotope ratios are $\pm$ 3%; nuclide abundances are accurate to better than 6% for He, Ne and Ar and to better than 25% for Kr and Xe. Differences larger than these values between the two specimens are ascribed to sample heterogeneity.

The mean 4-He/3-He ratio of 6.0 is close to the cosmogenic production ratio which leaves only exceedingly little radiogenic 4-He. An absolute upper limit to the 4-He gas retention age is 35 m.y. which follows from the U and Th contents (4) and assuming all 4-He to be of radiogenic origin. This is very much younger than the 40-Ar retention age of 3800 m.y. Cosmogenic 3-He, 21-Ne and 38-Ar are present in the ratio 3.04:1.13:1; the production ratios are predicted (7) to be 11:1.1:1 which indicates a loss of ca. 70% of spallogenic helium. Note, however, that the 21-Ne/38-Ar ratio is as predicted. Actually, a 21-Ne/38-Ar ratio of 1.13 indicates the irradiation by the cosmic radiation to have occurred at a depth of approximately 10 gcm^{-2} (7). Preferential diffusion losses of 21-Ne would feign a larger-than-real amount of shielding so that we take this as an upper limit to the depth of burial at the time of irradiation. All investigated samples of the lunar regolith from such depths contain large amounts of solar-wind implanted noble gases which Y 82192 does not. We therefore conclude that Y 82192 was exposed to the cosmic radiation as a small body during its transit from Moon to Earth. The exposure age - 10 m.y. from both 21-Ne and 38-Ar - is then a strict upper limit to this transit time.

There is no indication that Y 82192 contains, or ever contained, any solar-wind implanted noble gases. Although "Y 82192 and Y 82193 have less regolith components than the other lunar meteorites" (4) this cannot be the explanation that trapped-gas concentrations are lower by at least 2 orders of magnitude than those in the lunar regolith or in the two other lunar meteorites (Y 791197 and AH 81005). It rather appears that there exist samples of the lunar regolith which have not partaken in the soil gardening to the extent that they were ever exposed to the solar wind to any considerable length of time. The concentrations of trapped gases and their abundance pattern are similar to those in a large lunar rock (8) or in "normal" chondrites of high petrologic grade (9). It remains to be seen whether a precise isotope analysis of Kr and Xe allows to distinguish between the two possibilities.

This study was performed as part of the Consortium organized by R.Ostertag. We very much appreciate the generosity of Prof.K.Yanai for making available the sample.

1. Marvin U.B. (1983), Geophys. Res. Letts. 10, 775-778.

2. Bischoff A. and Stoeffler D. (1985), Lunar Planet. Sci. XVI, 63-64.

3. Yanai K. and Hideyasu K. (1985), 10th Symp. Antarctic Met. (abstract) 87-89.

4. Bischoff A. et al. (1986), this volume

5. Bogard D.D. and Johnson P. (1983) Geophys. Res. Letts. 10, 801-803.

6. Takaoka N. (1985), 10th Symp. Antarctic Met. (Abstract), 114-116.

7. Hohenberg C.M. et al. (1978), Proc. 9th Lunar Planet. Sci. Conf. 2311-44.

8. Leich D.A. et al. (1975), The Moon 14, 407-444.

9. Marti K. (1967), Earth Planet. Sci. Letts. 2, 193-196.

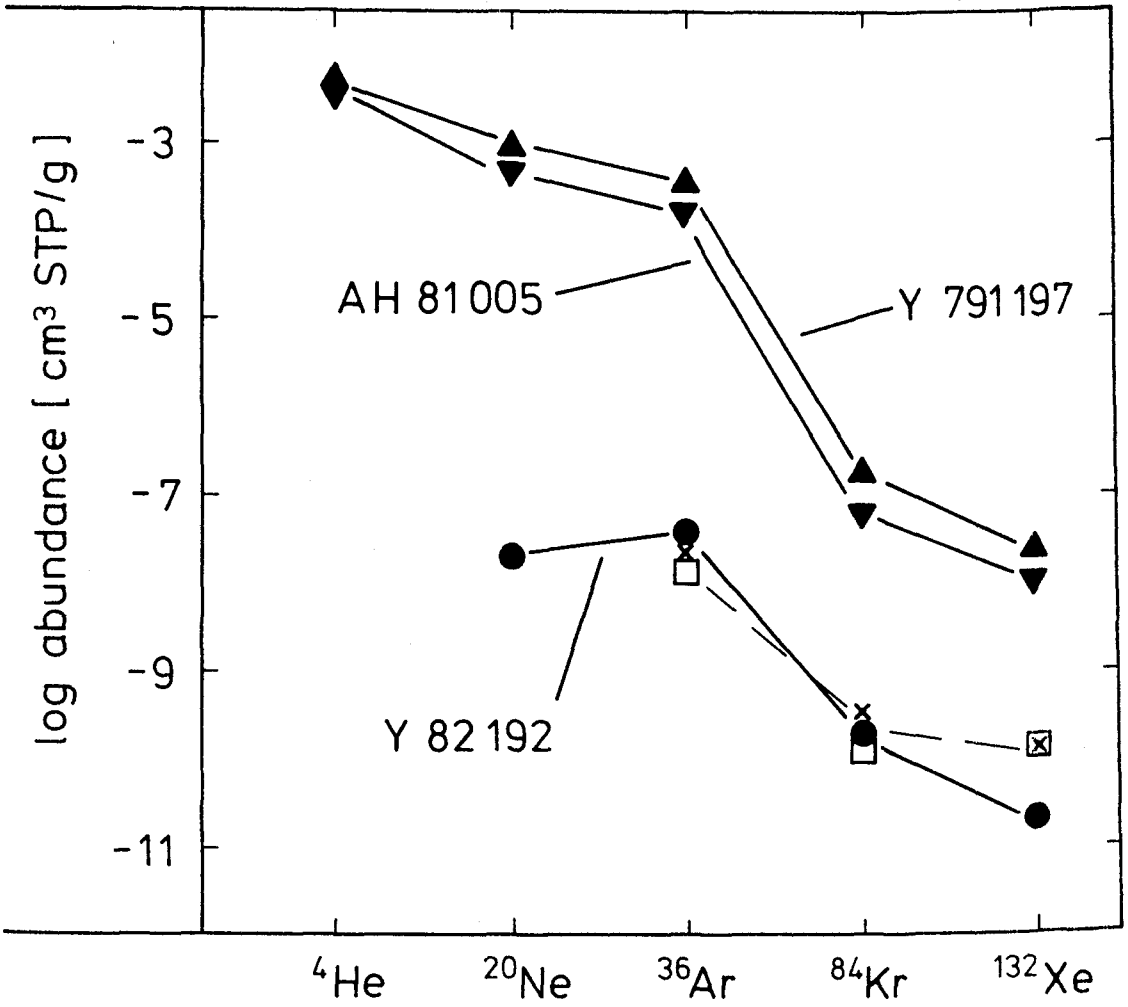

Nuclide abundance patterns in three lunar meteorites. In Y 791197 and AH 81005 the abundances of all nuclides except 4-He are very similar to those in the lunar regolith. Y 82192, on the other hand, is much more similar to normal chondrites of high petrologic grade (□) and to the Apollo XVII boulder (Shown are the results (×) for the anorthositic breccia AnBx (8)).

21—1

^{40}Ar-^{39}Ar ANALYSES OF YAMATO-82192, AN ANORTHOSITIC REGOLITH BRECCIA FROM ANTARCTICA

Kaneoka, I.* and Takaoka, N.**
* Geophysical Institute, Faculty of Science, University of Tokyo, Bunkyo-ku, Tokyo 113.
** Department of Earth Sciences, Faculty of Science, Yamagata University, Yamagata 990.

Yamato-82192 together with Yamato-82193 have been characterized as anorthositic regolith breccias, which are classified as lunar meteorites (1). Among a large amount of meteorites recovered from Antarctica, Allan-Hills A81005 and Yamato-791197 have been identified to have come from the moon (2,3). Among these meteorites, the age is only known for Yamato-791197, which has been reported to be 4065Ma as an ^{40}Ar-^{39}Ar age (4). In this study, we have tried to get information on the age of Yamato-82192 by the ^{40}Ar-^{39}Ar method.

For ^{40}Ar-^{39}Ar anlyses, we tried to separate pure clasts from a portion of Yamato-82192,63D, where small clasts are relatively abundant. However the sizes of clasts in the present sample are generally less than 1mm and it is difficult to separate each clast. Hence a bulk sample with relatively abundant clasts (0.056g) was used for present analyses.

Sample was wrapped in Al-foil and irradiated with neutrons in the JMTR of Tohoku University with the total fast neutron fluence of about 4×10^{17} nvt/cm^2. The hornblende MMhb-I (K-Ar age: 519.5±2.5Ma) (5) was used as the age monitor. Ar gas was extracted and purified at the Isotope Center, University of Tokyo, and analysed on a Nier-type mass spectrometer with a resolving power of about 600 at the Yamagata University. Although nine temperature fractions(600 - 1600°C) were prepared for analyses, the 600°C fraction could not be measured due to the unexpected crack occurred in the Ar collector tube of Pyrex glass for the fraction. However only very small amounts of radiogenic ^{40}Ar would have been lost due to the lack of the 600°C fraction, which could have been inferred from the results for higher temperature fractions. Thus it gives no serious effect on the present result. Blanks and the effects of Ca- and K-derived interfering isotopes were corrected to calculate an ^{40}Ar-^{39}Ar age.

As preliminary results, it has been revealed that this sample shows a quite different degassing pattern from that of Yamato-791197, which shows a plateau age of 4065±93Ma at higher temperatures(900 - 1600°C). More than 90% of ^{39}Ar was degassed together with most radiogenic ^{40}Ar in the 1600°C fraction, where an apprent ^{40}Ar-^{39}Ar age of about 4200Ma has been observed. In the lower temperature fractions, the apparent ^{40}Ar-^{39}Ar ages often exceed 4500Ma, which are probably affected by the incorporation of the terrestrial atmospheric Ar to some extent. It is quite particular that most Ar was degassed only when the sample would be melted. Such pattern is observed in some lunar samples which had been seriously shocked. Under a microscope, both the clasts and the matrix in this sample show signs of intensive shocks (1). Hence probably the highest fraction would approxi-

mate the age when some intensive shock had affected this sample.

Since this sample contains relatively little amounts of trapped and cosmogenic components of Ar, it is further inferred that this portion might have been buried at some depth on the moon's surface.

References

(1) Yanai, K. and Kojima, H., Abstr. 10th Anatarctic Meteorite Symp., 87-89, Tokyo (1985).
(2) e.g.) Bogard, D. D., Geophys. Res. Lett., 10, 773 (1983).
(3) Yanai, K. and Kojima, H., Mem. Natl Inst. Polar Res., Spec. Issue 35, 18-34 (1984).
(4) Kaneoka, I. and Takaoka, N., Mem. Natl Inst. Polar Res., Spec. Issue (1985) (in press).
(5) Alexander, E. C. Jr., Mickelson, G. M. and Lanphere, M. A., U. S. Geol. Surv. Open-File Rep., 78-701, 6 (1978).

EXPOSURE HISTORY OF FOUR LUNAR METEORITES

K. Nishiizumi, J. Klein*, R. Middleton*, D. Elmore+, P. W. Kubik+ and J. R. Arnold; Dept. of Chemistry, B-017, Univ. of Calif., San Diego, La Jolla, CA 92093 ; *Tandem Accelerator Lab., Dept of Physics, Univ. of Pennsylvania, Philadelphia, PA 19104; +Nuclear Structure Research Lab., Univ. of Rochester, Rochester, NY 14627.

The Antarctic meteorites Yamato791197, Yamato82192, Yamato82193, and Allan Hills 81005 were identified to be lunar origin based on chemical composition and isotopic data [ex. 1,2, also see Sept. 1983 Geophys. Res. Lett.]. In particular, the mechanism for ejection of such meteorites from the surface of the moon and for transportation of them from the moon to the earth are very interesting. Even though these meteorites came from the moon, it is not clear whether Yamato 791197 and ALHA81005 are ejected by the same impact event; both meteorites have similar chemical compositions, but different bombardment histories. The case for pairing Yamato 82192 and 82193 as one fall is somewhat stronger, from radionuclide data only. Investigation of cosmogenic nuclides in the objects may help us to understand such dynamics by providing constraints. The lunar meteorites are expected to have cosmic ray exposure on the moon before their ejection and in space during transportation from the moon to the earth. The terrestrial age is also appriciable for the Antarctic meteorite. It is necessary to measure three or more cosmogenic nuclides in the same sample to determine the such complex history.

We report here measurements of the cosmogenic nuclides ^{36}Cl(half-life = 3.0×10^5 years), ^{26}Al(7.05×10^5 years), and ^{10}Be(1.6×10^6 years) in four lunar meteorites and ^{53}Mn (3.7×10^6 years) in ALHA81005. The ^{10}Be and ^{26}Al measurements were carried out using the University of Pennsylvania FN tandem Van de Graaff accelerator [3,4]. The ^{36}Cl measurements were carried out using the University of Rochester MP tandem Van de Graaff accelerator [5]. The ^{53}Mn was measured by neutron activation using the NBS reactor. The preliminary results are shown in Table 1 along with literature values for ^{10}Be and ^{26}Al in ALHA81005 [6]. The ^{53}Mn measurements in the other three meteorites are not completed at this time.

The production rates of cosmogenic nuclides and cosmic ray tracks in meteorites vary with the meteoroid's size and the depth of sample [e.g. 7,8]. The production rates of cosmogenic nuclides on the moon also change by the depth. The depth profiles of ^{36}Cl, ^{26}Al, ^{10}Be, and ^{53}Mn have been measured in the Apollo 15 deep drill core [9]. Those experimental results fitted one theoretical model [7]. Thus, the exposure history on the moon can be well defined using above four cosmogenic nuclides in the same sample. The measured activity A is produced by three different time periods

$$A = Pm\ (1-e^{-\lambda Tm})\ e^{-\lambda(Ts+Tt)} + Ps\ (1-e^{-\lambda Ts})\ e^{-\lambda Tt}$$

where Pm is the production rate(saturation activity) on the moon at the depth of exposure, Ps is production rate of each nuclide in meteoritic body in space. Ps changes with irradiation depth and the preatmospheric size, λ is the decay constant, Tm is the exposure age on the moon, Ts is the exposure age in space, and Tt is the terrestrial age at Antarctica. With other data and some assumptions, the cosmic ray irradiation histories of the four lunar meteorites can be explained as follows.

ALHA81005 : The meteorite was irradiated by cosmic rays at a depth of 140-170 g/cm^2 in the moon for at least 15 million years before being ejected. The low ^{36}Cl result can be explained by the terrestrial age of the meteorite. The terrestrial age of the meteorite is $(1.7\pm 0.5)\times10^5$ years. The transportation time from the moon to the earth must be very short, probably less than 1×10^5 years. This agrees with low TL (thermoluminescence) and almost no cosmic ray tracks [10, 11]. Our ^{36}Cl terrestrial age was supported by the ^{81}Kr age [12].

Yamato791197: Either the meteorite was ejected from the very surface (< 5 g/cm^2) and had much less than 1x10^5 years terrestrial age or it was ejected from a depth of 40-70 g/cm^2 and had about 1x10^5 years terrestrial age. The high ^{26}Al may be explained either by solar cosmic ray irradiation at a near surface depth on the moon or by secondary cosmic ray production at 40-70 g/cm^2 depth. The ^{10}Be production profile between the surface and 100 g/cm^2 is relatively flat so that the experimental value can be explained by either model. The ^{36}Cl production rate at the surface of the moon is similar to the observed value. The production rate is higher at 40-70 g/cm^2 due to mainly ^{35}Cl(n,γ)^{36}Cl reaction but a terrestrial age of 10^5 years would reduce this value to the measured. Without the ^{53}Mn result, the irradiation condition cannot be defined. In the former case, Yamato791197 and ALHA81005 are not same event on the moon.

Yamato82192 and Yamato82193 : High ^{10}Be results indicated that both meteorites were irradiated by cosmic rays in space with 4 π geometry. Even though we cannot calculate transportation time and terrestrial age of both meteorites accurately without chemical composition and ^{53}Mn dat, the exposure age was more than few million years and the terrestrial age was less than 1x10^5 years. These two meteorites are probably a paired fall.

We thank R. M. Lindstrom for the neutron irradiation. This work was supported by NASA grant NAG 9-33 and NSF grant PHY82-13598, PHY82-14295, and DPP-8409526.

REFERENCES:

[1] Yanai K. and Kojima H. (1984) *Mem. Natl. Inst. Polar Res., Spec. Issue, 35*, 18-34.
[2] Clayton, R. N. et al., (1984) *Mem. Natl. Inst. Polar Res., Spec. Issue, 35*, 267-271.
[3] Klein J. et al., (1982) *Nucl. Instr. and Meth. 193*, 601-616.
[4] Middleton R., et al., (1983) *Nucl. Instr. and Meth. 218*, 430-438.
[5] Elmore D., et al (1979) *Nature 277*, 22-25. ; Errata, *Nature 277*, 246.
[6] Tuniz C. et al., (1983) *Geophys. Res. Lett., 10*, 804-806.
[7] Reedy R. C. and Arnold J. R. (1972) *J. Geophys. Res. 77*, 537-555.
[8] Reedy R. C. (1985) *Proc. 15th Lunar Planet. Sci. Conf., J. Geophys. Res. 90*, C722-C728.
[9] Nishiizumi K. et al., (1984a) *Earth Planet. Sci. Lett. 70*, 157-163. and 164-168.
[10] Sutton S. R. (1985) *11th Symposium on Antarctic meteorites*, 111-113. (Natl. Inst. Polar Res.)
[11] Crozaz G. (1985) *11th Symposium on Antarctic Meteorites*, 110. (Natl. Inst. Polar Res.)
[12] Eugster et al., (1985) *Meteoritics 20*, 642-643.

TABLE 1. Cosmogenic Nuclides in Lunar Meteorites

	^{36}Cl	^{26}Al	^{10}Be	^{53}Mn
		(dpm/kg meteorite)		(dpm/kg Fe)
Yamato 791197,75	12.34 ± 0.86	85.1 ± 8.5	11.61 ± 0.46	
Yamato 82192,73	18.37 ± 1.13	106.6 ± 7.5	23.96 ± 1.20	
Yamato 82193,101	17.03 ± 0.94	138.9 ± 9.7	20.10 ± 1.00	
Allan Hills 81005,16	8.81 ± 0.44	41.3 ± 4.1	6.33 ± 0.25	181 ± 15
		46 ± 3*	4.1 ± 0.5*	

* Tuniz et al.,(1983)

Special Lecture

Professor William A. Cassidy

Early History of the United States Antarctic Meteorite Program and the Value of Antarctic Meteorites

Cassidy W.A.
Department of Geology and Planetary Science, 321 Old Engineering Hall, University of Pittsburgh, Pittsburgh, PA. 15260, USA

1. We owe a substantial debt to scientists involved in the Japan Antarctic meteorite program, both for their early field work and their help to U.S. scientists in early stages of the U.S. program.

2. A common question is, when will our meteorite collections be large enough so that we can end the programs? Sampling standards become important in answering this question.

3. Study of frequency distributions within types may help in deciding if meteorites collected at one Antarctic site can be comparted to meteorites collected at another.

4. It can be difficult to compare Antarctic meteorites to modern world falls because of the Antarctic meteorite pairing problem. In some cases, it might be better to compare masses from each source.

5. Antarctic meteorites can be a source of information on the recent history of the ice sheet. The latest field season near the Beardmore glacier may yeild some insights on this but it also presented some new questions.

Wednesday, March 26, 1986

0900 - 1205	*Symposium, Auditorium*
1300 - 1620	*Special session: Yamato-691 enstatite chondrite*
1620 - 1720	*Special Lecture* *Professor Ahmed El Goresy* *(Max-Planck-Institut für Kernphysik, Heidelberg, FRG)*

24—1

A siderophile-rich clast in the polymict eucrite Y-790266

Y.Ikeda, H.Palme, F.Wlotzka, B.Spettel and H.Wänke

Max-Planck-Institut für Chemie

A small siderophile-rich clast (4.47 mg) was separated from the polymict eucrite Y-790266, and the major and trace element concentrations were determined by INAA. The clast contains a large amount of troilite (about 16 wt%) with minor metals (about 1 wt%). The clast has a nearly flat REE, and its lithophile element concentrations are similar to those of the Malvern howardite except for alkalis, which deplete in the clast.

On the other hand, siderophile element concentrations (W, Ir, Ni, Co, Fe and Au) of the clast are higher than those of Malvern. The ratios of Ir/Co and Au/Co of the clast resemble those of metallic phases of the Mincy mesosiderite. The siderophile-rich clast is considered to be produced as a mixture of howarditic materials similar to Malvern and sulfuridized phases of mesosiderite metals.

MINERALOGY OF SOME CLASTS IN NEW ANTARCTIC POLYMICT EUCRITES AND HOWARDITES WITH REFERENCE TO THEIR PARENTAL MASSES

Toyoda, H.[1], Takeda, H.[1], and Ishii, T.[2]
[1]Mineralogical Inst., Faculty of Science, University of Tokyo, Hongo, Tokyo 113. [2]Ocean Research Institute, University of Tokyo, Nakano-ku, Tokyo 164

Both Antarctic achondrites and non-Antarctic achondrites provide us many information about their origin, but there is some difference between them about statistics on populations for different classes of achondrite (1). For example, the number of the Antarctic achondrites is grater than that we expected from the non-Antarctic collections (1), and the number ratio of polymict eucrite to howardite in Antarctic collection is higher than that in non-Antarctic collection (1). To account for this difference, many hypotheses have been proposed (2, 3), and one possibility is that many of them are pieces from a single fall, and the number of the statistics is depend on this uncertainty (4). We investigated six thin sections of new Antarctic achondrites, together with those with only preliminary description with an optical microscope and an electron microprobe. They contain some unique clasts which will give us clue to identify parental masses.

Y-790991 is a typical howardite, rich in pyroxene fragments. The thin section shows abundant lithic fragments similar to diogenites, cumulate eucrites and eucrites. Microprobe analyses show a wide range in pyroxene composition as is shown in Fig. 1a. Some pyroxene compositions extend beyond the most Mg-rich diogenite to nearly $Wo_{0.3}En_{83.7}Fs_{16.0}$ and the most Fe-rich eucrite to nearly $Wo_{8.7}En_{24.2}Fs_{67.1}$. Plagioclase ranges from $An_{78}An_{95}$. Two large diogenetic clasts, up to 4.2x3 mm in size, show fine-grained granoblastic textures of orthopyroxene. One olivine clast, 1.8x0.9 mm in size was present and its chemical composition is Fo_{63-66}. One Fe-rich eucritic pigeonite shows exsolution of augite on (001). Several cumulate eucritic pyroxenes, inverted pigeonites with exsoloved thick augite lamellae with (001) and thin augite lamellae on (100) in the host, exist. One clast, 0.4x0.5 mm in size consists of orthopyroxene with a few thickened and thinned lamella-like augite on (001). It may be a low Ca inverted pigeonite. Y-791573 is similar to Y-790991.

Y-790113 is a polymict eucrite and contains three large basaltic clasts up to 4x2.5 mm. Pyroxenes, up to 1x0.8 mm, in basaltic clasts show chemical zoning and one of their compositions is from core pigeonite $Wo_{10}En_{64}Fs_{30}$ to rim pigeonite $Wo_{10}En_{51}Fs_{39}$ and plagioclase $Ab_{11}An_{88}Or_1$ to $Ab_{15}An_{84}Or_1$. Other part is breccia including several suboptic clasts generally less than 1-2 mm. The chemical compositions of pyroxene in the clasts show also chemical zoning from $Wo_6En_{63}Fs_{33}$ to $Wo_{13}En_{35}Fs_{52}$. Microprobe analyses data of pyroxene are plotted in pyroxene quadrilateral (Fig. 1b). A shock-recrystallized sub-round clast, 1.5x2 mm, consists of plagioclase, pigeonite, augite and silica mineral. Several pyroxenes show exsolved lamellae. Some of them are Fe-rich pigeonite with fine exsolved augite lamellae parallel to (001) (Juvinas type). Others are partly inverted pigeonite with (001) and (100) exsolution lamellae (Moore County type). Inverted pigionites with blebby inclusions (Binda type) have not been detected. Y-790006 and Y-790114 are similar to Y-790113.

Y-791960, polymict eucrite, contains some unique clasts. A cumulate eucritic clast, 3x1 mm in size, consists of plagioclase (An_{88-91}) and inverted pigeonite ($Wo_2En_{51}Fs_{47}$) with augite lamellae ($Wo_{43}En_{37}Fe_{20}$). A

clast, 1x0.8 mm in size displays a gabbroic texture with crystals of pigeonite, plagioclase and chromite. One fragment, 0.5x0.4 mm in size, consists of a inverted pigeonite ($Wo_3En_{38}Fs_{59}$) with augite lamellae($Wo_{41}En_{29}Fs_{30}$). A Y-75032-type clast, 1.5x0.4 mm in size is aggregate of minor plagioclase (An_{94}) and orthopyroxene ($Wo_{3-6}En_{62-64}Fs_{31-34}$).

The bulk chemical composition$of Y-790991 and Y-791573 analyzed by H. Haramura are similar to Y-790727, Y-791208 and Y-791492 and plot in the middle of the diogenite-eucrite trend in the Al_2O_3 vs. CaO diagram, close to that of the three howardite (4). From these facts and similarity of their textures and mineral compositions, there is a possibility that they are pieces from a single fall. The above data, suggest that Y-790006, Y-790113, Y-790114 and Y-790007, Y-790020, might be a pieces of a single fall. As is shown in Fig. 1, Y-791960 differs from other Yamato polymict eucrites (e.g., Y-790113), because it contains only minor surface eucritic component, more cumulate eucrites, and a small amount of diogenitic component. It is also distinct from Yamato howardite (e.g., Y-790991).

In summary, we investigated two howardites and four polymict eucrites, but the total number of the Antarctic howardite falls did not increase and only one possible additional new fall has been identified for polymict eucrite. However, the parental masses of Y-791960 may still be the same as other Yamato polymict eucrites, since the amount of diogenitic components may vary from one place to the other in the mass. A study on local variation of the clast type within a single large polymict eucrite is required before proposing the meteorites flux variation between Antarctic and non-Antarctic falls (1).

Acknowledgments We thank Dr. K. Yanai's parties of JARE and NIPR for providing us with Yamato meteorite samples and H. Haramura and I. Kushiro kindly provided with bulk chemical compositions of the Yamato achondrites.

References:(1) Takeda. H.(1985) Workshop on Antarctic Meteorites, 49-51, Lunar planet. Inst. (2) Takeda. H. and Yanai. K.(1982) Mem. Natnl. Inst. Polar Res. Spec. Issue 25, 97-123. (3) Takeda. H., Wooden. J. L., Mori. H., Delaney. J. S., Prinz. M. and Nyquist. L. E.(1983) Proc. Lunar Planet. Sci. Conf. 14th, in J. Geophys. Res. 88, B245-B256. (4) Takeda. H., Mori. H., Ikeda. Y., Ishii. T. and Yanai. K.(1984) Mem, Natnl. Inst. Polar Res. Spec. Issue 35, 81-101.

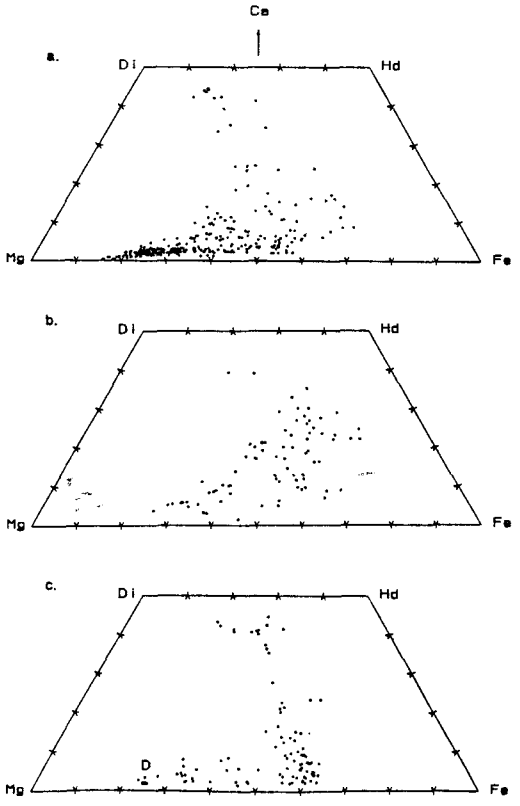

Fig. 1. Pyroxene quadrilaterals for the Yamato achondrites. D: diogenite component.
a. Y-790991
b. Y-790113
c. Y-791960

ABSORPTION SPECTRA AND COMPOSITIONS OF ACHONDRITIC POLYMICT BRECCIAS AND ITS APPLICATION TO IDENTIFICATION

Aoyama, T., Hiroi, T., Miyamoto, M.* and Takeda, H.
Mineral. Inst., Faculty of Sci., Univ. of Tokyo, Hongo, Tokyo 113
*College of Arts and Sci., Univ. of Tokyo, Komaba, Tokyo 153

We measured spectral transmittances of 19 thin sections of the HED achondrites (howardites, eucrites, diogenites) to determine the wavelength range of pyroxene absorption band for the meteorite types. Measurements were done at wavelengths of every 0.5 nm in the visible and near-infrared region (250-2550 nm), and detailed measurements were done every 0.0625 nm in the region from 800 nm to 1050 nm. The wavelength position of the pyroxene absorption band around 900 nm was calculated from the detailed spectra. We also examined a relationship between the wavelength position of the pyroxene absorption band around 900 nm and the Mg/(Mg+Fe) ratio of the bulk chemical compositions of the HED achondrites.

1) Diogenites: Y-74013 is a recrystallized diogenite and mainly composed of orthopyroxene. Y-75032 is a unique meteorite intermediate between diogenites and cumulate eucrites with respect to chemistry and mineralogy, and contains small amounts of plagioclase in addition to orthopyroxene mostly inverted from low-Ca pigeonite (Takeda et al., 1985). (2) Cumulate Eucrites: A thin section of Moore County contains plagioclase (ca. 60 vol%) and pigeonite, which exsolved thick augite lamellae on (001) and is partly or totally inverted to orthopyroxene. (3) Ordinary Eucrites: Juvinas contains Fe-rich and compositionally uniform pigeonites. Y-791186 is a rare Antarctic monomict eucrites (Takeda et al., 1985) and shows evidence of an original minor chemical zoning of pyroxenes. Pasamonte contains chemically zoned pyroxenes. The core is as Mg-rich as diogenites but the rim is Fe,Ca-rich. (4) Howardites: Y-790727, Y-790991, Y-791208 and Y-791492 are the mixtures of diogenitic and eucritic components. Y-7308 is very rich in diogenitic components, but the area of the thin section is not large enough to give significant absorption. (5) Polymict Eucrites: Y-791960 and ALH78006 contain minor diogenitic components (Delaney et al., 1984). Y-791960 is a new Yamato polymict eucrite (Toyoda et al., 1986), and cumulate eucrite components have also been discovered in these breccias. Y-74159, Y-790006, Y-790007, and Y-790266 contain chemically zoned pyroxenes from lava-like eucrites. Y-790007 contains cumulate eucrite components more than other Yamato polymict eucrites. Y-790266 is a thin section of a crystallized clast and should be included in ordinary eucrites. No intensive microscopic exsolution has been detected (Takeda et al., 1982, 1983). Y-790113 and Y-790114 have not been used for detailed measurement.

The HED achondrites contain more than 92 vol% of pyroxenes and feldspars (Delaney et al., 1984). Although the major minerals which absorb source light must be pyroxenes and feldspars, feldspar has only weak absorption bands around 1.2 μm. The transmittance spectrum of the HED achondrites looks like that of pyroxene, because the HED achondrites can be characterized by the absorption bands of pyroxene. The absorption of pyroxene is caused by Fe^{2+}, and the more Fe or Ca are contained in pyroxene, the longer its wavelength positions of absorption bands will be (Adams J. B., 1974). Most of Mg and Fe in the HED achondrites is contained in pyroxenes. Therefore, we have investigated the relationship between the wavelength positions of the pyroxene absorption bands and the Mg/(Mg+Fe) ratio from bulk chemical compositions of the HED achondrites.

Representative spectra of different types of the HED achondrites are compared in Fig. 1. Detailed profiles of spectra (800-1050 nm) show that different types of the HED achondrites give the different wavelength positions of the absorption band. The absorption of 250-400 nm is caused by a glass slide, and absorptions around 2020-2550 nm and around 500 nm are due to resin. The discontinuity of spectra about 350 nm is the result of lamp change. The wavelength positions of the absorption bands are calculated from the detailed profile of spectra by using a peak search program (Hiroi, 1986) on HITAC-M280H. As shown in Fig. 2, they are divided into 3 types (diogenites, howardites, eucrites). Howardites give the wavelength position of the absorption bands between 919 nm and 923 nm and polymict eucrites give bands between 927 nm and 931 nm. For preliminary measurements in Fig. 2, the wavelength positions of the absorption bands are calculated from the spectra at interval of 0.5 nm.

A pyroxene crystallized in early stage is rich in Mg, and may sink in deeper portion of the HED achondrites parent body (Takeda, 1979). Because the Mg/(Mg+Fe) ratio is the criterion for the distinction between howardites and polymict eucrites, we plotted the wavelength position of the absorption compositions analyzed by Haramura (Fig. 3). Fig 3 shows that howardites group distribute in an area clearly distinct from polymict eucrites, and there is a positive correlation between the wavelength position of the absorption band and the Mg/(Mg+Fe) ratio. Y-7308, however, shows the longest wavelength of the absorption band (923 nm) among the howardites examined, even though Y-7308 is one of most enriched in diogenetic components. In conclusion, by using the transmittance spectrum of this sections, we can distinguish howardites which contain dominant diogenitic components with Mg-rich orthopyroxene from polymict eucrites which contain only eucritic components.

It has been a subject of controversy where we set a devide between howardites and polymict eucrites, which form a continuum between them. For example, ALH-78006 was once described as a howardite. Although 10 % divide of the diogenitic components has been proposed by Delaney et al. (1983), it has been difficult to measure the amount of the diogenitic components. The measurement of spectral transmittance of the thin section is one of the easiest methods to distinguish howardites from polymict eucrites.

We thank the National Institute of Polar Reseach and American Museum of National Histry for providing us with meteorite samples.

References:

Adams, J. B. (1974) J. Geophys. Res., 79, 4829-4836.

Delaney, J. S., Takeda, H., Prinz, M., Nehru, C. E. and Harlow, G. E. (1983) Meteoritics, 18, 103-111.

Delaney, J. S., Prinz, M. and Takeda, H. (1984) J. Geophys. Res., 89, 251-288.

Takeda, H. (1979) Icarus, 40, 455-470.

Takeda, H. and Yanai, K. (1982) Mem. Natl, Inst. Polar Res., Spec. Issue, 25, 97-123.

Takeda, H., Mori, H., Delaney, J. S., Prinz, M., Harlow, G. E. and Ishii, T. (1983) Mem. Natl. Inst. Polar. Res., Spec. Issue, 30, 181-205.

Takeda, H. and Mori, H. (1985) J. Geophys. Res., 90, 636-648.

Toyoda, H., Takeda, H., and Ishii, T. (1986) Abstract 11th Symp. Antarctic Meteorites NIPR (This volume).

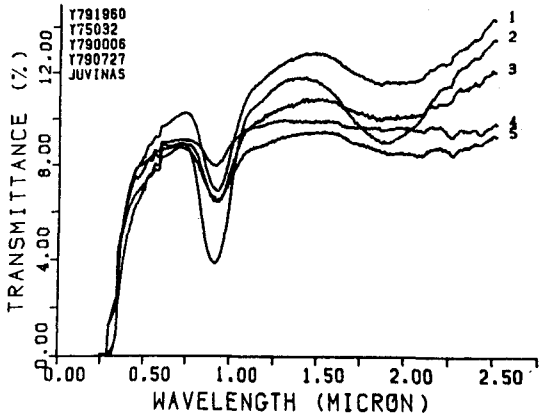

Fig.1 Comparison of transmittance spectra (250-2550nm) of different types of the HED achondrites.

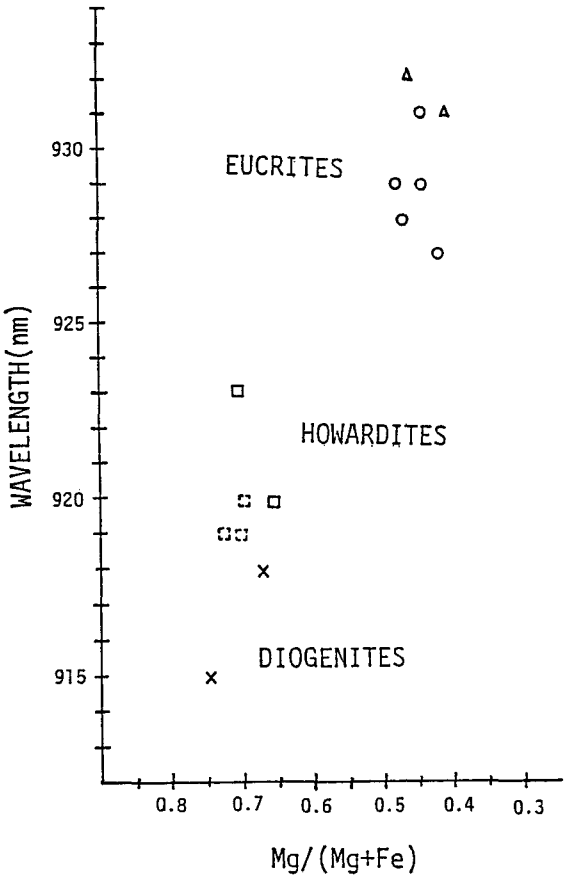

Fig. 3 The wavelength position of the absorption band around 900nm vs. the Mg/(Mg+Fe) ratio of the HED achondrites.

× DIOGENITE
□ HOWARDITE
△ MONOMICT EUCRITE
○ POLYMICT EUCRITE
[ ] Preliminary

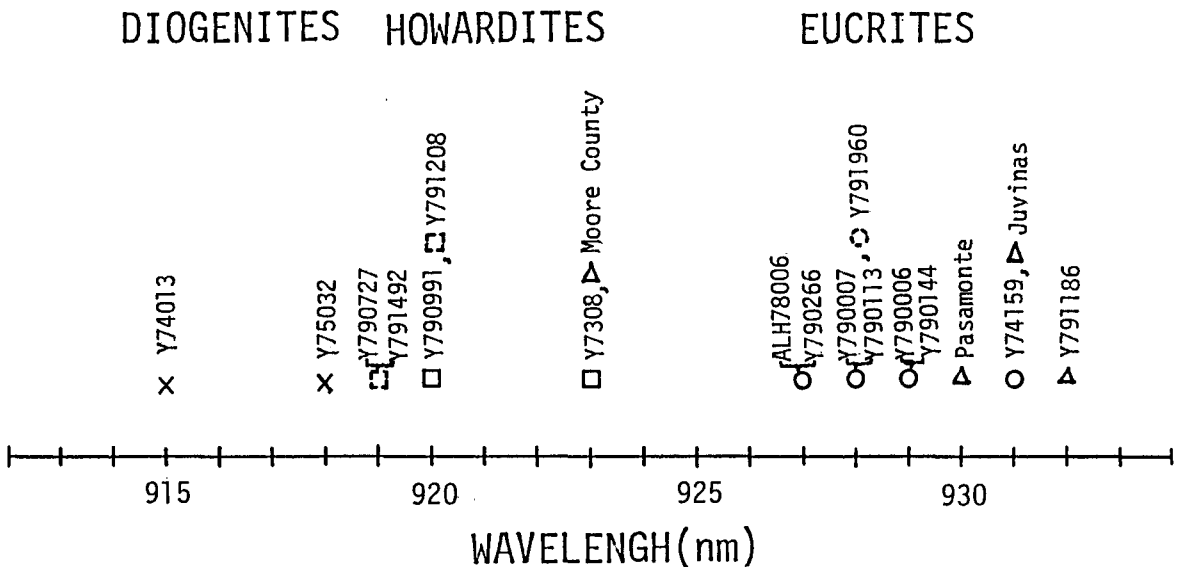

Fig. 2 The wavelength position of the absorption band around 900nm of the HED achondrites.

Diffraction characteristics and thermal histories of the meteoritic and terrestrial Ca-rich plagiclases

Tagai, T., Takeda, H. and Tachikawa, O.
Mineralogical Institute, Faculty of Science
University of Tokyo, Hongo, Tokyo, 113 Japan

Calcic plagioclase is commonly found in meteorite. It shows complicated microstructures, which are characterized by the thermal histories during subsolidus cooling.
In this work, the diffuse scattering in calcic plagioclase, which has usually been interpreted as the result of domain structure, was studied by means of X-ray diffraction.

Calcic plagioclase shows four kinds of reflections in the X-ray diffraction diagram. These reflections are named as a-, b-, c- and d-reflections according to their indices, namely a-reflection with (h+k=even and l=even), b-reflection with (h+k=odd and l=odd), c-reflection with (h+k=even and l=odd) and d-reflection with (h+k=odd and l=even).

The feature of these reflections in the diffraction diagram is characteristic of the thermal history of the feldspar :
The a-reflection is always observed to be sharp and strong and, therefore, the intensity distribution is essentially unaffected by the variation of chemical composition and cooling rate. The b-reflection loose its intensity at about 1200 ^{o}C and in the course of cooling, it appears and sharpens according to the cooling rate (Tagai et al., 1981). The c- and d-reflections loose their intensities not only by elevating temperature but also by increasing sodium content. They loose gradually their intensities up to 500 ^{o}C and their diffuseness is closely connected to the cooling rate (Adlhard et al., 1980a,b). In the plagioclase of about An_{90} from volcanic rocks, only very diffuse streaks are observed in the positions of the c- and d-reflections in the diffraction diagram except sharp a- and b-reflections.

In this study, the following calcic plagioclases in eucrites were investigated and were compared with the terrestrial calcic ones;

1) An_{94} from Moama
2) An_{93} from Serra de Magé
3) An_{90} from Moore County.

In the diffraction diagram, the three plagioclases show very sharp b-reflections and considerably sharp c- and d-reflections in spite of relatively high sodium content. Especially, in the plagioclase from Serra de Magé, remarkably sharp c- and d-reflections were observed. These facts indicate that all these three meteorites were slowly cooled in the temperature range of 1200 - 1000 ^{o}C and 500^{o}C - room temperature. The plagioclase from Moore County was observed to be exsolved to intermediate plagioclase (sodic phase) and anorthite. This plagioclase is one of the most calcic one which shows exsolution. The most interesting fact is that the very diffuse e-reflections (satellites beside b-reflections) are observed in the intermediate plagioclase and sharp c- and d-reflections in calcic phase. It can be assumed that the cooling rate was slow enough to sharpen b-reflections

but not slow enough to make e-reflections sharp at high temperature and that at lower temperature plagioclase was cooled slowly enough to sharpen c- and d-reflections. This thermal history is consistent with those deduced from the pyroxene data (Mori & Takeda, 1981).

In the terrestrial plagioclase, three samples were considered;
4) An_{100} from Pasmeda (metamorphic origin)
5) An_{100} from Miyake (volcanic origin)
6) An_{70} from Sognefjord (plutonic origin).

The anorthites from Pasmeda and Miyake show different diffraction diagrams in spite of the same chemical composition. In Pasmeda, sharp a-,b-, c- and d-reflections were observed but in Miyake, considerably diffuse c- and d-reflections, which can be interpreted as the difference of cooling rate in lower temperature. The plagioclase from Sognefjord show the exsolution between well ordered sodic plagioclase and the calcic one (about An_{85}) with very diffuse c- and d-reflections.

The thermal history of meteorites which include feldspar can well be studied by applying X-ray diffraction method to investigating the microstructure of feldspar with combining electron microscopy.

The authors thank Prof. T. Nagata for the Serra de Magè sample, Dr. M. Prinz for Moore county sample and Prof. J.F. Lovering for Moama sample.

W.Adlhart, F.Frey & H.Jagodzinski (1980a): Acta Cryst. A36, 450-460.
W.Adlhart, F.Frey & H.Jagodzinski (1980b): Acta Cryst. A36, 461-470.
H.Mori & H.Takeda (1981): Meteoritics 16, 362-363.
T.Tagai & M.Korekawa (1981): Phys. Chem. Minerals 7, 77-81.

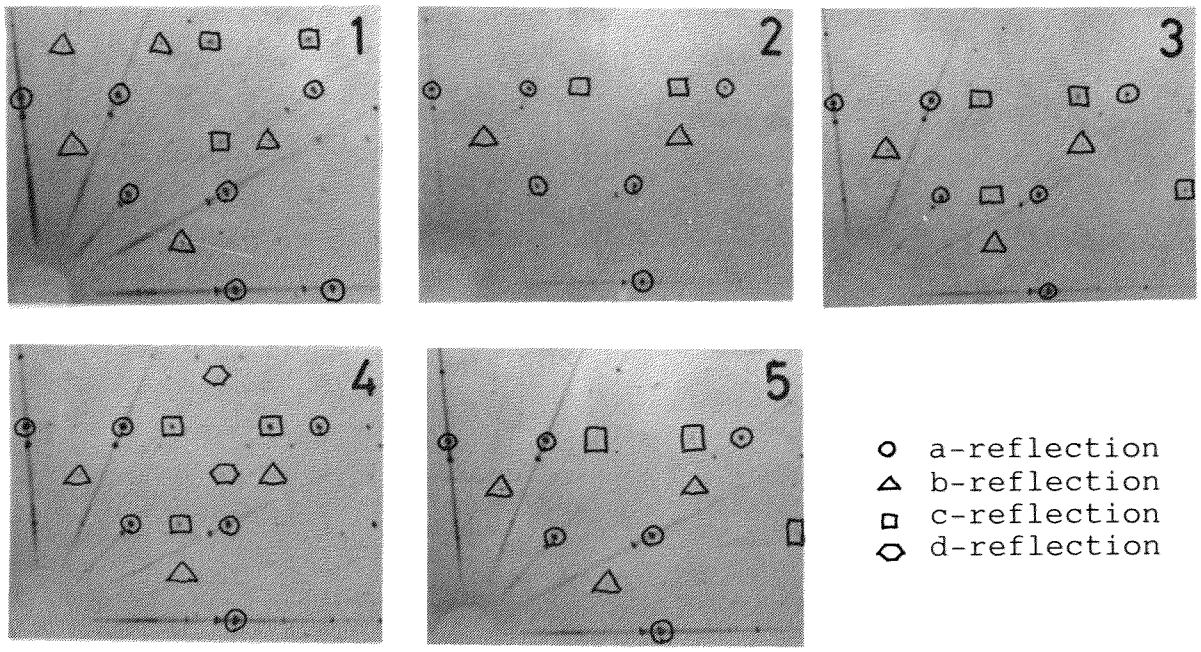

X-ray diffraction photographs of the meteoritic and terrestrial plagioclases

Chemical Zoning of Chondrules in the Allende and ALH-77003 chondrites.

Y.Ikeda*, M.Kimura**and F.Wlotzka*

Max-Planck-Institut für Chemie (*), Ibaraki University (**).

Two chondrules in Allende (CV3) and two chondrules in ALH-77003 (CO3) show remarkable chemical zoning in the groundmasses which are directly in contact with matrix surrounding the chondrules. Zones I, II, III and IV from the core to the rim of the zoned chondrules were defined to be original groundmass, continuous zoning region, discontinuously high-Na and low-Ca zone, and discontinuously high-Al zone, respectively. A zoned chondrule No.4 in Allende includes all zones from I to IV, showing remarkable increase of Na and decrease of Ca from the core to the rim (Fig. 1).

In order to clarify the chemical zoning of chondrules, we carried out heating experiments using synthetic glass beads, the chemical composition of which is represented by a mixture of anorthite and diopside in nearly equal amounts. The glass beads were set in a reagent (NaCl, Na_2CO_3 or $NaSiAlO_4$) and heated at constant temperatures of 800°, 750° and 700°C with a duration ranging from 5 to 320 hours. One result of the heating experiments is shown in Fig. 2, which shows a chemical zoning similar to that of chondrule No.4 in Allende (Fig. 1).

The comparison of the zoned chondrules with the results of heating experiments suggests that the zoned chondrules were formed after the chondrule-formation by the reaction with a nebular gas which might have been produced by evaporation of C1-like materials. The reaction temperatures were lower than 750°C and higher than 300°C.

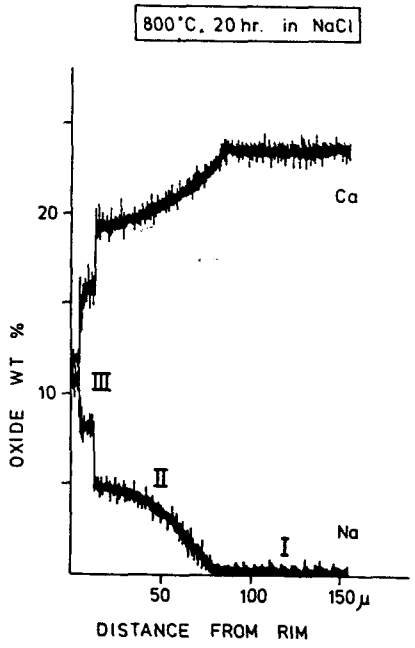

Fig. 2.

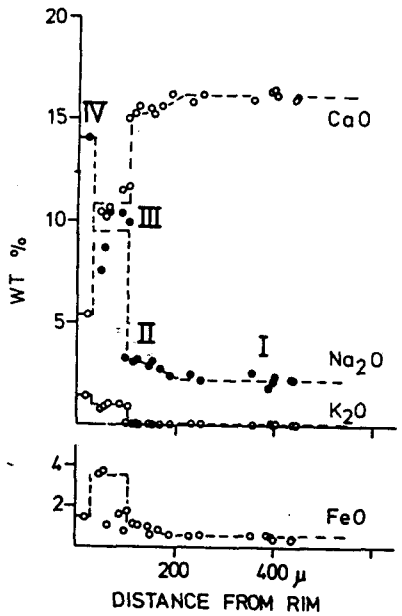

Fig. 1.

PYROXENE CRYSTALLIZATION IN CHONDRULES
- AUTOMETAMORPHIC EVOLUTION OF CHONDRITES -

Masao KITAMURA, Seiko WATANABE and Nobuo MORIMOTO
Department of Geology and Mineralogy, Faculty of Science,
Kyoto University, Sakyo, Kyoto, 606, Japan

Olivine and pyroxene show large compositional variation in type 3 chondrites, but they become homogeneous as the petrologic type increases. The homogeneity in a chondrite has been interpreted to represent the degree of metamorphism of the chondrite. Two models have been presented on the metamorphism (Fig. 1); (i) prograde metamorphism, and (ii) autometamorphism. The former model derives the chondrites of the higher petrologic types from the primitive type 3 chondrite through the metamorphism due to reheating after accretion. In the latter model, the chondrites of different petrologic types represent different cooling rates before or during the accretion process.

The characteristics, which have been used to define the petrologic types [1], have been considered to indicate the prograde metamorphism model. However, recent analytical electron microscopic study on the fine textures of pyroxenes in chondrules has suggested the autometamorphism model [2]. In the present paper, the chemical zoning of the pyroxenes in chondrules has been studied to elucidate the crystallization process of the pyroxenes and the possibility autometamorphism.

Chemical zoning of pyroxenes in chondrules of the ordinary chondrites (H, L and LL) was studied by a backscattered electron imaging method (BEI) and an electron probe microanalyzer. Enstatite and carbonaceous chondrites have been studied with E3 and C3. Augite and pigeonite are different in the appearance and texture among the petrologic types. In type 3, augite occurs mostly as thin rims of the Ca-poor pyroxene (see Figure 1 in Watanabe et al. in the present symposium) and rarely as small dendrites in the mesostasis. As the petrologic type increases, the augite rim becomes thicker, and augite also appears as single crystals. In type 3, pigeonite generally appears as thin rims of the Ca-poor pyroxene. A few single crystals of pigeonite were observed in types 4 and 5.

In both metamorphic models, the chemical zoning of pyroxene in type 3 can be explained by rapid cooling. The chemical zoning in the higher petrologic types is differently explained. However, in the prograde metamorphism model, there arise some difficulties in explaining the formation of the chemical zoning of pyroxenes. The first difficulty is on the increase of thickness of the augite rim by increase of the petrologic types. Since augite was considered to have coarsened through the devitrification of glass, the mesostasis near the thick augite rim should be depleted in augite component. However, no significant depleted zone was observed (Figure 2).

The second difficulty is on the formation of pigeonite. Pigeonite in the chondrites is stable only above ~1100°C. If the chondrites are reheated upto the temperature of ~1100°C, not only the metal-sulfides but also the silicate minerals partially remelt. However, no chondrites show evidence of the partial melting. Therefore, pigeonite must not be recrystallized by reheating but be left metastably after the primary crystallization at the chondrule formation. Since pigeonite should decompose into orthopyroxene and augite under the metamorphic temperatures (400°C - 800°C) [3], and no such decomposition has been observed in the microscopic scales (Figure 3), the diffusion distance in pigeonite during reheating must have been very small. This seems to conflict with the requirement of the wide range diffusion to explain the similarity of compositions of pyroxenes among the chondrules in the type 4 and 5 chondrites.

In the autometamorphism model, the thickening of pigeonite and augite can be well explained by the cooling processes as shown in Figure 1a. The homogeneity in composition among the pyroxenes in the higher petrologic types is also well explained.

In conclusion, the compositional zoning and appearance of pyroxenes in the ordinary chondrites can be better explained by the autometamorphism model than the other model.

REFERENCES

[1] Van Schmus,W.R. and Wood,J.A.; Geochim. Cosmochim. Acta, **31**, 747-765, 1967.
[2] Watanabe,S., Kitamura,M. and Morimoto,N,; Earth Planet. Sci. Lett., **72**, 87-98, 1985.
[3] Dodd,R.T.; Geochim. Cosmochim. Acta, 33, 161-203, 1969.

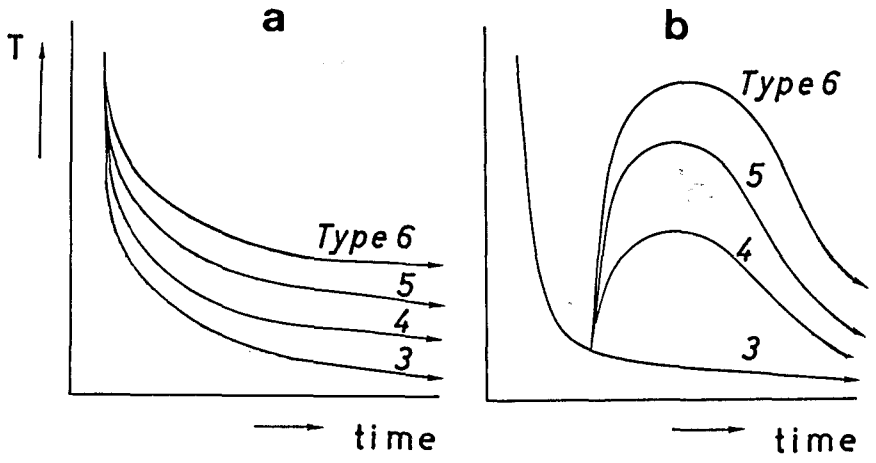

Figure 1 Schematic diagram of the temperature change on time for the autometamorphism model (a) and the prograde metamorphism model (b).

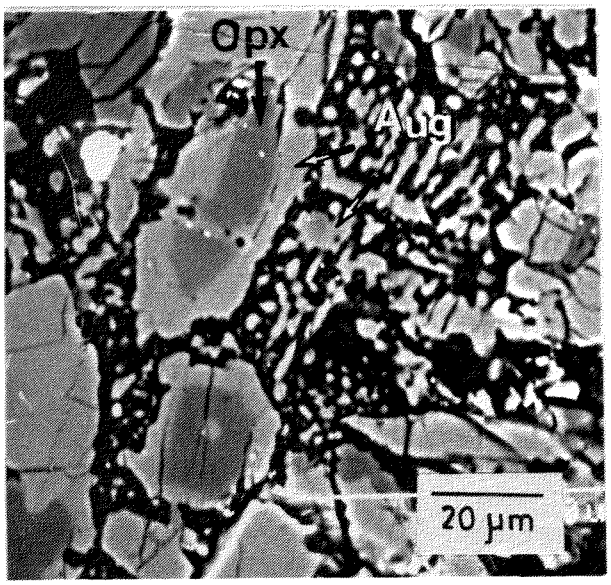

Figure 2. Porphyritic pyroxene chondrule in H5. Thick augite rim and small grains of augite in the mesostasis.

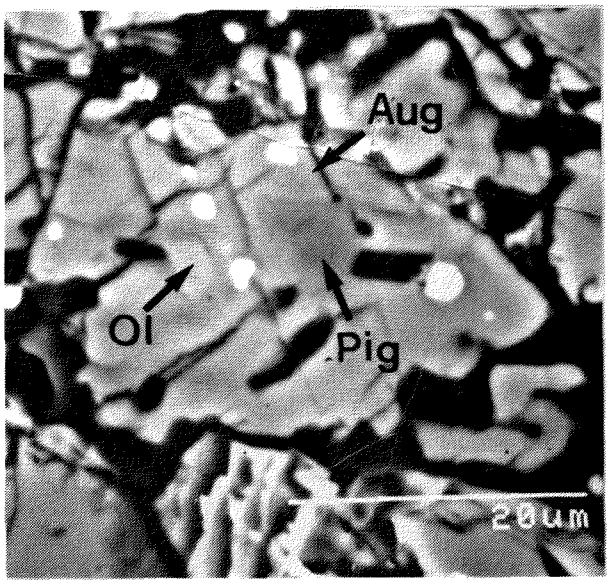

Figure 3. Porphyritic pyroxene chondrule in H5. Pigeonite and augite coexit with a sharp boundary.

OSCILLATORY ZONING OF PYROXENES IN ALH-77214 (L3)

Seiko WATANABE, Masao KITAMURA and Nobuo MORIMOTO
Department of Geology and Mineralogy, Faculty of Science, Kyoto University, Sakyo, Kyoto 606, Japan

Compositional zoning of pyroxenes in porphyritic chondrules in ALH-77214 (L3) has been studied by the backscattered electron image (BEI) method. Though the Ca-poor pyroxenes widely show an increase of the Fe- and the Ca-component from the core to the rim, close examination of the fine textures indicates that most of them show the oscillatory changes in composition.

Figure 1 is a typical example of a chondrule of which pyroxenes show several growth bands as the oscillatory zoning parallel to the rim. Figures 2 (a) and (b) are BEI's of two pyroxene grains in a chondrule. The width of each growth band is similar between the two pyroxenes. EPMA analyses across the oscillatory zoning were carried out on the two pyroxene grains (Figs. 2(a) and (b)). Characteristics of these zonings (Figs. 3(a) and (b)) are;

(1) Oscillatory zoning is due to the oscillatory change of the Mg-Fe-Ca ratios in pyroxenes. The change from bright to dark corresponds to abrupt increase of the Mg-component (dotted lines in Figs. 3(a) and (b)).

(2) Two pyroxene grains in a chondrule have the similar oscillation in composition (Fig. 3), in addition to in width of growth bands (Fig. 2).

Since the chondrules cooled in the surrounding gas and/or dusts, the oscillation of the Mg-Fe-Ca ratios in pyroxenes are considered to have taken place either by change of the circumstances where the chondrules formed, or by local fluctuation of the condition within chondrules. The similarity in oscillatory zoning of the two pyroxene grains suggests that the oscillation was controlled by the circumstances. In order to explain the abrupt increase of the Mg-component by the fluctuation of temperatures, the growth front with the Fe-rich composition should once melt. However, since all the growth bands are parallel to the rim, it is difficult to explain the oscillatory zoning by the fluctuation of temperatures. The most probable explanation is the fluctuation of the redox condition, that is, reducing circumstances should have caused the reduction of Fe^{2+} in the chondrule melts, resulting in the abrupt increase of the Mg-component.

The oscillatory zoned pyroxenes occur commonly in chondrules in ALH-77214, and may also in other type 3 chondrites.

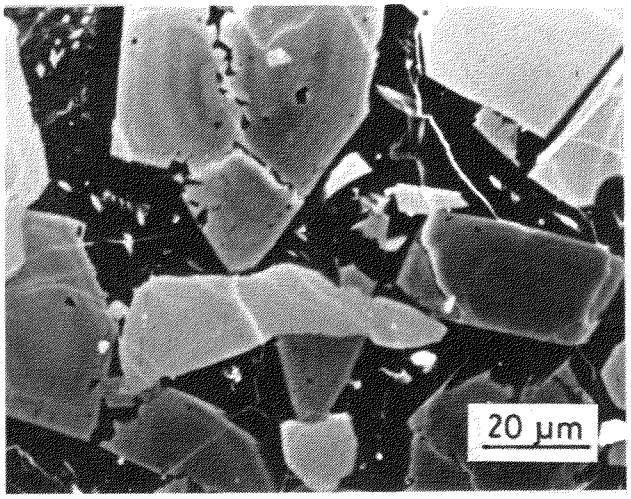

Fig. 1 BEI of a porphyritic chondrule. Pyroxene shows the concentric changes in contrast.

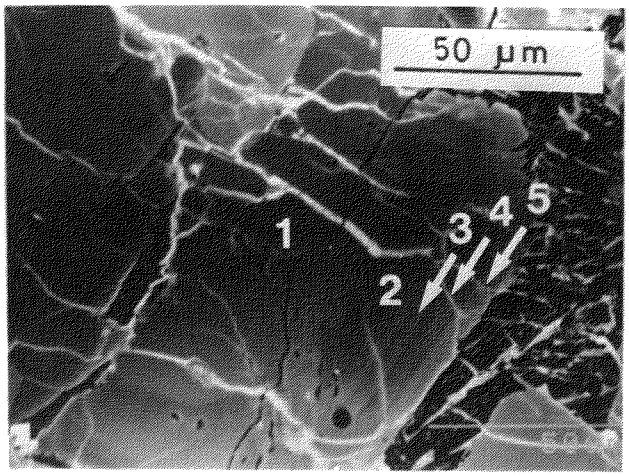

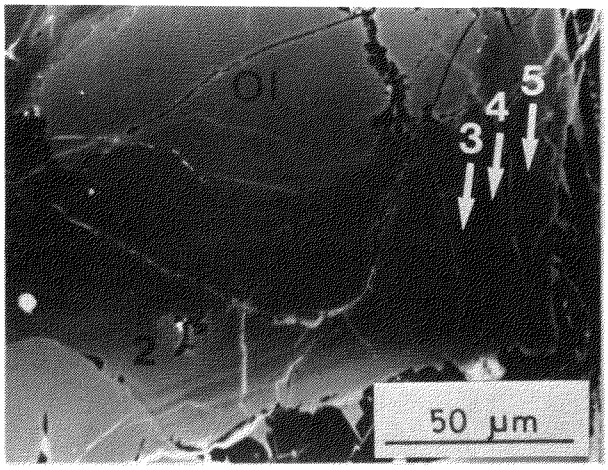

Figs. 2(a) and (b) BEI of two pyroxenes in a chondrule. Note the similarity in the width of growth bands between (a) and (b).

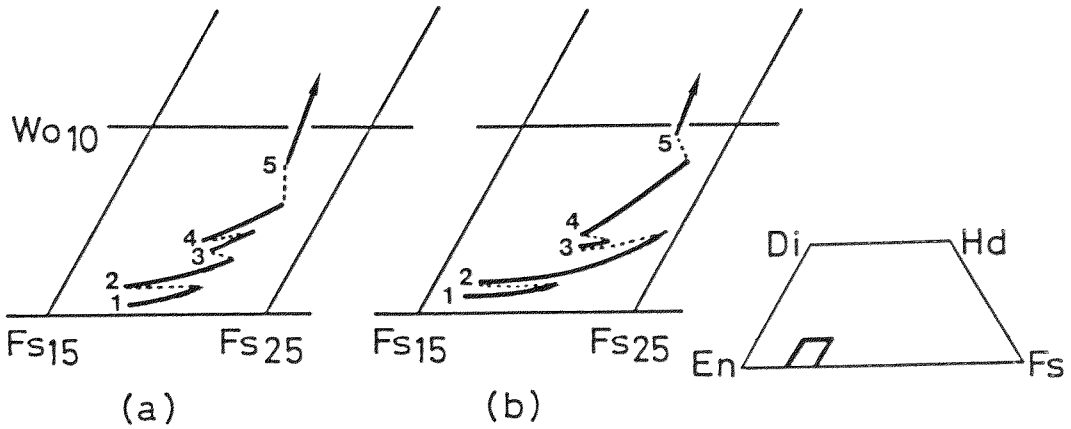

Figs. 3(a) and (b) Compositional change across the zoning of pyroxenes in Figs. 2(a) and (b), respectively. Number corresponds to that for each growth band.

TEXTURAL AND CHEMICAL STUDIES OF SOME ANTARCTIC IRON METEORITES

Saito, J., Tagai, T., Tachikawa, O. and Takeda, H.
Mineralogical Institute, Faculty of Science, Univ. of Tokyo,
Hongo 7-3-1, Tokyo 113

The preliminary description by Clarke et al. (1981) reported that ALH-77283 contains the carbonado-type diamond and lonsdalite nodules previously described from the Canyon Diablo meteorite. In this study, the pressure and temperature of a shock event of ALH-77283 are estimated.

Typical micrographs of the texture of the ALH-77283,52 are shown in Fig. 2 and 3. These micrographs indicate that the shock textures of ALH-77283 is in general simillar to the Canyon Diablo meteorite. Since the shock textures of iron-nickel minerals were described in detail by Heymann et al. (1966), this study has been carried out comparing the previous description of the shock textures.

On the etched surface of kamacites of ALH-77283,52, neumann-bands have been observed but they are of little use.

There are shock-hatched kamacites on the sample. The bristles of shock-hatched kamacites are very fine and sharp. The shock-hatched kamacites appear in localized areas, and not throughout the entire specimen. The sample contains a few isolated patches of shock-hatched kamacites. The appearance of these isolated patches of shock-hatched kamacites is simillar to those of the Canyon Diablo meteorite reported by Heymann et al.(1966). These shock-hatched kamacites are useful for estimation of shock pressure.

We found partially recrystallized kamacites on the microscope scale (Fig. 3). They appear in localized areas, mainly beside the cohenites. By combining these results, we can estimate the shock pressure and temperature.

At the pressure greater than 130 kb, a transformation structure appears on kamacites. The appearance of shock-hatched kamacites changes with pressures from 130 to 600 kb showing a progression of metallographic structures (Heymann et al. 1966). Differences were found in meteoritic iron artificially shocked to 190-600 kb (Heymann et al. 1966). From this study, they stated that at the lower pressure, the neumann bands begin to show a slight amount of feathering and at higher pressure, the neumann bands show a well developped transverse hatching. The appearance of shock-hatched kamacites is more simillar to that produced at about 600 kb than that of at about 190 kb of Canyon Diablo meteorite.

The relationships between shock pressure and residual temperature are well known for pure iron, and this data can be apllied to kamacite with small error (Heymann et al. 1966). Clarke et al. (1981) estimated the shock pressure of 200-750 kb by employing Heymann's procedure. However, we think that the shock pressure will be estimated more accurately by detail study of shock-hatched kamacites.

Heymann et al. (1966) suggested that the kamacites begin to recrystallize at the temperature around 500°C (Fig. 1). The partially recrystallized kamacites observed in ALH- 77283 may indicate the temperature about 500°C.

In summary, we can estimate the pressure and temperature of the shock event by plotting our data on Fig. 1 . From the shock-hatched kamacites, we estimate the pressure at 600-750 kb and from the recrystallized kamacites, we estimate the temperature at about 500°C. These estimation is

within the range of the diamond formation.
Acknowledgements: We thank National Institute of Polar Research for meteorite sample.

References: Clarke, R.S.Jr., Applemen, D.E. and Ross, D.R. (1981) Nature 291, 396-398, Heymann, D., Lipschutz, M.E., Nielsen, B. and Anders, E. (1966) J. Geophys. Res. 71, 619-641

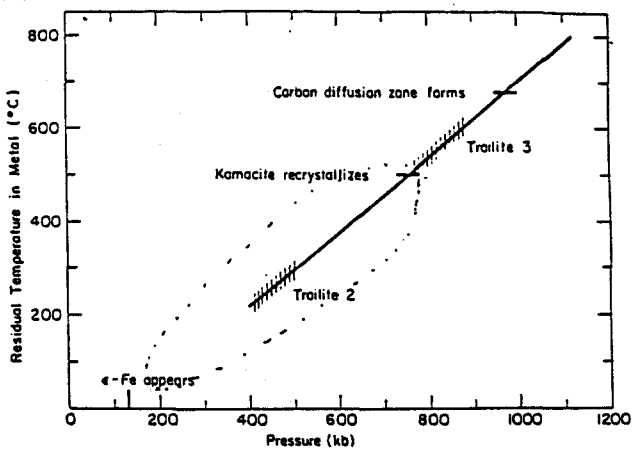

Fig. 1 Residual temperature of shocked iron

Fig.2 SEM photograph of shock-hatched kamacite

Fig.3 Recrystallized kamacite

Spinel-group Minerals in Ordinary Chondrites

Hideo YABUKI[1)], Makoto KIMURA[2)] and Ahmed EL GORESY[3)]

1) The Institute of Physical and Chemical Research, Wako, Saitama 351-01
2) Ibaraki University, Mito, Ibaraki 310
3) Max-Planck-Institut fur Kernphysik, 6900 Heidelberg, Germany

Because of their wide range in composition, spinel-group minerals bear various informations on the circumstances under which they crystallized out. Previously we reported that Mg-Al-rich members of spinels can be seen as an accessary mineral in all types of L- and LL-chondrites except in petrologic type 6 (1). Including those found in H-chondrites we will discuss here the chemistry of spinels and of coexisting phases as well as its relation to the bulk composition of chondrules.

In contrast with chromite, almost all of Mg-Al-rich spinels are included in chondrules or chondrule fragments and show distinct compositional zoning. Those chondrules are mostly porphyritic and rarely barred, olivine and glass ones. Zoning of spinels can be devided into three different types, i.e. (a) with Mg-Al-rich core and Fe-Cr-rich rim ("normal" zoning), (b) its reverse ("reverse" zoning) and (c) a special case of "normal" zoning, in which compositional change is not gradual but Mg-Al-rich core is entirely or partly surrounded by Fe-Cr-rich rim with a sharp boundary ("jump" zoning, Fig.1). These three types of zoning features occur in the same chondrite but never in the same chondrule. In matrices of H-chondrites of low petrologic types hundred-micron-sized clasts are noticeable, which are mainly composed of glassy material and fine-grained spinels without zoning (Fig. 2).

The occurrense of "jump" zoning is suggestive that it is resulted from the reaction with Fe-Cr-rich melt (or gas) before aggregation. "Reverse" zoning is still puzzling but the capture of chromite or Mg-Al-chromite by Mg-Al-rich chondrule melt might be one of the possible interpretations. In L- and LL-chondrites most spinels show either "normal" or "reverse" zoning. On the other hand, over one half of spinel grains in H-chondrites do not show distinct zoning, and especially "reverse" zoning could not be seen in any of them. "Jump" zoning is contrarily fairly common in H-chondrites of low petrologic types and quite rare in other clans. As an exceptional case, a spinel grain with this type of zoning was found in an LL5 chondrite (Fig. 1), which brings up a question to us because thermal metamorphism would have readily changed "jump" zoning into gradual one. Though spinels are generally rare in type 5 chondrites as compared with in lower petrologic types, clear zoning is observable in over half of them.

Zoning of spinels ranges usually from plaonaste to Mg-Al-chromite and never reaches to the composition of chromite in matrices. This compositional gap implies that there is no genetic relationship between zoned spinels in chondrules and matrix chromites. Fe/(Fe+Mg) ratios of spinels, especially of Mg-Al-rich ones, show a clear-cut trend of H<L<LL in every

petrologic type. They are strongly correlative with the Fe/(Fe+Mg) ratios of host chondrules. Coexisting phases with spinels in chondrules are usually olivine, pyroxenes and mesostasis as glassy materials. Crystallization sequence seems to be olivine, spinel, and then pyroxenes, according to their occurrence. Pyroxenes are bronzite or hypersthene, pigeonite and Ca-rich pyroxenes, all of which usually show remarkable enrichment with aluminum. Their Al_2O_3 contents reach to 17.2, 7.5, and 15.3 wt%, respectively. Fassaite can be also seen in some cases. It seems to be indicating that spinels are crystallized from fairly Ca-Al-rich chondrule melt. Distinct linear relationship can be noticed between Al/(Al+Cr) of spinels and Al/(Al+Na+K) of chondrule bulk.

(1) YABUKI, H. et al., (1983), Meteoritics 18, 426-427.

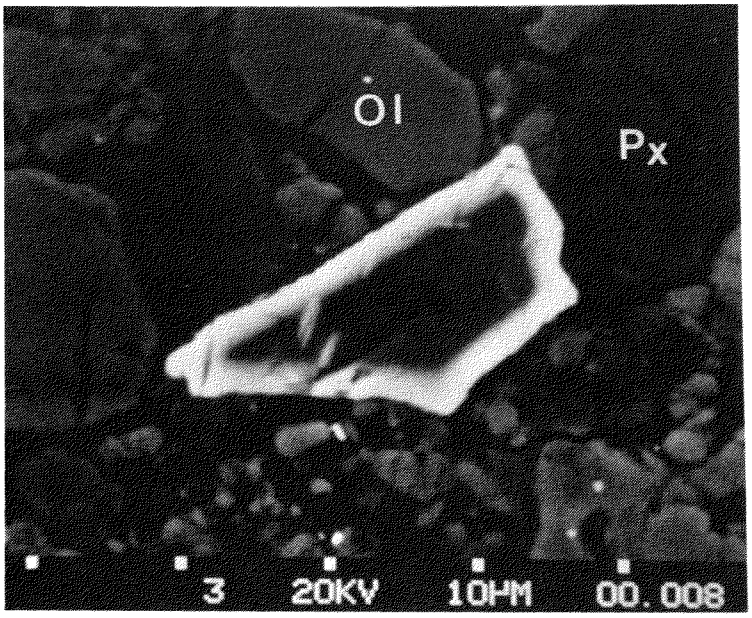

Fig. 1. A fine grain of spinel showing "jump" zoning. Dark, Mg-Al-rich core (MgO 14%, Al_2O_3 64%, FeO 19%, Cr_2O_3 2%) is surrounded by bright Fe-Cr-rich rim (MgO 3%, Al_2O_3 16%, FeO 30%, Cr_2O_3 46%) with a sharp boundary. Thin inclusion is ilmenite. Ol and Px represent olivine and pyroxene, respectively. Krahenberg (LL5). Backscattered electron image.

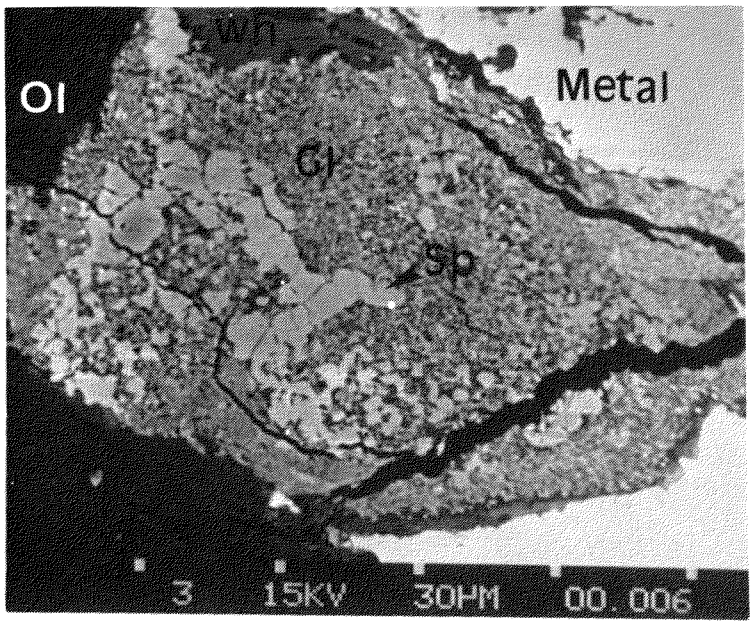

Fig. 2. A clast composed of glassy groundmass (Gl), spinel (Sp) and whitlockite (Wh) at the margin. Olivine (Ol), and metallick nickel-iron (Metal) are seen next to the clast. Dhajala (H3). Backscattered electron image.

PERRYITE PROBLEM

Akihiko Okada* and Klaus Keil**

* Institute of Physical and Chemical Research, Wako, Saitama
**Department of Geology and Institute of Meteoritics, University of New Mexico, Albuquerque, NM 87131, USA

Of the known meteoritic minerals, perryite, a nickel silicide mineral containing minor amounts of iron and phosphorus, has not yet been well characterized because of the lack of the knowledge about its crystal structure. This mineral is usually present as fine-grained inclusions, less than 20 micrometers wide, within kamacite and as a very thin rim around kamacite of enstatite chondrites (Hvittis, Indarch, Khairpur, Kota-kota, St. Mark's, South Oman, Allan Hills A77156, Yamato 691 etc.), enstatite achondrites (Mount Egerton and Norton County) and an unusual iron meteorite, Horse Creek. Ramdohr (1963) described perryite as $(Ni, Fe)_x(Si, P)_y$, and later he suggested that the X-ray powder pattern of perryite is very similar to that of kamacite, and that it may be $(Ni, Fe)_2(Si, P)$ having a body-centered cubic structure (Ramdohr, 1964). However, the molecular formula is not consistent with the compositional data obtained by electron probe microanalysis. The atomic ratio, (Ni, Fe)/(Si, P), of perryite is 2.30-2.78 (Fredriksson and Henderson, 1965; Okada, Keil and Taylor, 1986; Reed, 1968; Wai, 1970). Wai (1970) proposed an ideal molecular formula, $(Ni, Fe)_5(Si, P)_2$, based on the structural formula calculated from electron microprobe data. No X-ray study of perryite has yet been reported so far in spite of its importance for the understanding of the chemical and physical properties of the mineral. It might be the reason why the separation of fine-grained perryite from the host kamacite is technically difficult. In this work, perryite crystals were separated from kamacite of Norton County enstatite achondrite by using $CuCl_2$-KCl solution which dissolves only metallic nickel-iron. In addition, synthetic crystal was prepared by reacting nickel, iron, silicon and Ni_5P_2 in argon gas and solidifying the melt slowly from 1350°C. Although both meteoritic and synthetic perryites are twinned, the reciprocal nets examined by single crystal X-ray diffraction indicate that perryite is rhombohedral with possible space group, R3c, R32 or R$\bar{3}$c. The lattice dimensions based on hexagonal setting are $a \cong 6.7$ and $c \cong 38$ A. Compared with Ni_5Si_2 which has trigonal symmetry with a=6.67-6.68 and c= 12.28-12.29 A (Saini et al., 1964; Frank and Schubert, 1971), the dimension of c-axis is three times longer.

REFERENCES: Frank, K. and Schubert, K. (1971): Acta Cryst., B27, 916; Fredriksson, K. and Henderson, E. P. (1965): Trans. Amer. Geophys. Union, 46, 121; Okada, A., Keil K. and Taylor, G. J. (1986): Chem. Erde (to be published); Ramdohr P. (1963): J. Geophys. Res., 68, 2011; Ramdohr, P. (1964): Sitzungber. deutsch. Akad. Wiss. Berlin (Chem. Geol. Biol.), No.5, 1; Reed, S. J. B. (1968): Mineral. Mag., 36, 850; Saini, G. S., Calvert, L. D. and Taylor, J. B. (1964): Can. J. Chem., 42, 1511; Wai, C. M. (1970): Mineral. Mag., 37, 905.

MG-FE PLAGIOCLASE COMPOSITIONS IN ANTARCTIC CHONDRITES (I)

Miura, Y.[1], Yanai, K.[2] and Abe, T.[1]
1) Department of Mineralogical Sciences and Geology, Faculty of Science, Yamaguchi University, Yoshida, Yamaguchi, 753.
2) National Institute of Polar Research, Itabashi, Tokyo 173.

Differences in Mg and Fe contents of plagioclase(-like) phases indicate the different formation condition and process [1-5]. Remarkable differences in the Mg-Fe plagioclase compositions in twenty-five chondritic meteorites are summarized on the basis of relation between the ratio Mg/(Mg+Fe) [i.e. *mg*] and An-content as follows (cf. Figs. 1 and 2):

1. Maximum values of *mg* ratio and An-content are observed in EH3 and LL3 chondrites, respectively.
2. Maximum values of MgO and FeO in the plagioclase(-like) phases are 8.8 and 9.5 wt.%, respectively.
3. Petrologic type 3 chondrites contain much (amorphous) Mg-rich phases with scarce data.
4. Petrologic type 6 chondrites involve much (crystalline) Fe-rich phases with the continuous data expressed by the similar compositional trend as shown in Figs. 1 and 2.
5. Differences in chemical groups of E, H, L and LL can be explained by the An-content of the Mg-rich phases as shown in the different overall chemical trends of Figs. 1 and 2.
6. The Mg-rich phases (with the An-rich) considered as the one of the primordial products are assumed to be formed under the condition of the higher temperature and rapid cooling, whereas the Fe-rich phases are formed at lower temperature and slower cooling.
7. The Mg-rich phases with the higher An-content are observed in LL chondrites, whereas those with poor An-content are found in E chondrites.
8. The continuous data of the various *mg* ratios depend upon the accretion process to chondritic body.

In conclusion, the formation condition and process in the various chondritic meteorites can be discussed by the plagioclase(-like) compositions as shown in Figs. 1 and 2.

The authors thank Mr. H.Miura, graduate student of Yamaguchi University, for his help of the calculation of EPMA data.

REFERENCES:

[1] Miúra, Y. (1984): Mem. Natl Inst. Polar Res., Spec. Issue,35, 226-242.
[2] Miúra, Y. et al. (1984): ibid., 210-225.
[3] Miúra, Y., K. Yanai and T. Tanosaki (1985): Proc. Symposium on Antarctic Meteorite X (Tokyo), 66-68.
[4] Miúra, Y.(1986): Lunar and Planetary Science XVIII (Houston) pp.2 (in press).
[5] Miúra, Y. (1986): Proc. Symposium on Antarctic Meteorite XI (in this volume). pp.3.

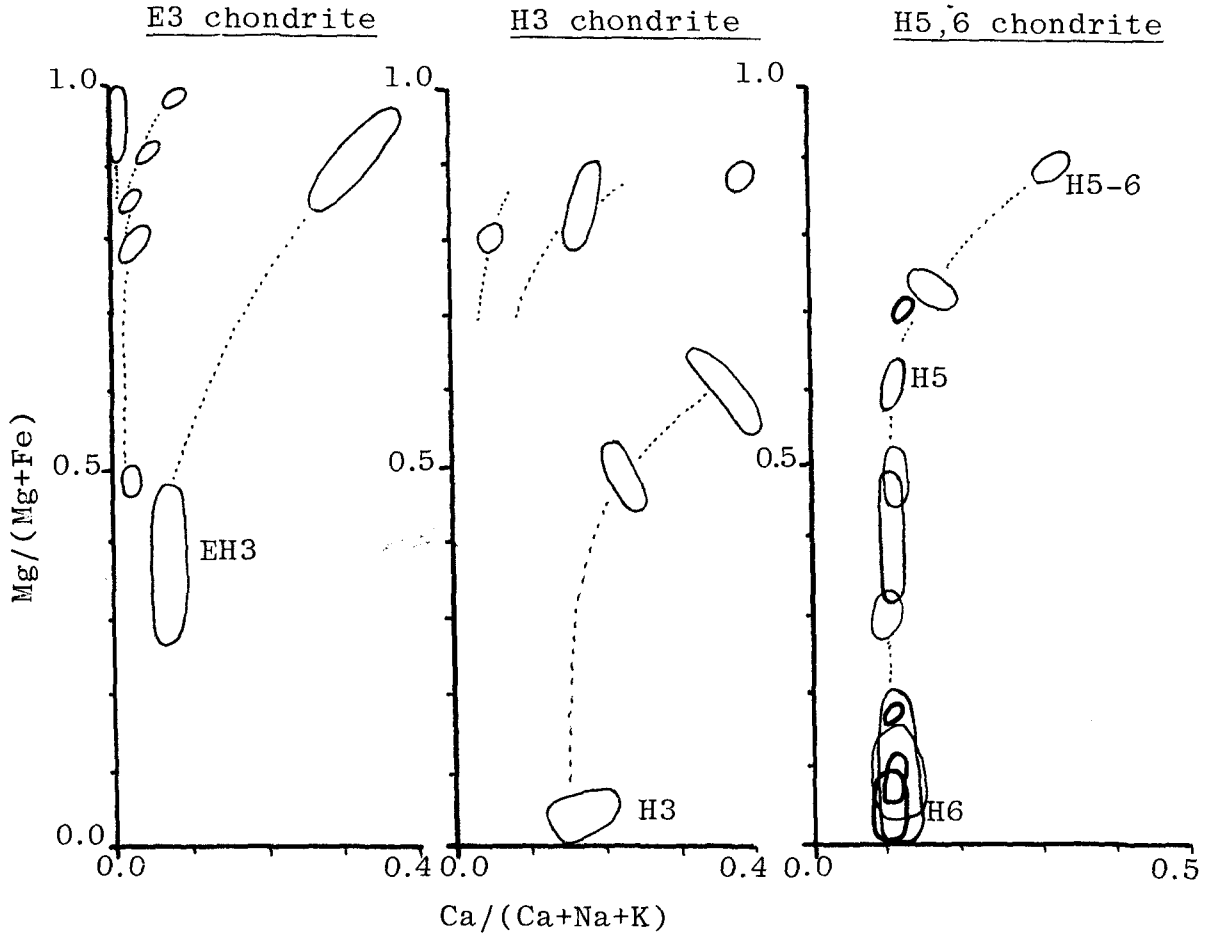

Fig.1. Relation between Ca/(Ca+Na+K) and Mg/(Mg+Fe) of plagioclase(-like) compositions in E3, H3 and H5·6 chondrites:

EH3: Yamato-691,80-1
Yamato-691,89
Yamato-74370,81-4

H5 : Plainview

H5-6:Yamato-75647,95-3

H3: Nio-3(Miyano)
ALH-77299,6
Yamato-791500,80-1

H6: Yamato-74640,81
ALH-768,65-2
ALH-77288,64

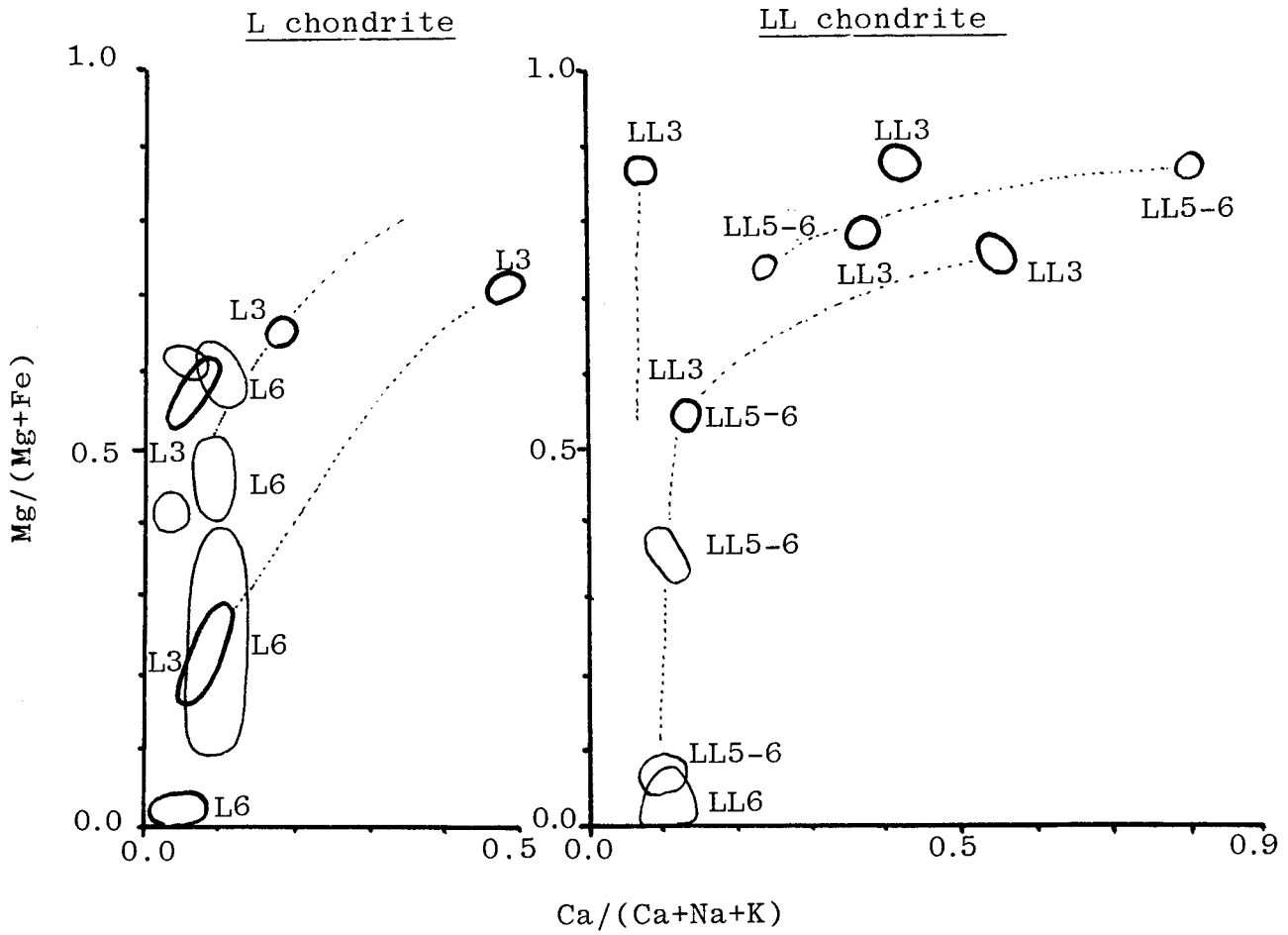

Fig. 2. Relation between Ca/(Ca+Na+K) and Mg/(Mg+Fe) of plagioclase (-like) compositions in L and LL chondrites:

L3 : ALH-77214,90-1
ALH-77214,93

L6 : Yamato-74190,72-3
Yamato-74362,84-3
Yamato-75102,74
Yamato-75115,91-2
ALH-769,85-3
ALH-769,75
Holbrook
Willard

LL3: Yamato-74660, 84-3
ALH-77278,85-3

LL5-6: Yamato-74646,93

LL6: Yamato-75258,97

REE PARTITIONING AND THE SHERGOTTY PARENT MELT: EVIDENCE FOR COMPLEX PETROGENESIS AND AGAINST METASOMATIC ALTERATION.

G. McKay (SN4, NASA-JSC, Houston TX 77058), J. Wagstaff, and L. Le (Lockheed, 1830 NASA Rd. 1. Houston, TX 77258)

Introduction. The shergottites are a group of igneous-textured meteorites which may be from mars [e.g.,1]. Despite extensive study by the Shergotty Consortium (see [2] and ref's. therein), chronology and petrogenesis of the Shergotty meteorite remain controversial. One aspect of this controversy concerns whether Shergotty has undergone metasomatic alteration [3,4]. Another concerns the Sm/Nd ratio of the Shergotty parent melt (SPM), and the resulting implications for the complexity of melt generation processes. While Shergotty's bulk Sm/Nd is greater than chondritic, the source region (SR) is constrained by isotopic systematics to have Sm/Nd less than chondritic [3,5,6]. If $Sm/Nd_{SPM} < Sm/Nd_{SR}$, this melt could have been generated by simple processes such as equilibrium partial melting of common mafic mineral assemblages [7]. However, if $Sm/Nd_{SPM} > Sm/Nd_{SR}$, more complex processes (e.g., batch melting [8]) are required.

Because Shergotty is a PX cumulate, the composition of its parent melt must be inferred from bulk or mineral compositions and appropriate PX/LIQ D's. Following [9], Smith *et al.* [7] noted a correlation with Fe/Mg among literature phenocryst/matrix D(CPX,REE) (Fig. 1, data from [10]), and used D's so derived to obtain $Sm/Nd_{SPM} < Sm/Nd_{SR}$, and hence inferred simple petrogenetic processes. McKay *et al.* [11,12] experimentally measured D(REE,PX/L) for PX and melts similar in major ele. comp. to the homogeneous magnesian cores of Shergotty PX phenocrysts and the inferred SPM of [13], found much lower D's than those used by [7] (Fig. 1), consequently obtained $Sm/Nd_{SPM} > Sm/Nd_{SR}$, and hence inferred complex petrogenetic processes. This conclusion rested on two assumptions: First, that only the homogeneous PX cores are cumulus (the zoned rims being adcumulus [13]), and second, that Shergotty has been a chemically closed system since crystallization (a requirement of the method used to calculate the trace element (TE) content of the melt [14]). If portions of the zoned rims are cumulus [15], and if D's increase markedly with Fe/Mg [7], previously measured D's [11,12] would not apply, and effective D's might be large enough to permit $Sm/Nd_{SPM} < Sm/Nd_{SR}$. Also, if the bulk REE content of Shergotty has been altered since crystallization, the method used to compute melt TE content is invalid, Sm/Nd_{SPM} becomes poorly constrained, and little can be inferred about the processes by which the SPM was generated.

In [16] and this abstract we report D's measured for evolved PX and melt derived through ~50% crystallization of a synthetic SPM starting composition, thereby addressing the case in which portions of the zoned PX rims are cumulus. In addition, we discuss implications of recently reported Sm and Nd analyses of separated pyroxenes [3,4] for the issue of whether Shergotty has undergone metasomatic alteration. Finally, we address the issue of whether LREE enrichments observed in Fe-rich pyroxene separates [3,4] are a consequence of simple closed-system crystallization.

Experimental Results. Experimental and analytical techniques are similar to our earlier ones [11,12]. Charges quenched from 1035, 1045, and 1052°C (QFM) consisted of ~50% glass, subequal amounts of CPX (aug. zoned to ferropig.) and PL, and minor Ti-magnetite. The composition of glass from the 1045°C run is Si=50.2; Ti=1.8; Al=9.2; Fe=24.1; Mn=0.60; Mg=1.4; Ca=8.3; Na=1.7; K=0.56; Nd=0.47; Sm=0.22 (wt% oxide). PX compositions from the three runs are shown in Fig. 2, along with PX for which we previously measured D's [11,12], and Shergotty homogeneous cores [13]. In contrast to our earlier study, PX from the present runs spans a large range of Fe/Mg, comparable to that observed in Shergotty [13].

D's for Sm and Nd are plotted against WO in Fig. 3 and mg' in Fig 4. Correlations with WO are in general agreement with those from our previous experiments [13]. Although no correlation with mg' is apparent from Fig. 4, multiple least squares analysis shows a weak negative correlation. The lack of a strong correlation with mg' suggests that factors in addition to Fe/Mg are largely responsible for the correlation of phenocryst/matrix D's with mg' in Fig. 1. Such factors probably include melt composition and (T,P) of equilibration.

REE Pattern of the SPM. The major result of the present study is that D's for Shergotty zoned PX rims do not differ markedly from those for the homogeneous cores, at least well past initial PL crystallization. (Absence of a Eu anomaly argues against the presence of cumulus plagioclase in Shergotty [13,15].) Hence use of D's measured for the core compositions does not lead to significant errors in calculated melt TE content, even if portions

of the zoned rims are cumulus. Thus the present results support the validity of our previous SPM calculated melt compositions [11,12].

Those melt REE compositions are shown in Fig. 5. They are based on the bulk Shergotty composition reported by [5], also shown. Two extreme melt compositions are shown. One corresponds to 70% trapped intercumulus liquid (TL), the case where only the homogeneous PX cores are cumulus as proposed by [13], and the other to 30% TL, an extreme lower limit if Eu-based arguments for the absence of cumulus plagioclase are accepted. Isotopically constrained Sm/Nd ratios of the Shergotty SR are shown (at arbitrary absolute levels) for two extremes of proposed crystallization age [5,17]. All permissible values of Sm/Nd_{SPM} are much greater than all permissible values of source Sm/Nd, thereby precluding simple petrogenetic processes, unless bulk Sm/Nd has been altered by metasomatism.

EVIDENCE AGAINST METASOMATISM. Also shown in Fig. 5 is the SPM REE composition calculated by [4]. Sm and Nd values were obtained simply by dividing the abundances in a very primitive augite [3] by D's previously reported by us [12]. This calculation assumes that the augite is uncontaminated cumulus material, unaltered since crystallization. Excellent agreement between those mineral-based Sm and Nd values and the ones we obtained from the bulk REE content for the homogeneous cumulate case (Fig. 5, TL=.7) suggests two possibilities: (1) If the cumulates were homogeneous then neither primitive augite nor bulk sample were affected by metasomatic alteration of Sm and Nd. (2) If the cumulates were zoned (TL<.7), then Sm, Nd, and Nd/Sm of the bulk sample were increased by metasomatism, relative to primitive augite, and agreement for TL=.7 is fortuitous. In light of experimental and petrographic arguments [13], we regard the former as much more likely. Other elements in the SPM pattern of [4] were scaled from a less primitive PX. Lack of agreement with our TL=.7 pattern (Fig. 5) may indicate selective metasomatism of REE other than Sm and Nd (unlikely), REE evolution prior to crystallization of the more evolved PX (most likely), or problems with the scaling procedure.

LREE ENRICHMENTS ARE NOT INTRINSIC TO LATE-STAGE PYROXENES. Separates of Fe-rich Shergotty PX were found to be strongly enriched in LREE relative to chondrites and Mg-rich pyroxene separates [3,4,6]. These LREE enrichments were originally believed to be intrinsic enrichment to PX, resulting from the effects of closed system crystallization [6]. However, we noted that extremely high PX D-values are required to produce the observed enrichments via closed system crystallization [18]. Subsequently, [3] and [4] attributed the enrichments to the presence of a LREE-rich minor phase in their PX separates. The low D-values for Fe-rich CPX reported here confirm that the LREE enrichments cannot be intrinsic to pyroxene, and must result from a minor phase. The presence of such a phase suggests that caution be exercised in interpreting the 350 MY Sm-Nd "PX" isochron of [3].

CONCLUSIONS. (1) Sm and Nd D's for Shergotty zoned augite rims do not differ markedly from those for magnesian cores of similar WO. (2) Factors in addition to PX Fe/Mg are responsible for the apparent correlation with pheno/matrix D's. (3) Similarity of D's for rims and cores supports our previous estimate of the REE content of the Shergotty parent melt. (4) Agreement between SPM Sm and Nd contents calculated from mineral separates and from bulk sample argues against metasomatic alteration. (5) Extreme LREE enrichment in Fe-rich PX separates is NOT intrinsic to PX.

References: [1] Bogard and Johnson (1983) Science 221, 651. [2] Laul (1986) The Shergotty Consortium and SNC Meteorites: An Overview. GCA, in press. [3] Jagoutz and Wanke (1986) Sr and Nd isotopic systematics of Shergotty Meteorite. GCA, in press. [4] Laul et al. (1986) Chemical Systematics of the Shergotty Meteorite and the Composition of its Parent Body (Mars). GCA, in press. [5] Shih et al. (1982) GCA 46, 2323. [6] Jagoutz and Wanke (1985) LPSC XVI, sup. A, 15. [7] Smith et al. (1984) PLPSC 14th, B612. [8] Ma et al. (1982) PLPSC 12th, 1349. [9] Nakamura et al. (1982) GCA 46, 1555. [10] Schnetzler and Philpotts (1970) GCA 34, 331. [11] McKay et al. (1985) PLPSC 16th, 540. [12] McKay et al. (1986) CPX Distribution Coefficients for Shergottites: The REE Content of the Shergotty Melt. GCA, in press. [13] Stolper and McSween (1979) GCA 43, 1475. [14] Paster et al. (1974) GCA 38, 1549. [15] Smith and Hervig (1979) Meteoritics 14, 121. [16] McKay et al. (1986) LPSC XVII, in press. [17] Jones (1985) LPSC XVI, 406. [18] McKay et al. (1986) Meteoritics 20, 710.

Fig. 1

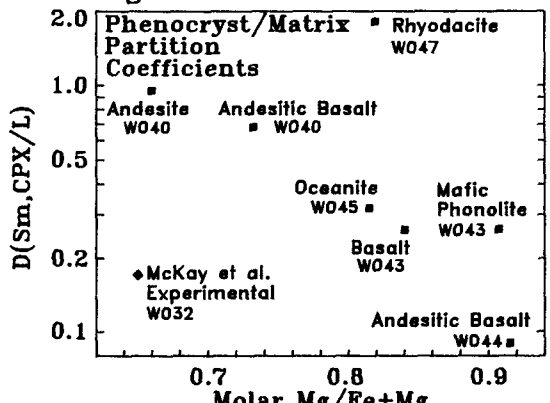

Fig. 2

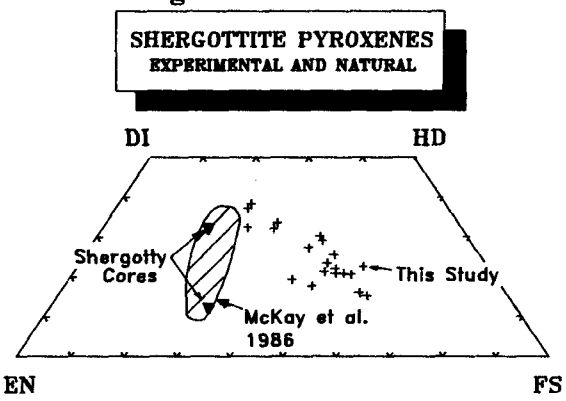

Fig. 3

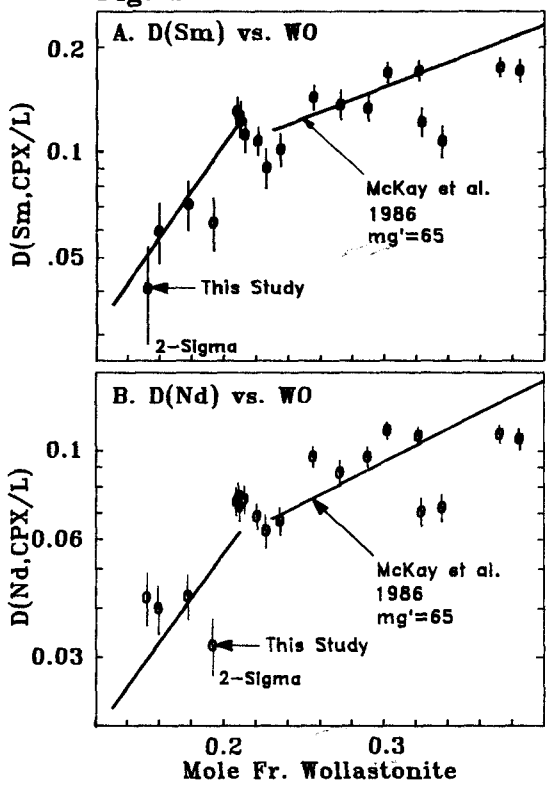

Fig. 4

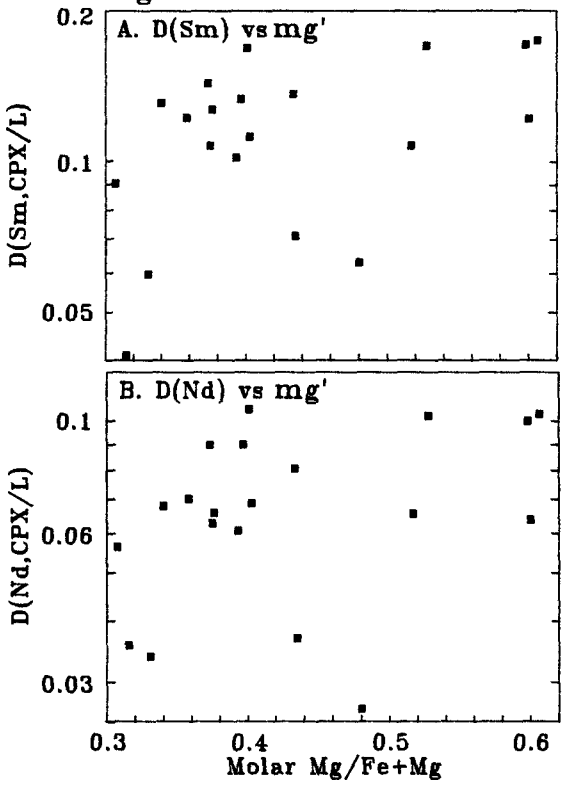

Fig. 5

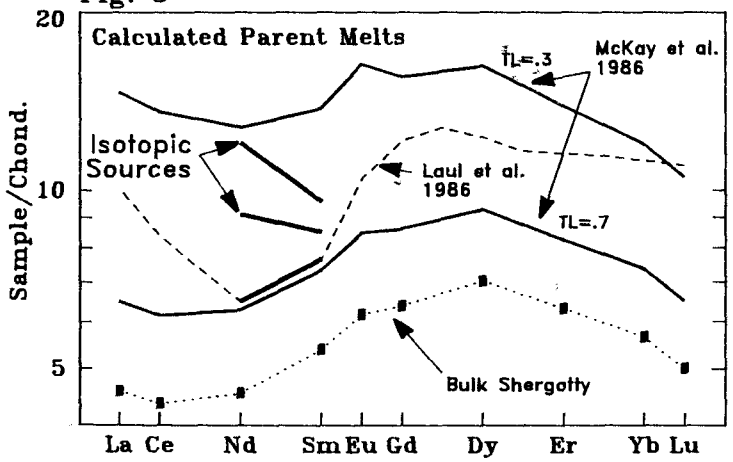

Special Session: Yamato-691 Enstatite Chondrite

1300 - 1720

Yamato-691 E3 chondrite; recovery, curation and allocation

Yanai K. and Kojima H.
National Institute of Polar Research, 9-10, Kaga 1-chome, Itabashi-ku, Tokyo 173

Yamato-691 was the first meteorite discovered in the Yamato Mountains region. This specimen was named as Yamato(a) first, but the specimen was officially renamed as Yamato-691 at the Committee on Antarctic Meteorite Research, NIPR in 1975.

Yamato-691 (Y-691) meteorite was accidentally found on snow-firm area by an oversnow glaciology party of the 10th Japanese Antarctic Research Expedition(JARE) in December 21, 1969, near the number 18 site of a glaciological triangulation chain of the southern Yamato Mountains. Yamato-691 was found as one of nine specimens which were collected from very closed area at the same time, within a region of approximately 5 x 10 km. But among them only Yamato-691 was located in the snow-firm area. This is very rare occurance in Antarctic meteorites, because occurances most of Antarctic meteorites had been limitted on the bare ice surface. A preliminary data of the Yamato-691 as follow;

Yamato-691 Enstatite chondrite (EH3)

Weight: 715 gms Location: Yamato Mountains, Antarctica
Dimension: 10 cm 71°50'55"S 36°31'10"E
Degree of Weathering: A/B Original Number: 1
Degree of Fracturing: A Found: Dec. 21, 1969, M. Yoshida et al.

Physical Description:
A neartly complete stone with thin dull black fusion crust covering of the surface; a sawn surface shows abundant white to dark gray chondrules in a black matrix. Rusty limonitic weathering is extensive throughout the meteorite. Specific gravity of this specimen is 3.58 (g/cm3).

Petrogrphic Description:
the section shows numerous small chondrules (most about 0.5 mm in diameter) and chondrule fragments in groundmass consisting of opaque material with numerous small grains of enstatite and clinoenstatite, but a few also contain some forsterite grains. Weathering is moderate and has converted not a few of the nickel-iron to limonite. Microprobe analyses give the following results: olivine (Fa0.1-1.3), pyroxene (Fs0.5-6.7).

Sample allocation of Yamato-691 for consortium studies show the Table .

Sub No.	P.I.Name	Bulk weight(g)	Remarks
2	K.Yagi	29.2	Petrology and mineralogy
3	M.Shima	23.8	Chemistry(bulk,trace), 26Al meas.
11	I.Kushiro ※	10.928	Bulk chemical analyses
62	T.Nagata		Magnetic properties
71	J.F.Lovering	3.0	?
72	W.Birch	4.0	?
73	A.Masuda	2.97	Chemical analyses, REE, trace
74	E.Gibson	3.769	Abundances of Carbon and S

78	Curator	1.586	for P.T.S.
79	Curator	0.977	for P.T.S.
80	Curator	0.765	for P.T.S.
82	El Goresy ※	0.482	Petrology and mineralogy
83	F.Podosek	1.182	Xe-Xe, Ar-Ar analyses
84	M.Ebihara ※	0.642	Chemistry
88	T.Fukuoka ※	0.053	Chemistry, trace elements
89	Y.Miura ※	0.327	Petrology
90	M.Lipschutz ※	0.406	Chemistry, trace elements
91	M.Honda	0.442	26Al, 52Mn measurement
92	J.Annexstad	0.995	for P.T.S.
93	M.Higgins	0.365	Boron abundances
94	N.R.Clayton	0.017	Oxygen isotope
100	T.Tanaka※	0.194	Nd isotope
101	J.Wasson※	0.543	Chemistry, NAA
102	Y.Ikeda ※	2.320	Petrology
104	El Goresy ※	0.375	Petrology
105	N.Muller※	0.698	Age determination
106	M.Miyamoto	0.492	Reflectance
142	T.Fukuoka ※	0.027	Chemistry, NAA

Sub No.	P.I.Name	P.T.S.	Remarks
2	M.Miura ※	P.T.S.	Petrology
78-1	J.Akai※	P.T.S.	Mineralogy
78-2	H.Nagahara※	P.T.S.	Petrology
78-3	J.Wasson※	P.T.S.	Petrology
78-4	H.Matsueda※	P.T.S.	Mineralogy
78-5	(Save)	P.T.S.	
78-6	N.Morimoto※	P.T.S.	Mineralogy
79-1	Y.Ikeda ※	P.T.S.	Petrology
79-2	J.Wasson※	P.T.S.	Petrology
79-3	El Goresy ※	P.T.S.	Petrology
80-1	I.Sunagawa	P.T.S.	Mineralogy
80-2	Y.Ikeda ※	P.T.S.	Petrology
80-3	M.Prinz	P.T.S.	Mineralogy
80-4	(Save)	P.T.S.	

(※ Consortium Member)

A review of Y-691

Yukio Ikeda
Ibaraki University , Mito 310

COMPOSITIONAL CHARACTERIZATION OF YAM6901 AND OTHER EH3 CHONDRITES

Gregory W. Kallemeyn
Institute of Geophysics and Planetary Physics,
University of California, Los Angeles, CA 90024, USA

The enstatite chondrites comprise two groups: high-Fe EH and low-Fe EL [1]. The EH group consists of petrologic types 3-5. Qingzhen was classified as the first EH3 chondrite [2]. Differences in mineral compositions provide natural hiatus for determining whether an EH chondrite is type 3 or 4 (Table 1). Several EH chondrites have now been classified as EH3, including seven in this study: Allan Hills A77295, Allan Hills A81189, Kota-Kota, Parsa, Qingzhen, Yamato 6901 and Yamato 74370. The tentative classification of Yamato 6901 as type 3 [3], based on its textural features and silicate mineral compositions [4], has been confirmed by further studies of its opaque mineral compositions [5].

Because of the major differences in mineral compositions between EH3 and EH4,5 chondrites it seemed possible that there might also be differences in their bulk compositions. Weeks and Sears [6] studied two EH3 chondrites and compared them to literature data for EH4,5. They found that EH3 lithophile and siderophile abundances are indistinguishable from EH4,5 abundances, but that EH3 abundances of moderately volatile chalcophiles (Cr, Mn, Na, K, Se and Zn) fall at the lower end of the EH range. In the present study concentrations of 30 elements were determined in 30 replicates of 16 enstatite chondrites by instrumental and radiochemical neutron activation analysis.

In Fig. 1 are histograms of siderophile/Mg ratios in EL falls, EH4,5 falls, and all EH3 chondrites. The seven EH3 chondrites are indistinguishable from the EH4,5 falls. This clearly indicates a strong compositional link between EH3 and EH4,5 chondrites. Element ratios plotted in Fig. 2 give variable support to the Weeks-Sears inference that moderately volatile chalcophiles are lower in EH3 than in EH4,5 chondrites. Only the Se/Ni (Fig. 2b) ratio consistently shows EH3 lower than EH4,5 ratios, while six of the seven EH3 chondrites show lower Na/Mg ratios (Fig. 2a). In most cases, though, the element ratios for EH3 falls show somewhat higher ratios than the finds, and low ratios are also found in the EH5 find Reckling Peak A80259. It may be that weathering has reduced the contents of most of these elements in EH finds.

Of the six EH finds in our sample set, five are from Antarctica, and thus presumably experienced similar weathering conditions. In Fig. 3 are chondrite/EH abundance ratios for 28 elements in the five Antarctic finds: EH3 A81189, EH5 A80259, EH3 Y6901, EH3 Y74370 and EH3 A77295. Since numerous elements (Al, Sc, Yb, Lu, Ir) are very near the mean EH falls abundance levels, Mg loss has probably been negligible. The A77295 sample shows an unusual pattern and is probably not typical of the whole rock. The remaining four show similar patterns. Elements with abundance ratios <0.93 in those four finds are Ca, Eu, Mn, Na, K, Re, Fe, Au, As, Ga, Sb, Se and Te. Labile elements such as Na and K are expected to be among the most leachable. The decreasing ratios from Te through Sb could reflect the existence of a highly reactive sulfide, that contains a proportionately greater fraction of each element through the same sequence. Despite the general contention that oldhamite (CaS) is especially prone to destruction by weathering, Ca shows the highest abundance ratio (0.925) among these elements.

An interesting mineralogical difference between EH3 and EH4,5 chondrites is the lower Ni and Si contents in EH3 kamacite relative to EH4,5 kamacite. An explanation may be provided by perryite $(Ni,Fe)_5(Si,P)_2$, which occurs in EH3 chondrites [2,3,5] and has very high contents of Ni and Si. Perryite may have formed by corrosion of metal at high nebular temperatures, and survived to low temperatures in EH3 chondrites, but dissolved into the metal during the metamorphic heating of EH4,5 chondrites. This is supported by petrograhic observations of Qingzhen [2] and mass-balance arguments.

This study shows that mean elemental abundances in pristine EH3 chondrites are very similar to those in pristine EH4,5 chondrites. Thus, the mineralogical differences

between EH3 and EH4,5 chondrites can be interpreted as changes resulting from the metamorphic reheating of the latter.

References: [1] Sears D.W., Kallemeyn G.W. and Wasson J.T. (1982) Geochim. Cosmochim. Acta 46, 597-608. [2] Rambaldi E.R., Rajan R.S., Wang D. and Housley (1983) Earth Planet. Sci. Lett. 66, 11-24. [3] Prinz M., Nehru C.E., Weisberg M.K. and Delaney J.S. (1984) Lunar Planet. Sci. 15, 653-654. [4] Okada A. (1975) Mem. Natl. Inst. Polar Res. 5, 14-66. [5] Kimura M. (1985) 10th Sym. Ant. Met., 29-31. [6] Weeks K.S. and Sears D.W.G. (1985) Geomchim. Cosmochim. Acta 49, 1525-1536. [7] McKinley S.G., Scott E.R.D. and Keil K. (1984) Proc. Lunar Planet. Sci. Conf. 14th, B567-572. [8] Keil K. (1968) J. Geophys. Res. 73, 6945-6976.

Table 1. Differences in phase compositions between EH3 and EH4,5 chondrites [3,7,8].

phase	component	compositional range EH3	EH4,5
kamacite	Si (mg/g)	23-26	33-35
	Ni (mg/g)	24-33	65-79
schreibersite	Ni (mg/g)	108-155	63-136
troilite	Cr (mg/g)	5-18	15-28
niningerite	Mg (mg/g)	235-260	89-193
	Ca (mg/g)	3.5-6.5	13-30
	Cr (mg/g)	1.4-3.1	16-20
	Mn (mg/g)	116-152	40-71
	Fe (mg/g)	130-156	271-370
oldhamite	Mg (mg/g)	5-9	7-17

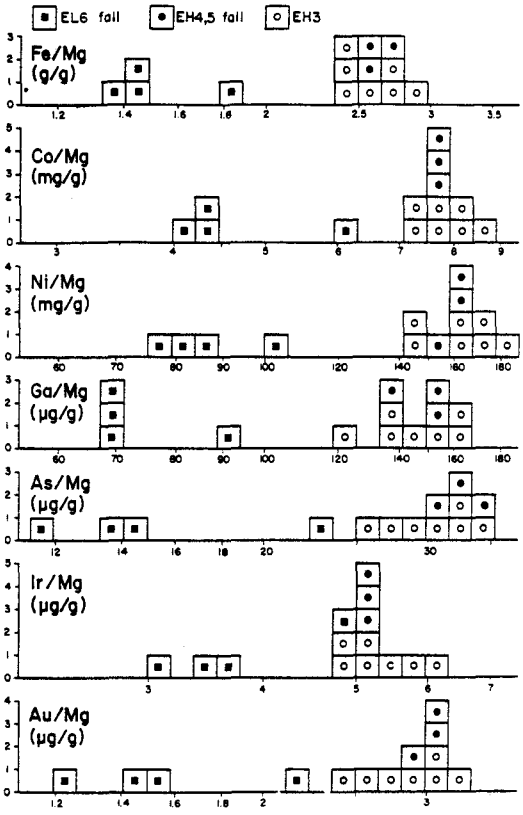

Fig. 1

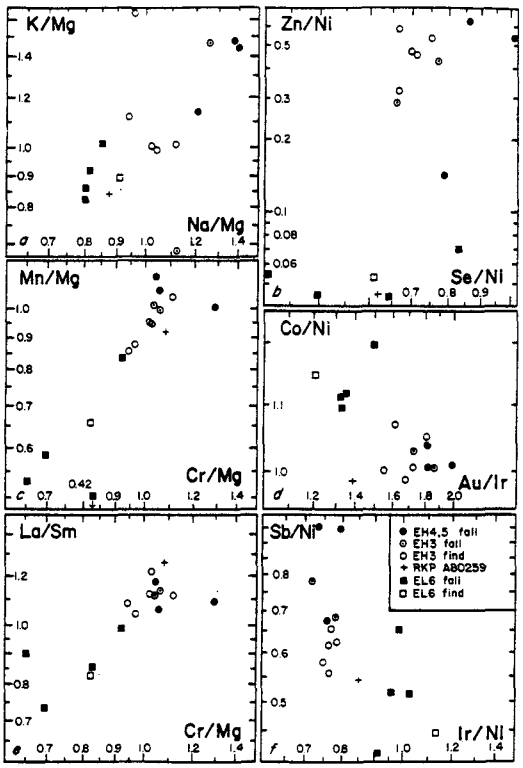

Fig. 2

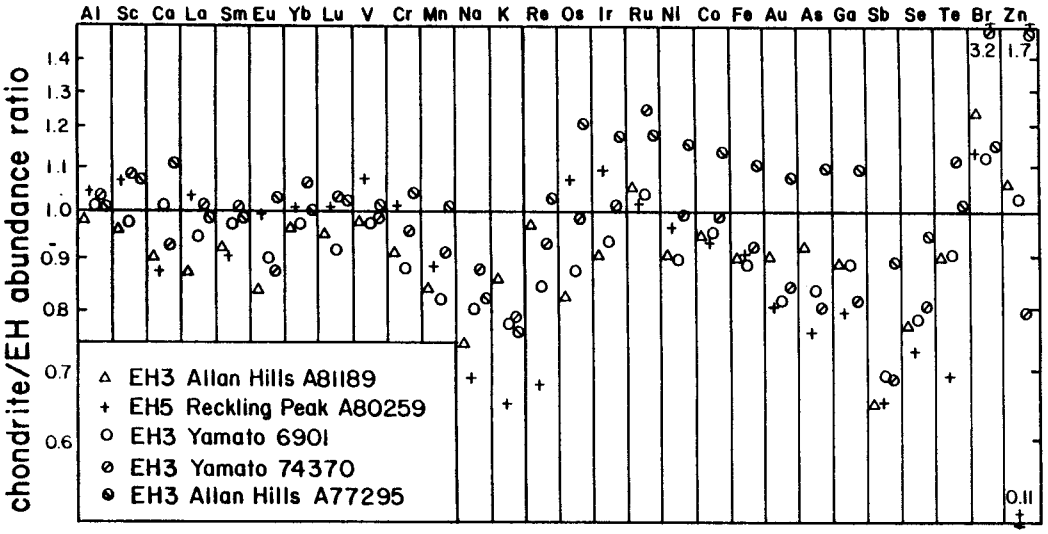
Al Sc Ca La Sm Eu Yb Lu V Cr Mn Na K Re Os Ir Ru Ni Co Fe Au As Ga Sb Se Te Br Zn
chondrite/EH abundance ratio
1.4
1.3
1.2
1.1
1.0
0.9
0.8
0.7
0.6
3.2
1.7
0.11
△ EH3 Allan Hills A81189
+ EH5 Reckling Peak A80259
○ EH3 Yamato 6901
⊘ EH3 Yamato 74370
⊘ EH3 Allan Hills A77295

Fig. 3

Mineralogical study on Y-691 enstatite chondrite

Makoto Kimura
Ibaraki University, Mito 310

Enstatite chondrites show unique features such as their mineralogy and redox state, which are fairly different from ordinary chondrites. Thus, many authors have studied these enstatite chondrites and clarified their mineralogical features and condition of their formation. This paper describes the features of constituent units of Y-691, and discusses the condition of formation of units and genetic relations between units.

Y-691 enstatite chondrites consists of chondrules, and silicate and opaque mineral fragments. Chondrules are small in size, in comparison with those of ordinary chondrites. They often contain fine-grained opaque minerals. Fine-grained silicate and opaque minerals fill the interstices among coarse-grained opaque mineral fragments (OMF's hereafter) and chondrules, which is matrix of enstatite chondrites. Such silicate minerals often show the same features as those in chondrules. The kinds of opaque minerals in chondrules and matrix are same as those of OMF's, although they are small in size and are not aggregates like OMF's in general. Fine-grained silicate minerals are often included in OMF's.

Kimura (1985) described OMF's in Y-691 and discussed that various phases in OMF's, such as schreibersite, perryite, sphalerite, and so on, originated from primary OMF's, which had been Fe-Ni metal alloy. Bulk compositions of OMF's have similar composition to cosmic elemental abundance, and they had primarily contained Si, Zn, Ti, Mn and Cr, in addition to Fe, Ni, Co, P. Such features of OMF's show that they were primary condensates and they formed under very low oxygen fugacity condition.

In general, enstatite chondrites have been believed that they formed under high reduced condition, which is also suggested

from OMF's as mentioned above. However, enstatite chondrites have also the evidences that the part of them formed under slightly oxidized condition. Nagahara (1985) found ferrous silicate minerals in Y-691. Such features are also found in OMF's. Fine-grained silicate minerals in OMF's mostly comprise silica mineral and pyroxene, with minor amount of albitic plagioclase and roedderite. Silica mineral are abundant, in comparison with pyroxene, which is different from phenocrysts in chondrules. Silica minerals are often accompanied by perryite and troilite in Fe-Ni metal. Kimura (1985) suggested that perryite and troilite formed simultaneously from Fe-Ni metal below 700 °C. These evidences suggest that silica mineral formed simultaneously with perryite and troilite from Fe-Ni metal which had contained Si. Such a environment was under slightly oxidized condition.

Chondrules often contain fine-grained opaque minerals among silicate phenocrysts or in them. Since the kind of these minerals is same as that of OMF's, chondrules formed from precursors which had contained fragments of OMF's. Thus, the formation of chondrules took place after the formation of various minerals in OMF's and their fragmentaion. Opaque minerals in chondrules generally show similar composition to those of OMF's. However, Si-contents of some Fe-Ni metals in chondrules are lower than those of OMF's, although Ni/(Ni+Fe) ratios of them are similar to each other. Such a evidence also suggests the oxidized condition. It is probable that some chondrules in enstatite chondrites formed under slightly oxidized condition, although such a oxidization state is still lower than that of ordinary chondrites.

Thus, the redox state of the formation of enstatite chondritic material changed from highly reduced condition under which OMF's primarily formed, to slightly oxidized condition under which some OMF's are oxidized and chondrules formed.

[References] Kimura M. (1985): Abs. 10th Symp. Antarctic Meteorite, 29-32.; Nagahara H. (1985): Abs. 10th Symp. Antarctic Meteorite, 12-14.

PYROXENES IN Y-691

Masao KITAMURA, Seiko WATANABE and Nobuo MORIMOTO
Department of Geology and Mineralogy, Faculty of Science, Kyoto University, Sakyo, Kyoto 606, Japan

Pyroxenes are one of the major constituent minerals of Y-691 (EH3) and are common in chondrules, mineral fragments and lithic fragments. They are identified to be clinoenstatite (CEn), orthopyroxene (OPx), diopside (Di), diopside rich in Ca-Tschermak mole (CaTs), and pigeonite (Pig) under an optical microscope and a back scattered electron image (BEI).

Pyroxenes in the chondrules:

All the chondrules contain pyroxenes in our thin section. The chondrules can be roughly classified into five groups by their mineral assemblage as follows; (1) En + glass, (2) En + Di + glass, (3) Ol + Di + SiO_2 + glass, (4) SiO_2 + Di + glass, (5) relict Px including Ol + CEn + Pig + glass. Among these groups, (1) (Figure 1) is the most common.

Single crystals of diopside were found in (2), (3) and (4) groups (Figure 2). Although single crystals of diopside have been reported only in Qingzhen (E3) (Grossman et al., 1985) among the E chondrites, they are considered to occur widely in the E3 chondrites. However, in the EH4, diopside was considered to react with sulfur and form the oldhamite (Rubin, 1984).

Relict olivines in the chondrules and fragments commonly have Fe metal inclusions by reduction during the chondrule formation (Figure 3). Relict Ca-poor pyroxenes do not have the metal inclusions but can be distinguished by their Fs rich compositions from Ca-poor pyroxenes which crystallized during the formation of chondrule.

A new relict Ca-poor pyroxene was found which includes poikilitically relict olivines (Figure 4). Fe metal inclusions are observed in the relict olivine but not in the relict pyroxene. The Mg/(Mg+Fe) ratio of the olivine including Fe metal (~0.93) is almost same as that of the relict pyroxene (~ 0.93), suggesting that they were kept in an equilibrium state. Therefore, this grain with the poikilitic texture implies that the precursor of the chondrules was the rocks.

Pyroxene in the lithic fragments:

Diopsides anomalously rich in CaTs component were found in two lithic fragments. The first (Figure 5) consists of three Ca-poor pyroxenes distinguished by Al_2O_3 content, two diopside also distinguished by Al_2O_3, silica mineral, and glass (or albite). The other fragment (Figure 6) also includes diopside rich in CaTs. Coexistence of the Al-rich and poor diopsides cannot be explained by a single monotonic process. Since the Al-rich diopside formed under about 20 kbar (Gasparik and Lindsley, 1980), a shock process should have taken place. The timing of the shock process must be before or during the chondrule formation, because pyroxenes and olivines are reduced as the relict grains.

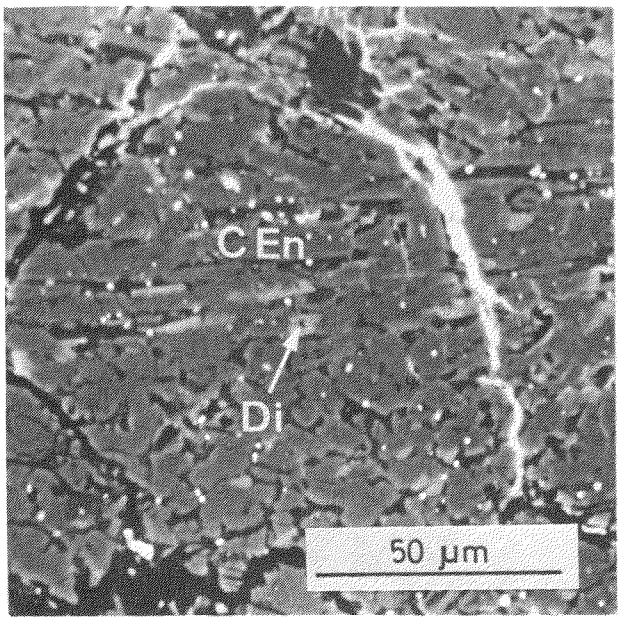

Figure. 1. Radial pyroxene chondrule (BEI). Diopside (Di) overgrew on the rim of clino-enstatite (CEn).

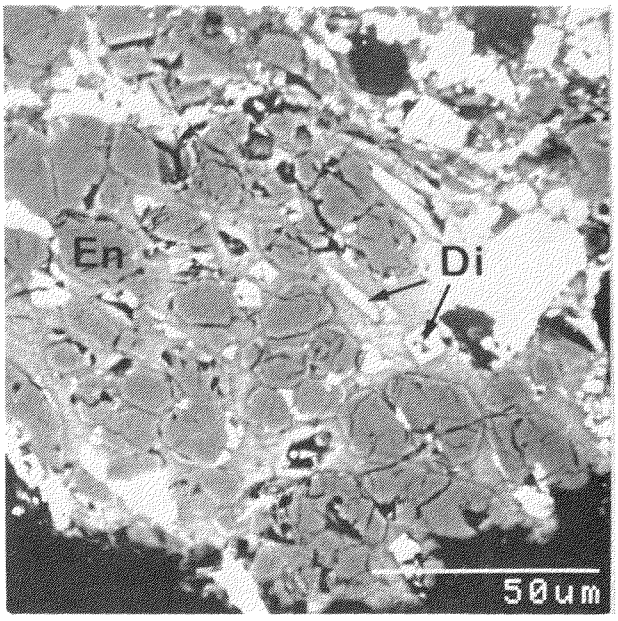

Figure 2. Porphyritic chondrule (BEI). Enstatite and diopside are single crystals. Groundmass is glass.

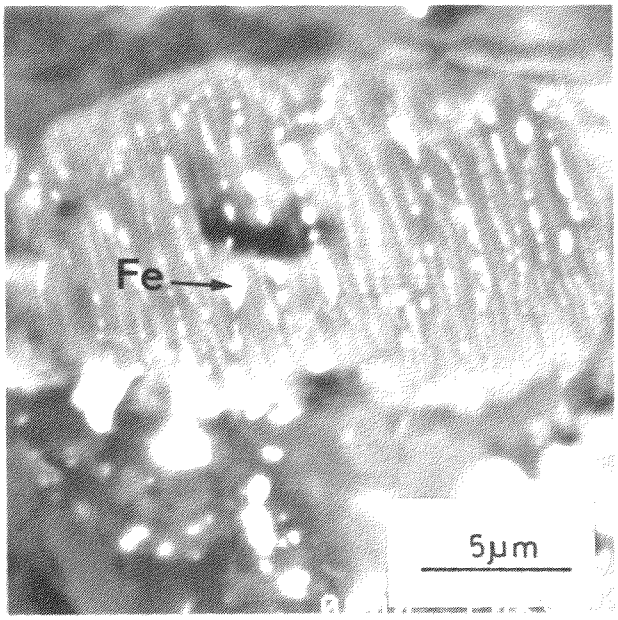

Figure 3. Relict olivine as a mineral fragment. Fe metal inclusions are observed.

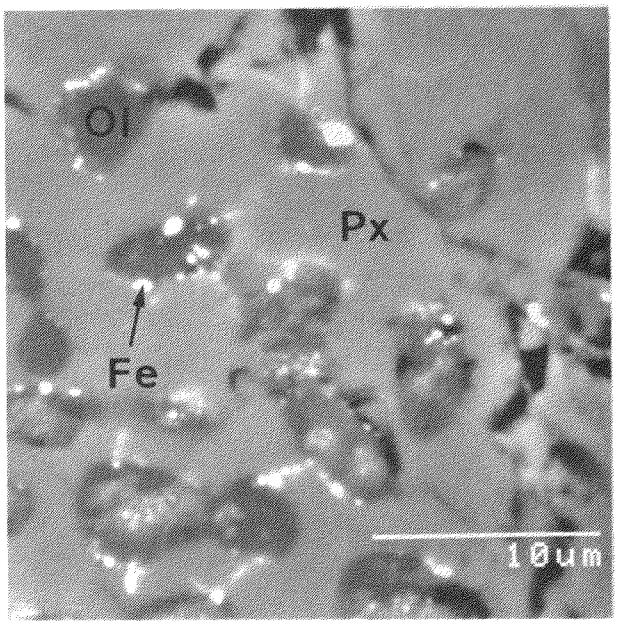

Figure 4. Relict pyroxene poikilitically includes olivines with Fe inclusions.

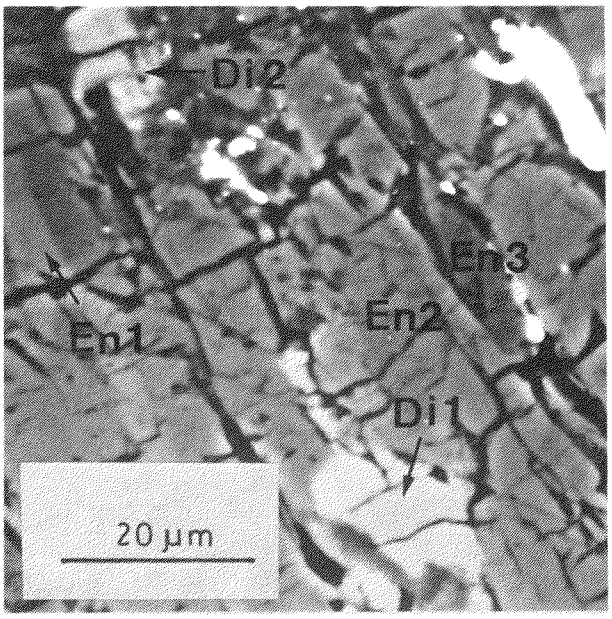

Figure 5. Lithic fragment with Al-rich diopside (BEI). Two kinds of diopsides and three of enstatites coexist.

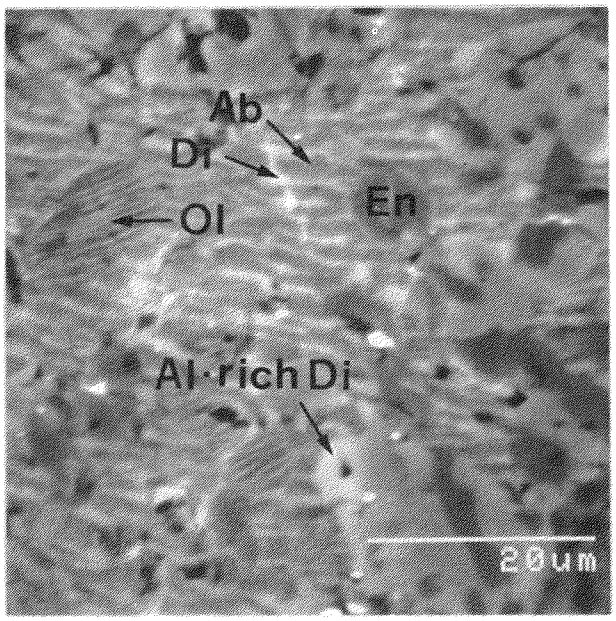

Figure 6. Lithic fragment with Al-rich diopside (BEI). Olivine with Fe-lamellae, and lamellar intergrowth of albite and diopside are observed.

[REFERENCES]
Gasparik,T. and Lindsley,D.H. ; in Pyroxenes, eds. C.T.Prewitt, Mineral. Soc. Amer., 328 (1980)
Grossman,J.N., Rubin,A.E., Rambaldi,E.R., Rajan,R.S. and Wasson,J.T. ; Geochim. Cosmochim. Acta **49**, 1781-1795 (1985)
Rubin,A.E. ; Earth Planet. Sci. Lett., **67** 273-283 (1984)

MINERALOGY OF Y-691 BY AEM AND HREM
(PRELIMINARY REPORT)

Junji Akai

Fac. Sci. Niigata Univ. Niigata 950-21

Mineralogy of Y-691 is already reported by some investigators (1),(2),(3). However, very fine-grained minerals such as those in the matrix have not been known in detail. EM, AEM and HREM are potential for characterization of these fine-grained minerals and also usefull for investigation of fine textures of minerals which often record previous history of the mineral experienced. In this study,matrix minerals were examined by EM, AEM and HREM (JEM 200CX with TN2000). The specimen of matrix was prepared by cutting off from polished thin section and ion-thinned ,which contained many small grains of various sizes and also contained small fragments of chondrules and/or Opaque Mineral Fragments (OMF's according to Kimura(2)). This paper preliminarily reports the mineralogy of the fine-grained minerals in the matrix of Y-691.

1. Metals

Metal phase previously reported in Y-691 was only kamacite (1),(2),(3). In this study, however, the following types of metal phases could be recognized.

i) Kamacite with about 2 % Si

This is most abundant in the fine grained matrix as well as in OMF's. Fig. 1 shows EM and ED pattern of this type,and small precipitates are found present. Fig.2 shows HREM of such region. Composition of this type is shown in Table 1-[1-11] and indicates some chemical variations.

ii) Si-poor (~Si-free) Kamacite

This type was rarely found in the matrix. The composition is shown in Table 1-[12]. In EM image (Fig.3) precipitates were not observed.

iii) Taenite

Table 1-[13,14] show the composition of this type. Small amounts of grains were found adjacent to kamacite (type i) (Fig.4). Taenite has very rarely been observed in enstatite chondrite (4) and this may be the third occurrence in it.

iv) Ni-free kamacite in an olivine in the matrix

Rounded small metal grains are found arranged in an olivine grain (Fig.5). Impure composition of this metal grain by a little contribution of host olivine ($Fo_{98.3}$) is shown in Table 1-[15]. It is found that no Ni is contained. These metal grains might be formed in-situ reduction of olivine.

The present data of metals suggest large variations of composition in fine-grained minerals and may indicate the larger degree of unequilibrium. The presence of various types of metals is similar to those in Quingzhen (4).

2. Other opaque minerals

Among the mineral species found in OMF's (2),(3), troilite, niningerite,schreibersite, oldhamite and perryite were found as fine grained minerals in the matrix for the present. However, some of them may be those of small OMF's in the matrix. Compositions of some of these minerals are shown in Table 2.

All these data for very fine-grained minerals in the matrix can not be compared with the previous EPMA data in a strict sense. However, compared with the sulfide composition in the other enstatite chondrites (4),(5),(6), several differences are revealed. Approximate similarities are characteristic between the present data and those in Quingzhen (4),(5) (for instances, in niningerite composition) , although slight differnces between them are also present. As suggested in Quingzhen(4), Y-691 might not be reheated after accretion.

3. The other minerals

Compositions of enstatite grains varies to a considerable extent. The variations were characteristic in Fe, Ca, Al and Na contents. Other minerals which have not been reported were found ; for example, augite with lamellae structures and plagioclase of bytownite composition. Other very small grains of corundom , zircon , albite and Ca-mineral (calcite?) were found often in interstices of relatively larger grains ,but doubts of being artifacts should be cleared away. A detailed study is in progress.

References :
(1) Okada,A.(1975) :Mem.Natl.Inst.Polar Res.,5,14,(2) Kimura,M. (1985) Abs. 10th Symp.Ant.Meteorite NIPR,29 , (3) Nagahara,H.(19 85) ibid 12 ,(4)Rambaldi,E.R. et al. (1983) :Lunar Planet. Sci. XIV,626. ,(5) El Goresy et al. (1983) : Meteoritics, 18,293. (6) Keil,K.(1968) : J. Geophys. Res.,73,6945.

Table 1 Compositions of metals in Y−691 matrix by AEM (wt%)

gr. No.	Si	P	Fe	Co	Ni	Cr
Kamacite						
1	1.9	0.0	93.3	1.3	3.4	0.0
2	2.2	0.0	93.9	0.0	3.9	0.0
3	2.2	0.0	94.7	0.0	3.1	0.0
4	2.2	0.0	93.8	0.9	3.1	0.0
5	2.1	0.0	93.0	2.0	2.9	0.0
6	2.4	0.0	93.7	0.7	3.2	0.0
7	3.1	0.0	92.5	0.9	3.5	0.0
8	2.2	0.0	91.9	2.3	3.7	0.0
9	3.1	1.5	88.2	0.0	7.1	0.0
10	2.7	0.8	90.6	0.0	5.8	0.0
11	2.9	0.0	93.3	1.0	2.7	0.0
Si−free Kamacite						
12	0.2	0.0	92.6	2.1	5.0	0.0
Taenite						
13	10.1	0.9	55.0	0.0	34.0	0.0
14	3.3	0.9	78.3	0.0	17.6	0.0
Kamacite in olivine (see text)						
15	6.1	0.0	93.1	0.0	0.0	0.8

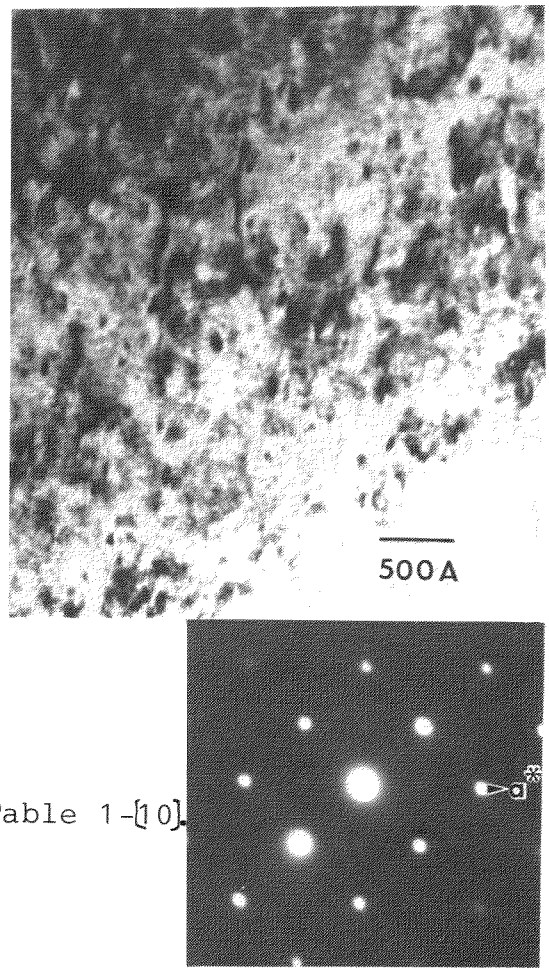

Fig.1 EM of kamacite (type i).
Corresponding composition is Table 1-[10].

Table 2 Compositions of some sulfides in Y－691 matrix (wt %) by AEM

Troilite

gr.	No.	S	Ti	Cr	Mn	Fe	P	Ni
	1	37.9	0.15	3.5	0.0	57.5	0.8	0.15
	2	36.4	0.0	1.1	0.0	58.4	0.4	0.0
	3	36.3	0.0	0.9	0.0	60.5	0.4	0.0
	4	38.7	0.0	1.0	0.1	56.8	1.1	0.1

Niningerite

No.	Mg	S	Ca	Cr	Mn	Fe	P	Si
1	31.3	49.2	0.5	0.2	5.4	11.6	1.6	0.3
2	31.1	49.1	0.8	0.0	5.5	12.3	1.1	0.0
3	29.7	48.5	0.4	0.1	5.3	13.4	1.6	0.9
4	30.5	49.2	0.3	0.0	5.5	13.2	1.0	0.3
5	31.9	47.0	0.5	0.1	7.2	11.8	1.3	0.0
6	28.7	47.0	0.4	0.0	6.4	16.1	1.1	0.3
7	32.2	49.9	0.5	0.2	5.2	10.1	1.4	0.3
8	31.2	49.2	0.4	0.2	6.0	12.0	1.2	0.0
9	26.0	47.7	0.7	0.1	6.9	17.1	0.9	0.5
10	29.9	51.4	0.4	0.0	5.5	11.5	0.9	0.2

Schreibersite

No.	Si	P	Fe	Co	Ni	Mg	Zn
1	0.0	12.1	72.6	0.0	13.9	0.9	0.5
2	0.3	13.2	70.4	0.0	15.7	0.4	0.0

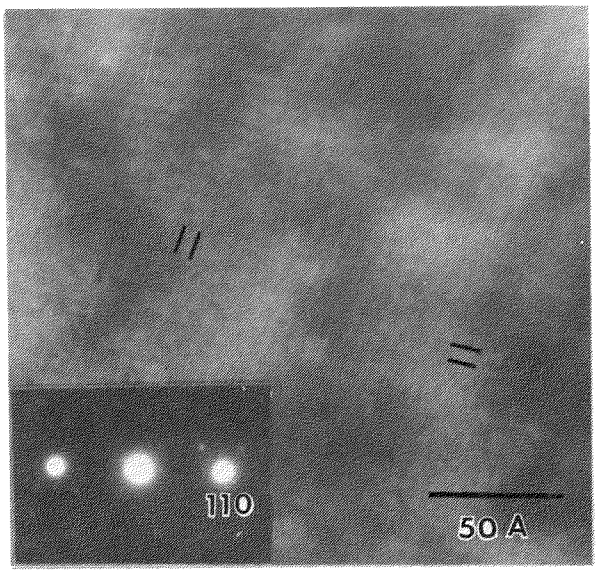

Fig.2 HREM of kamacite (type i)
Composition: Table 1-[4]

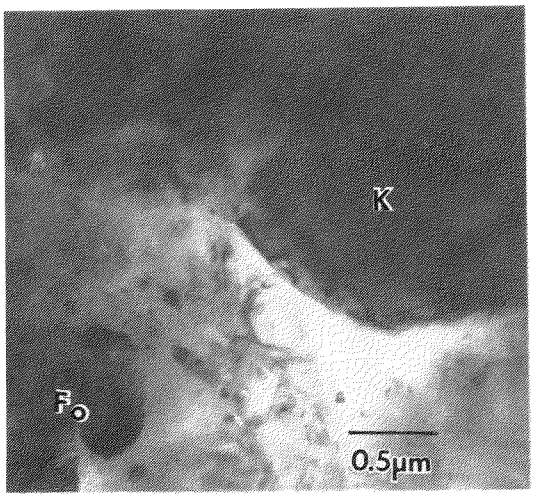

Fig.3 EM of Si-poor kamacite.
(composition ; Table 1-[12])

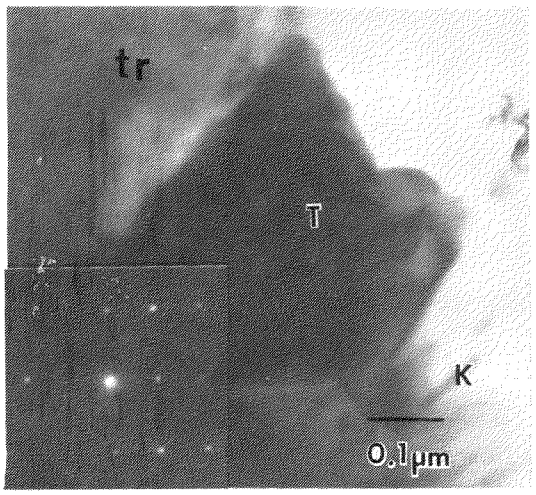

Fig.4 EM of taenite.
(composition ;Table 1-[13])

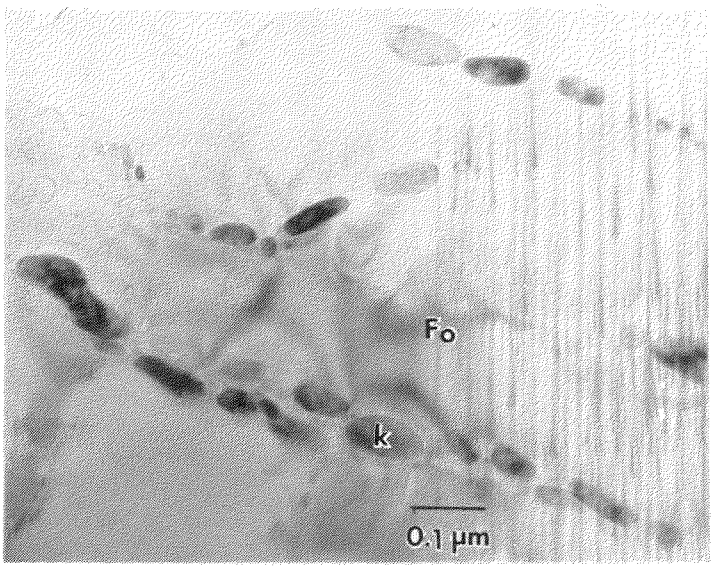

K : kamacite
T : taenite
tr :troilite
Fo :forsterite

Fig.5

EM of rounded small Ni-free kamacite grains arranged in an olivine grains ($Fo_{98.3}$)

FORMATION PROCESS OF YAMATO-691 CHONDRITE FROM MG-FE PLAGIOCLASES AND OSUMILITE-GROUP MINERALS.

Miúra, Yasunori
Department of Mineralogical Sciences and Geology, Faculty of Science, Yamaguchi University, Yoshida, Yamaguchi, 753.

The formation process of Yamato-691 (EH3) chondrite is discussed by the compositions and structure of Mg-Fe plagioclase (-like) and osumilite-group minerals [1-8] in the two fragments of the Yamato-691,80-1 and Yamato-691,89 chondrites.

Plagioclase(-like) phases

The composition of the Mg-Fe plagioclase(-like) phase has been reported so far [1-4,6-7], though few large crystal of typical plagioclase has been observed in type 3 chondrite. The Mg-Fe plagioclase observed in the matrix of pyroxene (Fo_{98-99}) chondrule of the Yamato-691,80-1 chondrite, however, shows composition of $(Na_{0.7}Ca_{0.02}\ K_{0.01}FM_{0.27})(Al_{0.9}Si_{2.9}FM_{0.2})O_8$. The other various phases between the amorphous and the crystalline with plagioclase(-like) compositions show A site vacancy (~34 mole%) and higher contents of Mg (~4.3 wt% MgO) and Fe (~6.3 wt% FeO) in the EPMA analyses of eleven elements.

The Mg-Fe plagioclase(-like) phases are separated at least into two regions in the diagram of *mg* ratio and An content (Fig. 1). The Mg-rich phases (*mg*=0.8~1.0) have various An contents from 0 to 40 (mol%) than the Fe-rich phases (*mg*=0.2~0.5). Figure 1 suggests that the Fe-rich phase consists moreover of the intermediate and Fe-rich end-members, and that the Mg-rich phase might be separated into two regions of An content; that is, Ab-rich (~10mole%) and An-rich (~40mole%) regions.

The crystalline plagioclases in the Yamato-691,89 chondritic fragments have anomalous structural data of the unit-cell dimensions corresponding to those of the terrestrial sodic plagioclase, together with diffraction pattern of the terrestrial calcic plagioclase (i.e., a:33%, b:18%, c:31%, d:18%). This discrepancy suggests that the sodic plagioclase suffered the progressive thermal metamorphism under reducing condition still involves the memory of the structure type of the primordial plagioclase.

Osumilite-group mineral

Various types of osumilite-group mineral have been reported in the various meteorites [3,8]. The Mg-Fe and Mg-Na types of the osumilite group minerals are observed in the Yamato-691,89 fragments (Fig. 2). The Mg-Na phases are found also in H3 chondrites [3,5,10] and iron meteorite (as Yagiite and Roedderite), whereas the Fe-Na type phase observed in sugilite [9] is the first description in extraterrestrial materials. Thus, the characteristics of the Yamato-691 chondrite are the coexistence of two different Mg-rich and Fe-rich osumilite-group minerals with the same potassium content.

Formation Process

The pyroxene chondrule (Fo_{97-99}) has variable compositions of the plagioclase(-like) and osumilite-group phases. The coexisting of two different compositions of Mg- and Fe-rich phases

indicates that the Yamato-691 chondrite is formed at least in two stages; at first, during progressive thermal metamorphism in the parental body at reducing condition, followed by the mixing by impact; and second, accretion to chondritic body.

The distribution of the analytical data in Figs. 1 and 2 suggests the coexisting (or mixing by impact) of the following phases in the Yamato-691 chondrite: that is, (1) Fe- and Na-rich phase, (2) Mg- and Na-rich phases, and (3) Mg- and Ca-rich phases. The separation to the chondrules with Mg (and/or Ca) - or Fe (and/or Na) - rich region (cf. Figs. 1 and 2) are finally formed by thermal metamorphism probably in the individual parental body, followed by the complete mixing by impact process. The two compositional trends between the two sections of the Yamato-691 chondrites (in Fig. 1), therefore, are assumed to be formed within the primordial parental body prior to chondrule formation.

In conclusion, the Yamato-691 chondrite contains the various products resulted from the multi-stage formations, which can be discussed by the compositions of plagioclase(-like) and osumilite group minerals in detail.

The author thanks to Dr. K. Yanai and Mr. H. Kojima of the National Institute of Polar Research of Japan for their help in preparing the polished thin sections of the Yamato-691,80-1. The fragments of the Yamato-691,89 are polished for thin sections, and the grains are picked up for collecting of X-ray data by the help of the my graduate student, H. Miura.

REFERENCES:

[1] Miúra, Y. (1984): Mem. Natl Inst. Polar Res., Spec. Issue,35, 226-242.
[2] Miúra, Y. et al. (1984): ibid., 210-225.
[3] Miúra, Y. et al. (1985): Lunar and Planetary Science XVI (Houston), 2, 563-564.
[4] Miúra, Y. (1985): ibid., 561-562.
[5] Miúra, Y. (1985): Proc. Symposium on Antarctic Meteorites X (Tokyo), 210-212.
[6] Miúra, Y., K. Yanai and T. Tanosaki (1985): ibid., 66-68.
[7] Miúra, Y. (1986): Lunar and Planetary Science XVIII (Houston) pp.2 (in press).
[8] Miúra, Y. (1986): ibid., pp.2 (in press).
[9] Kato, T., Y. Miúra and N. Murakami (1976): Mineralogical Journal, 8, 184-192.
[10]Miúra, Y. (1986): Proc. Symposium on Antarctic Meteorite XI (in this volume).

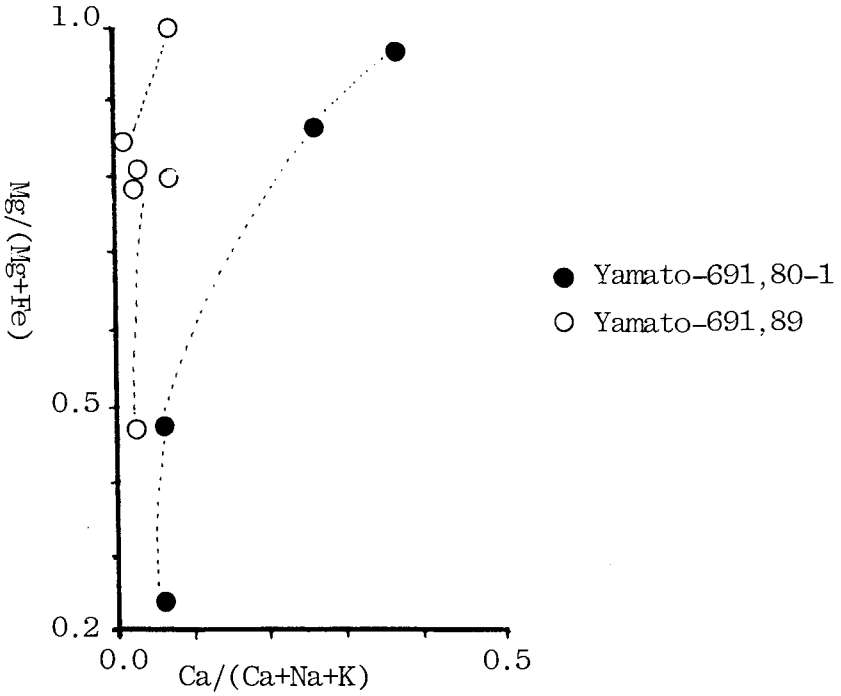

Fig.1. Relation between Ca/(Ca+Na+K) and Mg/(Mg+Fe) in Yamato-691 chondrite (EH3). Compositions of plagioclase(-like) are referred.

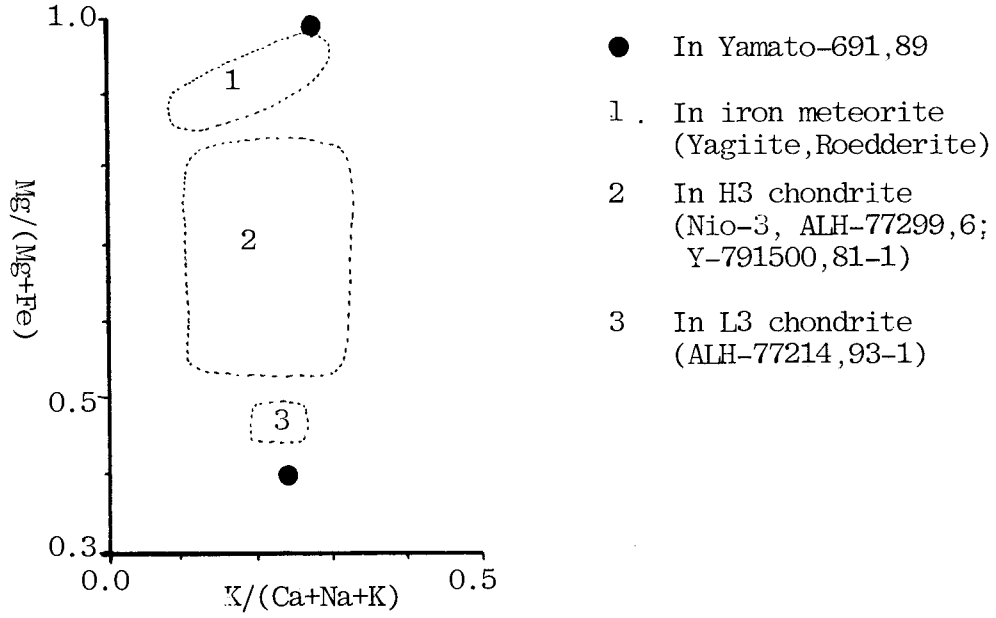

Fig.2. Relation between K/(Ca+Na+K) and Mg/(Mg+Fe) of osumilite-group minerals in several meteorites.

CHEMISTRY OF ENSTATITE CHONDRITE, YAMATO 691 (E3) ANTARCTIC METEORITE

Fukuoka, T.

Department of Chemistry, Gakushuin University, Mejiro, Toshima-ku, Tokyo 171

For the study of chemical evolution on the parent body of enstatite chondrite including the metamorphism, chemical data of type 3 enstatite chondrite play important role. Because the meteorites of E3 type are lack, Yamato-691 (E3) meteorite is one of the precious sample. We analized more than 20 major, minor and trace elements in Yamato 691 meteorite sample (Sub. No. 88) which was provided from National Institute of Polar Research of Japan, by instrumental neutron activation analysis (INAA).

The preliminary analytical results are shown in Table 1 together with the results of standard rock, JB-1 and Allende meteorite (bulk). The chemical abundances of this meteorite (1) and Qingzhen meteorite (E3)(2) are compiled in Table 1 for comparison. Our results generally agree well with earlier reported values (1), but Mn, Cr, Co and Ni contents are higher in our results and Os, Ir and Au contents are lower in our results. Our results also agree well with the averaged values of Qingzhen meteorite (2). This suggests that type 3 enstatite chondrites have close chemical compositions.

Rare earth elements (REE) and Sc data, normalized to volatile-free Cl chondritic abundances (3), are plotted in Fig. 1 for Y-691 and Qingzhen meteorites (4). These patterns show flat unfractionated REE and Sc patterns which is similar to it of Cl chondrites.

From the comparisons with the chemical abundances of other types E chondrites, we will discuss more on the chemical evolution of the parent body of enstatite chondrite.

REFERENCES: (1) Shima, M. and Shima, M. (1975) Mem. Natl Inst. Polar Res., Spec. Issue 5, 9-13. (2) Weeks, K. S. and Sears, W. G. (1985) Geochim. Cosmochim. Acta 49, 1525-1536. (3) Anders, E. and Ebihara, M. (1982) Geochim. Cosmochim. Acta 46, 2363-2380. (4) Ebihara, M. (1984) Mem. Natl Inst. Polar Res., Spec. Issue 35, 243-249.

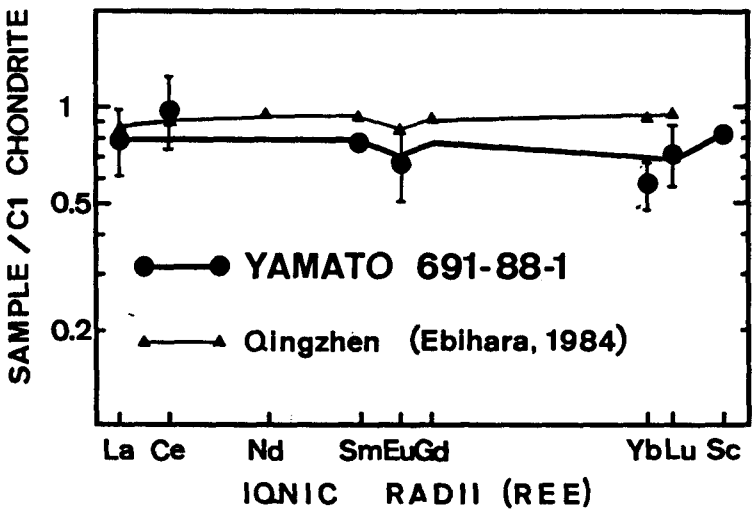

Fig.1. Cl chondrites (non-volatile) normalized abundance patterns of REE and Sc of Y-691 and Qingzhen meteorites.

Table 1. Preliminary results of chemical abundances by INAA

		YAMATO 691		Qingzhen	JB-1	Allende	Error*
		88-1	1)	2)			(%)
Wt	mg	13.0			20.6, 19.8	9.70	
Ti	%	0.05	0.045		0.73		40
Al	%	0.86	0.82	0.86	7.46		1
Fe	%	31.6	29.8	31.3	5.94	24.5	0.5
Mg	%	10.9	11.6	11.3	5.43		3
Ca	%	1.1	1.04	0.91	6.43		15
Na	%	0.88	0.64	0.60	1.91	0.38	0.5
K	%	0.051	0.070	0.081	1.18		28
Mn	%	0.224	0.191	0.201	0.123		0.5
Cr	%	0.403	0.286	0.316	0.046	0.376	0.5
Sc	ppm	6.28		6.27	25.6	12.5	0.5
V	ppm	59		55	225		4
La	ppm	0.25		0.26	36.5	0.60	25
Ce	ppm	0.8			64.2	1.5	25
Sm	ppm	0.15		0.14	4.95	0.36	3
Eu	ppm	0.049		0.038	1.39	0.12	25
Yb	ppm	0.12			2.24	0.27	17
Lu	ppm	0.023			0.31	0.063	22
As	ppm	2.4			1.9	1.5	20
Co	ppm	964	890	910	34.0	649	0.5
Ni	%	2.46	1.86	2.05	0.016	1.55	0.5
Os	ppb	465	1400		n.d.	674	7
Ir	ppb	606	900	554	n.d.	853	0.5
Au	ppb	316	490	343	n.d.	157	1

* Errors for INAA are due to counting statistics.
Values indicate for Y691-88-1 only.
1) Shima and Shima (1975), 2) Average of Weeks and Sears (1985)

44—1

Comsortium studies on E3 chondrite Yamato-691

Dennisson J.E. Kaczaral P.W. Verkouteren R.M. and Lipschutz M.E.*

See No. 17.

SPECTRAL REFLECTANCE (0.25-25 μm) OF THE YAMATO-691 ENSTATITE CHONDRITE

Miyamoto, M.

College of Arts and Sciences, University of Tokyo, Komaba, Tokyo 153.

As part of consortium studies on the Yamato-691 enstatite chondrite, we measured spectral reflectances in the UV-Visible-Near infrared (UV-VIS-NIR) wavelength region and middle infrared region, and compared them with reflectances of an iron meteorite. These meteorites give similar spectra without strong absorption bands in the UV-VIS-NIR region (1), whereas reflectances of meteorites in this wavelength region have been used to interpret mineral assemblages of asteroidal surfaces (e.g., 2). Reflectances in the middle infrared region may give additional information on identification of surface materials. Most previous works have measured 'transmission' spectra of meteorites or minerals in the middle infrared region (e.g., 3). Although meteorites usually show low refelectivity, development of Fourier transform infrared spectrophotometer enabled us to measure reflectances of dark materials in the middle infrared region.

We used two spectrophotometers. [1] Beckman UV 5240 in the UV-VIS-NIR region (0.25-2.5 μm) with an integrating sphere by using Halon as a standard, [2] JASCO FT/IR-3 Fourier transform infrared spectrophotometer in the middle infrared region (2.5-25 μm) equipped with a diffuse reflectance attachment (DR-81) by using an aluminum-coated mirror as a standard. We passed dry air into the spectrophotometer. We used plates of the Y-691 enstatite chondrite and Mundrabilla iron meteorite (octahedrite).

In the UV-VIS-NIR region, the reflectance of Y-691 does not show any strong absorption bands, because pyroxene (enstatite) does not contain Fe^{2+}. Mundrabilla also does not show any absorption bands. Absorption bands which correspond to the crystal field splitting energy of transition metals are dominant in this wavelength region. Therefore, it is difficult to distinguish the E chondrite from the iron meteorite on the basis of reflectances in the NIR region alone.

In the middle infrared region, the reflectance of Y-691 shows absorption bands of pyroxene mainly caused by vibrations of atoms (Fig. 1). The iron meteorite does not show any strong absorption bands in the middle infrared region as expected from the chemical composition. The sharp absorption band at about 4.3 μm is caused by atmospheric CO_2. Noisy spectra around 2.6 μm are caused by residual H_2O in dry air.

We can distinguish the E chondrite from the iron meteorite by reflectances in the middle infrared region. Middle infrared spectra are helpful in interpreting asteroidal surface materials combined with UV-VIS-NIR spectra.

References: (1) Gaffey, M. J. (1976) J. Geophys. Res., 81, 905. (2) Gaffey, M. J. & McCord, T. B. (1977) Proc. Lunar Sci. Conf. 8th, 113. (3) Sandford, S. A. (1984) Icarus, 60, 115.

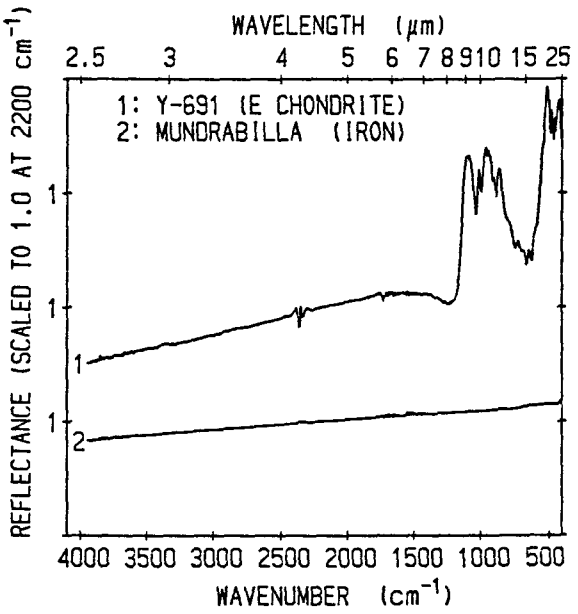

Fig. 1 Comparison of middle infrared reflectances of Y-691 and Mundrabilla.

46—1

DISTRIBUTION OF RARE EARTH ELEMENTS IN SOME ENSTATITE CHONDRITES INCLUDING YAMATO-691

Mitsuru Ebihara

Department of Chemistry, Faculty of General Studies, Gunma University, 4-2 Aramaki, Maebashi, Gunma 371

Enstatite chondrites contain a large variety of unique minerals, most of which are thought to have been formed in the highly reduced condition. For instance, calcium and manganese are known well to be present for the most part in the form of sulfides (oldhamite and alabandite, respectively), hence these elements must have behaved as chalcophile elements instead of lithophile elements as usually recognized at the formation of enstatite chondrite parent bodies.

Host phase(s) of rare earth elements (REEs) in enstatite chondrites have been examined for many years by several investigators. In spite of a great effort taken so far, this problem is still enigmatic. Using a dissolution method, Shima and Honda (1967) were possibly the first to try to make clear the host phase(s) in enstatite chondrites. They found that most of the calcium, which were thought to be attributable to oldhamite, were leached out in acetate buffer solution, whereas REEs were leached out for the most part in ammoniacal EDTA solution (pH 9.5). These results suggested that REEs were not hosted by oldhamite. Sears et al. (1983) and Frazier and Boynton (1985) tried to separate oldhamite mechanically. Though they could not isolate the oldhamite mineral, they come to the conclusion that oldhamite was the host mineral for the REEs. Recently, Larimer and Ganapathy succeeded in isolating oldhamite mechanically in Indarch (E5) and found that REEs were present in this mineral with an enrichment factor of 100 relative to the bulk abundances.

In this work, REEs were studied for their distribution in enstatite chondrites, Abee (E4), Indarch (E4), Qingzhen (E3) and Yamato-691 (E3). A stepwise dissolution method, modified after a Shima and Honda's method, were applied for phase separation. Some results are shown in Figure 1. In Abee, the dissolution patterns of calsium and REEs (La and Sm) are identical, whereas the dissolution patterns of REEs do not follow that of Ca in Indarch and Qingzhen. These results do not suggest that oldhamite is an only host phase for REEs in enstatite chondrites.

References:
Frazier, R.M. and Boynton, W.V. (1985), Meteoritics, 20, 197-218.
Larimer, J.W. and Ganapathy, R. (1983), Meteoritics, 18, 334 (abstract).
Sears, D.W., Kallemeyen, G.W., and Wasson, J.T. (1983), Earth Planet. Sci. Lett., 63, 180-192.
Shima, M. and Honda, M. (1967), Geochim. Cosmochim. Acta, 31, 1995-2006.

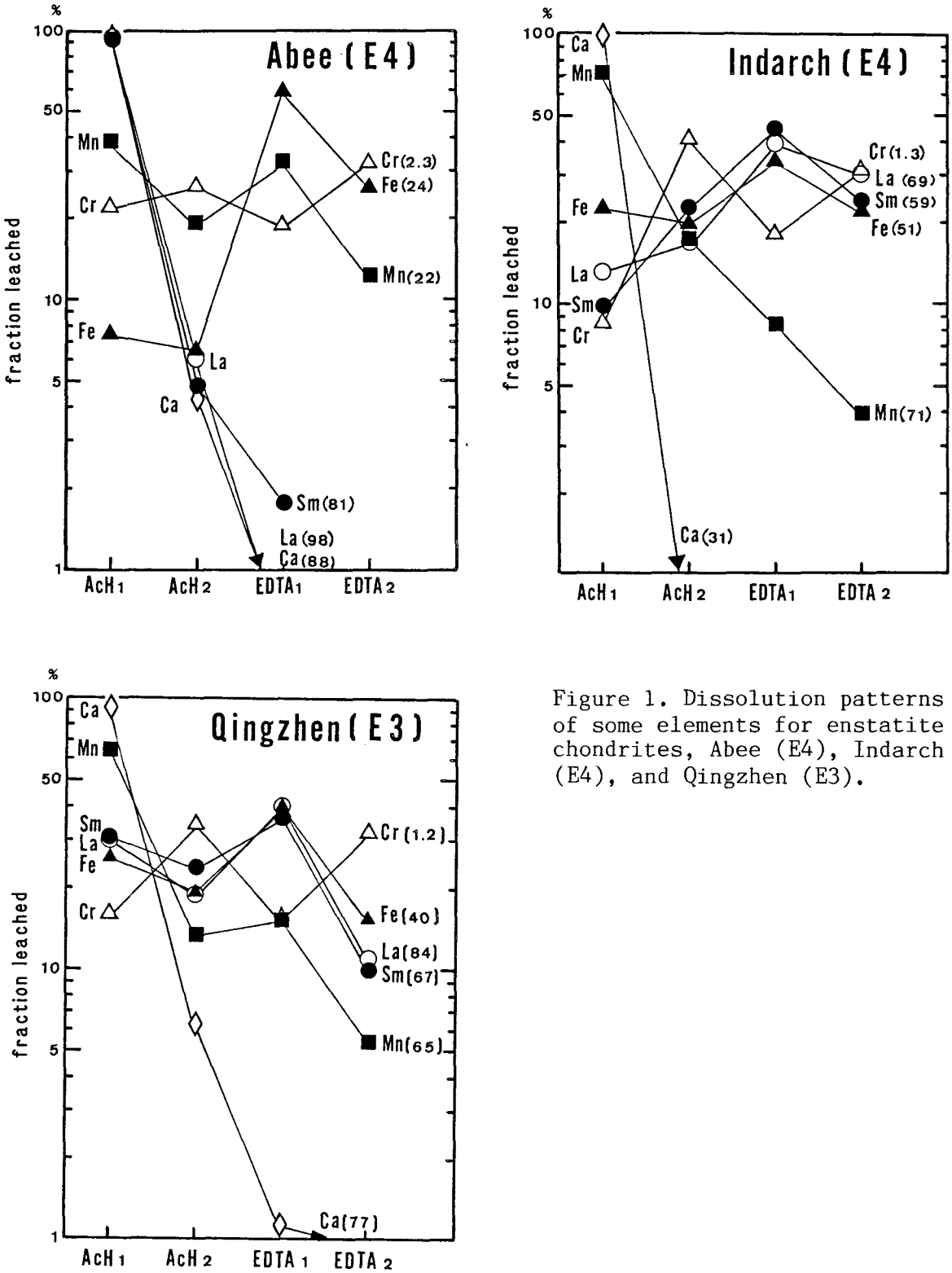

Figure 1. Dissolution patterns of some elements for enstatite chondrites, Abee (E4), Indarch (E4), and Qingzhen (E3).

Special Lecture

Professor Ahmed El Goresy

YAMATO 691: EVIDENCE FOR PLANETARY METAMORPHISM t < 1.1 BILLION YEARS IN THE EH PARENT BODY

El Goresy, A.[1], Woolum, D.S.[2] and Ehlers, K.

[1]MPI Kernphysik, Heidelberg, FRG; [2]Calif. State Univ. Fullerton, CA, USA; [3]University of Heidelberg, FRG

The unequilibrated EH chondrites are aenigmatic and the least understood among the enstatite chondrite clan. Abundances of the siderophile elements resemble those of typical EH (1). However, the moderately volatile chalcophile elements in some of them appear to be intermediate between EH and EL (1). The geochemical behaviour of many typical lithophile elements is entirely different from behaviour of these elements in ordinary and carbonaceous chondrites as a result of the low fO_2 during their formation and evolution. Ca is almost exclusively present in oldhamit (CaS), major part of Mg is incorporated in ningerite (Mg,Fe,Mn)S, and the metal phases contain considerable amounts of Si alloyed with them (1-14 wt% Si). In the unequilibrated EH chondrites both Na and K occur as sulfides (2). However, these elements display a remarkable fractionation in varous complex sulfide lithologies (2). This fractionation is well pronounced in Yamato 691, Qinzhen and Yamato 77295. K is incorporated in djerfisherite $(K_3Cu(Fe.Ni)_{12}(S.Cl)_{14}$ while Na is associated with Cr in several sulfide phases, e.g. caswellsilverite $(NaCrS_2)$(2,3).

Textures and mineral relations in Y691 are indicative of an unequilibrated EH. Likewise in Qinzhen (2) and Kota Kota (6) metals and sulfides occur in rounded, lenticular, and angular complex clasts. All alkali sulfides reside in the matrix. Minerals encountered include Si-bearing kamacite, perryite, Ti-bearing troilite, oldhamite, djerfisherite, caswellsilverite, a hydreous Na-Cr sulfide, two new complex Na-Cu-Cr-sulfide and Na-Cu-Zn-sulfide presumably related to caswellsilverite. Djerfisherite displays breakdown textures similar to the one described from Qinzhen (2,3). However, the reaction in Yamato 691 is more advanced.

PETROGRAPHY & MINERAL CHEMISTRY: Niningerite usually displays segmental zoning, thus suggesting lack of equilibration or a late thermal episode. Compositions of niningerites in EH chondrites (St. Marks, Kaidun III, Qinzhen, Indarch, Y74370, Kota Kota and Y691) are resolved in three distinct chemical groups in the MgS-FeS-MnS compositional diagram (Fig. 1): a a group with the lowest MnS (3.6-6.7) and the highest MgS-contents (73.2-82.9) only comprising Y691; b medium MnS (7.5) and lowest MgS (58.65.5) represented by Indarch & c high MnS (12-14) and medium to high MgS (61-75); Kaidun III, St. Marks, Kota Kota, Qinzhen, and Y74370. Compositional variations of niningerite analyses in a meteorite reflects usually zoning features (e.g. Y691, Indarch).

All groups plot as well separated flat elongated fields lying parallel to the MgS-FeS join (Fig. 1). This relationship may reflect either the difference in bulk Mn or differences in partitioning of Mn between enstatite and niningerite as a function of fS_2.

The heavy cluster of Kaidun III, St. Marks, Kota Kota, Qinzhen, and Y74370 may represent an evolution sequence: Y74370 the most primitive and Kaidun III the most equilibrated in this subgroup. In Y691 djerfisherite compositions vary thus manifesting the unequilibrated nature of the meteorite (50.9-51.5 Fe, 0.49-2.94 Ni, 4.73-2.09 Cu, 7.94-6.91 K, 1.14-1.68 Na, 1.45-1.5 Cl). Breakdown of djerfisherite is advanced to complete. Only residual patches of djerfisherite occur in a complex assemblage of breakdown products consisting

of major troilite, a mixture of idaite and bornite (48.0 Cu, 19.2 Fe, 0.12 Zn, 30.0 S), covellite (CuS) and sphalerite (25.6 Fe, 2.24 Mn, 33.0 Zn, 1.23 Cu, 0.17 Ga, 35.3 S). The occurence of sphalerite in this assemblage is intruiging since: a djerfisherite does not contain detectable Zn (< 0.01%) and hence Zn was introduced during this metamorphic episode, and b sphalerite can be used as a cosmic barometer for estimation of the total pressure during the metamorphic event in the parent body (7). Both secondary troilite and sphalerite contain numerous bubbles presumably formed by release of ^{40}Ar during the metamorphic event and indicating simultaneous formation of the sphalerite-troilite pair. This troilite contains minor Cl (0.18) evidencing a genetic link to djerfisherite breakdown. Caswellsilverite (15.3 Na, 36.5 Cr, 1.00 Fe, 1.28 Cu, 0.14 Zn, 45.9 S) adjacent to breakdown assemblages in djerfisherite displays remarkable variation in its Cu-content (1.28-15.0 Cu). Several idiomorphic caswellsilverite crystals are surrounded by narrow rim of a new Cu-Zn-rich variety (1.86 Na, 32.5 Cr, 0.65 Fe, 0.76 Ca, 7.62 Cu, 9.97 Zn, 0.3 K, 42.8 S). In some cases a hydrous Cu-rich Na-Cr sulfide was encountered (1.22 Na, 32.1 Cr, 1.6 Fe, 18.0 Cu, 0.14 Zn, 0.46 K, 41.6 S). Major part of oldhamite was removed by weathering. In djerfisherite breakdown assemblage oldhamite (55.5 Ca, 0.52 Fe, 0.29 Mg, 0.2 Cu, 0.13 Zn, 43.1 S) is intact indicating that leaching of CaS was achieved during terrestrial weathering and not during the metamorphic episode. Perryite (73.6 Ni, 9.85 Fe, 0.21 Cu, 3.56 P, 12.48 Si) occurs usually as idiomorphic crystals in kamacite (94.7 Fe, 0.37 Co, 2.33 Ni, 2.07 Si). This texture is not suggestive of formation of perryite as a result of sulfidization of kamacite. Primary troilite displays considerable variations in its minor element concentrations (0.69-2.24 Cr, 0.03-0.32 Ti). Primary sphalerite (29.5 Fe, 1.18 Mn, 33.8 Zn, 0.2 Cu, 0.14 Ga, 33.8 S) was encountered in a primary assemblage coexisting with niningerite, FeS, αFe, CaS, and schreibersite (70.0 Fe, 14.4 Ni, 0.14 Si, 13.9 P).

DISCUSSION: Both Y691 and Qinzhen have low K-Ar ages 1.1 Ga and 2.88 Ga respectively (4 & 5). $^{39}Ar/^{40}Ar$ laser age measurements revealed ≈ 4.4 Ga for unaltered djerfisherite and an age of < 1.4 Ga for the breakdown product in Qinzhen (5). The low age of Y691 (4) even hints to a much younger event for this meteorite. The metamorphic episode in Y691 seems to have mainly modified or altered the alkali sulfides i.e. breakdown of djerfisherite, mobilization and introduction of Zn and Cu to caswllsilverite ... etc. The P-T history of Y691 is quite complex. Composition of sphalerite occuring in the breakdown products may allow estimation of the P-T conditions during the metamorphic episode (7). The P-T isopleths of primary and secondary sphalerites (Fig. 2) are well separated indicating that little or no equilibration took place in the primary assemblage during the metamorphic event. Idaite and covellite places the maximum temperature of this episode at 507°C, thus below the estimated 600°C as a blocking temperature of the primary sphalerite (7).

We estimate a pressure of 800 bars and T = 350°C for the metamorphic reaction and hence conclude it must have taken place in Y691 parent body as a result of an endogenic metamorphic episode.

REFERENCES: (1) Weeks & Sears, GCA (1985), 1525. (2) El Goresy et al., Meteoritics 18 (1983), 293. (3) El Goresy, Meteoritics (1985) in press. (4) Shima et al. EPSL 19 (1973), 246. (5) Müller & Jessberger, Lunar Planet. Sci. XVI (1985), 595. (6) Leitch & Smith GCA (1982), 2083. (7) Hutchison & Scott, GCA (1983), 101.

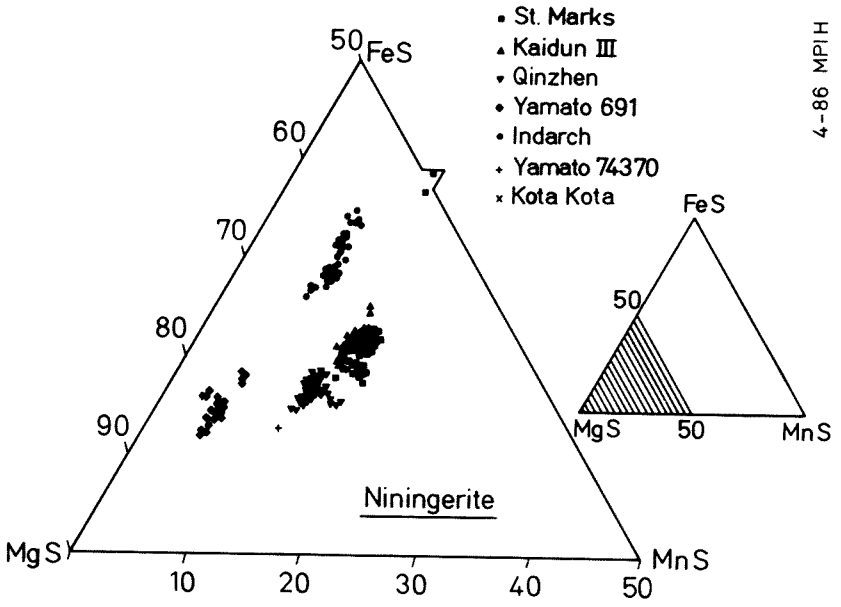

Figure 1:

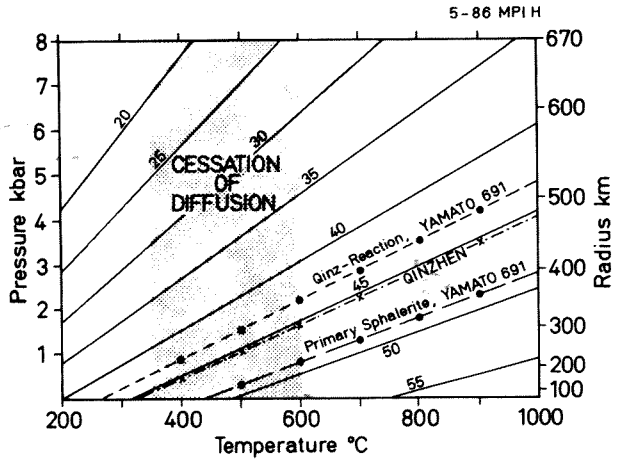

Figure 2: Experimentally determined P-T isopleths (mole % FeS) of sphalerite formed in equilibrium with troilite (from 7). Isopleths for sphalerites in Qinzhen and in Y691 are calculated from present results.

Thursday, March 27, 1986

0900 - 1510	*Symposium, Auditorium*
1540 - 1630	*Special Lecture*
	Professor Michael E. Lipschutz
	(Purdue University, Lafayette, USA)

PRIMITIVE REE FRACTIONATION IN ALLENDE CHONDRULES

KEIJI Misawa and NOBORU Nakamura
Department of Science of Material Differentiation, Graduate School of Science and Technology, also at Department of Earth Sciences, Kobe University, Nada, Kobe 657, JAPAN

More than twenty individual chondrules from the Allende chondrite were analysed for REE, Sr, Rb, K, Mg and Ca by isotope dilution method. In addition, petrographic examinations were carried out for thin sections of some samples analysed for the trace elements.

Results show that REE abundances between each one of the analysed chondrules vary at least a factor of ten, and are more or less fractionated. Furthermore, it is worth noting that most of chondrules have variable amount of negative Eu anomaly, and that negative or positive Ce and/or Yb anomalies are frequently observed. However, the magnitude of these anomalies do not show a direct correlation to those of REE abundances.

Two BO (barred olivine) chondrules, two RP (radial pyroxene) chondrules and a chondrule rich in opaque minerals exhibit distinct HREE and LREE fractionations (Fig.1). BO chondrules are enriched in HREE and present superimposed large negative Eu and Yb anomalies. On the other hand, RP chondrules and the chondrule rich in opaque minerals show LREE enrichment with large positive Yb anomalies. In despite of these REE fractionations, K and Rb, two moderately volatile elements, exhibit no relative fractionation, showing a straight correlation to that of $(Rb/K)_{CI}$ ratio (Fig.2).

In Fig.3, the elements are arranged according to their cosmochemical volatilities (Boynton and Cunningham, 1981). Most of chondrules have negative Ca anomalies (i.e. a high REE/Ca ratio than CI) and a constant Mg abundance (1.5 - 3 X CI). Alkaline element abundances are not correlated to other lithophile elemental abundances. It is pointed out that CI-normalized pattern do not form any smooth curve when plotted against elemental volatilities. In accordance with previous results (Gooding et al., 1980, 1983; Grossman and Wasson, 1982, 1983), these lithophile elemental fractionations suggest that chondrules were not formed by melting of CI chondrite-like materials. Considering the enrichment in most refractory REE of two BO chondrules and the depletion in these elements of two RP chondrules, it seems likely that their patterns are related to elemental volatility, and therefore, it is expected that gas/solid fractionation took place during formation process of

chondrule precursor materials. It is suggested that early nebula condensates and/or evaporation residue can be invoked as alternative REE carriers in the Allende chondrules.

In Allende, the Ce anomaly is known in two CAI's (Boynton, 1978, Davis et al., 1982). However, there has been only a little amount of information about these anomalies (Tanaka et al., 1975, Hamilton et al., 1979). Our results suggest that Ce anomalies seemed to be much more widespread in chondrules, reflecting chondrule precursor material(s) or chondrules those may have formed under more oxidizing conditions.

REFERENCES

Boynton W.V. (1978) Lunar Planet. Sci. IX, 120.

Boynton W.V. and Cunningham C.C. (1981) Lunar Planet. Sci. XII, 106.

Davis A.M., Tanaka T., Grossman L., Lee T and Wasserburg G.J. (1982) GCA,46, 1627.

Gooding J.L., Keil k., Fukuoka T. and Schmitt R.A. (1980) EPSL,50, 171.

Gooding J.L., Mayeda T.K., Clayton R.N. and Fukuoka T. (1983) EPSL, 65, 209.

Grossman J.N. and Wasson J.T. (1982) GCA,46, 1081.

Grossman J.N. and Wasson J.T. (1983) GCA,47, 759.

Hamilton P.J., Evensen N.M. and O'Nions R.K. (1979) Lunar Planet. Sci. X, 494.

Tanaka T., Nakamura N., Masuda A. and Onuma N. (1975) Nature, 256,27.

Fig.1. CI-normalized REE pattern of chondrules from the Allende chondrite. Barred olivine chondrules (O), radial pyroxene chondrules (∇) and opaque mineral-rich chondrule (Δ) show fractionated REE patterns.

Fig.2. CI-normalized K vs. Rb variation of Allende chondrules. Most chondrules follow CI-ratio.

Fig.3. Enrichment factor of lithophile elements normalized to CI chondrite, in the Allende chondrules.

Fig.1.

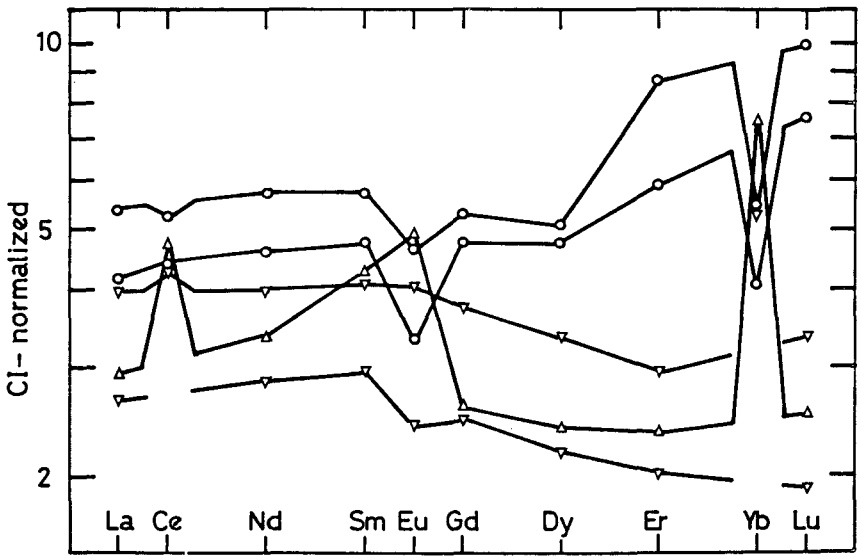

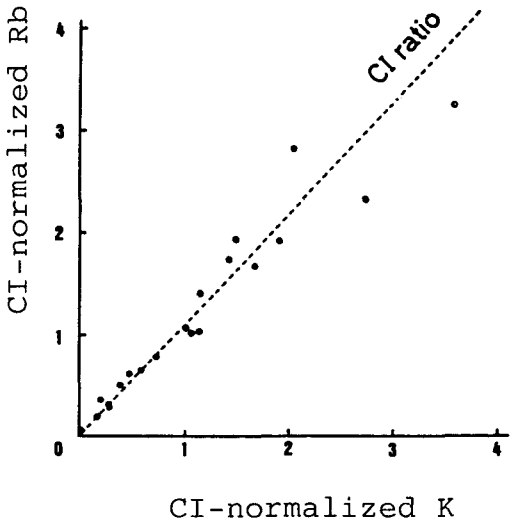

Fif.2.

Fig.3.

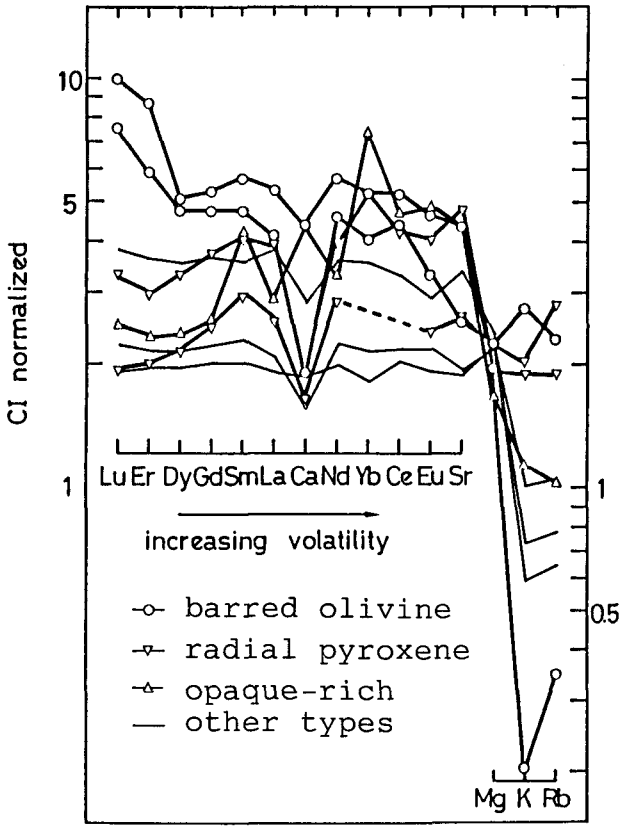

Fractionation of REE among individual chondrules from the Bjurböle (L4) chondrite.

Tomoko Nakayama and Noboru Nakamura
Department of Earth Sciences, Faculty of Science, Kobe University, Nada-ku, Kobe 657 Japan

Concentrations of REE, K, Rb, Sr, Mg and Ca in 11 individual chondrules from the Bjurböle chondrites (L4) were determined by the mass spectrometric isotope dilution method. Major chemical compositions of constituent minerals and bulk chondrules were also examined using electron microprobe analyzer.

As shown in Fig.1, fayalite contents in olivine grains within individual chondrules are homogeneously distributed,indicating that the major elements such as Fe and Mg are well-"equilibrated" in the grains.

Based on chondrites-normalized REE patterns, chondrules are classified into three groups (A,B,C in Fig.2). Every group is characterized by its petrologic features; Group A chondrules show radial-pyroxene texture; Group B chondrules have porphyritic olivine (and pyroxene) together with microcrystalline plagioclase; Group C chondrules include porphyritic olivine (and pyroxene) grains enbeded in a "least-crystallized", black chondrule matrix.

Light REE depleted patterns of Group A and B are qualitatively explained in terms of "equiliblium" distribution of REE among constitunent minerals of chondrules.

However, REE patterns of group C chondrules which are generally flat and have negative Eu anomaly are similar to those of many chondrules in unequilibrated chondrites. Furthermore, REE are most abundant in chondrule matrix (Fig.3).

Therefore, REE in C-3 (and C-7) seems to be less re-distributed compared to those in group A and B.

Fig. 1

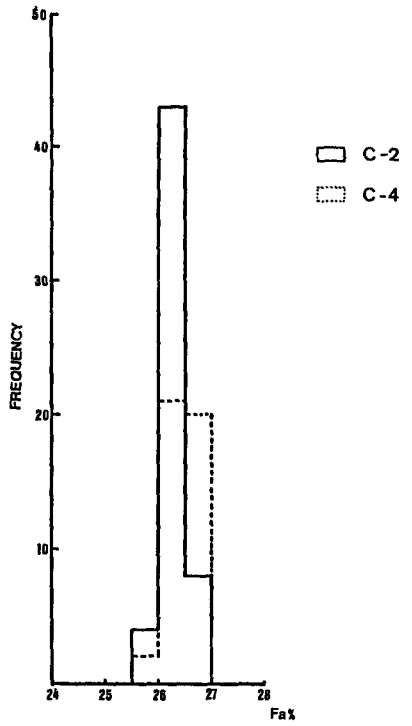

Fig. 2

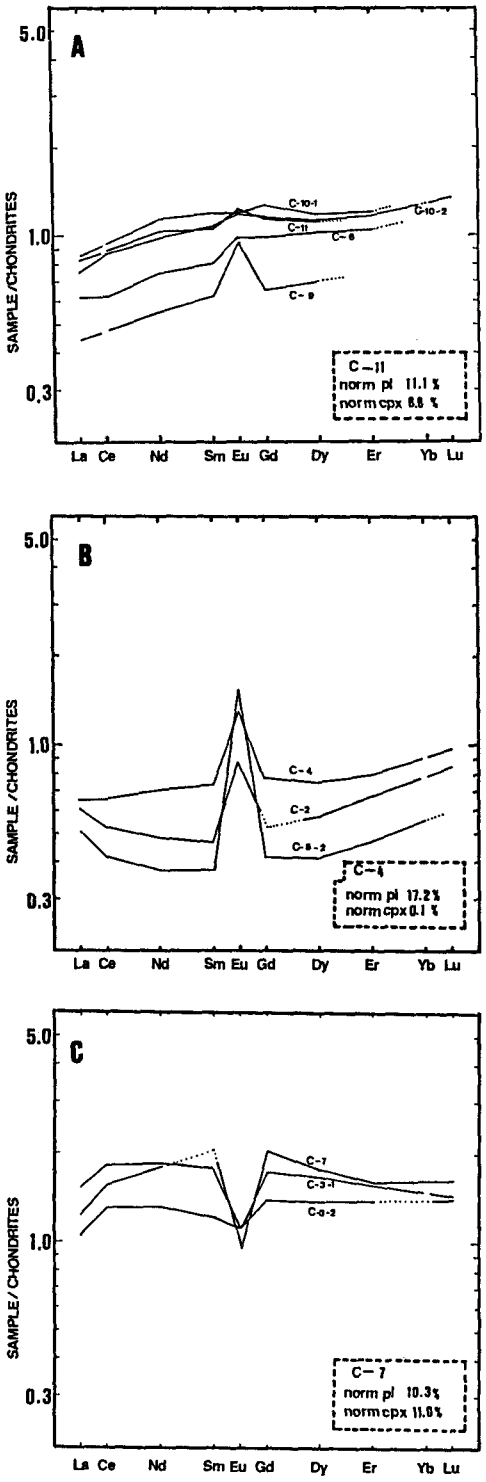

Fig. 3

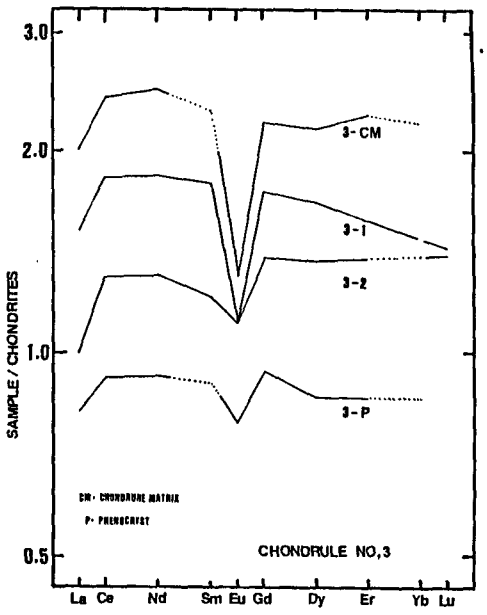

Fig. 1 The histogram of fayalite (Fe_2SiO_4) contents of olivines from C-2 and C-4 chondrules.

Fig. 2 Three classified groups of chondrules based on REE patterns.

Fig. 3 REE patterns of the C-3 chondrule.

DISTRIBUTION OF RARE EARTH ELEMENTS IN UNEQUILIBRATED ORDINARY CHONDRITES

Misuru Ebihara

Department of Chemistry, Faculties of General Studies, Gunma University, 4-2 Aramaki, Maebashi, Gunma 371

Distribution of rare earth elements (REEs) among some component phases of Antarctic unequilibrated ordinary chondrites (UOCs) was studied. A selective dissolution method was applied for phase separation. REEs were determined by radiochemical neutron activation analysis.

In Equilibrated ordinary chondrites (EOCs) of petrological types of 4-6, more than 80% of the light and middle REEs were confirmed to be located in Ca-phosphates (apatite and merrillite) (Shima and Honda, 1967; Ebihara and Honda, 1983). The residual parts of the REEs were present in HCl-insoluble phases, most of which were pyroxene and plagioclase. These figures, however, seem to be quite different in UOCs. In Yamato 74191 (L3), as much as 51% of the total Sm were observed to reside in HCl-insoluble phases. ALH78084 (H3) showed the distribution of 30% of the total Sm into such phases. The present results for Sm budgets in some chondrites are summarized in Table 1 including those for the Allende carbonaceous chondrite (Ebihara and Honda, submitted).

Figure 1 shows the fraction of the REEs attibutable to Ca-phosphates. Bruderheim (L6) shows the high concentrations of the REEs with a large Eu depletion, whereas the UOCs show relatively small enrichment and a small Eu depletion. In fact, no Eu depletion was confirmed for the Ca-phosphate phase in Y74191. Figure 2 shows the C1 chondrite-normalized REE abundance patterns for HCl-insoluble phases of UOCs and EOCs. The relative enrichment and degree of the inclination are apparently different between them. These differences between UOCs and EOCs, and even among UOCs, may reflect the difference in metamorphic activities on their parent bodies.

Table 1. Approximate Sm budgets in some chondrites.

meteorites	type	Ca-phosphate	pyroxine + plagioclase
Allende	C3	10-15	50-60
Y74191	L3	49	51
ALH78084	H3	70	30
Kesen	H4	80	20
Richarton	H5	90	10
Bruderheim	L6	82	18
St.Severin	LL6	88	12

References:
Ebihara, M. and Honda, M. (1984), Meteoritics, 19, 69-77.
Shima, M. and Honda, M. (1967), Earth Planet. Sci. Lett., 2, 344-348.

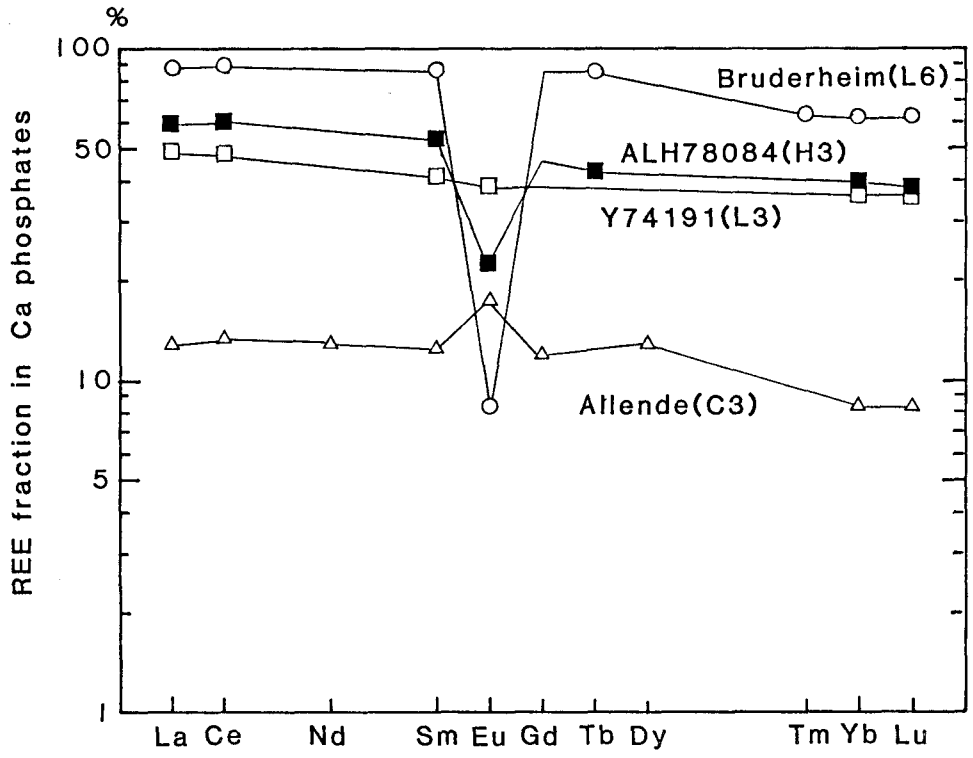

Figure 1. REE fraction in Ca-phosphate phases.

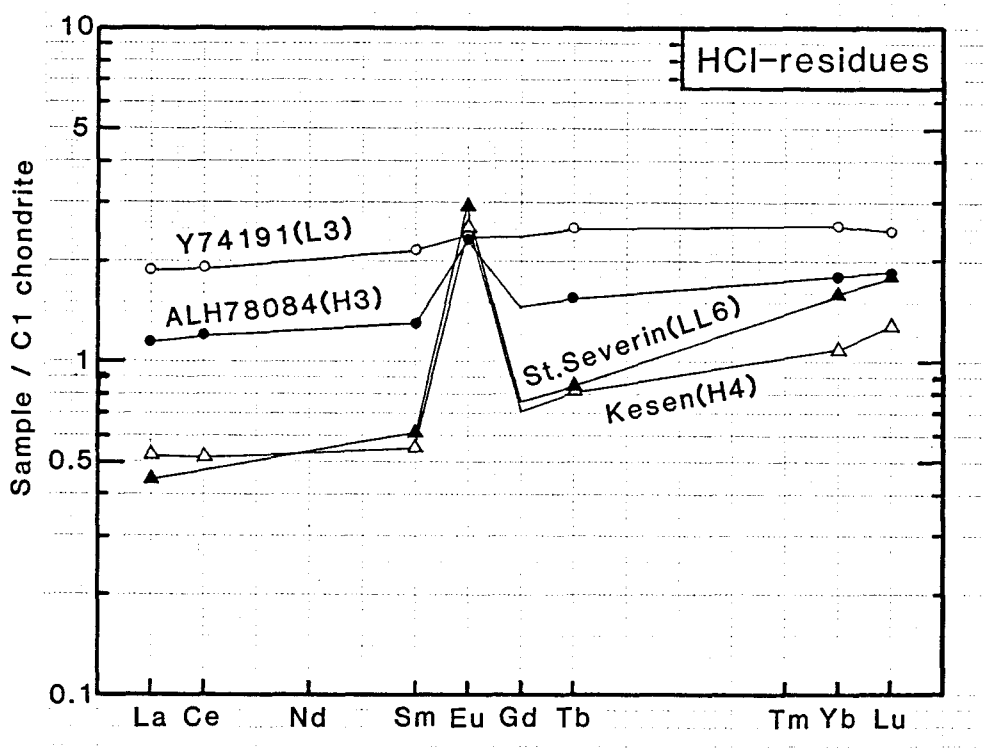

Figure 2. C1 chondrite-normalized REE abundance patterns for HCl-insolbule phases.

TRACE ELEMENTS IN SOME IRON METEORITES.

M.HONDA, H.NAGAI, Nihon Univ.,Dept. of Chem.,Sakura-josui, Setagaya-ku,Tokyo,156.
and T.SHIMAMURA, Marubun Corp.,Nihonbashi,Chuoh-ku,Tokyo,103.

Several species of siderophile elements and some non-volatile cosmogenic stable isotopes have been determined in iron meteorites by neutron activation (NAA) and by glow discharge mass-spectrometry (GDMS).

Relative contents of siderophile elements such as platinum group,Ga,Ge,As,Re,Au and others at ppm levels were analyzed non-destructively by NAA and GDMS. The data were compared with reported values appeared in literatures. The samples tested were Canyon Diablo,Odessa,Boxhole,Treysa and Grant. The NAA method has also been applied further for some other types of irons including antarctic meteorites.

In the same samples, Sc,Cr and Mn which contain cosmogenic products at ppb levels were also studied by GDMS nondestructively and Sc was by radiochemical NAA method. The natural contamination levels of the first transition elements covering Sc to Mn are found to be close to those of the cosmogenic products, but still they seem to be parallel with the pattern of their solar abundances.

Two sets of the results so far obtained by NAA and by GDMS are compared in Table 1. A fairly good mutual agreement can be illustrated among the data obtained by different methods. In some cases,however, disagreements are detected such as in the cases of As and Au. On the whole, depending upon the classfications,A and B, Ir contents are remarkably variable by a factor of 10^3,in contrast to a smaller variation of Au. The relative abundances of Re and Os seem approximately parallel with that of Ir.

Reference:
T.Shimamura,H.Nagai and M.Honda,Elemental Analysis of Iron Meteorites by Glow Discharge Massspectrometer. abstract for Lunar and Planetary Sci.,XVII,Mar.1986,Houston,Tex,U.S.A.

Table 1. Contents of Trace Elements found in Iron Meteorites.

	Content in Canyon Diablo, IA		Contents(normalized to C.D.)											
			Odessa, IA			Boxhole, IIIA			Treysa, IIIB			Grant, IIIB		
			NAA.	MASS	LIT.	NAA.	MASS	LIT.	NAA.	MASS	LIT.	NAA.	MASS	LIT.
Sc	0.26	ppb	0.1	-	-	0.2	-	-	1.8	1.6	1.8	1.4	1.4	-
Ti	1300	ppb	-	260	-	-	100	-	-	170	-	-	160	-
V	30	ppb	-	40	-	-	260	-	-	21	40	-	30	-
Cr	11	ppm	-	15	-	-	110	66	-	1	1	-	0.4	1.1
Mn	-	ppb	-	-	-	-	-	-	-	-	60*	-	40	50*
Ni	6.0	%	-	6.1	7.3	-	7.7	7.7	-	7.5	9.5	-	8.1	9.3
Co	0.51	%	-	0.44	0.48	-	0.44	0.49	-	0.53	0.57	-	0.47	0.60
Ga	80	ppm	70	60	75	17	15	18	20	14	20	16	16	20
Ge	320	ppm	300	323	285	32	32	38	42	42	42	35	48	54
As	2	ppm	2.0	2.2	-	0.5	0.3	-	2.1	1.2	-	2.2	0.7	-
Re	0.23	ppm	0.23	0.20	0.25	1.50	1.33	-	0.10	0.07	0.09	-	0.003	0.005
Os	2.2	ppm	2.0	2.0	2.6	11	16	-	0.70	0.46	0.57	-	0.02	0.10
Ir	1.6	ppm	1.8	1.8	1.9	10	10	8	1.1	0.8	1.1	(0.02)	0.02	0.03
Pt	5.4	ppm	3.8	5.4	8.6	9	12	-	5.3	5.7	-	(1.6)	1.1	-
Au	1.3	ppm	1.3	-	1.9	0.4	-	-	1.3	-	-	1.3	-	-

* estimated for cosmogenic products

A 1.2 B.Y. IMPACT EVENT ON LL-CHONDRITE PARENT BODY: EVIDENCE FROM RB-SR SYSTEMATICS AND RARE GAS COMPOSITIONS OF PAIRED LL-CHONDRITES FROM ANTARCTICA.

O. OKANO[1], N. NAKAMURA[1,2], K. NAGAO[3] and H. HONMA[4]

1) Dept. of Science of Material Differentiation, Graduate School of Science and Technology, Kobe University, Nada, Kobe 657.
2) Dept. of Earth Sciences, Faculty of Science, Kobe University, Nada, Kobe 657.
3) Okayama University of Science, Ridai-cho, Okayama 700.
4) Institute for Study of Earth's Interior, Okayama University, Misasa, Tottori 682-02.

Many shock ages determined by the K-Ar(Ar-Ar) method have been reported so far for meteorites but the ages were rarely re-examined by other chronological method such as Rb-Sr or U,Th-Pb method. The use of these methods have been limited by experimental difficulties and mainly because of irregular homogenization and/or absent of fractionation in the melted portions. Recently, we presented a 1.2 b.y.-Rb-Sr isochron age for a "wholly" impact-melted LL-chondrite, Yamato-790964(Nakamura and Okano, 1985). Here we present an additional Rb-Sr data, newly determined K-Ar ages and chemical data for additional five Yamato-79 LL-chondrites.

As shown in Table 1, K-Ar ages determined for six Antarctic LL-chondrites are substantially identical except for that of Yamato-790143, which seems to have suffered slight Ar loss after the major shock event at 1.2 b.y. ago. For these meteorites, cosmic-ray irradiation ages(Table 1) and other rare gas compositions as well as K-Ar ages are all quite similar to each other, indicating that they were originary a single stone. Rb-Sr isotopic compositions, however, are quite different from chondrite to chondrite and from portion to portion even in a same meteorite. While the Yamato-790964 shows a well-defined isochron of 1.20 ± 0.05 b.y. age, the Yamato-790723 does not yield any meaningful isochron at all(Fig. 1). However, the Yamato-790519 seems to be intermediate between these two, that is, data for mineral concentrates from this meteorite, as a whole, do not form a specific isochron but fall within a zone nearly pararelled with the 1.2 b.y. line. These Sr isotopic variations are closely related to their petrographical features which indicate that they have been more strongly affected by the shock in following order: Yamato-790964, Yamato-790519, Yamato-790723. Anyway, the Rb-Sr age of 1.2 ± 0.05 b.y. are fairly confirmed by the K-Ar ages. It is interesting that this age is the youngest and well-defined isochron age so far known among chondrites.

Our results suggest that the shock melting at 1.2 b.y. ago induced rather random and small-area migration of variable amounts of melts followed by fractionation of Sr and REE, to some extent evaporation of alkali metals and nearly complete degassing of rare gases such as He, Ne and Ar.

The post-shock residual temperature and cooling rate were roughly estimated to be around 1300°C and 1-10°/h respectively on the basis of petrographical texture and mineral chemistry.

Present results suggest that the Yamato-79 LL-chondrites

were surface regolith materials and that prominent shock event(s) occurred on the LL-chondrite parent body at around 1.2 b.y. ago.

Reference
N. Nakamura and O. Okano(1985): Nature 315, 563-565.

Table 1. K-Ar gas retention ages and ^{21}Ne cosmic-ray irradiation ages(T_{21}) for the Yamato-79 LL-chondrites.

	K-Ar age (b.y.)	T_{21} (m.y.)
Yamato-790143	1.03	20
Yamato-790345	1.26	17
Yamato-790397	1.32	19
Yamato-790519	1.31	19
Yamato-790723	1.31	18
Yamato-790964	1.26	20

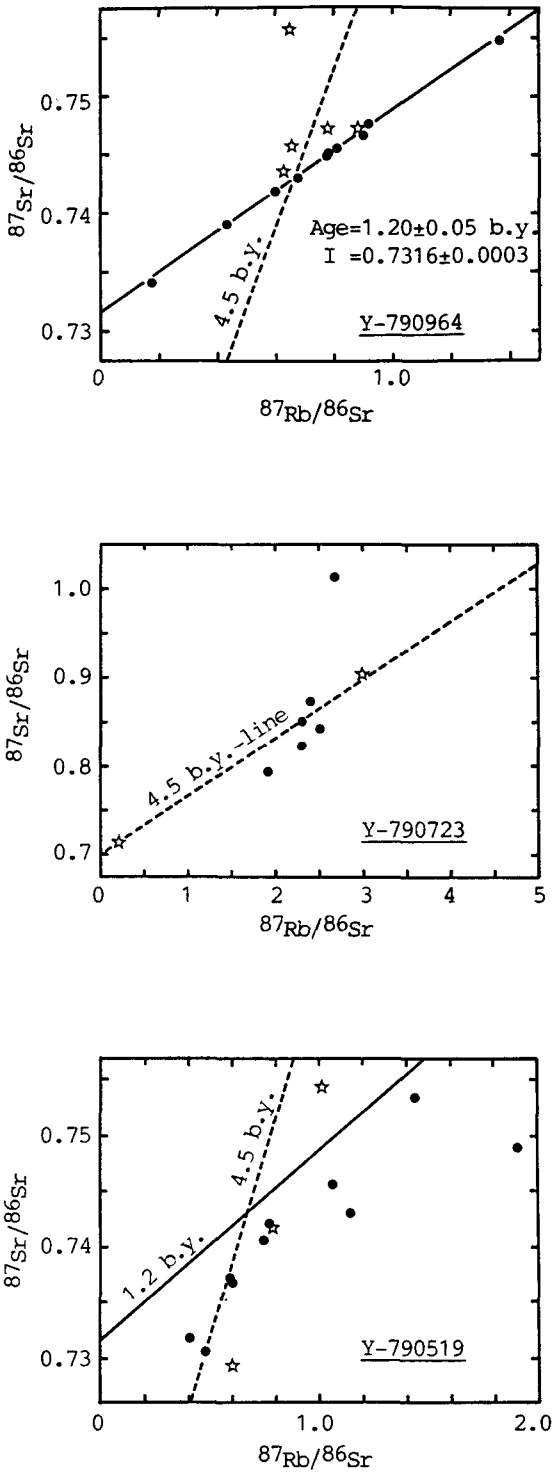

Fig. 1 ^{87}Rb-^{87}Sr evolution diagrams for the Yamato-790964, Yamato-790723 and Yamato-790519. (Star and dot represent whole rock and mineral concentrate respectively.)

INVESTIGATION OF THE SHOCK EFFECT ON THE ANTARCTIC METEORITES BY THE 40Ar-39Ar METHOD

Takigami, Y.* and Kaneoka, I.**
* Institute for Cosmic Ray Research, University of Tokyo, Tanashi-shi, Tokyo 188
**Geophysical Institute, Faculty of Science, University of Tokyo, Bunkyo-ku, Tokyo 113

In order to investigate the shock effect on meteorites, the 40Ar-39Ar analyses were performed to the Antarctic LL-chondrites, Y-790964(LL) and Y-790448(LL3), which have been identified to be shocked and unshocked meteorites, respectively. Y-790964 was investigated by the Rb-Sr method and the age of 1197+-54 Ma was obtained as the time of the shock event [1].

Sample chips were selected from the outerpart (Y-790964,97;0.75g, Y-790964,67;0.81g and Y790448.88;0.79g) and the inner part (Y-790964,96;0.75g and Y-790448,75;0.81g) of each meteorite in order to compare the differences of the shock effect on the 40Ar-39Ar systems in these meteorites.

The experimental procedures are almost the same as those reported before [2], except that a quadrupole mass spectrometer was used for measuring Ar isotopic ratios [3]. Data were corrected for the system blanks and the effects of Ca- and K-induced interfering isotopes.

The results of this study are summarized as follows and age spectra are shown in Figs.1 and 2.

(a) Y-790964 (LL, shocked) (Fig.1)

The age spectra of the inner part (96) and two outer parts (97 and 67) indicate similar patterns, though that of 97 is more scatterd slightly than that of 96 and the 600C fraction of 67 is higher than those of 96 and 97. Total fusion ages (96;about 1240Ma, 97;about 1210Ma, 67;about 1260Ma) are similar among each portion and these ages almost agree with the reported Rb-Sr age (1197+-54Ma). Moreover, the age spectra show almost the same ages through the whole degassing temperatures. These results suggest that the shock event to Y-790964 was very intensive and all K-Ar and Rb-Sr systems were resetted about 1200Ma ago.

(b) Y-790448 (LL3, unshocked) (Fig.2)

The age spectra of the inner (75) and outer (88) parts are similar each other. The highest temperature fraction (1600C) of 75 was lost due to an experimental failure and an apparent old age for the 1000C fraction of 88 may have been caused by some improper experimental procedures. The age of 75 (600C-900C;about 4490Ma) is older than that of 88 (600C-900C;about 4360Ma).

The age spectrum of this meteorite shows an inverse stair-type, where the age becomes younger with the increse of the

Futher study is required to settle this problem.

References

[1] Okano, O. and Nakamura, N., Abstracts for the Tenth Symposium on Antarctic Meteorites, 67 (1985)
[2] Kaneoka, I., Mem. Natl. Inst. Polar Res., Spec. Issue 30, 259 (1983)
[3] Takigami, Y., Nishijima, T., Koike, T. and Okuma, K., Mass Spectroscopy, 32, 227 (1984)
[4] Turner, G., in "Paleogeophysics" ed. by S. K. Runcorn, 491 (1970)
[5] Turner, G., Enright, M. C. and Cadogan, P. H., Proc. Lunar Planet. Sci. Conf. 9th, 989 (1978)
[6] Podosek, F. A. and Huneke, J. C., Geochim. Cosmochim. Acta, 37, 667 (1973)

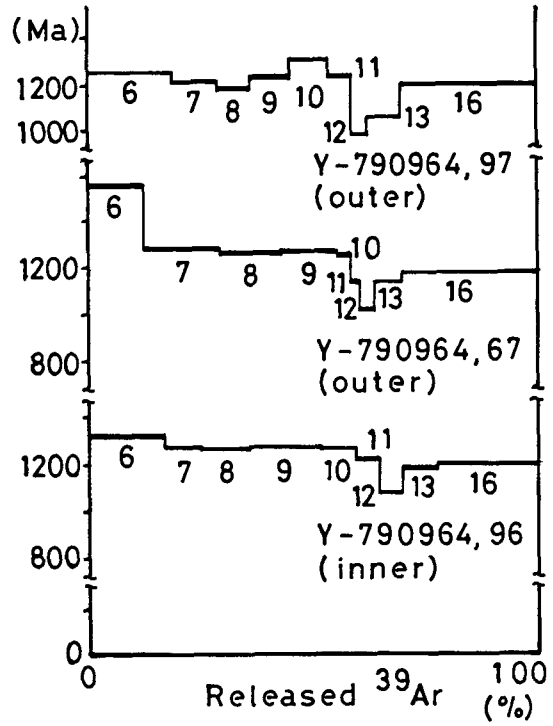

Fig.1
Age spectra of the shocked meteorite Y-790964 (LL).
The numerical figures at each column indicates the degassing temperature in hundred centigrade degrees.

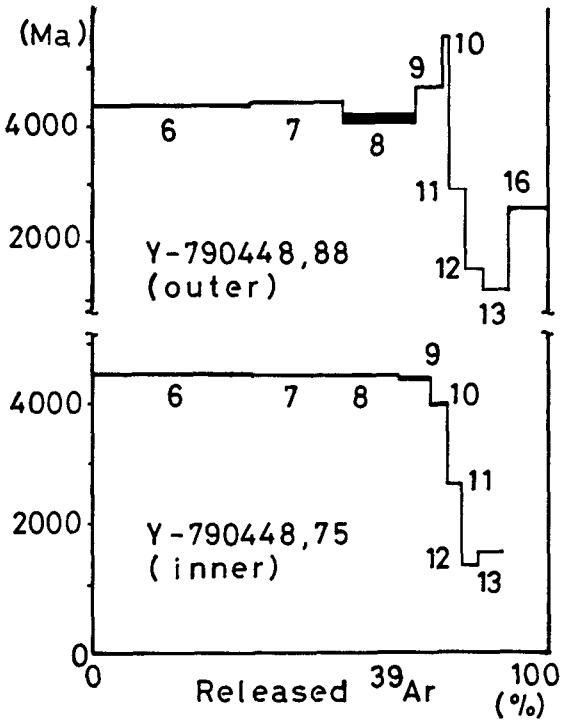

Fig.2
Age spectra of the unshocked meteorite Y-790448 (LL3).
The numerical figures are the same as those of Fig.1.

Magnesium Isotope Abandance in Allende and Antarctic Meteorites

Okano Jun, Uyeda Chiaki, Suzuki* Mari, Nishimura** Hiroshi
Institute of Geological Science, College of General Education, Osaka University
* Department of Physics, Faculity of Science, Osaka University
**Naruto University of Teacher Education

Since the excess of ^{16}O was found in refractory inclusions in Allende by Clayton et al.[1], it has been generally accepted that the early solar nebula consisted of two or more isotopically different components. In connection with this, we reported that an excess of ^{24}Mg was found in some meteorites.[2] In this paper, results on the measurements of magnesium isotope ratios in ALH-77216(L3), ALH-764(LL3), Y 790992(C3), Y 791500(H3) and four specimens of Allende(C3) will be repoted. And the correlations of the ^{24}Mg excess with Si/Mg and Fe/Mg ratios of the measured area on the specimens will be shown.

A modified Hitachi IMA-2A ion microprobe mass analyzer was used for this work. The primary ions were 9 keV O_2^+ with the beam current of about 1μA. The spot size was 50-100μm. The measurements, the caluculation of the isotope ratios and the errors were automatically carried out with a minicomputer. The errors due to the interference of molecular and multiply charged ionic species were thoroughly examined and estimated to be less than one permil in normal experimental conditions. The isotope ratios were measured for more than twenty spots on each specimen. From the mass spectra and the δ values (see below) obtained for each spot, the correlation between the ^{24}Mg excess and the elemental composition was evaluated. Terrestrial Mg-rich olivine from Ehime Prefecture in Japan(FO) was used as a laboratory standard throughout this work.

Figure 1 shows the results for Allende(AL855). The horizontal and vertical axes are :

$$\delta(\,m/25\,) = \left\{ \frac{(^{m}Mg/^{25}Mg)_{sample}}{(^{m}Mg/^{25}Mg)_{FO}} - 1 \right\} \times 1000, \quad m = \begin{cases} 24 \text{ for horizontal axis} \\ 25 \text{ for vertical axis} \end{cases}$$

The isotope ratios for FO were measured in every run with the same experimental conditions as those for meteorites. The FO data in every run were taken as the origin of the figure. The data points for AL855 were clearly shifted to the right side of the origin showing the excess ^{24}Mg of 9.1 permil in the average. For comparison, the same data were plotted in Fig.2 where δ(26/24) and δ(25/24) were taken as the axes. This type of figure appeared in many papers describing magnesium isotope anomalies in meteorites. The data points roughly distribute along the line through the origin with the gradient -1, showing again an enrichment of ^{24}Mg compared with FO. In the figure, the data for the three different inclusions and the matrix were plotted by the separate symbols.

In a figure like Fig.1, we denote the deviation of the data point from the normal mass fractionation line(NMFL) in the direction of the horizontal axis as Δ_{24}.($\Delta_{24}=\delta(24/25)+\delta(26/25)$) Figure 3 shows the correlation between Δ_{24} and the intensity ratio of $^{28}Si^{+}/^{24}Mg^{+}$. The line with the negative gradient in the figure was obtained by a regression analysis. The correlation coefficient was -0,34 in this case. Figure 4 shows the regression lines for ten specimens(including four Allende specimens). All specimens have negative gradients although the correlation coefficients for some specimens were small. These results suggest that the host minerals with the excess of ^{24}Mg would be those with low Si/Mg ratios such as forsterite. The correlations between Δ_{24} and $^{56}Fe^{+}/^{28}Si^{+}$ ratio are shown in Fig.5. Here again, all regression lines have negative gradient. However, the correlation coefficients are generally small in these cases.

The relation between $\delta(24/25)$ and $\delta(26/25)$ for three groups of samples was shown in Fig.6. In this figure, the absolute magnesium isotope ratios reported by Schramm et al.[3] was taken as the origin. For the reference, the absolute ratios reported by Catanzaro et al.[4] is also shown. The first group of the samples, A, are of the terrestrial olivines, the data points of which are expressed by large open circles. The second group of the samples, B, includes the fellowing meteorites; Bruderheim(L6), Y 74190(L6), Potter(L6), Leedy(L6), ALH77278(L3), ALH77307(C3), Y 74191-1(L3), Y 74640(H6) and Y75028(H3). The data points of this group are expressed by large black circles. The third group, C, includes ALH764(LL3), ALH77216(L3), ALH77003(C3), Allende 851, 852, 853, 855(C3), Y 791500(H3) and Y790992(C3) and these data points expressed by small black circles with the error bars. The data for Allende 852-855, Y 790992 and Y791500 are taken from arbitrarily selected area on the specimens while the other data were taken from Mg-rich area on the specimens. The measurements of the samples of group A and B were carried out for relatively small number of areas per one specimen (less than fifteen areas), while those of group C samples were carried out for large number of areas (larger than twenty, typically thirty) per one specimen. The data points and the error bars of the group C shows the averge of the data obtained for all the measured areas and the standard deviations.

The data points of the terrestrial olivines are fairly well on the NMFL through the origin. The data points of highly metamorphosed meteorites fall near the NMFL except Y 74640(H6). Contrary to this, those of low metamorphosed meteorites (type 3) deviate to the right side of the NMFL, excepting the data points for Allende 853 and Y 790992. As far as the result obtained so far are concerned, the host materials with the excess ^{24}Mg were preferentilly found in the portions with high Mg/Si ratios in the low metamorghosed primitive meteorites.

Reference

1) Clayton, R. N., Grossman, L, and Mayeda, T. K., Science,182, 485(1973)
2) Nishimura,H., Okano,J., Mem.Natl.Inst. Polar Res., Spec.Issue, 25, 171(1982)ibid, 30, 332(1983)
Nishimura,H., Okano,J., Meteoritics, 16, 368(1981)
Nishimura,H., Okano,J., Secondary Ion Mass Spectrometry, SIMS IV, ed. A. Benninghoven et al., Springer-Verlag, P475(1984)
Okano,J., Uyeda,C. and Nishimura,H., Mass Spectroscopy, 33, 245(1985)
3) Schramm,D.N., Tera,F. and Wasserburg,G.J., Earth Planet. Sci. Lett., 10 44(1970)
4) Catanzaro,E.J., Murphy,T.J., Garner,E.L. and Shields, W.R., J.Res. Natl. Bureau Stand., 70A, 453(1966)

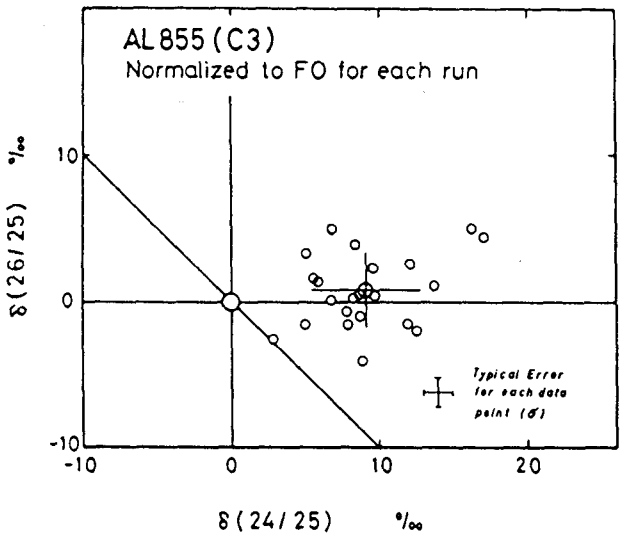

Fig.1 Three isotope plot for Allende(AL855). The data points show the results on twenty two measured areas. The average and the standard deviation are shown.

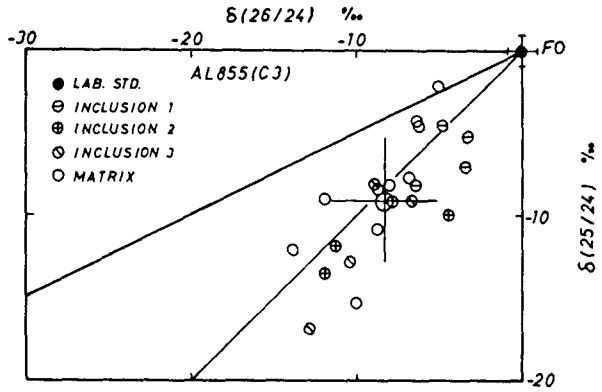

Fig.2 Replotted data of AL855 taking $\delta(26/24)$ and $\delta(25/24)$ as the axes. The data of the three inclusions and the matrix are shown by the separate symbols. The straight line with the gradient 1/2 is the NMFL and that with the gradient 1 is the line showing 24-Mg enrichment.

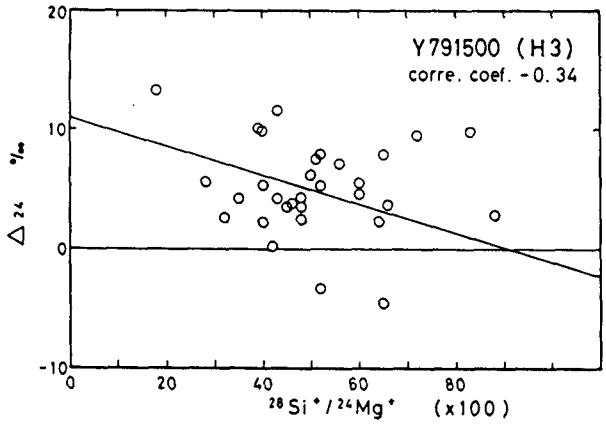

Fig.3 Relation between the 24-Mg exess, Δ_{24}, and the Si^+/Mg^+ ratio. The straight line with the negative gradient is obtained by a regression analysis.

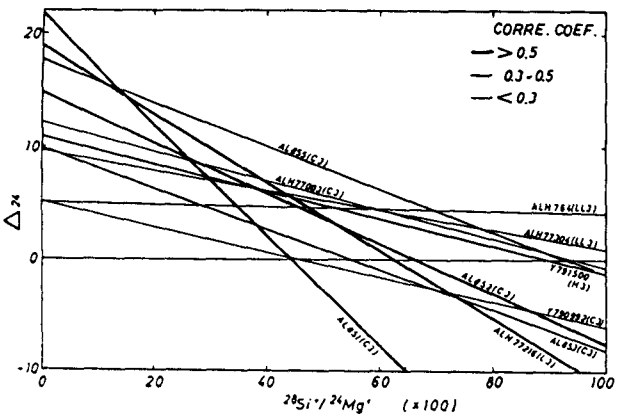

Fig.4 The Δ_{24}-Si/Mg regression lines for the ten specimens. All the lines have negative gradients showing that the hosts of the excess 24-Mg are minerals with high Mg/Si ratios.

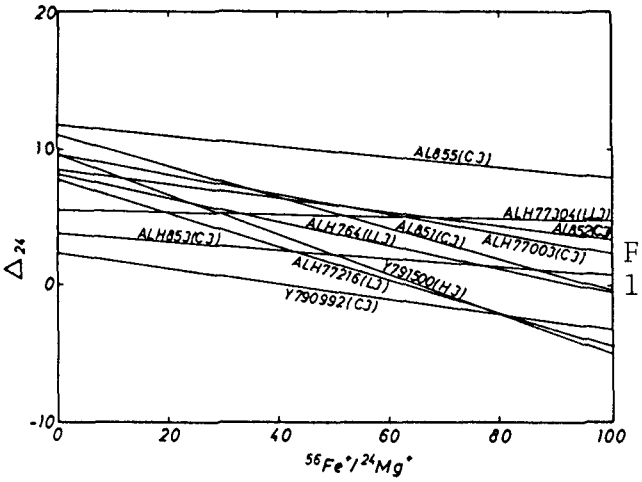

Fig.5 The Δ_{24}-Fe/Mg regression lines for the ten specimens.

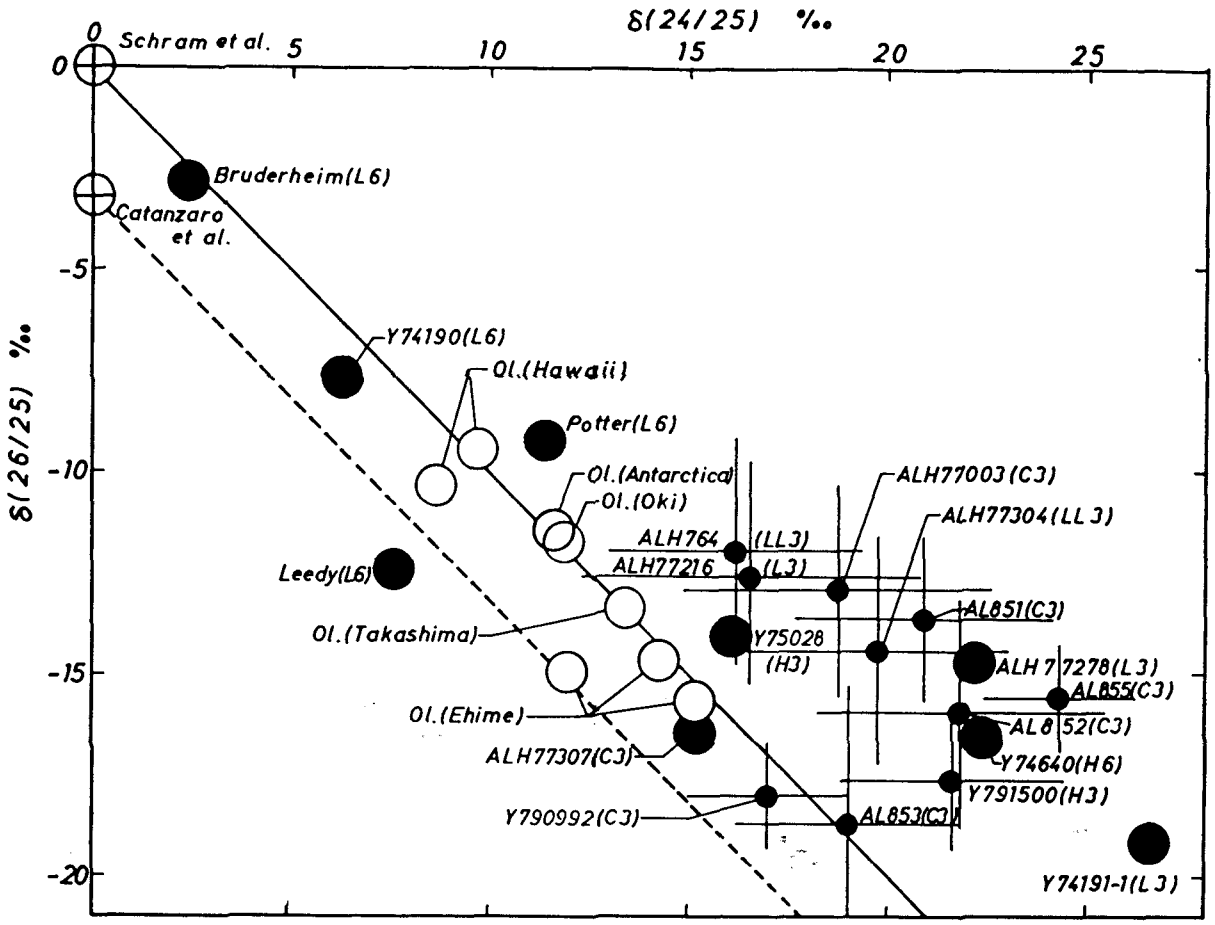

Fig.6 Magnesium three isotope plot of the results obtained so far. The absolute magnesium isotope ratios reported by Schram et al. is taken as the origin and the NMFL is shown. (see text)

RARE GAS STUDIES OF ANTARCTIC METEORITES

K. NAGAO* and J. MATSUDA**
* Okayama University of Science, ** Kobe University

Rare gas isotopic compositions have been measured for two L6-chondrites, five achondrites and C3-chondrite. Rare gas from C3-chondrite was extracted by stepwise heating. The preliminary results are presented in Table.

Cosmogenic helium and neon are dominant for all the meteorites except for Y-790727 howardite. Since the howardite has relatively large amount of trapped helium and neon, it may be a gas-rich meteorite such as other howardites, Kapoeta and Bununu. However, we could not know whether the trapped helium and neon are solar type or not because of the presence of cosmogenic helium and neon in this meteorite.

Rare gas composition of Y-74190(L6) is different from those reported by Kamaguchi and Okano(1979). Our data do not indicate the presence of trapped helium and neon in this meteorite. K-Ar age of this meteorite caluculated with 40Ar content determined in this work and potassium content by Kamaguchi and Okano (1979) is 0.5 b.y., which indicates that this meteorite belongs to the group of the L-chondrites with age of about 0.5 b.y.

Rare gas composition of Y-74136 diogenite is similar to those for Y-74 diogenites which are considered to be a meteorite shower.

Though Kr and Xe isotopic compositions are not presented here, cosmogenic xenon is predominant for two eucrites and howardite. 244Pu fission component was found in these meteorites. Cosmogenic Xe is also evident in other meteorites(L, Di, She).

Stepwise heating experiment on Y-790992(C2) indicates that most of the helium was released at the lowest temperature and most of heavier rare gases Ne, Ar, Kr and Xe were evolved at 1100° C. Helium and Neon isotopic ratios for all the extraction temperatures are nearly constant. 40Ar/36Ar ratios were different among the temperature fractions. The lowest ratio is 5.6 at 1100°C, which is much lower than the atmospheric ratio of 295.5. Xenon isotopic ratios are similar to that of AVCC-Xe except for the 700, 900 and 1800°C fractions. CCF-Xe was found in 700 and 900°C fractions of this meteorite. Light isotopes of cosmogenic Xe are dominant in 1900°C fraction.

Sample	$^{4}He^{*}$	$^{3}He/^{4}He$	$^{20}Ne^{*}$	$^{20}Ne/^{22}Ne$	$^{21}Ne/^{22}Ne$	$^{36}Ar^{*}$	$^{38}Ar/^{36}Ar$	$^{40}Ar/^{36}Ar$	$^{84}Kr^{\#}$	$^{132}Xe^{\#}$
Y-74118(L6)	580	0.010	2.1	0.83	0.89	0.45	0.82	9800	0.57	0.82
Y-74190(L6)	190	0.11	8.5	0.85	0.95	1.8	0.73	130	0.44	0.53
Y-74136(Di)	240	0.096	12	0.82	0.91	0.74	1.5	49	0.23	0.083
Y-790260(Euc)	680	0.013	2.8	0.82	0.84	1.7	1.5	890	0.13	0.18
Y-790727(How)	3000	0.0023	27	4.2	0.59	2.4	0.61	170	0.47	0.21
ALH-765(Euc)	470	0.0074	1.4	0.82	0.87	0.92	1.4	1100	0.40	0.44
ALH-77005(She)	15	0.17	0.82	0.93	0.78	0.42	0.51	634	1.4	0.52

Y-790992(C3) 231.7mg

Temp.(°C)	$^{4}He^{*}$	$^{3}He/^{4}He$	$^{20}Ne^{*}$	$^{20}Ne/^{22}Ne$	$^{21}Ne/^{22}Ne$	$^{36}Ar^{*}$	$^{38}Ar/^{36}Ar$	$^{40}Ar/^{36}Ar$	$^{84}Kr^{\#}$	$^{132}Xe^{\#}$
700	490	0.019	1.2	1.4	0.79	2.2	0.22	180	1.4	1.3
900	280	0.015	1.8	1.3	0.81	16	0.20	9.7	9.5	6.6
1100	120	0.019	3.1	1.3	0.82	82	0.20	5.6	52	36
1300	15	0.013	0.85	1.0	0.84	16	0.20	10	14	15
1500	4.1	0.022	0.43	0.85	0.87	1.2	0.23	12	0.98	1.1
1800			0.11	0.87	0.89	0.11	0.27	30	0.14	0.18

* $10^{-8}cm^{3}STP/g$ # $10^{-10}cm^{3}STP/g$

THE EXTRA-TERRESTRIAL NOBLE GAS IN DEEP-SEA SEDIMENTS

S.AMARI[1),2)] AND M.OZIMA[2)]

1) Division of Science of Materials, The Graduate School of Science and Technology, Kobe University, Nada, Kobe 657, Japan
2) Geophysical Institute, University of Tokyo, Tokyo 113, Japan

In order to characterize the carrier of extra-terrestrial noble gases in deep sea sediments, we separated deep-sea sediments into magnetic and non-magnetic fractions. From He analysis, we have confirmed that the carrier of extra-terrestrial noble gases concentrate in magnetic fractions. Judging from ^{3}He contents, the concentration of the carrier in magnetic fraction is a few hundred times as high as that in bulk sediments. Lately, we suggested that these extra-terrestrial noble gases were trapped by IDPs (Interplanetary Dust Particles), which fell on the earth and were incorporated in deep-sea sediments[1)].

By stepwise heating we studied noble gas elemental abundance and isotopic compositions on magnetic fractions of several deep-sea sediments from the Pacific Ocean. In high temperature fractions the constant $^{3}He/^{4}He$ ratio ($\sim 2 \times 10^{-4}$) is observed in all samples. The ratio is different from He-A and He-B and considered to be a unique component. In case of Ne, $^{21}Ne/^{22}Ne$ ratios vary in the range of 0.03 ~ 0.06. From these the amount of spallogenic Ne is negligible: at most 2% of total Ne. $^{20}Ne/^{22}Ne$ ratios are constant (11.3 ± 0.5) in all temperature fractions in all samples. This ratio is different from known Ne component and considered to be a unique component as well as He. For Ar, $^{40}Ar/^{36}Ar$ ratios lower than the atmospheric ratio are observed in high temperature fractions. While $^{38}Ar/^{36}Ar$ ratios is indistinguishable to the atmospheric ratio, which means spallogenic Ar is negligible. The isotopic ratios of Kr and Xe is the same as the atmospheric ratios within experimental error. Combining isotopic data of Kr and Xe with elemental abundance pattern, Kr and Xe are considered to be of air origin.

A maximum size for IDPs to retain noble gas during atmospheric entry is likely to be less than a few ten microns. Also, while less energetic solar wind particles (~1KeV) would be more easily lost than high energy solar flare noble gases during sedimentation, higer energy particles (>5MeV) would go through IDPs. Considering these, we conclude that solar flare noble gases with inermidiate energies (< a few MeV) implanted on IDPs are responsible to the extra-terrestrial noble gas in deep-sea sediments.

1) Amari,S and Ozima, M. Nature,317,520,1985

YAMATO 82042: AN UNUSUAL CARBONACEOUS CHONDRITE WITH CM AFFINITIES

Grady, M. M., [1] Barber, D., [2] Graham, A., [3] Kurat, G., [4] Ntaflos, T., [4] Palme, H. [5] and Yanai, K. [6]

[1] Dept. of Earth Sciences, Open University, Milton Keynes, U. K.
[2] Dept. of Physics, University of Essex, Colchester, U. K.
[3] British Museum (Natural History), London, U. K.
[4] Naturhistorisches Museum, Wien, Austria.
[5] Max-Planck-Institut, Mainz, West Germany.
[6] National Institute of Polar Research, Tokyo, Japan.

Yamato 82042 is an unusual carbonaceous chondrite consisting of abundant phyllosilicates which form a fine-grained matrix; irregularly dispersed within this matrix are grains of olivine, carbonates (calcite and dolomite), iron oxides and sulphides. No high temperature CAI's or pyroxenes have so far been found, and metal only occurs as rounded grains included within olivine. No veins cross the specimen, which is coherent and unweathered. In thin section this material consists of sub-rounded aggregates of phyllosilicates embedded in a groundmass of apparently almost amorphous material. Transmission electron microscopy shows that the matrix phyllosilicates are mainly 7Å serpentine-type minerals, ranging from virtually amorphous to crystalline in character and exhibiting a wide variety of growth forms. Minor amounts of chlorite-montmorillonite have also been identified. Within the groundmass are areas of poorly characterized phases (PCP) giving distinctive electron diffraction patterns, now believed to indicate tochilinite, but with the main d-spacing (≈ 10.5Å) slightly lower than normal. In the optical microscope, this matrix seems similar to that of Cold Bokkveld, but is distinct from that of other CM chondrites, e. g. Murray and Mighei. Modal abundance of olivine is lower than in other type 2 carbonaceous chondrites, while that of carbonates seems to be higher. Olivines are mainly forsterites with very few more iron-rich than Fa_2. Most are surrounded by a corona of dark brown phyllosilicates and show some internal zoning, iron content increasing slightly out towards the rims. One olivine crystal was found which showed two distinct minor element contents and no gradation between them. Within this olivine are round blebs of low-Ni metal and Ca-Al-rich glass. Some of the forsterites contain rounded metal grains up to 10μm across, with 6.3 - 7.6% Ni, 0.4% Si, 0.5% P and 0.4% Co.

Carbonate is present throughout the section either as crystals in matrix or as rounded chondrule-like objects. Within the carbonate "chondrules" is Mg-Cr spinel; irregular carbonate-rich aggregates also occur containing small grains of Mg-Al spinel and Al-rich phyllosilicates. These irregular aggregates are enveloped by dolomite, and are similar in form to the Ca-Al-rich inclusions rimmed by diopside which occur in CM2 meteorites. Matrix carbonates, mainly twinned dolomites, range

up to 30μm in size, some with an unusual meteoritic composition, rich in manganese (up to 4 wt%). Most of the carbonate grains have indistinct boundaries since their outer regions grade into porous phyllosilicates and hydrous calcium sulphates which are not exclusively gypsum. The presence of calcium silicate sulphate hydrate (apatite structure) and carbonate fluorapatite has been established.

Pentlandite occurs with two compositions, one with 13% Ni, 49% Fe and 0.22% Co and the other has 34% Ni, 29% Fe and 3.2% Co. There are also two dominant oxide compositions: one with chondritic Ni/Co ratio, but the other, produced by oxidation of the metal, with Ni/Co ratio of ≈ 10.

The bulk major and minor element analysis of Yamato 82042 (see table and figure) shows it to be a CM meteorite: oxygen isotopic data ($\delta^{18}O$ = +8.46‰; $\delta^{17}O$ = +2.35‰) are within the CM range and confirm the classification. However the petrography shows a higher modal proportion of phyllosilicate than other CM stones, hence this meteorite may be the first CM1 recognized.

Dissolution of Y 82042 in orthophosphoric acid yielded 2025 ppm carbon with $\delta^{13}C$ = +36.6‰, presumably derived from calcite. After an extended reaction period, a further 944 ppm carbon with $\delta^{13}C$ = +50.1‰ was extracted from dolomite. These carbon isotopic signatures fall well within the range of those of CM chondrites. Stepped combustion indicated that there is also 0.55 wt% organic material with $\delta^{13}C$ ≈ -9.4‰. The total carbon content of 1.05 wt% is low for a CM meteorite, and the weighted $\delta^{13}C$ value of +9.8‰ isotopically heavier. This reflects the preponderance of carbonate minerals and the very low percentage of organic matter present in Y 82042.

The total nitrogen concentration is 534 ppm with weighted $\delta^{15}N$ ≈ +3.0‰; although the nitrogen abundance is just within the range of values for CM chondrites, the isotopic composition is light, indicating that ^{15}N-enriched organic matter found in other CM chondrites is absent. The total sulpur content of 2.88 wt% is similar to other CM meteorites, sulphur occuring as both sulphates and sulphides (including PCP) and also as a constituent of organic material.

CONCLUSIONS:

Formation of phyllosilicates occurred prior to assembly of the stone and the olivines accreted with their skin of brown phyllosilicate. Occasional rounded phyllosilicate chondrule-like objects occur with a distinct boundary to the matrix, but these are rare. The high temperature component is limited to some olivines and very rare Mg-Al spinels. The delicate structures within the matrix are preserved so there has been little or no loading or reheating of the stone following accretion. Dolomites are twinned, but there is no veining and little serpentinisation of the olivines.

ACKNOWLEDGEMENTS: Thanks are due to R. N. Clayton for oxygen data and R. Burgess for the sulphur analysis. Gratitude is extended to the N.I.P.R. for financial assistance.

Bulk major and trace element contents (ppm) of Y 82042

C	10504	Se	12.4
N	534	Mo	0.91
Na	3540	Sb	0.11
S	28784	La	0.30
K	365	Sm	0.20
Ca	1000	Eu	0.065
Sc	7.76	Dy	0.34
Cr	2730	Yb	0.20
Mn	1625	Lu	0.030
Fe	194800	Hf	0.14
Co	534	Re	0.046
Ni	12800	Os	0.68
Cu	110	Ir	0.563
Zn	200	Pt	1.1
Ga	7.99	Au	0.160
As	1.84		

Comparison of Y 82042 with Mighei and Murchison CM2 chondrites

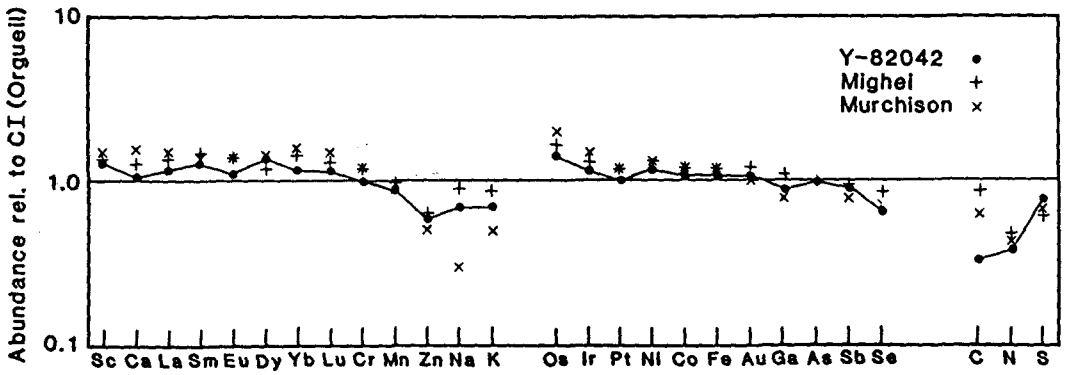

AN INVESTIGATION OF ^{13}C-RICH MATERIAL IN C1 AND C2 METEORITES.

Wright, I.P., McGarvie, D.W., Grady, M.M., Gibson, E.K.Jnr[1] and Pillinger, C.T.
Department of Earth Sciences, The Open University, Walton Hall, Milton Keynes MK7 6AA, England.
[1] SN4, Experimental Planetology Branch, NASA Johnson Space Center, Houston, Texas, U.S.A.

C1 and C2 carbonaceous chondrites are meteorites which appear to have formed in a regolith-type environment. As such, they have been subjected to processes which cause brecciation and aqueous alteration. Notwithstanding the petrological changes accompanying these events, the meteorites are chemically primitive, with C1 chondrites in particular having a similar composition to the Sun. However, small fractions of these meteorites are composed of materials which, on the basis of isotopic measurements, are decidedly non-solar. These components have traditionally been recognised by detection of noble gases with anomalous isotopic signatures (e.g. 1). More recently, analyses of some of the host materials have uncovered unusual isotopic compositions in elements such as carbon and nitrogen (2,3). Detection and measurement of the small amounts of isotopically anomalous noble gases, carbon or nitrogen involves much care and effort and is very time consuming. For these reasons most investigations have been confined to a small number of samples. The present study was aimed at assessing the abundance and distribution within C1 and C2 meteorites of the ^{13}C-rich carbonaceous materials which are thought to have resulted from the operation of processes pre-dating the formation of the solar system.

Two CI1 meteorites (Orgueil and Alais), the unusual C1 meteorite Y82042 and ten CM2 meteorites were selected for study. Whole-rock specimens contain carbonates with slight ^{13}C-enrichments (possibly arising from isotopic fractionation in the solar nebula) hence all samples were dissolved in HCl (12M, 24 hours at 18°C) to ensure complete removal of the carbonate minerals. The HCl-resistant residues were then subjected to gas-phase oxidation under conditions of increasing temperature (stepped combustion) followed by extraction, purification and mass spectrometric determination of the carbon dioxide. Since the HCl-resistant residues contain between 2 and 7 wt% carbon as macromolecular organic material (see table) it was necessary to repeatedly combust the samples at 500°C in order to try and remove this component. The meteorites were then generally combusted in 25°C increments for 30 minutes under a pressure of 200 to 500 torr of oxygen.

The table below shows the integrated carbon yield and $\delta^{13}C$ values for data acquired by stepped combustion between 700 and 1300°C. In all cases, carbon which combusts above 700°C is isotopically heavier than the majority of the carbon in the residue (mostly macromolecular organic material which combusts below 600°C and has $\delta^{13}C$ values of between -10 and -19‰). The $\delta^{13}C$ values of the high

temperature carbon are undoubtedly compromised somewhat by the presence of small amounts of uncombusted organic material and indeed there is a relationship between carbon yield and $\delta^{13}C$ (with the lowest carbon yields generally displaying the largest ^{13}C-enrichments). In general, between 10 and 100 ppm of carbon are found to combust above 700° although in the case of Pollen, 331 ppm were obtained and only a modest ^{13}C enrichment observed. This is because Pollen contains quite large amounts of carbon (3.61 wt% as compared to 2.02 to 2.57 wt% for the other CM2 samples studied) and it is likely that some organic carbon has survived combustion to higher temperatures. The $\delta^{13}C$ value for Pollen of -18.9‰ is lower than other CM2 samples and suggests the addition of some contaminant terrestrial organic material ($\delta^{13}C$ typically -25‰). For samples other than Pollen three, or possibly four, different ^{13}C-rich components may be discerned from the stepped combustion data, two of which have been recognised previously (a and b in the list below).

(a) Carbon-alpha (Cα) is thought to be the host of Ne-E(1) (4) and combusts at relatively low temperatures (600-800°C). The largest ^{13}C-enrichment so far observed for Cα has been in a highly processed residue from Murchison (2C10c) where a $\delta^{13}C$ value of +338‰ has been recorded. In this study of relatively simple HCl residues, $\delta^{13}C$ values only achieve -8‰ (Mighei), -7‰ (Murchison) and +9‰ (Cold Bokkeveld).

(b) Carbon-beta (Cβ), the putative host of s-process xenon (4) which burns somewhere between 850 and 1050°C. Maximum $\delta^{13}C$ values of this component have reached +1100‰ (again in highly processed residues, e.g. 2C10f from Murchison) but in this study $\delta^{13}C$ values of between +100 and +160‰ were obtained for CM2 meteorites (it could not be discerned in Kivesvaara) and +160 and +180‰ for the CI1 samples.

(c) The third component of ^{13}C-rich carbon combusts at a very similar temperature to Cβ (albeit somewhat lower, between 800 and 900°C) and indeed may be related to it. Evidence for this component is seen in Kivesvaara ($\delta^{13}C$=+6‰), Cold Bokkeveld ($\delta^{13}C$=+22‰), Mighei ($\delta^{13}C$=+31‰) and Orgueil ($\delta^{13}C$=+85‰).

(d) The fourth component is that carbon which combusts above 1100°C and in all cases shows the largest ^{13}C-enrichments ($\delta^{13}C$ between +100 and +400‰ for CM2 samples and about +475‰ for CI1 meteorites). This material is presumably that carbon which can be identified in the highest temperature steps of the Murchison residue 2C10m (2,5). Due to the apparent widespread occurrence of this component the operational term carbon-epsilon (Cε) seems appropriate for its description (Cδ and Cγ having already been assigned to other components, ref. 2).

(References and table overleaf).

METEORITE	<1300°C		700-1300°C	
HCl-RESIDUE	YIELD (Wt%C)	$\delta^{13}C$	YIELD (ppmC)	$\delta^{13}C$
Alais	7.15	-14.9	84	+25.8
Orgueil	6.47	-16.7	39	+82.7
Cold Bokkeveld	-	-	13	+53.7
Kivesvaara	2.29	-16.1	106	+21.2
Mighei	2.57	-17.5	11	+60.6
Murchison	2.20	-10.4	13	+155.6
Murray	2.02	-15.2	79	+10.0
Pollen	3.61	-18.9	331	-10.9

(1) Anders, E. (1981). Proc. R. Soc. Lond. A 374, 207-238.
(2) Swart et. al. (1983). Science 220, 406-410.
(3) Lewis et. al. (1983). Nature 305, 761-771.
(4) Alaerts et. al. (1980). Geochim. Cosmochim. Acta 44, 189-209.
(5) Carr et. al. (1983). Meteoritics 18, 277.

THERMOBAROMETRY OF DIOGENITES

MUKHERJEE AMALBIKASH and VISWANATH T. A.
Department of Geology and Geophysics
Indian Institute of Technology, Kharagpur-721302,W.B.,India

One of the tests for the validity of layered HED (Howardite, Eucrite, Diogenite) parent planets is quantitative thermobarometry - aiming to establish a reasonable and realistic P-T-f_{O_2} profile across the presumed sequence of diogenites at the deeper level followed upwards by howardites and eucrites. We address here the problem of thermobarometry of diogenites, based essentially on the equilibration of orthopyroxene, chrome spinel and silica. Fe^{2+}- Mg exchange equilibrium between the major orthopyroxene and spinel components is governed by the reactions:

$$FeSiO_3 + MgCr_2O_4 = MgSiO_3 + FeCr_2O_4 \quad \ldots \quad (1)$$

$$FeSiO_3 + MgAl_2O_4 = MgSiO_3 + FeAl_2O_4 \quad \ldots \quad (2)$$

$$FeSiO_3 + MgFe_2O_4 = MgSiO_3 + Fe_3O_4 \quad \ldots \quad (3)$$

These three reactions may be combined to give the following equilibrium equation:

$$\frac{a^{Opx}_{MgSiO_3} \cdot (a^{Sp}_{FeCr_2O_4})^{Y^{Sp}_{Cr}} \cdot (a^{Sp}_{FeAl_2O_4})^{Y^{Sp}_{Al}} \cdot (a^{Sp}_{Fe_3O_4})^{Y^{Sp}_{Fe^{3+}}}}{a^{Opx}_{FeSiO_3} \cdot (a^{Sp}_{MgCr_2O_4})^{Y^{Sp}_{Cr}} \cdot (a^{Sp}_{MgAl_2O_4})^{Y^{Sp}_{Al}} \cdot (a^{Sp}_{MgFe_2O_4})^{Y^{Sp}_{Fe^{3+}}}}$$

$$= \exp\left[-\left(Y^{Sp}_{Cr} \left(\Delta G^{o}_{1} - \Delta S^{o}_{1} (T - 298.15) \right) + Y^{Sp}_{Al} \left(\Delta G^{o}_{2} - \Delta S^{o}_{2} (T - 298.15) \right) + Y_{Fe^{3+}} (\Delta G^{o}_{3} - \Delta S^{o}_{3} (T - 298.15)) \right) / RT \right] \quad \ldots \quad (4)$$

where $a^{Opx}_{MgSiO_3}$ and $a^{Sp}_{FeCr_2O_4}$ and similar expressions represent activity of an orthopyroxene and a spinel end-member in orthopyroxene and spinel respectively. Y^{Sp}_{Cr} and similar expressions stand for the mole fraction of an R^{3+} ion in the octahedral site of the spinel, i.e. $Y^{Sp}_{Cr} = X^{Sp}_{Cr} / (X^{Sp}_{Cr} + X^{Sp}_{Al} + X^{Sp}_{Fe^{3+}})$. ΔG^{o}_{1}, ΔG^{o}_{2}, ΔG^{o}_{3} and ΔS^{o}_{1}, ΔS^{o}_{2}, ΔS^{o}_{3} stand for the standard state (298.15°K and 1 bar) Gibbs free energy and entropy of the reactions 1, 2 and 3. ΔV of the reactions being extremely small were neglected. For calculating the end-member activities, we adopted for the orthopyroxenes the relationship: $a^{Opx}_{MgSiO_3} = X_{Mg,M1} \cdot X_{Mg,M2}$ (and a similar expression for $FeSiO_3$) where M1 and M2 stand for the M1 and M2 sites. For the spinels, we used the activity formulations of Sack (1982), ignoring all other spinel components except the 6 used in our equation 4. Applying the thermometer to the Johnstown diogenite, using data of Floran et al. (1981), we get 1061°C as the orthopyroxene - spinel equilibration temperature. Using an ideal Temkin-type activity-composition relationship for the spinel, we get 1093°C for the same assemblage. We calculated the equilibration pressure of the Johnstown diogenite from the reaction:

$$\underset{\text{(in pyroxene)}}{MgAl_2SiO_6} = \underset{\text{(spinel)}}{MgAl_2O_4} + \underset{\text{(tridymite)}}{SiO_2} \qquad \ldots \qquad (5)$$

using the ΔG^{o}, ΔS^{o} and ΔV^{o} from Wood and Banno (1973). At 1093°C, the equilibration pressure is 21.8 kbar.

For the ΔG^{o} and ΔS^{o} in equation 4, we used data from Robie, Hemingway and Fisher (1979), Helgeson et al. (1978) and Engi (1978).

The thermometer yields 1347°C for the Yamato 75032 diogenite (data from Takeda et al. 1978) and 1828°C for the Yamato 74013 diogenite (rim composition data of chromite and pyroxene from Mukherjee and Viswanath (communicated for publication)), on the basis of ideal spinel activities. While the error in the temperature estimate due to ignoring the nonideality of mixing in the spinels is possibly not more than 60°C (Sack, 1982), the other sources of errors include mismatching of pyroxene and spinel (i.e. ignoring core-to-rim growth stages, growth domains e.g. large euhedra and small matrix grains etc) grains used for the analysis. In Yamato 74013, the large chromite euhedra have the characteristic zoning pattern of high temperature presilicate spinel and may not be equilibrated even at their rim with the orthopyroxene. On the other hand, the significantly lower temperature for Yamato 75032 diogenite is in accord with its eucritic affinity and a possible location at a shallower level of the HED parent body compared to Yamato 74013.

REFERENCES: Engi M. (1978)Ph.D.thesis,Swiss Fed.Inst.Tech.

Floran R.J.,Prinz M., Hlava P.F.,Keil K.,Spettel B. and Wänke H. (1981) Geochim. Cosmochim. Acta, 45, 2385

Helgeson H.C.,Delany J.M.,Nesbitt H.W. and Bird D.K.(1978) Am. J. Sci., 278-A, 1

Robie R.A.,Hemingway B.S. and Fisher J.R.(1979):US Geol.Surv. Bull 1452

Sack R.A.(1982): Contrib. Mineral.Petrol.,79,169

Takeda H., Miyamoto M., Yanai K. and Haramura H.(1978): Proc. Second Symp. Antarctic Meteorites, 170

Magnetic properties of tetrataenite in Ni-rich at ataxites

Takesi Nagata[1], Minoru Funaki[1] and Jaques Danon[2], 1) National Institute of Polar Research, Tokyo, Japan. 2) Centro Brasileiro de Pesquisas Fisicas, Rio de Janeiro, Brazil

ON THE POSSIBLE TRANSPORT OF VOLATILE TRACE ELEMENTS IN METEORITE PARENT BODIES

N. Sugiura, J. Arkani-Hamed and D.W. Strangway

Department of Geology, University of Toronto, Toronto, Canada, L5L 1C6

Concentrations of volatile trace elements such as Bi,Tl and In decrease with increasing metamorphic grade of chondrites. It has been debated whether this fractionation was due to a nebula condensation process or due to the metamorphism in parent bodies. We examined the latter possibility in this study.

The parent body model used in this study is the same as the one adopted for the possible transport of carbon (1). The model is based on the experimentally determined gas permeability of chondrites and a plausible thermal history of 30-50 km radius parent bodies. Vapourization process is assumed to be the reverse reaction considered in condensation models (2). Trace elements, vapourized from interior, condense near the surface of the parent body as their partial pressure exceeds their vapour pressure. The effect of a carrier gas (carbon monoxide) on the transporation of trace elements was also examined.

Vapour pressures of the trace elements strongly depend on the presence of pure phases, which in turn depends on the solubility of the elements in solid solution (2). Table 1 shows relative volatility of some elements which is defined by the ratio of the amount of the element in the vapour phase to the amount in the starting (solid) material. Heat of solution from (2) was used in the case of solid solution. CI abundance was used for the concentration in the starting material. It is seen that pure phases of Tl,Bi,In and Cd are more volatile than carbon, but if these elements are in the solid solution they are less volatile. (In is more volatile at 1000 K but becomes less volatile at higher temperatures.) In our previous calculation on the carbon transport (1), it was shown that carbon can be transported during metamorphism only if rather stringent conditions were met. Therefore, it was expected that transport of these elements would be difficult if they were in solid solution.

Numerical simulation of the transport of these elements, based on the thermodynamic data of (2), showed that these elements were mostly in the solid solution during metamorphism, and they (except for Cd) could not be removed from the interior of the parent body. The effect of a carrier gas was found to be rather small in the present models. The thermodynamic data (heat of solution (Table 1) and activity coefficient which was assumed to be 1) are, however, very uncertain. Within the uncertainty of the thermodynamic data, vapour pressures of these elements in equilibrium with their solid solution could be 1000 times higher than those shown in table 1. If we assume such higher vapour pressures, substantial amounts of Cd, In, Tl, Bi and Pb could be transported in the parent body during the metamorphism. Fig. 1 shows an example of the transport of Tl with an assumed heat of solution (30 kcal/mol).

References

1. N. Sugiura, J. Arkani-Hamed, D.W. Strangway and T. Matsui: in Abstract for 48th Meteoritical Society Meeting, 1985.
2. J. Larimer: Geochim. Cosmochim. Acta 37 (1973) 1603.

Table 1

	reaction	Hs(kcal/mol)	Mv/Ms at 1000°k Solid-solution	Pure phase
Tl	Tl(s)=Tl(g)	14	1.1×10^{-4}	1.9×10^{-1}
Bi	Bi(s)=Bi(g)	15	2.0×10^{-5}	2.9×10^{-2}
Pb	Pb(s)=Pb(g)	15	1.6×10^{-5}	1.0×10^{-3}
In	Fe+2InS=FeS+In_2S(g)	19	1.1×10^{-2}	$8.7 \times 10^{+1}$
Cd	Fe+CdS=FeS+Cd(g)	9	6.5×10^{-4}	1.1
Zn	Fe+ZnS=FeS+Zn(g)	(9)	9.2×10^{-7}	2.1×10^{-6}
C	C+Olivine=Fe+SiO_2+CO	-	-	2.3×10^{-3}

Mv : amount in the vapour phase
Ms : amount in the starting material
Hs : Heat of solution from Larimer (1973)

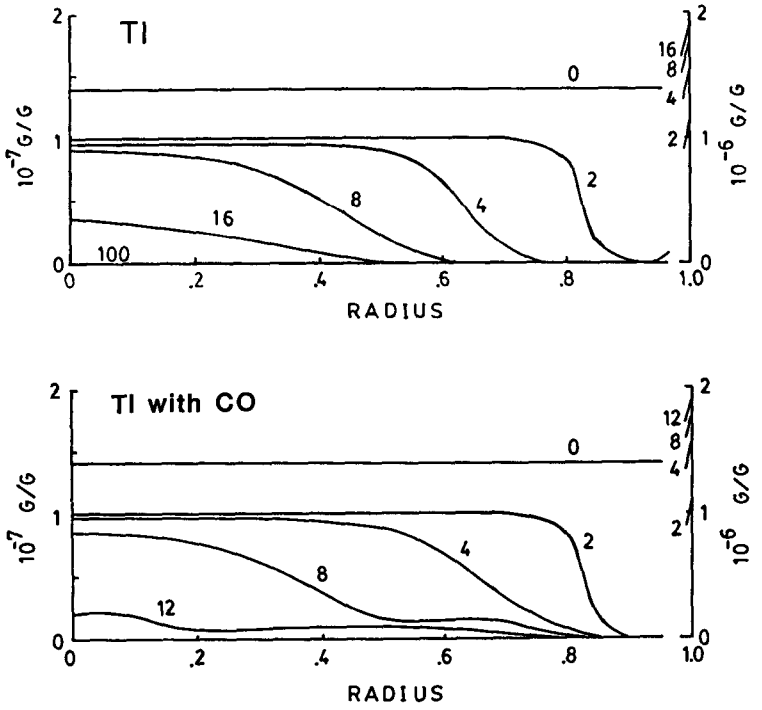

Fig.1 Concentration of Tl as a function of radial distance at various time steps (in million years) in a 40km parent body. A rather high heat of solution (30kcal/mol) was assumed. Note the scale for the concentration is different at the surface. Top: transportation of Tl alone. Bottom: transportation of Tl with a carrier gas (carbon monoxide).

62—1

SHAPE ANALYSIS OF METALLIC GRAINS AMONG ANTARCTIC ORDINARY CHONDRITES

Naoyuki FUJII, Keisuke ITO, and Masamichi MIYAMOTO(#)
Department of Earth Sciences, Kobe University, Nada, Kobe 657.
(#)College of General Education, The Univ. of Tokyo, Meguro, Tokyo 153.

We have developed several approaches to characterize the irregular shape of metallic grains in ordinary chondrites. By introducing several appropriate parameters for selected Antarctic ordinary chondrites including Y-74142(H3), ALH-77233(H4), ALH-77115(H6), Y-74094(H6), Y-74417(L3), ALH-77230(L4), Y-74117(L6) and ALH-77105(L6), some differences in general trend are clarified among petrologic types in these chondrites.

Boundary lines of metallic grains with the area larger than 0.001 mm^2 are digitized by using the microcomputer-aided picture analyzing system for the photographs of polished or thin sectioned samples. The shape irregularity of metallic grains are characterized by the frequency distributions and mutual relationships of several parameters: 1) the shape parameter, $SP(L/\sqrt{S})$, 2) the axial ratio, $\underline{b}/\underline{a}$, 3) the non-circularity (P) and non-ellipticity (Q) parameters, and 4) the fractal dimension, FD (= -logN/logd), respectively. L, S, N, and d are the total perimeter length (with d of 0.01 mm), the area, the number of segments of the perimeter and the divider opening, respectively. $\underline{a}$ and $\underline{b}$ are the major and semi-major axial lengths calculated by the principal component analysis. $P\ (= 2\cdot\Sigma B_k^2)$ and $Q\ (= P - 2\cdot B_2^2)$ are obtained from the Fourier Descriptors B_k in which a radial distance R_j from the topographical center of a grain is expanded in a finite Fourier series as a function of the perimeter length, i.e. $R_j/R_o = 1 + 2\cdot\Sigma B_k\cdot COS(j\cdot k/N - D_k)$.

As previously pointed out by our series of investigations, the distribution of each parameter for different petrologic types shows a slight tendency that the shape irregularity of Fe-Ni grains is likely to be reduced with increasing metamorphic grade of parent bodies. Figure 1 shows that the relation between the shape parameter (SP) and $\underline{b}/\underline{a}$ for H4, H6, L4 and L6 of ALH-chondrites. The distribution of data indicates that values of SP scatter more widely in type 4 chondrites than that in type 6 chondrites for both H and L chondrites. It means that type 6 chondrites have less irregular shape than type 4. The similar tendency is also seen in Figure 2, where the shape parameter vs logQ diagrams are shown for four different types of chondrites. The shape parameter vs FD diagrams also indicate that smaller values of FD and shape parameter are more frequent in type 6 chondrite when compared with those of relatively non-equilibrated chondrites.

Although there remain several difficulties to obtain physically meaningful averages of these parameters and to relate with the mechanical characteristics of different petrologic types of chondrites, this approach could provide some clues to investigate the mechanisms of lithification and deformation processes within chondritic parent bodies. Other factors, such as the variation of Ni content and shock-melted effects for each grain, would contribute to cause a variety of the shape irregularity of metallic grains with some correlations among petrologic types of ordinary chondrites.

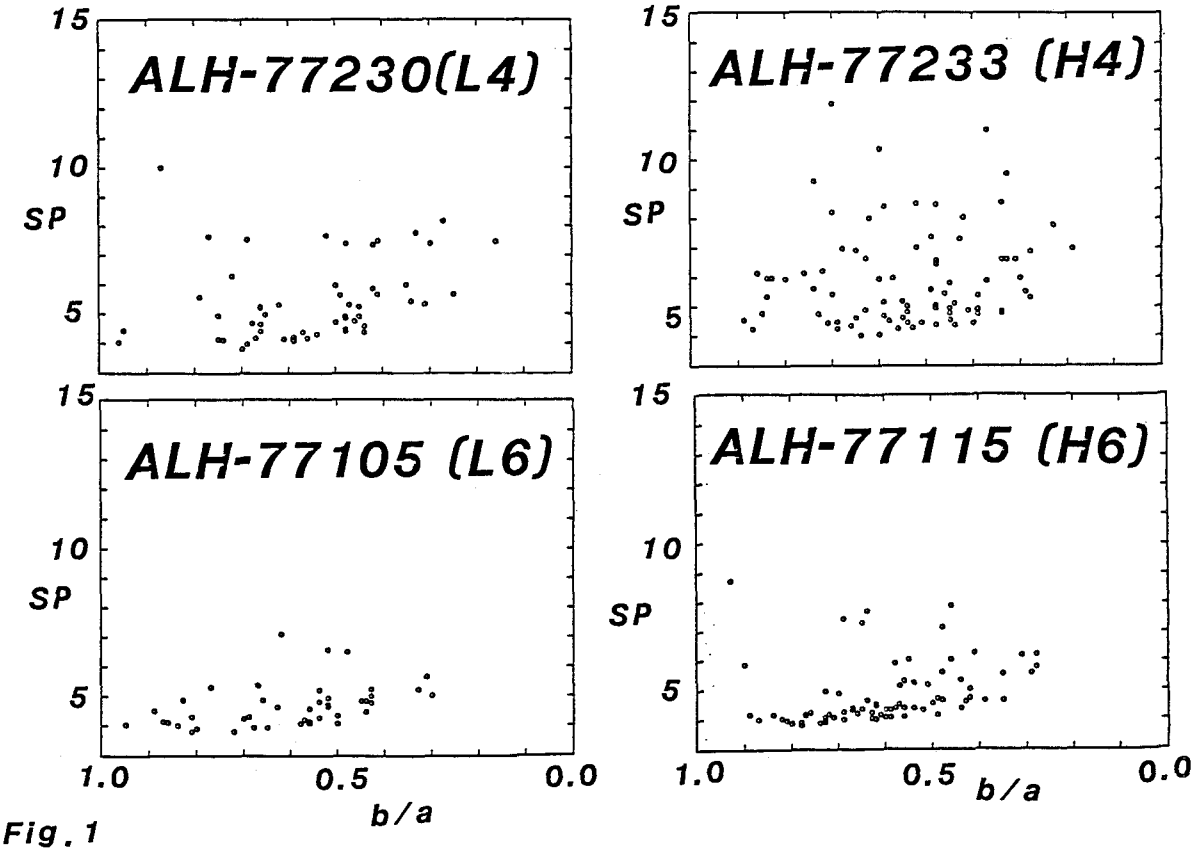
ALH-77230(L4)
ALH-77233 (H4)
ALH-77105 (L6)
ALH-77115 (H6)
SP
15
10
5
1.0
0.5
0.0
b/a

Fig. 1

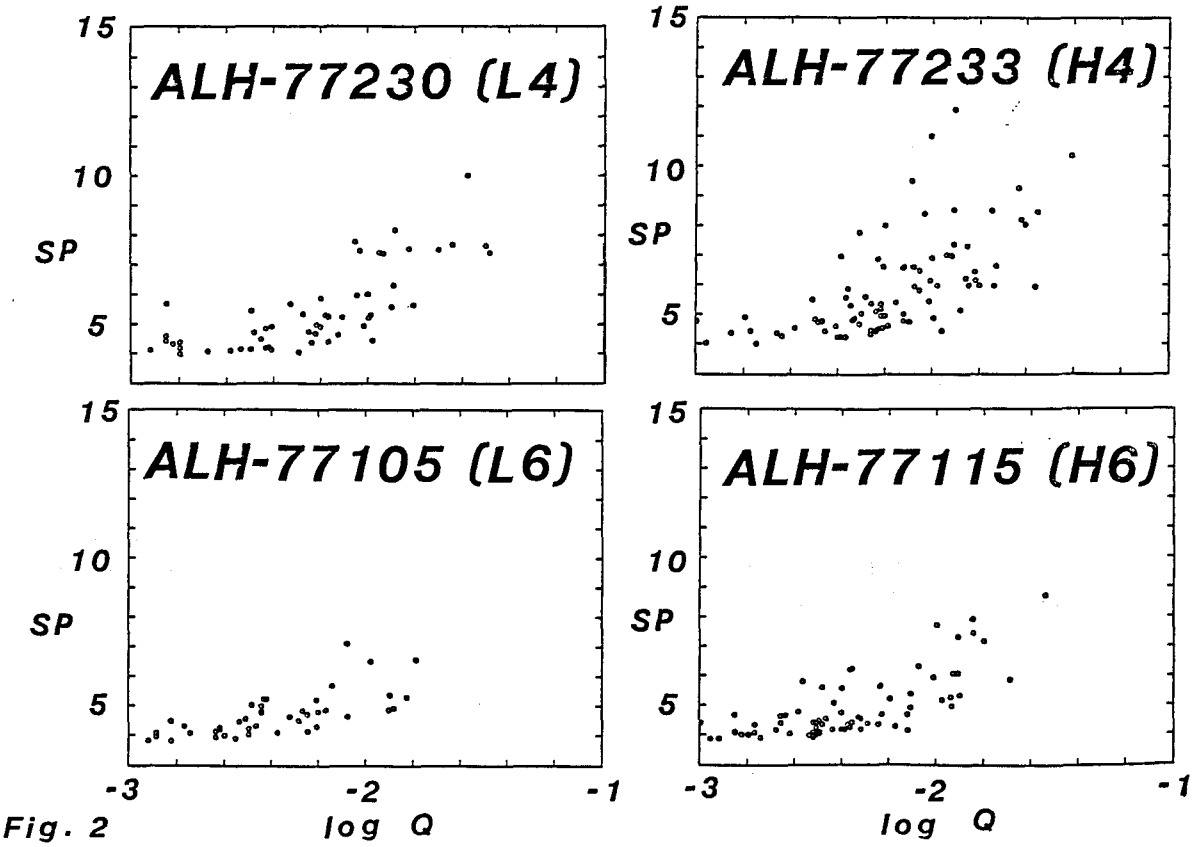
ALH-77230 (L4)
ALH-77233 (H4)
ALH-77105 (L6)
ALH-77115 (H6)
SP
15
10
5
-3
-2
-1
log Q

Fig. 2

Non-destructive analysis of meteorites by using a high-energy X-ray CT scanner

Akimasa Masuda[1], Isamu Taguchi[2] and Kohki Tanaka[2]

1) Faculty of Science, The University of Tokyo,
2) R & D Laboratories-I, Nippon Steel Corporation

I. Introduction

The high-energy X-ray computed tomographic scanner (CTS) was developed in order to non-destructively investigate the internal structures and components of iron and steel samples. In this paper, CTS was applied to non-destructive study of five Antarctic meteorites. Internal structures of the meteorites were successfully observed by CTS.

II. Experimental

(1) Antarctic meteorites Yamato 74364 (H-chondrite, 722.97 g), Yamato 74454 (L-chondrite, 569.00g), Yamato 74450 (Eucrite, 147.28g), ALH-78132 (Eucrite, 187.15g) and ALH-77219 (Mesosiderite, 292.60g) were used.

(2) CTS The high-energy X-ray computed tomographic scanner (CTS) was developed for iron and steel sample analysis[1]. The principle of analysis is the same as that of a medical CT. CTS is shown in Photo 1 and its specifications and operating conditions are given in Table 1. The main features of CTS are high X-ray transmission and high resolution capability. The CTS data were processed by the image analyzer, TOSPIX II.

III. Results

(1) CTS observation CTS observations of the meteorites were performed. For example, the results of Yamato 74364 (H-condrite) and Yamato 74454 (L-condrite) are given in Photos 2 and 3.

(2) Average CT value The average CT values are as follows.

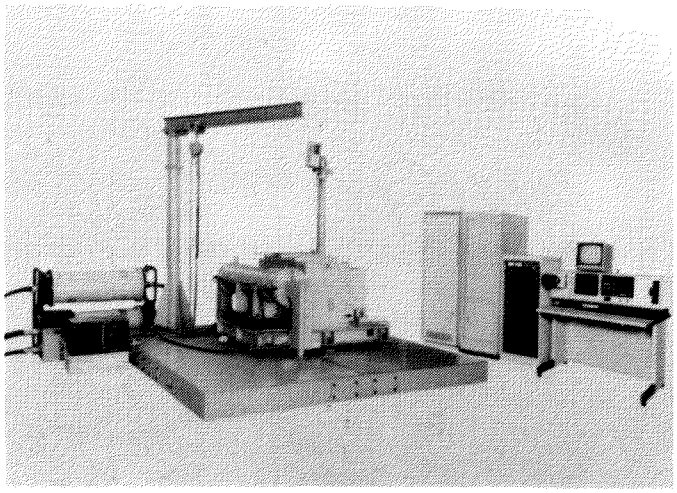

Photo 1 CTS (High-energy computed tomographic scanner)

Table 1. Specification and operating conditions of CTS

1. CT type	2nd generation CT, 8 channel, S-R-S type
2. X-ray tube	420 kV, 3mA
3. X-ray detector	BGP-PMT
4. Scanning method	6° revolution and traversing, 30 times
5. Collimator slit	0.5 mm square
6. Filter	Iron, 7mm
7. Image matrix	240 x 240 pixel
8. Data collection time	5 min.
9. Image reconstruction time	1 min.
10. Sample size	62mm (max.) in dia.
11. Spatial resolving capacity	0.25 x 0.25 mm

Yamato	74364	90.9
Yamato	74454	84.5
Yamato	74450	75.5
ALH-	78132	76.8
ALH-	77219	96.8

CT value (C) is related with density (D, g/cm^3) as shown in the following equation.

$$D = 0.0515C - 0.747$$

(3) Particle analysis Areal ratios (%) of the particles in the CTS pictures, which showed over 115 (CT value), are as follows.

Yamato	74364	6.85% at 5mm*
		6.84% at 10mm*
Yamato	74454	2.86% at 70mm*
		2.71% at 75mm*

* height

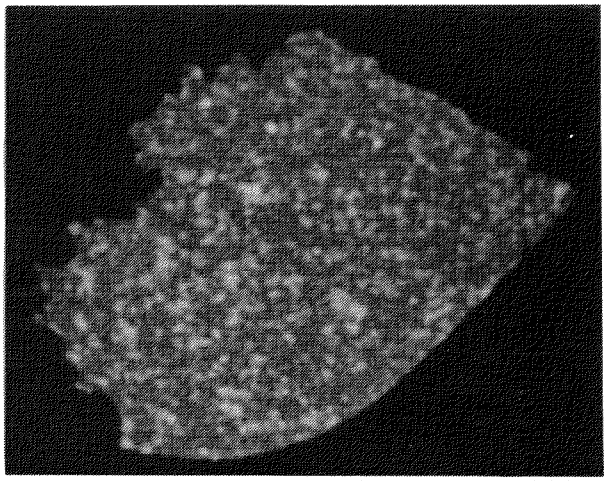

Photo 2. CTS analysis of Yamato 74364 (H-chond., Slice Position: 10mm)

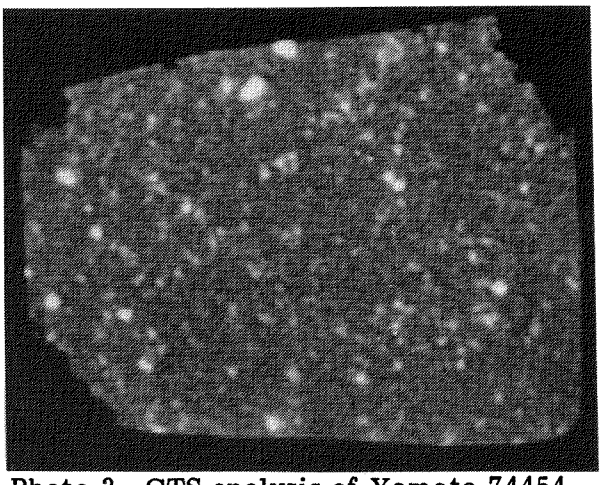

Photo 3. CTS analysis of Yamato 74454 (L-chond., Slice position: 75mm)

IV. Summary

CTS was found to be a suitable tool for very rapid classification and analysis of meteorites. Information for metallic phase size distribution was also obtained.

Reference

1) I. Taguchi: Analytical Sciences p.93 (1985).

HUGONIOT OF SOME ORDINARY CHONDRITES

Takafumi Matsui[1], Kouki Kani[2] and Yasushi Matsushima[3]
1) Geophysical Institute, University of Tokyo, Tokyo 113.
2) Faculty of Education, Okayama University, Okayama 700.
3) College of General Education, Okayama University, Okayama 700.

One of the major problems of meteoritics is to reveal impact fragmentation history of the meteoritic material. The Hugoniot is obviously one of the most fundamental physical properties when we study impact processes. However, no Hugoniot measurements have been conducted on meteorites. We have measured the shock wave velocity - particle velocity Hugoniot of 5 ordinary chondrites (Wellman (H5), Gilgoin Station (H5), Farmington (L5), Bruderheim (L6) and Leedey (L6)).

The specimen with the size of roughly 5x5x2 mm was impacted by the copper-plate projectile accelerated by the single-stage vertical powder gun. The impact velocity of the projectile and the shock wave velocity were measured by the magnet flyer method and the pin-contactor method (see Figure 1), respectively. The particle velocity was determined by the impedence-matching method.

The shock wave velocity - particle velocity Hugoniot of 5 ordinary chondrites are shown in Figure 2. The data are rather scattered but this is possibly due to either high porosity of chondrites or thinnes of specimen or both. Judging from inhomogenity in texture of chondrite, the thickness of the specimen, 2mm, may be too thin to represent a bulk physical property of the specimen (Yomogida and Matsui, 1983). It is hard for some chondrites (specifically Farmington) to approximate the data points by the linear relationship. This may be due to a phase change of some composite mineral judging from the existence of break in specific volume versus pressure curve. The Hugoniot calculated from the bulk composition of H and L chondrites by using the Munson & Schuler's formulation (Munson and Schuler, 1971) has a higher shock wave velocity. This is probably due to the prosity effect. Although we have measured only two H chondrites and three L chondrites, we can see the trend that the shock wave velocity of H chondrites is higher than that of L chondrites. It also appears that the shock wave velocities of L chondrites are more widely scattered than those of H chondrites.

References

K. Yomogida and T. Matsui, Physical properties of ordinary chondrites, J. Geophys. Res., 88, 9513-9533, 1983.
D. E. Munson and K. W. Schuler, Shock waves and the mechanical properties of solid, Syracuse Univ. Press, pp185, 1971.

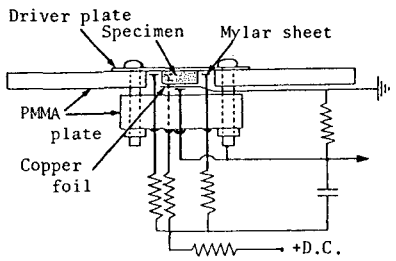

Fig.1 Specimen assembly and measuring circuit.

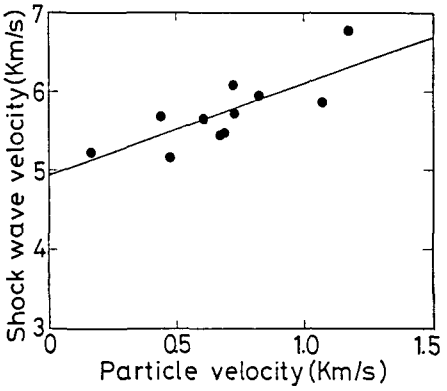

(a)

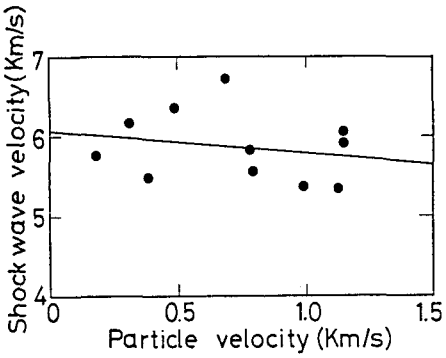

(b)

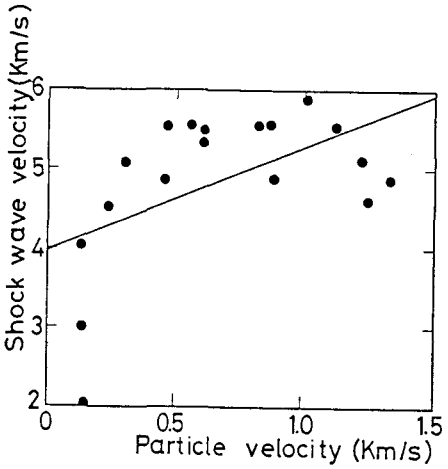

(c)

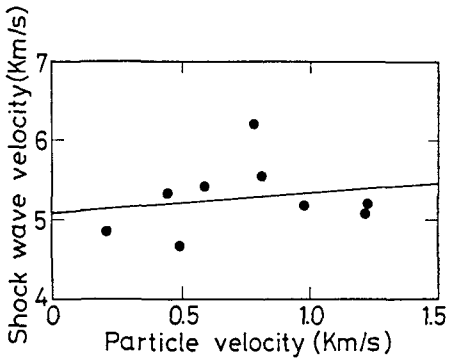

(d)

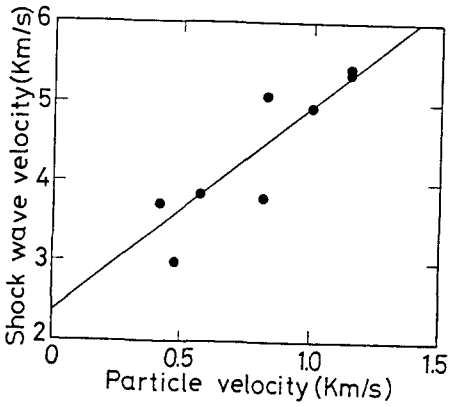

(e)

Fig. 2 The shock wave velocity - particle velocity Hugoniot.
(a) Wellman (H5), (b) Gilgoin Station (H5),
(c) Farmington (L5), (d) Bruderheim (L6), (e) Leedey (L6).

Thermomagnetic "Hump" in Antarctic Stony Meteorites

Minoru FUNAKI and Takesi NAGATA

National Institute of Polar Research

(1) Thermomagnetic Hump Phenomenon.

The thermomagnetic Hump (TM-hump) is a newly found particular phenomenon looking just like a "hump" on the initial heating thermomagnetic curve (TM-curve) of some stony meteorites, as shown in Fig. 1 for example. The TM-hump is defined as follows: In a course of increasing temperature (T), magnetization I(T) discontinuously begins to increase at $T=\Theta_h$, and after reaching a maximum value I(T) decreases with T down to a magnetic transition point at $T=\Theta_C$, the I(T) curve forming a hump shape extended from Θ_h to Θ_C. No hump appears on the first cooling TM-curve nor on the subsequent TM-curves.

(2) Antarctic Stony Meteorites accompanied by TM-Hump.

Antarctic stony meteorites which are accompanied by a TM-hump are listed in Table 1. As shown in Table 1, all meteorites accompanied by a TM-hump are achondrites, which do not contain metalic grains larger than 10^2 μm in linear size. Θ_h is in a range from 325°C to 360°C and Θ_C in a range from 535°C to 565°C.

(3) Thermomagnetic Hump in Silicate Component of St. Séverin Chondrite.

It is found that the silicate component of St. Séverin LL chondrite also is accompanied by a TM-hump as given in Table 1, though the TM-hump is buried within a stronger magnetization of metallic component in the bulk TM-curves. Fig. 2 shows the first- and second-run TM-curves of the St. Séverin silicate and Table 2(A) summarizes the magnetic hysteresis parameters at room temperature for the original state, after heating to 400°C near the maximum of TM-hump and after the thermal annealing at 900°C. Since the St. Séverin silicate (matrix) contains tetrataenite (Fe-Ni γ′-phase) in its very fine grains of metal too, and Θ_h=330°C is in agreement with th transition temperature of $\gamma' \rightleftarrows \gamma$ of $Fe_{50}Ni_{50}$ metal, the experimental

Table 1. Antarctic Achondrites accompanied by Thermomagnetic Hump

Meteorite	θh(℃)	θc(℃)	I_s (emu/g)	I_R (emu/g)	Hc (Oe)	H_{RC} (Oe)
Y-791186 (Eu)	330	535	0.28	0.028	32	190
Y-6902 (Di)	350	565	0.19	0.0035	42	—
Y-74013 (Di)	330	565	0.445	0.0025	17	210
Y-74037 (Di)	360	550	0.218	0.0045	73	140
Y-74097 (Di)	325	545	0.318	0.0040	13	210
Y-74648 (Di)	350	540	0.20	0.0075	85	520
St. Séverin Silicate	335	560	0.163	0.0245	278	1790

I_S : Saturation magnetization. I_R : Saturation Remanence
Hc : Coercive Force. H_{RC} : Remanence Coercive Force

results shown in Fig. 2 and Table 2(A) may indicate that the magnetically highly coercive component of Fe-Ni γ′-phase is broken down to form a new ferromagnetic phase by amalgamating with the surrounding paramagnetic γ-phase component at temperatures above 330°C. Such a phenomenon of a break-down and amalgamation with paramagnetic γ-phase for Fe-Ni γ′-phase has already been observed in the St. Séverin metallic component and Santa Catharina iron meteorite (Nagata et al., 1985). In the present case of fine powder, however, the break-down and amalgamation processes proceed relatively rapidly.

(4) Thermomagnetic Hump of Y-74013 and Y-791186.

As shown in Fig. 3 and Table 2(B), an increase of I_S caused by a formation of a TM-hump is same as in case of the St. Séverin silicate, but I_R, H_C and H_{RC} considerably increase by the TM-hump formation effect in Y-74013 diogenite instead of their characteristic reduction for the St. Séverin silicate. However, an annealing effect by heating twice to 870°C results in a considerable decrease in I_R and H_C to their medium levels higher than their respective initial values, while H_{RC} still increases even after the annealing procedure. Similar thermomagnetic measurements of Y-791186 eucrite result in similar characteristics of a TM-hump effect to those of Y-74013 (Table 3(C)). Namely, I_S, I_R, H_C and H_{RC} increase by the TM-hump formation effect, and the annealing at 850°C results in a reduction of I_S, I_R and H_C to their medium levels while a further increase of H_{RC}. These characteristics of TM-hump of Y-74013 and Y-791186 are considerably different from those of the St. Séverin silicate.

Table 2. Changes in Ferromagnetic Hysteresis Parameters in Association with TM Hump.

Obs. No	Temp. (℃)	Remarks	I_s (emu/g)	I_R (emu/g)	H_C (Oe)	H_{RC} (Oe)
(A)	(St. Séverin Silicate)					
1	24	Initial	0.163	0.0245	278	1790
2	24	After heating to 400℃	0.365	0.0595	158	450
3	24	After heating twice to 900℃	0.34	0.008	38	230
(B)	(Y-74013)					
1	21	Initial	0.445	0.0025	17	210
2	22	After heating to 360℃	0.48	0.00265	72	330
3	22	After heating to 490℃	0.675	0.071	134	325
4	22	After haeting to 590℃	0.70	0.0965	208	410
5	22	After heating twice to 870℃	0.42	0.0195	120	530
(C)	(Y-791186)					
1	18	Initial	0.28	0.028	32	190
2	21	After heating to 350℃	0.32	0.015	69	290
3	20	After heating to 490℃	0.62	0.081	137	370
4	20	After heating to 590℃	0.745	0.133	173	410
5	18	After heating twice to 850℃	0.43	0.064	160	570

(5) Type (A) and Type (B) of Thermomagnetic Hump.

The TM-hump subjected to the characteristics observed for the St. Séverin silicate (called Type A here) is very likely to be produced by a break-down of Fe-Ni γ'-phase of fine size into the ordinary γ-phase which amalgamates with surrounding paramagnetic γ-phase, as already mentioned. Possible mechanisms for a TM-hump of Type B for Y-74013 and Y-791186 may be more complicated, so that the present experimental data do not seem to be sufficient for suggesting a reasenable theoretical interpretation. One of possible hypothetical mechanisms might be as follows:-

The creation of a TM-hump of Type-B is due to a formation of fine ferromagnetic prolate particles of γ-phase of about 50% Ni by amalgamation of paramagnetic γ-phase with superparamagnetically fine nuclei of γ'-phase. Then an increase of I_R, H_C and H_{RC} during the formation process can be understood. The annealing effects could be attributed to an almost complete rearrangements in a high temperature γ-phase of the Ni-rich metallic parts.

Fig.1

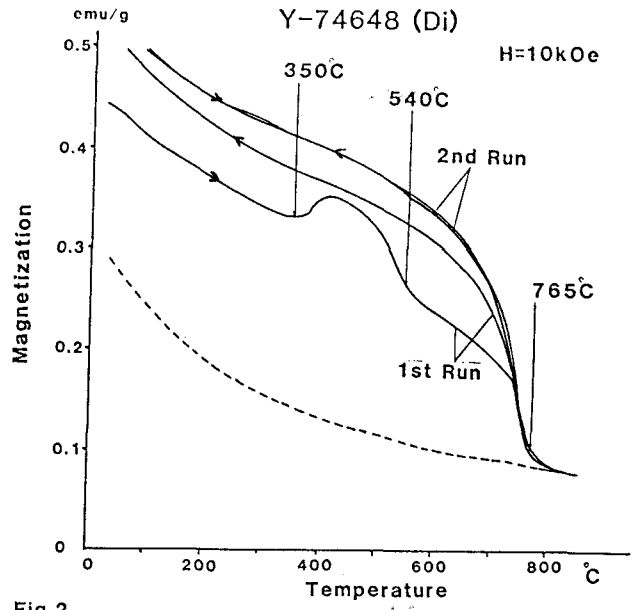

Fig.2

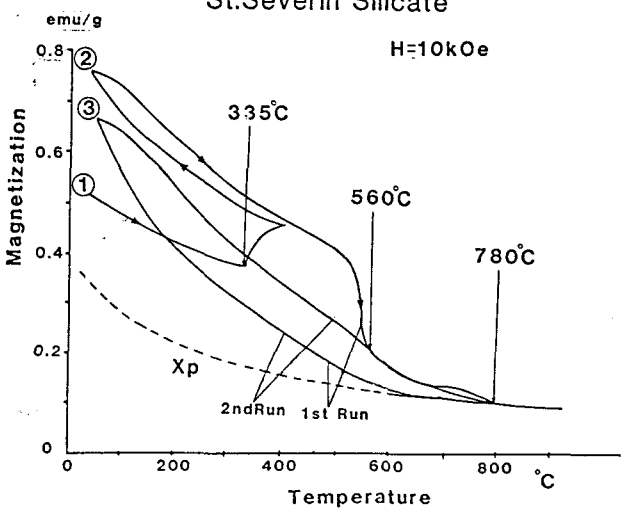

Fig.3

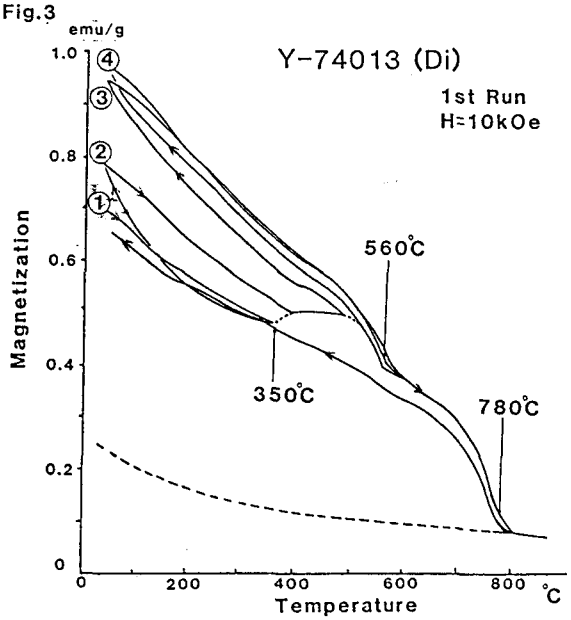

Tetrataenite Phase in Antarctic Stony Meteorites

Takesi NAGATA and Minoru FUNAKI

National Institute of Polar Research

(I) Tetrataenite (γ'-phase of Fe-Ni metal) in meteorites.

As the ordered taenite (tetrataenite: γ'-phase of FeNi) having an approximate composition of 50%Fe50%Ni in atomic ratio has a crystal structure of a large crystalline anisotropy, presence of this γ'-taenite phase in meteorites seems very significant in the ferromagnetic properties of meteorites. From this point of view, several stony meteorites which contain a fair amount of tetrataenite in their metallic components are magnetically and metallographically examined (Nagata and Funaki, 1982; Nagata, Funaki and Danon, 1985). It seems likely, on the other hand, that the so-callled plessite phase in metallic components of stony meteorites may contain a certain amount of the tetrataenite phase in the Ni-maximum edges of their M-shape distribution of Ni in taentie zones, because Curie point of the magnetic phase to represent a presence of plessite component is always in approximate agreement with Curie point of tetartaenite, 550-570°C.

(II) Standard γ'-rich stony meteorites.

Taking St. Séverin LL_6 chondrite (containing 51wt% γ'-phase in metallic component) and Appley Bridge LL_6 (containing about 80 wt% γ'-phase in metallic component) as the two standard samples of γ'-rich stony meteorites, all Antarctic stony meteorites (except C-chondrite), which have been magnetically analyzed (total member N=42) are re-examined in order to look for γ'-phase in their metallic components. 27 stony meteorites among 42 examined samples have the plessite component whose Curie point (Θ_C(pl)) is 550-575°C (Fig. 1). Characteristic magnetic properties of the standard γ'-rich chondrites are summarized as follows:

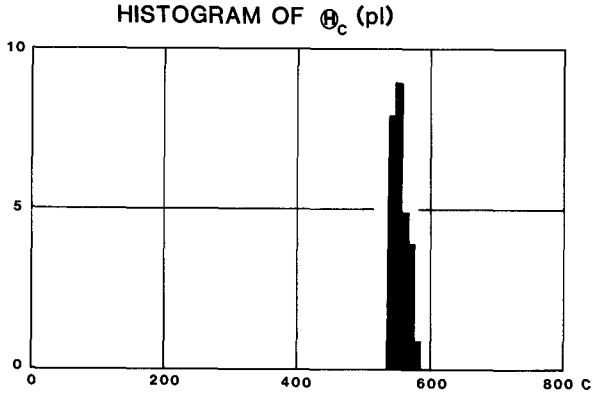

Fig. 1

(1) Remanence coercive force (H_{RC}) and coecive force (H_C) are anomalously large ($H_{RC}\gtrsim 500$ Oe, $H_C\gtrsim 100$ Oe).
(2) Curie point of γ'-phase is around 560-570°C.
(3) The initial heating thermomagnetic (TM) curve of γ'-phase is flat up to about 500°C and then sharply decreases to Curie point.
(4) After heating up above 800°C, γ'-phase is broken down to the ordinary disordered γ-phase. Hence the first cooling and subsequent TM curves have characteristics of those of the disordered γ-phase.
(5) Because of the break-down of γ'-phase by the heating procedure H_C and H_{RC} after the heating are much reduced from their respective pre-heating values.

A set of TM curves of one of the standard γ'-phase chondrite (St. Séverin) is shown in Fig. 2(a), and H_C, H_{RC}, saturation magneitzation (I_S) and saturation remanence (I_R) before and after the heating procedure to break-down the γ'-phase of the two standard samples are given in Table 1.

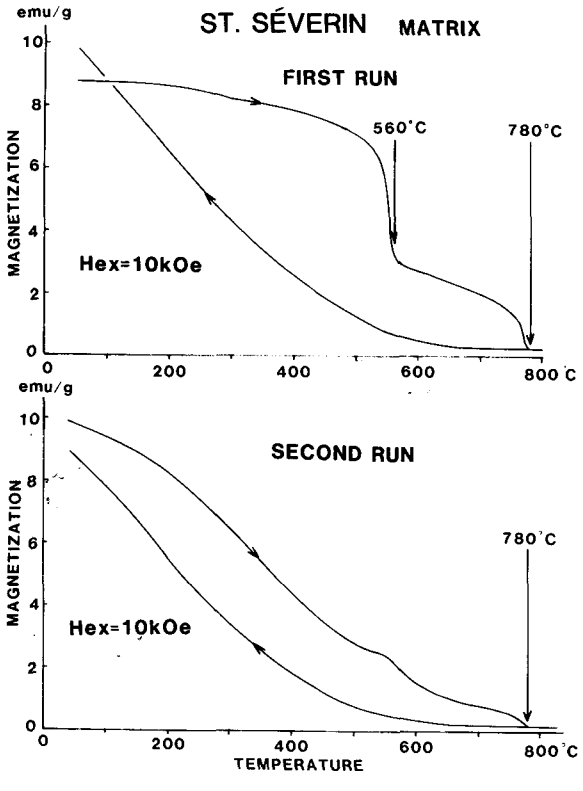

Fig. 2(a)

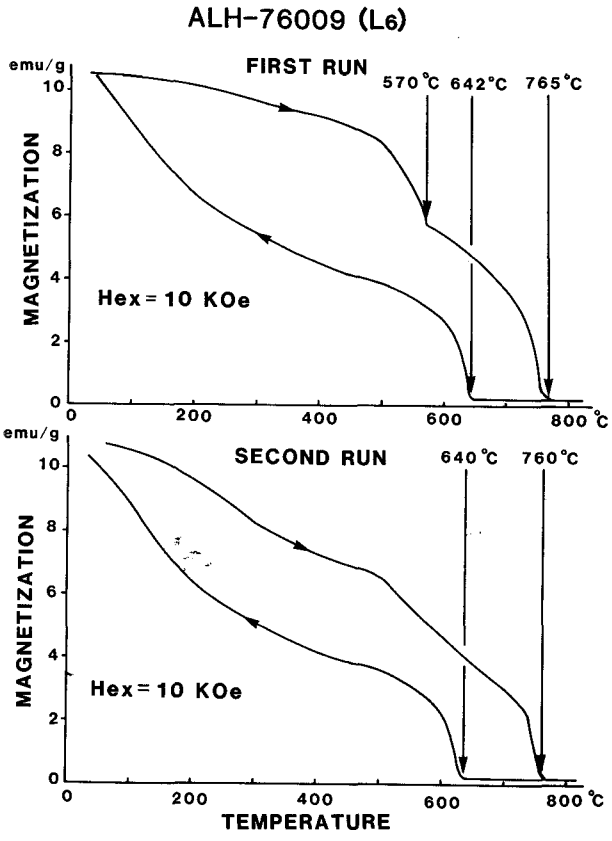

Fig. 2(b)

(III) γ'-phase characteristics in Antarctic Stony Meteorites.

Fig. 2(b) shows a set of TM curves of ALH-76009 L_6 chondrite. The TM curves of ALH-76009 are closely similar to those of the standard sample given by Fig. 2(a), both TM curves consisting of α- and γ'-phases (plus γ-phase too). The bottom half of Table 1 summarizes the characteristic magnetic transition temperature of plessite component, θ_C(pl), and magnetic hysteresis parameters, I_S, I_R, H_C and H_{RC}, at room temperature befor and after the heat treatment to break down γ'-phase, for ALH-76009 together with those of Y-74160 LL-condrite and Y-74648 diogenite. Approximate agreements of the characteristic θ_C(pl) values and noticeable decreases of I_R, H_C and H_{RC} values after the γ'-phase break-down heat treatment of the three Antarctic stony meteorites with those of the standard γ'-rich chondrites may indicate presence of γ'-phase in these Antarctic stony meteorites.

Some other Antarctic chondrites whose θ_C(pl) values are about 550-570°C, have unusually large values of H_{RC}, as summarized in Table 2. As an unusually large H_{RC} compared with H_C, indicates co-existence of an unusually coercive magnetic component, such as the Fe-Ni γ'-phase, together with another medium or soft magnetic component, these Antarctic chondrites also have a reasonably high possibility for containing a small amount of Fe-Ni γ'-phase. Further experimental studies on checking presence of Fe-Ni γ'-phase in these condrites will be continued.

Table 1. Magnetic properties of γ'-rich standard chondrites and Antarctic Meteorites.

Meteorite	θ_c(pl) (℃)	I_S (emu/g) (1) (2)	I_R (emu/g) (1) (2)	H_C (Oe) (1) (2)	H_{RC} (Oe) (1) (2)
St. Séverin (LL_6)	560	2.80→3.95	0.50 →0.021	520→ 9.5	1840→110
Appley Bridge (LL_6)	565	1.73→2.42	0.12 →0.031	160→ 14.55	470→ 70
Y-74160 (LL_7)	565	1.59→2.63	0.16 →0.008	255→ 8.0	460→240
ALH-76009 (L_6)	570	9.8 →9.4	0.37 →0.043	110→ 10.0	2470→130
Y-74648 (Di)	555	0.50→0.55	0.109→0.008	225→100	420→180

(1) : Before heating. (2) : After heating.

Table 2. Antarctic chondrites of θ_C(pl)=550-570 ℃ and $H_{RC}\gtrsim$1000 Oe

Meteorite	θ_C(pl) (℃)	I_S (emu/g)	I_R (emu/g)	H_C (Oe)	H_{RC} (Oe)
Y-7301 (H_4)	577	15.0	0.14	16	1.700
Y-74647 (H_{5-6})	561	27.9	0.34	14	1.080
Y-74191 (L_3)	558	6.8	0.22	30	1.330
Y-74354 (L_6)	545	21.8	0.71	66	2.620
Y-74362 (L_6)	560	8.1	0.27	160	2.100

Special Lecture

Professor Michael E. Lipschutz

ANTARCTIC AND NON-ANTARCTIC METEORITES: DIFFERENT POPULATIONS

Dennison, J. E., Kaczaral, P. W. and Lipschutz, M. E.

Department of Chemistry, Purdue University, W. Lafayette, IN 47907 USA

Among the 7000 Antarctic meteorite fragments, representing 1200-3500 separate finds, are many specimens of rare or unique types compared with non-Antarctic falls. Even at the coarsest classification level, distributions are peculiar: irons, stony-irons and LL chondrites are deficient in at least the Victoria Land population and the H/L chondrite ratio of 3 differs from the value of 1 in non-Antarctic falls or finds (Dennison et al., 1986). Iron meteorite subtypes from Antarctica differ in proportion from those in non-Antarctic regions (Clarke, 1985). These distribution differences, coupled with the long terrestrial ages of Antarctic meteorites and mass-distribution differences between non-Antarctic and Antarctic populations, hint that Antarctica may have sampled extraterrestrial parent sources differing from those that provide contemporary falls.

To study this, we determined by RNAA, concentrations of 14 trace and ultratrace elements (Co, Au, Sb, Ga, Se, Rb, Cs, Te, Bi, Ag, In, Tl, Zn and Cd) in a large number of unpaired Antarctic samples and non-Antarctic falls (Dennison et al., 1986; Kaczaral and Lipschutz, 1986). The distribution of each element in each population can be described by a normal or lognormal Gaussian. To establish compositional differences between sample populations, it is necessary to use standard statistical tests to establish how unlikely it is that two sample populations - e.g. Victoria Land and non-Antarctic falls - were drawn from the same parent population. At the 10% test level (90% confidence level), concentration of 2 of 14 elements might differ by chance: the larger the number of differing elements, the more likely it is that the population difference is meaningful. For Antarctic samples of weathering type A or B only, 8 elements each differ in H5 (11 Victoria Land /23 non-Antarctic) and L6 chondrites (13 Victoria Land/25 non-Antarctic) and 3 in LL6 samples (5 Victoria Land/11 non-Antarctic). Essentially the same numbers of differences are seen if samples of petrologic types 4-6 are studied. The H chondrite populations differ in shock history and ^{53}Mn content, in the correlation profile (pattern of statistically significant interelement relationships) and on 2-element diagrams involving Bi, In and Tl. Five Yamato Mts. H5 chondrites differ compositionally from 11 Victoria Land samples (8 elements) and from 23 non-Antarctic falls (5 elements). These differences do not seem to reflect weathering or analytical factors (modeling, bias, etc.) and seem instead to represent a preterrestrial population difference.

An usual, answering one question raises another. How do Antarctic samples preserve a memory of preterrestrial sources differing from those of contemporary, non-Antarctic falls? Differences in orbital inclinations seem quantitatively inadequate, leaving a time-variation as the least unlikely possibility. But this creates difficulties in the light of Monte Carlo orbital dynamic calculations. These random-walk calculations indicate that the near-earth meteoroid source distribution should be essentially constant over the 10^5-10^6 year terrestrial age of Antarctic

meteorites since asteroid ejecta is destroyed on the 10^7 year scale (Arnold, 1965; Wetherill, 1974; Opik, 1976). On the other hand, individual Apollo asteroids can contribute substantially to the Antarctic meteorite population over this time span according to recent calculations by Greenberg (personal communication; cf. Greenberg and Chapman, 1983). Problems presented by these samples may require us to ask more questions that we thought were long-since answered.

REFERENCES: Arnold, J. R., Astrophys. J. **141** 1536-1547 (1965); Clarke, R. S. Jr., Tenth Symp. Antarctic Meteorites, 188 (1985); Dennison, J. E., Lingner, D. W. and Lipschutz, M. E., Nature **319** 390-393 (1986); Greenberg, R. and Chapman, C. R., Icarus **55** 455-480 (1983); Kaczaral, P. W. and Lipschutz, M. E., Lunar Planet. Sci. XVII, in press (1986); Opik, E. J. Interplanetary Encounters (1976); Wetherill, G. W., Res. Earth Planet. Sci. **2** 303-331 (1974).

STUDY ON THE PRIMITIVE MATERIALS FORMING TERRESTRIAL PLANETS

Wang Daode
Institute of Geochemistry,Academia Sinica,Guiyang,Guizhou Province, The People's Republic of China

The primitive material which constitutes the Earth is probably IAB iron meteorite (the core of the Earth) and H-group chondrite (the mantle of the Earth). When the experimental temperature is higher than 1300 ^{o}C, noticeable magmatic differentiation takes place in the Jilin meteorite, and this is quite similar to the process of formation of the core and the mantle of the Earth. The metal-sulfide components within chondrite would sink to the core. During melting and recrystallization of the Jilin chondrite the partial FeO in olivine (mean olivine composition, Fa 18.46%, Fe 13.6%) can be reduced and Fe^{o} formed (mean melted olivine composition of 19 determinations:Fa 14.81%, Fe 11.0%). These reduced metal Fe also would move to the core.

Some large parent meteorite bodies seem to have undergone such a process leading to the formation of some iron meteorites and achondrites. The Fe-Ni-S phase in the experimental products may serve as an indicator in identifying the cosmic chondrules.

It seems reasonable to assume the mechanism of metal-silicate separation between the initial cores and mantles of terrestrial planets during their thermal evolution process as thermal diffusion of Fe-Ni metal in solid state, partial melting of metals and metal-sulfides, and full melting and differentiation of metals, metal-sulfides and silicates.

The differences in major elements, especially refractory elements, or rather, chemical compositions among different groups of meteorites, inner planets and outer planets bear witness to the fact that chemical fractionation took place between the beginning of condensation and the accretion of the solar nebula. As the distance from the sun increases the abundance of refractory elements and the oxidation state increases, while temperature and pressure decrease in the sequence of E-IAB-H,L, LL-CV,CO,CM,CI (Wasson, 1985). These features indicate different nebula temperature and pressure conditions for the environments in which they were formed.

On the basis of the core-mantle structure, chemical composition and physico-chemical conditions of formation of terrestrial planets, the result of simulant experiments on magmatism of the Jilin meteorite and its comparison with that of other meteorites, it is believed that the primitive materials for Mercury are EH and EL chondrites, for Vennus, IAB iron meteorites, for the Earth, IAB and H-chondrites, for Mars,H,L,LL chondrites. And the primitive materials for Jovian planets are carbonaceous chondrite and comets.

Reference: Wasson,J.T., Meteorites, Their Record of Early Solar -System History, W.H.Freeman and Company, New York,1985, 187-223.

A POTPOURRI OF APOLLO REGOLITH BRECCIAS: ANALOGS OF LUNAR METEORITES

Eric A. Jerde*, Paul H. Warren*, Grant H. Heiken§ and David T. Vaniman§

* Institute of Geophysics, U.C.L.A., Los Angeles, CA 90024, USA
§ Los Alamos National Laboratory, Los Alamos, NM 87545, USA

A typical sample of lunar regolith, say 50–200 mg, is a naturally-produced random assemblage of about 10^5 rock particles. Variations in regolith composition and petrology provide important clues to the nature of the underlying crust. Unfortunately, the maximum spread between points traversed on a single Apollo mission was only 12 km (Apollo 17). Variation among lunar soils from any given mission is commensurably limited. However, regolith breccias, which are essentially soils lithified by impacts, may be transported great distances. At least three lunar regolith breccias have been found in Antarctica: ALHA81005, Y-791197, and Y-82192 [1]. Because of this potential for exotic provenance, regolith breccias constitute important supplements to the Apollo and Luna collections of soils. Another key incentive for studying Apollo regolith breccias is to clarify the origin of lunar meteorites. For example, it is unclear whether ALHA81005, Y791197, and Y82192 were derived from a single impact or separate impacts on the lunar surface [2].

We employed INAA (at UCLA) and petrographic techniques including electron microprobe analysis (at LANL) to study 40 suspected regolith breccias, the majority of which had been essentially unstudied. This set comprised 23 samples from Apollo 14 (7 fragments from 14004, 10 from 14160, 5 from 14263, and one sample of 14315), 7 from Apollo 16, and 10 from Apollo 17. Nine of these samples turned out not to be regolith breccias (e.g., melt rocks).

Apollo 14. The most interesting regolith breccia from Apollo 14 is probably 14315, a 115-g rock that appears to be the richest in chondrule-like objects among all lunar samples: 5–10% chondrules [3]. However, only Rose et al. [4] and Keith et al. [5] previously analyzed its bulk composition, and these analyses omitted many key elements. The bulk composition of 14315 is as unusual as its texture. Compared to other Apollo 14 regolith samples, 14315 has far higher Al and far lower REE (e.g., Sm: Figure 1). It also has a higher mg ratio (0.654) than previously analyzed Apollo 14 regolith samples (0.608–0.630). Another Apollo 14 regolith breccia, 14160,128, has an exceptionally low mg ratio (0.587). Ratios of incompatible elements in 14315 conform to the KREEP pattern typical of Apollo 14 materials (see Fig. 1 in our companion abstract [2]). Dence and Plant [6] suggested that all four Apollo 14 breccias with chondrule-like objects (14301, 14313, 14315 and 14318) were derived from Triplet Crater, which is only about 0.25 km south of the landing site. However, the unique composition of 14315 suggests a more exotic provenance, probably many hundreds of meters and possibly many km from the site.

Regolith breccia 14004,63 has unusually high incompatible element contents, about 1.3 x normal for Apollo 14 regolith samples. The corresponding thin section, 14004,77, contains an ovoid granitic clast, about 50 x 30 μm, embayed in a large glob, about 180 x 100 μm, of ropy glass. Defocused beam analysis of the granitic clast indicates the following bulk composition in wt%: SiO_2 76.8, TiO_2 0.88, Al_2O_3 6.0, FeO 3.9, MnO 0.06, MgO 3.1, CaO 3.2, Na_2O 1.06, K_2O 2.6, and P_2O_5 1.5. The host ropy glass is also relatively granitic. The clast is similar in composition to other lunar granites [7]. It seems unlikely that these materials account for the high incompatible element contents of 14004,63. Lunar granites tend to have lower REE contents than

typical Apollo 14 soils, the clast and its host glass together constitute <<1% of the thin section, and the V-shaped REE pattern typical of lunar granites is not observed for 14004,63.

Apollo 16. Only three of the samples from Apollo 16 turned out to be regolith breccias. Last year McKay et al. [8] noted a "dichotomy" of mg ratio among Apollo 16 regolith breccias: of 16 such samples in the 1985 data base, the majority have mg = 0.69–0.72; members of another cluster, which tend to be more "mature" regolith samples, have mg = 0.65–0.67. But none had mg = 0.67–0.69. Our new data for 61504,8 (mg = 0.65) and 65925,1 (mg = 0.71) are consistent with this mg bimodality. However, our analysis of 67557,3 (mg = 0.684) extends the range of the high-mg group in the direction of lower mg (see Fig. 2 in our companion abstract [2]). The distribution of mg among Apollo 16 regolith breccias still appears bimodal, but the data set still comprises only 19 samples. The mg ratios of the soils (precursors of regolith breccias) and rocks from Apollo 16, while diverse, are not perceptibly bimodal. The majority of mature Apollo 16 soils (sensu stricto) have mg = 0.65–0.67, but a few immature ones have mg in the range 0.67–0.71. However, if pristine rocks alone are considered, mg is bimodal. Also, orbital geochemical data indicate that the Cayley Plains a few km west of the site probably have a far higher mg ratio than the Descartes material just east of the site [9, 10]. It will be interesting to see how well the bimodality holds up when more regolith breccias from Apollo 16 are analyzed. Equally important, the total range of mg among Apollo 16 regolith breccias remains limited to 0.65–0.72. This spread in mg is less than that between Y82192 and ALHA81005, and smaller still than that between Y791197 and ALHA81005, an observation that constitutes a key constraint on the origins of these meteorites [2].

Apollo 17. Most Apollo 17 regolith materials, breccias and soils, tend to obey simple trends produced by mixing local mare basalt with highlands material whose aggregate composition resembles a typical noritic breccia from this site (this resemblance is only approximate; e.g., the highlands component implied by the mixing trends is more Al-rich than the noritic breccias). Eight of the 9 regolith breccias we studied obey these same mixing trends. The exception is 72504,10, a 200 mg Station 2 fragment that Meyer [11] observed to be rich in black glass spheres and "unlike other soil breccias." Compositionally, this breccia is essentially identical to the famous orange-black glass soil, 74220 [e.g., 12] (Figure 2). A few of our data for 72504,10 are (in mg/g): Mg 90.4, Al 33.7, Si 181, Ca 52, Ti 53, Fe 178; (in μg/g) K 765, Zr 280, Ba 86, La 7.0, Sm 7.0, Eu 1.86, Tb 1.49, Lu 0.66, Th 0.60. This fragment was found 4.4 km southwest of Shorty Crater, on whose rim 74220 was found. The extreme concentration of the orange-black glass spherules in 74220 [13] attests to rapid deposition, entailing remarkably little dilution by pre-existing soil or contemporaneous impact ejecta. Apparently, assuming that 72504,10 was not also derived (i.e., ejected) from Shorty Crater, extreme concentration of orange-black glass spherules was a common phenomenon in the Taurus-Littrow Valley.

References: [1] Yanai K. and Kojima H. (1984) Proc. 9th Symp. Ant. Meteorites; [2] Warren P. H. and Kallemeyn G. W. (1985) Abstract, 11th Symp. Ant. Meteorites (this volume); [3] Nelen J. et al. (1972) Proc. Lunar Sci. Conf. 3; [4] Rose H. J., Jr. et al. (1972) Proc. Lunar Sci. Conf. 3; [5] Keith J. E. et al. (1972) Proc. Lunar Sci. Conf. 3; [6] Dence M. R. and Plant A. G. (1972) Proc. Lunar Sci. Conf. 3; [7] Warren P. H. et al. (1983) Earth Planet. Sci. Lett. 64, 175–185; [8] McKay G. A. et al. (1986) Proc. Lunar Planet. Sci.

Conf. 16; [9] Hubbard N. J. and Woloszyn D. (1977) Phys. Earth Planet. Int. 15, 287-302; [10] Andre C. G. and El-Baz F. (1981) Proc. Lunar Planet. Sci. Conf. 12; [11] Meyer C., Jr. (1973) Apollo 17 Coarse Fines (4-10 mm) Catalog: NASA Johnson Space Center, Houston; [12] Taylor S. R. (1982) Planetary Science, a Lunar Perspective; [13] Heiken G. H. et al. (1974) Geoch. Cosmoch. Acta 38, 1703-1718.

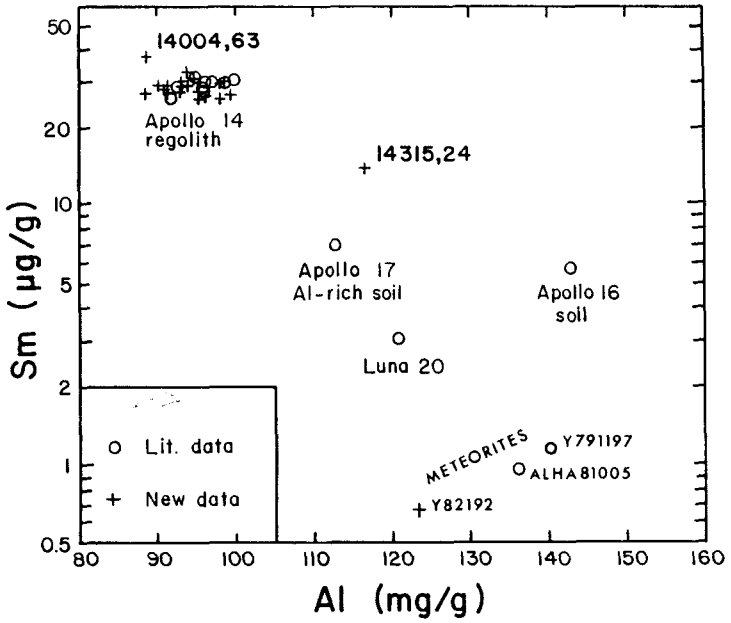

Fig. 1

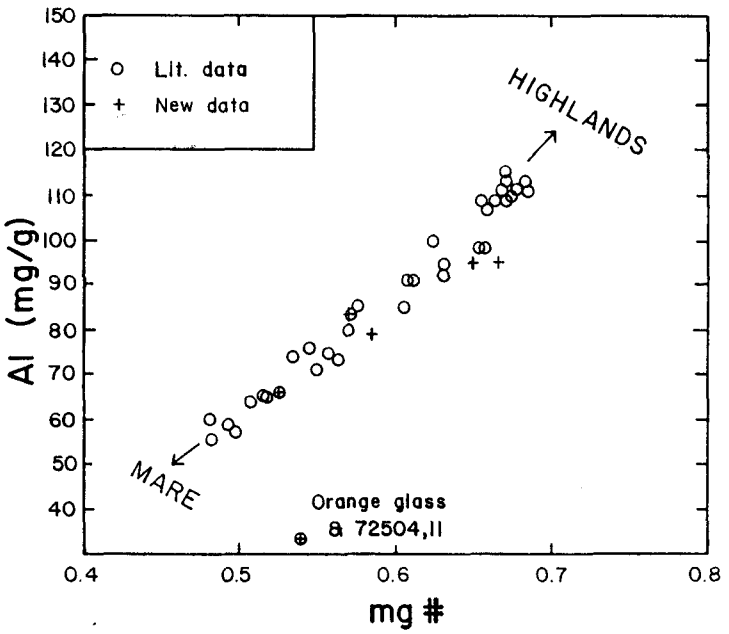

Fig. 2